AMERICAN UNIVERSITY OF BEIRUT

BIODIESEL PRODUCTION FROM WASTE FRYING OIL USING HETEROGENEOUS TRANSESTERIFICATION PROCESS

by
ELYSSA GEORGES FAWAZ

A dissertation
submitted in partial fulfillment of the requirements
for the degree of Doctor of Philosophy
to the Department of Civil and Environmental Engineering
of the Faculty of Engineering and Architecture
at the American University of Beirut

Beirut, Lebanon
September 2018

AMERICAN UNIVERSITY OF BEIRUT

BIODIESEL PRODUCTION FROM WASTE FRYING OIL USING HETEROGENEOUS TRANSESTERIFICATION PROCESS

by
ELYSSA GEORGES FAWAZ

Approved by:

Dr. Darine Salam, Assistant Professor
Department of Civil and Environmental Engineering
American University of Beirut
Advisor

Dr. Georges Ayoub, Professor
Department of Civil and Environmental Engineering
American University of Beirut
Chairperson of Committee

Dr. MakramSuidan, Professor
Department of Civil and Environmental Engineering
American University of Beirut
Member of Committee

Dr. Jean Daou, Professor
Institut de Science des Matériaux de Mulhouse
Université des Hautes Alsaces
Member of Committee

Dr. Pablo Campo Moreno, Assistant Professor
Cranfield Water Science Institute
Cranfield University
Member of Committee

Date of thesis defense: September 2018

AMERICAN UNIVERSITY OF BEIRUT

THESIS, DISSERTATION, PROJECT RELEASE FORM

Student Name: Fawaz Elyssa Georges
Last First Middle

○ Master's Thesis ○ Master's Project ⊗ Doctoral Dissertation

☐ I authorize the American University of Beirut to: (a) reproduce hard or electronic copies of my thesis, dissertation, or project; (b) include such copies in the archives and digital repositories of the University; and (c) make freely available such copies to third parties for research or educational purposes.

☒ I authorize the American University of Beirut, to: (a) reproduce hard or electronic copies of it; (b) include such copies in the archives and digital repositories of the University; and (c) make freely available such copies to third parties for research or educational purposes
after:

One ---- year from the date of submission of my thesis, dissertation, or project.
Two ---- years from the date of submission of my thesis, dissertation, or project.
Three ---- years from the date of submission of my thesis, dissertation, or project.

13/09/2018

Signature Date

ACKNOWLEDGMENTS

To my dear father: because I owe it all to you. Forever, thank you.

I am deeply grateful to my mother and sister for their unconditional love. I am also grateful to all my friends that I count as brothers and sisters for their unceasing encouragement, support and prayers.
I would like to thank my fellow lab-mates for the stimulating discussions we had at all levels, and I show acknowledgment to the lab staff for making special efforts in helping me at all times.

A very special gratitude goes to Dr. Nada Sabra for believing in me and encouraging me to pursue research.

I express my appreciation to the members of the dissertation committee: Drs. Georges Ayoub, Makram Suidan, Jean Daou and Pablo Campo Moreno for generously offering their time and efforts to review this work and provide insightful comments that significantly improved the thesis.
With a special mention to Dr, Jean Daou who responded readily and helped the progress of the research by providing his facilities.

Last, but by no means least, I deeply thank my thesis advisor Dr. Darine Salam for her continuous support of my PhD study and research, for her patience, motivation and immense insight. Her guidance and expertise helped me improve my research skills and made this work possible.

"by faith working through love"

AN ABSTRACT OF THE DISSERTATION OF

Elyssa Georges Fawaz for Doctor of Philosophy
Major: Environmental and Water Resources Engineering

Title: Biodiesel Production from Waste Frying Oil Using Heterogeneous Transesterification Process

Strategies to improve molecular diffusion limitations of HZSM-5 zeolites were investigated for the production of biodiesel. Zeolite crystals with short diffusion length and hierarchical porosity were compared with conventional coffin-shaped microcrystals for their catalytic activity in terms of acidic properties and pore structure. As-synthesized catalytic materials were characterized with instruments including XRD, SEM, TEM, BET/BJH porosimetry analysis, X-Ray fluorescence, and FTIR. Esterification of linoleic acid as a model reaction for biodiesel production and transesterification reactions were carried out at different reaction conditions (reaction time, reaction temperature, methanol to oil molar ratio, and catalyst loading) to investigate the effect of the reaction parameters on the behavior of the zeolite catalysts. The reactions were successfully catalyzed using hierarchical HZSM-5 zeolite catalysts produced in nanosheet and nanosponge morphologies as compared to highly acidic conventional big and nano-crystals of HZSM-5 zeolites. Improved accessibility and molecular transport of reactants from the outer mesoporous surface to the intrinsic active zeolitic framework resulted in achieving high conversions of 95.12 % for linoleic acid transesterification and 48.29 % for waste frying oil using HZSM-5 nanosheets at 4 h reaction time, 10 wt% catalyst loading, respective 6:1 and 12:1 methanol to linoleic acid/waste frying oil molar ratio and 180 °C. Although highly acidic, HZSM-5 nanosponges did not operate to their full potential as compared to HZSM-5 nanosheets given their higher hydrophilicity which favored water and glycerol adsorption to their surface and resulted in lower coverage of the less polar reactants. The correlation between the surface hydrophobicity and acidity of the zeolites with different Si/Al ratios and their catalytic performance was also assessed for biodiesel production. It was shown that Si/Al ratio of HZSM-5 zeolites determines their acidity and hydrophobic character with a combined effect on the esterification reactions. In addition, in economic feasibility on biodiesel production from waste frying oil in Lebanon using homogeneous catalysis was studied. By interacting with local authorities and creating a more covered supply chain coordination system, it would be possible to successfully reuse waste frying oil for the production of biodiesel on a national scale for the long term, and reduce the environmental damages caused by their disposal.

CONTENTS

ACKNOWLEDGMENTS…… v

ABSTRACT……. vi

LIST OF ILLUSTRATIONS…… xii

LIST OF TABLES…… xv

Chapter

1. INTRODUCTION..... 1

1.1 Biodiesel Production Using Zeolites: General Introduction……1

1.2 Thesis Objectives……..2

1.3 Thesis Significance……...3

1.4 Thesis Organization……..4

2. BIODIESEL PRODUCTION USING ZEOLITE CATALYSTS–REVIEW 6

2.1 Sources of Biodiesel Feedstock……....6

2.2 Biodiesel……...8

2.3 Transesterification……....9

2.4 Zeolites……...12

2.5 Non-Zeolitic Catalyzed Transesterifications……..16

2.5.1 Transesterification by Homogeneous Catalysts……16

2.5.2 Transesterification by Heterogeneous Catalysts……...18

2.5.2.1 Alkali-Heterogeneous Transesterification....….....18

2.5.2.2 Acid-Heterogeneous Transesterification……...20

2.5.3 Enzyme-Catalyzed Transesterification……..23

2.6 Zeolitic-Catalyzed Transesterifications……...24

2.6.1 Zeolitic alkali-heterogeneous transesterification……..24
2.6.1.1 Synthetic alkali zeolite catalysts……...24
2.6.1.2 Natural alkali zeolite catalysts……..27
2.6.1.3 Magnetic alkali zeolite catalysts……...28
2.6.2 Zeolitic acid-heterogeneous transesterification……29
2.6.2.1 H-Type Acid Zeolite Catalysts…….29
2.6.2.2 Modified Acid Zeolite Catalysts……...30
2.6.2.2.1 Post-synthesis modification of acid zeolite catalysts……..31
2.6.2.2.2 Direct-synthesis modification of acid zeolite catalysts……..32

2.7 Factors Affecting Biodiesel Yield Using Zeolite Catalysts……34

2.7.1 Reaction Temperature……...34
2.7.2 Molar Ratio of Alcohol to Oil……...35
2.7.3 Catalyst Type and Loading……...36
2.7.4 Reaction Time……...37

2.8 Synthesis of Zeolite Catalysts…….37

2.9 Characterization of Heterogeneous Zeolites……...38

2.10 Economic and Environmental Considerations of Biodiesel Production by Zeolite Catalysts……...39

2.11 Summary of the Review……..40

3. PRELIMINARY ECONOMIC ASSESSMENT OF THE USE OF WASTE FRYING OILS FOR BIODIESEL PRODUCTION IN BEIRUT, LEBANON 41

3.1 Introduction…….41

3.2 Methodology……...44

3.2.1 Waste Frying Oils Collection……...44
3.2.1.1 Data Collection…….45
3.2.1.2 Questionnaire Design……...46
3.2.2 Biodiesel Production……47
3.2.2.1 Reagents and Chemicals……...47
3.2.2.2 WFOs Sampling and Preparation…….47
3.2.2.3 Pretreatment and Transesterification……47
3.2.2.4 Purification……...49
3.2.2.5 Biodiesel Quality Characterization……...49

3.2.3 Assessment of Economic Feasibility of Biodiesel Production ……50

3.3 Results and Discussion …….50

3.3.1 Production……....50
3.3.2 Characterization of Biodiesel……...51
3.3.3 Analysis of the questionnaire……...52
3.3.4 Formation of the logistics costs……....54
3.3.5 Calculation of total cost...……....59
3.3.5.1 Acquisition cost of WFOs……59
3.3.5.2 Capital, manufacturing and chemicals' cost…….60
3.3.5.3 Labor cost and Utility and taxes costs……..61
3.3.5.4 Glycerin and FAEs credit…….....62
3.3.5.5 Biodiesel cost calculation and analysis……63
3.3.5.6 Sensitivity Analysis……..65
3.3.5.7 Long-Term Economic Assessment of Biodiesel…..66
3.3.6 Environmental and net energy benefit analysis……68

3.4 Conclusion……..70

4. COMPARATIVE STUDY ON THE CATALYTIC PERFORMANCE OF HZSM-5 ZEOLITES FOR BIODIESEL PRODUCTION: STRATEGY TO INCREASE CATALYST EFFECTIVENESS. 72

4.1 Introduction…….72

4.2 Experimental section……...74

4.2.1 Structure directing agent synthesis……...75
4.2.2 Catalysts Synthesis……...76
4.2.3 Catalysts Characterization……78
4.2.4 Esterification Reaction Procedure……79
4.2.5 Fatty Acids and Methyl Esters analysis……80
4.2.6 Determination of the kinetics of the esterification reaction ……82

4.3 Results and Discussion……...83

4.3.1 Catalyst Characterization……..83
4.3.2 Optimized Reaction Conditions of Esterification……90
4.3.2.1 Effect of Reaction Temperature on Esterification…90
4.3.2.2 Effect of Methanol to Linoleic Acid Ratio on Esterification……92
4.3.2.3 Effect of Reaction Time on Esterification……94

4.3.3 Mass transfer evaluation of the synthesized catalysts on the esterification reaction……..97

4.4 Summary and Conclusion……..102

5. HIERARCHICAL ZEOLITES AS CATALYSTS FOR BIODIESEL PRODUCTION FROM WASTE FRYING OILS TO OVERCOME MASS TRANSFER LIMITATIONS..... 103

5.1 Introduction……103

5.2 Experimental section……..105

5.2.1 Structure directing agent synthesis……..105
5.2.2 Catalysts Synthesis……..106
5.2.3 Catalysts Characterization……...108
5.2.4 Esterification Reaction Procedure……...109
5.2.5 Chemical Analysis……...110
5.2.6 Determination of the kinetics of the esterification reaction…….....111

5.3 Results and Discussion……..113

5.3.1 Catalyst Characterization ……...113
5.3.2 Optimized Reaction Conditions of Transesterification…...121
5.3.2.1 Effect of Catalyst Loading……..121
5.3.2.2 Effect of Methanol to WFO ratio on Transesterification……...122
5.3.2.3 Effect of Reaction Temperature on Transesterification……...124
5.3.2.4 Effect of Reaction Time on Transesterification…..126
5.3.3 Mass transfer evaluation of the synthesized catalysts on the esterification reaction……129

5.4 Conclusion……134

6. CATALYTIC STUDY ON THE ESTERIFICATION OF LINOLEIC ACID USING HZSM-5 ZEOLITES WITH DIFFERENT SI/AL RATIOS 136

6.1 Introduction……...136

6.2 Experimental section……138

6.2.1 Catalysts Synthesis……..138
6.2.2 Catalysts Characterization……...140
6.2.3 Esterification Reaction Procedure……...141

6.2.4 Method of Analysis……142
6.2.5 Determination of the kinetics of the esterification reaction……..143

6.3 Results and Discussion……..144

6.3.1 Catalyst Characterization……144
6.3.2 Optimized Reaction Conditions of Esterification……...148
6.3.2.1 Effect of Reaction Temperature on Esterification..148
6.3.2.2 Effect of Methanol to Linoleic Acid Ratio on Esterification……...150
6.3.2.3 Effect of External Mass Transfer Limitation……..153
6.3.2.4 Effect of Reaction Time on Esterification……..156
6.3.3 Effect of Si/Al Ratio on Esterification……157

6.4 Conclusion……159

7. CONCLUSION 160

7.1 Important conclusions……..160

7.1.1 With respect to the economic viability of homogeneous transesterification from WFOs in Lebanon……..160
7.1.2 With respect to the application of hierarchical heterogeneous zeolites for biodiesel production……..161
7.1.3 With respect to the effect of acidic and hydrophobic characters on the catalytic performance of zeolites with different Si/Al ratios.161

7.2 Future Work……..162

7.2.1 Shape selective effect of channels and cages of different hierarchical zeolites for biodiesel production……...162
7.2.2 Factors affecting biodiesel yield variation between linoleic acid esterification and WFOs transesterification……..…163
7.2.3 Quantification of enhanced acid site accessibility in hierarchical zeolites……...164

BIBLIOGRAPHY 165

Appendix

1. TABLES AND FIGURES……. 191

ILLUSTRATIONS

Figure 1. General transesterification reaction equation (Dias et al., 2008) 10

Figure 2. The framework structure of ZSM-5 (Cerius2, 1997) 13

Figure 3. Questionnaire data per typical working week 54

Figure 4. WFOs acquisition cost per 20 L WFOs..... 60

Figure 5. Total biodiesel cost..... 65

Figure 6. Variation of diesel oil cost in Lebanon 67

Figure 7. (a) Wide angle XRD patterns of calcined MC-ZSM-5, NC-ZSM-5, NSh-ZSM-5, and NS-ZSM-5, (b) Wide angle XRD patterns of exchanged and calcined MC-HZSM-5, NC-HZSM-5, NSh-HZSM-5, and NS-HZSM-5, (c) Low angle patterns of non-calcined NSh-ZSM-5, and NS-ZSM-5, (d) Low angle patterns of calcined NSh-ZSM-5, and NS-ZSM-5 85

Figure 8. Scanning electronic microscopy (SEM) images of (a) MC-HZSM-5, (b) NC-HZSM-5, (c) NSh-HZSM-5, and (d) NS-HZSM-5. 86

Figure 9. Transmittance electronic microscopy (TEM) images of (a) NSh-HZSM-5, and (b) NS-HZSM-5 87

Figure 10. N2 adsorption/desorption isotherms at −196 °C of the calcined MC-HZSM-5, NC-HZSM-5, NSh-HZSM-5 and NS-HZSM-5 samples. Full bullets represent adsorption isotherms and empty bullets, the desorption ones. 89

Figure 11 .Mesopore size distribution of the calcined exchanged hierarchical samples NSh-HZSM-5 and NS-HZSM-5 89

Figure 12. Effect of reaction temperature variation on the esterification of linoleic acid using MC-HZSM-5, NC-HZSM-5, NSh-HZSM-5, NS-HZSM-5 catalysts at methanol to linoleic acid molar ratio of 12:1, catalyst loading of 10 wt%, stirring rate of 550 rpm, and reaction time of 6 h 92

Figure 13.Effect of methanol to linoleic acid molar ration variation on the esterification of linoleic acid using MC-HZSM-5, NC-HZSM-5, NSh-HZSM-5, NS-HZSM-5 catalysts at catalyst loading of 10 wt%, reaction temperature of 180 °C, stirring rate of 550 rpm and reaction time of 6 h 94

Figure 14. Effect of reaction time on the esterification of linoleic acid using NSh-HZSM-5 catalyst at catalyst loading of 10 wt%, methanol to linoleic molar ratio of 6:1, reaction temperature of 180 °C, and stirring rate of 550 rpm..... 95

Figure 15. -ln(1-X_ML) versus reaction time plot at optimal reaction conditions using NSh-HZSM-5 96

Figure 16. XRD diffractograms of (a) calcined MC-ZSM-5 and MC-HZSM-5 at wide angle patterns, (b) calcined NC-ZSM-5 and NC-HZSM-5 at wide angle patterns, (c) calcined NSh-ZSM-5 and NSh-HZSM-5 at low and wide-angle patterns, (c) calcined NS-ZSM-5 and NS-HZSM-5 at low and wide-angle patterns 115

Figure 17. Scanning electronic microscopy (SEM) images of (a) MC-HZSM-5, (b) NC-HZSM-5, (c) NSh-HZSM-5, and (d) NS-HZSM-5. NS look beautiful in this picture 116

Figure 18. Transmission electronic microscopy (TEM) images of (a) NSh-HZSM-5, and (b) NS-HZSM-5. 117

Figure 19. (a)Adsorption/desorption isotherms of nitrogen on the calcined MC-HZSM-5, NC-HZSM-5, NSh-HZSM-5 and NS-HZSM-5 samples, at −196 °C, (b) Mesopore size distribution of the calcined exchanged hierarchical samples. 118

Figure 20. Effect of MC-HZSM-5, NC-HZSM-5, NSh-HZSM-5, and NS-HZSM-5 catalysts loading on the transesterification of WFO at the molar ratio of methanol to WFO of 12:1, reaction temperature of 140°C, stirring rate of 550 rpm, and reaction time of 6 h 122

Figure 21. Effect of methanol to WFO molar ration variation on the transesterification of WFO using MC-HZSM-5, NC-HZSM-5, NSh-HZSM-5, and NS-HZSM-5 catalysts, at catalyst loading of 10 wt%, reaction temperature of 140 °C, stirring rate of 550 rpm and reaction time of 6 h 124

Figure 22. Effect of reaction temperature variation on the transesterification of WFO using NSh-HZSM-5 catalyst at catalyst loading of 10 wt%, methanol to WFO molar ratio of 12:1, stirring rate of 550 rpm and reaction time of 6 h. 125

Figure 23. Effect of reaction time on the transesterification of WFO using NSh-HZSM-5 catalyst at catalyst loading of 10 wt%, methanol to WFOs molar ratio of 12:1, reaction temperature of 180 °C, and stirring rate of 550 rpm..... 126

Figure 24.-ln(1-X_FAMEs) versus reaction time plot at optimal reaction conditions using NSh-HZSM-5 128

Figure 25. Wide angle XRD patterns of exchanged and calcined HZSM-5 (45), HZSM-5 (25), and HZSM-5 (11.5)..... 145

Figure 26. Scanning electronic microscopy (SEM) images of (a) HZSM-5 (45), (b) HZSM-5 (25), and (c) HZSM-5 (11.5) 146

Figure 27. N_2 adsorption/desorption isotherms at −196 °C of the calcined HZSM-5 (45), HZSM-5 (25), and HZSM-5 (11.5) samples. Full bullets represent adsorption isotherms and empty bullets, the desorption ones. 147

Figure 28. Effect of reaction temperature variation on the esterification of linoleic acid using HZSM-5 (45), HZSM-5 (25), and HZSM-5 (11.5) catalysts at the molar ratio of methanol to linoleic acid molar ratio of 12:1, catalyst loading of 10 wt%, stirring rate of 550 rpm, and reaction time of 6 h 150

Figure 29. Effect of methanol to linoleic acid molar ration variation on the esterification of linoleic acid using HZSM-5 (45), HZSM-5 (25), and HZSM-5 (11.5) catalysts at catalyst loading of 10 wt%, reaction temperature of 180 °C, stirring rate of 550 rpm and reaction time of 6 h 152

Figure 30. $-ln1 - XML$ versus reaction time plot at optimal reaction conditions using HZSM-5 with different Si/Al ratios 154

Figure 31. Effect of reaction time on the esterification of linoleic acid using HZSM-5 (45), HZSM-5 (25), and HZSM-5 (11.5) catalysts at catalyst loading of 10 wt%, methanol to linoleic molar ratio of 6:1, reaction temperature of 180 °C, and stirring rate of 550 rpm 157

TABLES

Table 1. Physical and chemical properties of the biodiesel produced from WFOs……. 51

Table 2. Determination of vehicle capacity based on the suggested collection scenarios…56

Table 3. Total logistics cost per year for the different scenarios generated……. 57

Table 4.Total fixed and varied costs for biodiesel production from WFOsTable 4: total fixed and varied costs for biodiesel production from WFOs……. 63

Table 5. Influence of input parameter variation on Biodiesel cost……... 65

Table 6. Total energy use for biodiesel production…….. 70

Table 7. Textural properties by N2 sorption and acidity of the morphologically different HZSM-5 zeolites…… 90

Table 8. Thiele modulus variables data for linoleic acid esterification using MC-HZSM-5, NC-HZSM-5, NSh-HZSM-5 and NS-HZSM-5……. 99

Table 9. Textural properties by N2 sorption of the morphologically different HZSM-5 zeolites……..119

Table 10. Brønsted and Lewis acidity of the morphologically different HZSM-5 catalysts…….120

Table 11. Thiele modulus variables data for triglycerides transesterification using MC-HZSM-5, NC-HZSM-5, NSh-HZSM-5 and NS-HZSM-5……... 131

Table 12. BET surface area, porous volume and acidity of the H-ZSM5 catalysts with different Si/Al ratios……. 148

CHAPTER 1

INTRODUCTION

1.1 Biodiesel Production Using Zeolites: General Introduction

Biodiesel is an alternative fuel to the depletable petroleum diesel (Demirbas, 2005). Biodiesel from non-edible or waste renewable resources is most attractive as it reduces biodiesel production cost and greenhouse gas emissions in comparison with its production from crude vegetable oils. Also, it has the advantage of being biodegradable and nontoxic (Baskar and Aiswarya 2016; Živković et al. 2017). Various technologies and catalysts can be used for the production of biodiesel. Conventionally, biodiesel is produced using homogeneous mineral acid or alkali catalysts depending on the free fatty acid (FFA) content of the oil feedstock. However, one of the major disadvantages of homogeneous catalysts is that they cannot be regenerated unless more equipment is available for their separation, which results in higher production costs (Lourinho and Brito 2015; Tan et al., 2015). In addition, a large amount of wastewater is produced in the biodiesel purification step, which makes the process not environmentally friendly (Veljković et al., 2015).

The use of solid heterogeneous catalysts is an appropriate solution to overcome the issues associated with homogeneous catalysts (Salamatinia et al. 2013). Basic solids like CaO and MgO supported on alumina (El-Gendy et al., 2014), and acid heterogeneous catalysts such as sulfated zirconia (Thiruvengadaravi et al. 2012) have been used in biodiesel production from oils. Nonetheless, one of the major problems related to heterogeneous catalysts is the formation of three phases with the alcohol and the oil, which leads to diffusion limitations, lowering thus the rate of the reaction (Zabeti et al., 2009).

Catalysts with higher surface area are needed to overcome diffusion limitations and low catalytic activity.

Zeolites are microporous crystalline metallosilicates which possess molecular sieve and shape selective properties. They have found widespread applications in catalytic reactions, such as the transesterification of oils, due to their high surface area, and their controllable acidity, basicity, and hydrophobicity (Leclercq et al., 2001; Macario et al. 2010; Wang and Chen 2016). However, although the presence of ordered micropores in zeolitic materials enhances their acidity, their sole presence seems to impose intercrystalline diffusion limitations, contributing to the low usage of the zeolite active volume by hindering molecules' mass transfer (Taguchi and Schüth 2005; Tao et al. 2013). These properties set limitations for their use in the conversion of big molecules as the latter can't access acidic active sites within the pores of the zeolites rendering their catalytic performance during the transesterification reaction low (Kiss et al., 2006). In order to overcome this diffusion limitation, recent interest has emerged in synthesizing more accessible zeolitic catalysts (Sun et al., 2015). Two approaches including shortening micropores diffusion path length and introducing an additional (meso)porosity within the microporous zeolite crystal were adopted in this study to improve accessibility of molecules to the active sites confined in zeolites and enhance biodiesel production yield.

1.2 Thesis Objectives

In the present study, strategies leading to improved accessibility of the active sites confined within ZSM-5 zeolites framework for biodiesel production are proposed and applied. The main objective is to develop hierarchical acidic ZSM-5 zeolites for better

catalytic performance in biodiesel production by shortening the micropore diffusion path and by introducing an additional (meso)porosity within the microporous zeolite crystal. A second objective is to compare hierarchical zeolites to conventional ones in terms of their catalytic activity, hydrophobicity and selectivity. A third objective is to deliver a way to better understand the behavior of the catalysts produced under different transesterification conditions leading to optimal production that will subsequently enhance biodiesel yield and purity for commercially viable applications. A fourth objective is to assess the economic viability of the use of waste frying oils for biodiesel production in Lebanon using conventional one-step basic transesterification reactions.

1.3 Thesis Significance

Produced from post-consumer waste product, biodiesel derived from WFOs constitutes a green liquid fuel of dual environmental and economic value. Besides reducing the economy's dependency on limited resources and imports of petroleum-based diesel, WFOs-based biodiesel also helps reducing the amount of waste oil dumped into landfills and sewers. This ultimately contributes in mitigating a major environmental problem in Lebanon associated with the uncontrolled disposal of the waste oils. Furthermore, the use of biodiesel as alternative fuel to petroleum diesel significantly reduces the emission of harmful air pollutants improving air quality in Lebanon. In fact, a recent report on the first look on economic costs to Lebanon from Climate change was developed by the MoE (2015) and estimated the total costs might equal USD 1,900 million in 2020, rising to USD 138,900 million in 2080.

Considering that the water and FFA content have a negative influence on the homogeneous transesterification reaction, many heterogeneous catalysis transesterification using microporous zeolite have been assessed both qualitatively and technically. This study suggests using mesoporosity within zeolite framework to lower diffusion limitations and optimize the transesterification process. This study does not only provide a way to eliminate the drawbacks of homogeneous and zeolites nanocrystals' catalysis, but it also delivers a way to better understand the behavior of the catalyst under different transesterification conditions leading to optimal production that will subsequently enhance biodiesel yield and purity for commercially viable applications.

1.4 Thesis Organization

This thesis is paper-based and organized as follows:

In *Chapter 2*, a comprehensive overview of biodiesel production using different catalysts, focusing on the potential benefits and challenges of heterogeneous zeolitic catalysis are presented.

In *Chapter 3*, economic viability of the use of waste frying oils for biodiesel production in Lebanon using conventional one-step basic transesterification reactions is evaluated.

In *Chapter 4*, the influence of crystal morphology (conventional coffin-shaped microcrystals, nanocrystals, nanosheets, and nanosponges) on the catalytic properties of ZSM-5 zeolites in the esterification of linoleic acid as a model reaction for biodiesel production is investigated.

In *Chapter 5,* a comparison between the catalytic activity of conventional ZSM-5 conventional coffin-shaped microcrystals and nanocrystals, and hierarchical ZSM-5 nanosheets, and nanosponges, in the transesterification of waste frying oils is studied.

In *Chapter 6*, the correlation between surface hydrophobicity and acidity of ZSM-5 zeolites with different Si/Al ratios and their catalytic performance in linoleic esterification is assessed.

Chapter 7 summarizes the important conclusions and discusses future work.

CHAPTER 2

BIODIESEL PRODUCTION USING ZEOLITE CATALYSTS– REVIEW

In this chapter, benefits and challenges in various transesterification paths used for the production of biodiesel are discussed. Information regarding chemical and physical characteristics of oil feedstock to help determine the proper and most efficient catalytic method for biodiesel production are presented. Various catalysts used in biodiesel production are investigated focusing on zeolitic catalysts. Influence of transesterification reaction conditions using zeolitic catalysts such as, temperature, alcohol to oil ratio, catalyst loading, and reaction time are debated. And finally, zeolites production and characterization for catalytic activities in biodiesel production are explained.

2.1 Sources of Biodiesel Feedstock

Feedstock selection is a crucial step in biodiesel production, which affects yield, composition, purity and cost of the produced biodiesel (Gude et al., 2013; Mahdavi et al., 2015). Biodiesel is classified based of the source of the raw material used for its production; edible oil seeds, non-edible oil crops, waste oils, algae and genetically engineered oil crops.

The nature and availability of edible oil seeds depends on the geographical condition of the region (Singh & Singh, 2010). Biodiesel produced from oil seeds such as soybean, rapeseed and palm oil seeds seem to be economically sustainable in countries rich in fertile lands and accessible water resources (Panichelli et al., 2009). However, due to land use change, food crop cultivation will be reduced at the expense of edible food crops

used for biodiesel production and consequently, become high priced and unavailable for all classes of populations (Harvey and Pilgrim 2011).

Taking the above reasons into consideration, attention has turned to non-edible oils, such as non-edible energy crops and waste frying oils (WFOs), as feedstock sources for the production of biodiesel (Chakraborty & Das, 2012; Phan & Phan, 2008; Nik et al., 2012). There are two types of WFOs: brown and yellow grease. Brown grease has a high water and FFAs content (> 15%), while yellow grease contains lower FFAs content (< 15%) and can be used as a low cost raw material for biodiesel production (Adewale et al., 2015). The amount of yellow grease WFOs could be significant since over 80% of the vegetable oils are used in different food applications (Rosillo-Calle et al., 2009). Therefore, aside from the low cost of biodiesel production from WFOs, the use of waste raw materials doesn't compete with either land use, water or food supply (Akia et al., 2014). Biodiesel production from microalgae was assessed in different studies (Beetul et al., 2014; Talebi et al., 2015). Nonetheless, the cost of biodiesel produced does not compete with the cost of diesel fuel (Chisti 2013). Therefore, biodiesel produced from WFOs feedstock is the most viable economically and sustainable environmentally to be used as an alternative to petroleum diesel.

WFOs are characterized by their chemical and physical properties. They are waste of edible vegetable oils and their chemical and physical characteristics are different from those of vegetable oils as a result of the changes that occur during the frying process (Cvengroš and Cvengrošová 2004). They consist mostly of triglycerides and FFAs that vary in their carbon chain length and in the number of double bonds (Orsavova et al., 2015). Vegetable oils along with their chemical and physical properties are listed in APPENDIX

A: Table A. The chemical composition of vegetable oils dictates their viscosity which is around 14 times higher than that of petroleum diesel (Goering et al., 1982). The higher density and viscosity of fresh or waste vegetable oils restrict their direct use in diesel engines as they affect combustion phenomenon, carbon deposition, and plugging of fuel lines (Lam et al., 2010; Meher et al., 2006; Murugesan et al., 2009). To overcome the problems of direct feedstock use in engines, modifications are crucial to bring the combustion-related properties of vegetable oils closer to those of petroleum diesel. Modification methods include reactive distillation (de Lima da Silva et al., 2010), dual reactive distillation (Dimian et al., 2009), reaction absorption (Kiss et al., 2011), membrane reactor (Sdrula 2010), ultrasonic process (Van Manh et al., 2011), microwave heat (Motasemi and Ani 2012), and transesterification (Chung et al., 2008; Narkhede & Patel, 2014). Among the different methods available for the production of clean burning mono-alkyl ester based oxygenated fuel from vegetable oils feedstock, transesterification is the leading process (Meher et al. 2006). The resulting product called biodiesel holds comparable characteristics to petroleum diesel (Agarwal 2007).

2.2 Biodiesel

The American Society for Testing and Materials (ASTM) has defined biodiesel as a fatty acid (m)ethyl ester (FAME) (Demirbas, 2009). In contrast with petroleum diesel, biodiesel derives from biological sources thus the term ‘‘bio’’ (van Kasteren and Nisworo 2007). Since biodiesel is produced from virgin or waste oils, it is renewable, biodegradable and non-toxic and hence, superior to petroleum-based diesel (Aghbashlo & Demirbas, 2016; Hosseinpour et al., 2016; Knothe et al., 2006). APPENDIX B: Table B compares the

characteristics of biodiesel from WFOs and commercial diesel fuel. Besides better lubricity, flash point and ignition properties (Yusuf et al., 2011), biodiesel also emits 20%, 30%, and 50% less HC, CO, and smoke, respectively compared with diesel fuel (Shamshirband et al., 2016). However, it is worth mentioning that biodiesel faces storage stability problems, few operating disadvantages related to engine performance, and emits more NOx exhaust than petroleum diesel fuel (Datta and Mandal 2016; Knothe and Steidley 2009). Biodiesel could be blended with petroleum diesel in different proportions without the need for any engine modifications, as the mixture creates a stable fuel (Silitonga et al. 2011).

Various analytical methods exist for the qualitative and quantitative characterization of biodiesel (Baskar & Aiswarya, 2016; Felizardo et al., 2006; Knothe, 2001; Halim et al., 2009; Lertsathapornsuk et al., 2008; Tan et al., 2011), among which, gas chromatography in combination with a flame ionization detector (GC-FID) is mostly employed (Suppes et al., 2004; Wang & Chen, 2016). This analytical technique allows the detection of FAME peaks in the sample. The latter is compared with pure standards to determine the weight of the biodiesel produced, depending on the distribution area of each component (Elkady et al., 2015). FAMEs yield of the transesterification reaction is calculated based on the following equation (2-1):

$$\%\,Biodiesel\ yield = \frac{Total\ weight\ of\ FAMEs}{Total\ weight\ of\ oil\ in\ the\ sample} \times 100 \qquad 2\text{-}1$$

2.3 Transesterification

The transesterification reaction is the most common method used for the conversion of triglycerides from oil-based feedstock into biodiesel. In this process, the chemical

reaction occurs between triglycerides and a short chain alcohol. Many different alcohols can be used in this reaction, including, methanol, ethanol, propanol, and butanol. Methanol application is the most feasible owing to its low-cost and its physical and chemical characteristics, such as having the shortest chain and being polar (Ma and Hanna 1999). The transesterification reaction is a reversible reaction. To shift the equilibrium to the product side, excess alcohol is needed (Chisti 2007). Stoichiometrically, a 3:1 molar ratio of alcohol to triglycerides is required. However, in practice, the ratio must be higher to achieve a maximum ester yield. Fig. 1 shows the general equation of transesterification reaction whereby, triglycerides are converted to diglycerides, diglycerides are converted to monoglycerides, and finally monoglycerides to glycerol. Each step produces one ester molecule and, consequently, the reaction generates three ester molecules from one triglyceride molecule (Sharma and Singh 2008).

$$Triglyceride + ROH \leftrightarrow Diglyceride + R'COOR$$
$$Diglyceride + ROH \leftrightarrow Monoglyceride + R'COOR$$
$$Monoglyceride + ROH \leftrightarrow Glycerol + R'COOR$$

Figure 1. General transesterification reaction equation (Dias et al., 2008)

Various methods exist for biodiesel production from oils, consisting of non-catalytic and catalytic transesterifications. In order to produce high yields, non-catalytic transesterification occurs in the absence of a catalyst at very high pressures and at supercritical temperatures (220-260 ºC) wherein methanol would not only act as a solvent but also as an acid catalyst (Warabi et al., 2004). The use of supercritical alcohol for the

transesterification of vegetable oil is well described in different studies (Balat, 2008; Demirbas, 2006; Kusdiana & Saka, 2004). The presence of a catalyst improves the reaction rate and yield at mild reaction conditions and subsequently catalytic transesterifications are the most used reactions in the production of biodiesel. Different types of catalysts can be used in the transesterification reaction of oils including alkaline and acidic homogeneous and heterogeneous catalysts, and enzymatic catalysts. Depending on the undesirable compounds present in the oils (especially FFA and water), each catalyst has its advantages and disadvantages.

In an alkali-catalyzed transesterification reaction, the base reacts with the alcohol to form alkoxide and protonated catalyst. The nucleophilic alkoxide attacks the carbonyl atom of the triglyceride molecule to form a tetrahedral intermediate which will react with the alcohol to recover the anion. The tetrahedral intermediate is subjected to structural reorganization to form an ester molecule and a diglyceride. The same process is repeated for the diglyceride and monoglyceride (Singh & Singh, 2010).

In an acid-catalyzed reaction, the catalyst is a proton donor and the carbonyl group of the triglyceride is protonated resulting in carbocation. The positively charged compound is then subjected to a nucleophilic attack by the alcohol to produce an unstable tetrahedral intermediate. The glycerol is then removed, the ester is formed, and the catalyst is recovered (Schuchardt et al., 1998).

For both homogeneous and heterogeneous catalysis, though the alkaline transesterification has few advantages, the alkaline catalyst is not efficient for the conversion of oils containing high free fatty acid, the process being highly sensitive to water and FFA content in the feedstock. High water content causes the reaction to partially

change to saponification. Soap formation occurs by the hydrolysis of triglycerides in the presence of water leading to the formation of FFAs, which, in turn react with the alkaline catalyst to form soaps. Saponification pathway creates many problems in downstream purification and FAMEs recovery and causes reductions in the ester yield (Basu and Norris, 1996). The use of acid catalysts was thus proposed due to the insensitive nature they possess to free fatty acid content (Freedman et al., 1984). However acid catalyzed reactions are not recommended due to their comparatively slower reaction rate among other drawbacks. Another approach is to produce biodiesel from waste oils with high FFAs value combining both homogeneous acid esterification as a pre-treatment step followed by the homogeneous alkaline transesterification step (Yong Wang et al., 2007). However, this two-step transesterification is rather costly.

The use of solid heterogeneous catalysts is an appropriate solution to overcome the issues associated with homogeneous catalysts (Salamatinia et al., 2013). However, diffusion limitation of reactants or products from catalysts surface to their interior is a major problem related to heterogeneous catalysts. Catalysts possessing higher surface area such as zeolite are needed to overcome diffusion limitations and low catalytic activity. APPENDIX C: Table C summarizes the advantages and disadvantages of different catalyzed transesterification reactions of oil-based feedstocks, and APPENDIX C: Figure C presents a general scheme of biodiesel production from oils.

2.4 Zeolites

Zeolites are crystalline aluminosilicates of an extending mono, di and tri-dimensional, connected framework involving AlO_4 and SiO_4 tetrahedra sharing one oxygen

atom. The resulting structure is highly porous and contains channels and interconnected voids of molecular dimensions (2).

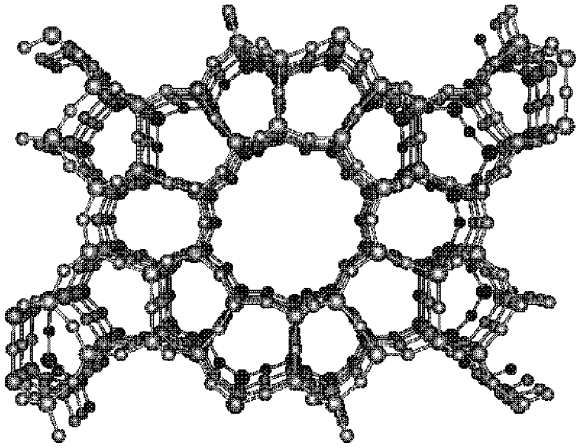

Figure 2. The framework structure of ZSM-5 (Cerius2, 1997)

Each AlO_4 tetrahedron has a net negative charge which is balanced by an extra-framework cation within the structure to keep the overall framework neutral (Auerbach et al., 2003). The most commonly used compensating cation is the inorganic cation Na^+. The important role played by both synthetic and natural zeolites as catalysts originates from their molecular sieve properties, their role as adsorbents, and their ion-exchange properties (Derouane et al. 2013). In particular, ion-exchange enables the generation of both base and acid active sites on the zeolite, indispensable for catalytic activities. Basicity and acidity can be introduced by a variety of ways among which ion exchange of a metal ion with the compensating cation (Na^+) (Hammett & Louis, 1932); and the impregnation of ion metals on the surface of zeolites (Benesi 1956). In both methods, the desired metal ion-containing liquid encounters the solid zeolite, and as a result, the suitable ion from the liquid is exchanged with the compensating ion or deposited on the surface of the solid. For instance, zeolites that have been modified by the decomposition of an impregnated alkali metal salt (KOH or NaOH) to active alkali-metal oxides have arisen as interesting solid bases capable

of catalyzing reactions that require a base site such as transesterification of low acid value oils (Al-Jammal et al., 2016; Takase et al., 2018). The base strength of the impregnated alkali ion increases with increasing electropositivity of the exchange cation.

H-type zeolites are prepared from Na-type zeolites by following the ion exchange procedure to produce acid zeolitic catalysts. The Na-type zeolite is added to a NH_4Cl solution at a specific mass ratio, and the mixture is stirred at around 80 °C for a limited duration. Then, the samples are washed with ultrapure water, filtered and dried at 100 °C, and finally calcined at around 550 °C (Alismaeel et al., 2018; Sun et al., 2015; Volli & Purkait, 2015).

Acidity has been introduced in the zeolites' framework to give rise to highly efficient solid acid catalysts. When the exchanged cation is a proton, it binds itself to one of the bridged oxygens directly connected to Al, forming a hydroxyl group. A zeolite can then be a proton donor and thus act as a Brønsted acid in reactions that require strong active acid sites such as the transesterification of high acid value oils (Doyle et al., 2017). However, in addition to Brønsted acid sites, zeolites can possess Lewis acid sites generated by dehydration of zeolite structures at calcination temperatures leading to the dehydroxylation of the Brønsted sites (Bolton, 1970). The relative abundance of both acidities determines the acid strength of the catalyst.

The properties of the exchanged zeolites can be adapted by adjusting synthesis parameters such as metal ions concentration and calcination temperature (Akia et al. 2014). A KOH/zeolite catalyst for biodiesel production was prepared by impregnation. KOH amounts were varied and assessed for the best catalyst performance during biodiesel production reactions. Increasing KOH loading from 20 wt% to 35 wt% improved FAMEs

yield, which is associated with increased concentration of K_2O active sites in the catalyst (Rezayan and Taghizadeh 2018). However, higher loading of KOH reduced FAMEs yield due to blockage of the pores by the agglomeration of KOH which decreased the surface area of the catalyst and hence the catalyst activity (Al-Jammal, Al-Hamamre, and Alnaief 2016). The effects of different Sr/ZSM-5, Ba–Sr/ZSM-5 mass ratios and calcination conditions on the catalytic activity were investigated by Feyzi and Khajavi (2014). The best calcination conditions were found to be at temperatures of 600 °C for 6 h and a mass ratio of 6Ba − 4Sr/ZSM-5 exhibited the best catalytic performance. These studies show that zeolites are superior to other heterogeneous catalysts by having controllable acidity and basicity. In addition to the chemical advantage that modified zeolites exhibit, zeolites have other properties that make them good catalysts for heterogeneous catalysis. They carry high thermal stability, large surface area, well defined pore structures with channels and cavities of specific molecular dimensions, and shape selectivity (Hammett & Louis, 1932). However, zeolites have usually been synthesized with crystal sizes in the micrometer range and, therefore, hold negligible external surface area. These properties set limitations for their use in the conversion of big molecules as the latter can't access active sites within the pores of the zeolites rendering their catalytic activity low (Kiss et al., 2006). In order to overcome this diffusion limitation, interest has emerged in synthesizing more accessible zeolitic catalysts. Okuhara et al., (2002) adjusted the pore size and structure of zeolite by varying the Si/Al ratio. Higher Si/Al ratio resulted in zeolite with larger-pore size but with weaker acidic strength (Okuhara 2002). Nanocrystalline hierarchical zeolites containing two types of porosity (micro- and mesopores) and high external surface area were more recently assessed for reactions involving large molecules like fatty acids and triglycerides

(Carrero et al., 2011; Sun et al., 2015). Additional advantages that the use of heterogeneous zeolites in catalytic processes such as the transesterification of oils provide, include the ease of separation from the liquid products, regenerability, and the reduction of toxicity, corrosion and environmental pollution (Gaurav et al., 2016; Zhang et al., 2015).

2.5 Non-Zeolitic Catalyzed Transesterifications

2.5.1 Transesterification by Homogeneous Catalysts

The homogeneously catalyzed transesterification of oil-based feedstocks is commonly performed in a one-step alkali process using base catalysts. The most common alkaline catalysts used in the transesterification of oils are alkali hydroxides such as potassium hydroxide (KOH), sodium hydroxide (NaOH), and alkoxides such as potassium methoxide (CH_3KO), sodium methoxide (CH_3NaO), and sodium ethoxide (C_2H_5ONa) (Lam et al., 2010; Narasimharao et al., 2007; Atadashi et al., 2013; Talha and Sulaiman, 2016). Khan and Dessouky studied the transesterification of vegetable corn oil using NaOH as a catalyst. A yield of 95% was achieved after 15 min upon increasing both the NaOH amount and the methanol to oil molar ratio to 0.5% and 6:1, respectively. An insignificant variation of the ester yield was observed in the range of 50-65 °C. (Khan et al., 2009). Keera et al. studied biodiesel production from castor oil by homogenous KOH transesterification. A conversion of 95 % was achieved at 1 wt% KOH, 60 °C, 9:1 methanol to oil ratio, and 30 min reaction time. Transesterification at temperature 30 °C gave a yield comparable with that obtained at 60 °C (Keera et al., 2018). Vicente et al. (2004) suggested adopting basic methoxide catalysts which lack the OH group necessary for saponification and near 100 wt.% biodiesel yields were obtained (Vicente et al., 2004). El Boulifi et al.

demonstrated a better catalytic activity of sodium methoxide as compared to NaOH during the transesterification of corn oil with an alcohol at 60 °C, with triglycerides' conversion of 90% (El Boulifi et al., 2010).

However, as discussed above, homogeneous base catalyst (KOH and NaOH) are effective for transesterification of oil having FFA content less than 2% (Nomanbhay & Ong, 2017). Therefore, many studies assessed one-step acid transesterification reactions of oils using strong acids which are insensitive to FFA content. Al-Widyan and Al-Shyoukh compared the catalytic performance of H_2SO_4 and HCl in the presence of ethanol for the transesterification of a high acid value WFOs. H_2SO_4 performed better than HCl at 2.25 M loading with 100% excess ethanol reducing the specific gravity of biodiesel (at 15/15 °C) from an initial value of 0.916 to a final value of 0.8737 after 3 h (Al-Widyan and Al-Shyoukh 2002).

However, high yields cannot be achieved at mild reaction conditions when adopting single step-acid transesterification reactions (Freedman et al., 1984). A few researchers proposed an alternative approach to produce biodiesel from waste oils with high FFAs value combining both acid esterification as a pre-treatment step followed by the alkaline transesterification step (Thanh et al., 2010; Van Gerpen & Knothe, 2005; Yong Wang et al., 2007). The purpose of including a pre-treatment acidic step is to reduce the excess FFA concentration in the original oil feedstock and minimize the chances of soap formation in the alkaline transesterification step (Jahirul et al., 2014; Ong et al., 2011; Hwai Chyuan Ong et al., 2014). The pre-treatment step is then followed by the alkaline transesterification step. However, the acid pretreatment step which reduces FFA concentration, also leads to the formation of water to which second-step alkaline transesterification process is sensitive.

The presence of water in the oil induces the formation of FFA by hydrolysis of triglycerides which facilitates the saponification reaction to occur (Atadashi et al., 2012).

For the different homogeneous transesterifications discussed, biodiesel is separated by gravity, to recover pure biodiesel from process byproducts (glycerol and alcohol). After it is separated from the glycerol layer, biodiesel is purified to remove impurities which include alcohol, catalyst, entrained glycerol and soap by excess methanol recovery (Issariyakul et al., 2007; Lapuerta et al., 2008) and a washing step (Predojević 2008). Biodiesel is then dried by either heating or the use of chemicals (Encinar et al., 2007; Murugesan et al., 2009).

2.5.2 Transesterification by Heterogeneous Catalysts

In contrast to the homogeneous catalysts which are hard to recover and which made the homogeneous transesterification process less competitive and uneconomic in terms of purification cost and wastewater produced, heterogeneous catalysts have the advantages of being non-corrosive, easily separable for reuse (Lee and Saka 2010), and environmental friendly requiring no washing step of the product and thus producing less waste (Saravanan et al., 2015).

2.5.2.1 Alkali-Heterogeneous Transesterification

Heterogeneous base catalysts include neat base catalysts (MgO, ZnO, CaO, $ZnAl_2O_4$ and solid KOH) (Chavarria-Hernandez et al., 2017; Chisti, 2013; Hajjari et al., 2017), loaded base catalysts such as oxides of alkali-doped metal oxides (CaO/ Al_2O_3,

Li/CaO, Na/SiO_2, CaO/SiO_2), alkali metal oxides (Na/NaOH/γ-Al_2O_3 reinforced on Al_2O_3 (Kligerman and Bouwer 2015), supported base nanocatalysts (KF/CaO, KF/CaO-MgO), and magnetic base catalysts (KF/$AlFe_3O_4$) (Tang et al., 2011), which researchers have used for transesterification reaction of biodiesel production. Hetafi et al. used MgO and ZnO base catalysts for biodiesel production and reported higher ester yield with MgO as compared to ZnO, which was ascribed to the higher effective reaction surface of the smaller MgO particles (Hatefi et al., 2014). CaO from snail shells was used in WFOs transesterification and achieved an ester yield higher than 96% within 1 h (El-Gendy, Deriase, and Hamdy 2014). $ZnAl_2O_4$ achieved low conversion (22% - 33%) in corn oil transesterification with methanol and ethanol at 150 °C and 200 °C, due to potential mass transfer limitations (Velázquez 2007). Sun et al. studied the transesterification of corn oil using solid KOH as a catalyst. The maximum yield of FAMEs (90.9 wt.%) was achieved for an alcohol to oil molar ratio of 9:1, 16.3 wt.% solid KOH, and a reaction time of 9 h (Sun et al., 2014). Meher et al. used Li, Na; and K- doped calcium oxides for the production of biodiesel from WFOs. Li/CaO was more effective than K/CaO and Na/CaO, and yielded 94.9% FAMEs in 8 h using 2 wt.% Li/CaO with 12:1 methanol to oil molar ratio at 65 °C (Meher et al. 2006). Akbar et al. used Na/SiO_2 catalyst (6 wt%) in the sol–gel method to obtain an optimum conversion of 99% of oil for a relatively short reaction time of 45 min at 65 °C, with a 1:15 methanol to oil molar ratio (Akbar et al., 2009). Moradi et al. used 70% CaO/SiO_2 and 40% CaO/γ-Al_2O_3 catalysts and obtained oil conversions of 85.6% and 79.1% after 8 and 5 h, respectively. Leached CaO by methanol was detected upon reuse of the impregnated catalysts (Moradi et al., 2014; Moradi et al., 2015). Hashmi et al. studied biodiesel synthesis from Jatropha curcas oil using CaO-Al_2O_3 nanocatalyst with a particle

size of 29.9 nm. They reported 82.3% conversion of the oil at 8:1 methanol to oil ratio and a reaction time of 3 h at 100 °C (Hashmi et al., 2016). KF/ CaO nanocatalysts of 30–100 nm particle size, prepared using the impregnation method, were used in the transesterification of stillingia oil to biodiesel. A yield of 96% was obtained after 2.5 h at 65 °C, with an oil to methanol ratio of 1:12 and 4 wt.% of catalyst (Wen et al., 2010). Yun Wang et al. used mesoporous nanosized KF/CaO-MgO catalysts of 100-300 nm particle size in the transesterification of rapeseed oil and obtained a biodiesel yield of 95% at a mass ratio of KF to CaO-MgO of 0.25 and a mass ratio of CaO to MgO of 8:2 (Yun Wang et al., 2009). Akia et al. used 30-35 nm sized particles of Cs/Al/Fe_3O_4 magnetic nanocatalysts for the transesterification of sunflower oil and achieved a biodiesel yield of 94.8% at 58 °C after 2 h, with a methanol to oil ratio of 14:1 (Akia et al. 2014).

2.5.2.2 Acid-Heterogeneous Transesterification

Heterogeneous alkali catalysts have the same disadvantage as homogeneous alkali catalysts of being sensitive to FFAs and water contents in the biodiesel feedstock. Heterogeneous acid catalysts can be used alternatively. These catalysts consist of zirconia catalysts (Sulfated Zirconia, WO_3/ZrO_2, MoO_3/ZrO_2), heteropolyacids (PW12), ion exchange resins (NKC-9, 001x7, D61), sulfated catalysts (Al (H_2SO_4), PSSA), supported solid acid nanocatalysts (TiO_2-ZnO, CsH2PW12O 40Fe–SiO_2, $TiO_2/PrSO_3H$), and carbohydrate derived solid acid catalyst.

Thiruvengadaravi et al. tested Sulfated Zirconia (1 wt.%) in the first-step esterification of high acid value karanja oil, reducing its acid value to 1.3 mg of KOH/g

after 2 h reaction time at 60 °C and 9:1 methanol to oil ratio. FAMEs yield of 95% was reached after the second-step transesterification carried out at 60 °C for 2 h, using 1% KOH and 6:1 methanol to oil ratio (Thiruvengadaravi et al. 2012). Park et al. compared sulfated zirconia, amberlyst 15, and tungsten oxide zirconia catalysts for biodiesel production from WFOs. Tungsten oxide zirconia (WO_3/ZrO_2 at 0.4 g/ml oil) showed the best catalytic activity with 96% FFA conversion at 150 °C for 2 h, using a 9:1 molar ratio of alcohol to oil (Park et al., 2010). Jacobson et al. evaluated the use of solid acid catalysts MoO_3/SiO_2, MoO_3/ZrO_2, $WO_3/SiO_2–Al_2O_3$, and ZS/Si for biodiesel production from WFOs. They found zinc stearate immobilized on silica gel (ZS/Si) to be the most active catalyst at a loading of 3 wt.%, with 98% oil conversion at 200 °C and 18:1 methanol to oil molar ratio (Jacobson et al., 2008). Cao et al. produced biodiesel from high acid value and water content WFOs using heteropolyacid (PW12) as catalyst. They achieved 87% transesterification conversion and 97% esterification conversion at 65 °C and 70:1 methanol to oil molar ratio after 14 h. The catalyst activity was not affected by the FFA and water content in the oil (Cao et al. 2008). Feng et al. used NKC-9, 001x7, and D61 cation-exchange resins as catalysts in biodiesel production from WFOs, and reported the highest yield (90%) with NKC-9 (Feng et al. 2010). Ramachandran et al. prepared the heterogeneous acid catalyst (Al (H_2SO_4)) by sulfonation of anhydrous $AlCl_3$ and used it in biodiesel production from WFOs at a 5 wt.% loading. A 81% conversion was obtained at the optimum conditions of 16:1 methanol to oil molar ratio, 220 °C reaction temperature, and 50 min reaction time (Ramachandran et al., 2011). Zhu et al. tested Poly Styrene Sulfonic Acid (PSSA) and Poly Vinyl Alcohol (PVA) blend membranes for biodiesel production from WFOs. They reported a conversion of 80% at temperatures higher than 80°C by a cross linker structure that emerged between PSSA

and PVA (Zhu et al. 2010). Madhuvilakku and Piraman assessed the transesterification of palm oil using TiO_2-ZnO and ZnO nanocatalyst metal oxides produced by urea using a glycerolnitrate combustion method. TiO_2-ZnO (0.91 wt.%) showed the best catalytic activity achieving a conversion of 92.2% after 5 h reation time at 60 °C and a methanol to oil ratio of 6:1 (Madhuvilakku and Piraman 2013). Feyzi et al. evaluated CsH_2PW12O 40Fe–SiO_2 nanocatalyst for the production of biodiesel from sunflower oil. They obtained a yield of 81% after 240 min of reaction at 60 °C with a methanol to oil ratio of 12:1 (Feyzi et al., 2014). Gardy et al. used mesoporous $TiO_2/PrSO_3H$ solid acid catalyst (4.5 wt.%) for the transesterification of WFOs and obtained a yield of 98.3% at 60 °C and methanol to oil ratio of 15:1 (Gardy et al., 2017).

To avoid the utilization of costly metal catalysts, carbon-based solid catalysts for biodiesel production from oils with high FFA content were tested (Lou et al., 2008). Glucose and C. inophyllum cake that remain after oil extraction were used by Dawodu et al. as a source of solid catalysts for biodiesel production. Both produced comparable yields, but C. inophyllum presented a lower stability than glucose catalyst (Dawodu et al., 2014a; Dawodu et al., 2014b). Ayodele and Dawodu tried to define a better carbonated catalyst for biodiesel production and demonstrated a high catalytic activity of sulfonated microcrystalline cellulose (MCC) with 99% FAMEs yield at optimum conditions, and high operational stability compared to glucose and C. inophyllum cake catalysts (Ayodele and Dawodu 2014). Chen and Fang used a catalyst prepared with glucose/starch mixture for the transesterification of a high acid value waste cottonseed oil. They reported a yield of 90% after 12 h reaction time (Chen and Fang 2011)

2.5.3 Enzyme-Catalyzed Transesterification

Enzyme-catalyzed transesterification has few advantages over chemical catalyzed transesterification, such as avoiding the use of toxic or corrosive chemicals and offering high operational stability (Arumugam and Ponnusami 2014). Lipase is the most commonly used enzyme in transesterification reactions. Lipase enzymes are abundant in nature, synthesized by microorganisms (fungi, yeast, and bacteria), plants and animals (Aarthy et al., 2014), and are most commonly used because of their low production cost and simple modification (Szczęsna Antczak et al., 2009; Vipin et al., 2016). In the biodiesel production through enzymatic catalysis, water plays a major role as the enzymatic hydrolysis of triglycerides takes place on the water/oil boundary layer (Lv et al., 2010). Arumugam and Ponnusami, produced biodiesel from C. inophyllum oil using immobilized lipase enzyme on mesosporous SBA-15 (Arumugam and Ponnusami 2014). Hosseini et al. studied the immobilization of *Bacillus subtilis* microbial lipase using celite in hexane for the transesterification reaction of waste sunflower oil (Hosseini et al., 2013). Vipin et al. assessed biodiesel production from non-edible rubber seed oil (FFA content = 26%) using Rhizopus Oryzae lipase as catalyst. A maximum conversion of 31% was obtained at a methanol to oil molar ratio of 4:1, a catalyst concentration of 15 wt.%, and a reaction time of 48 h (Vipin et al. 2016). There are different types of lipase enzymes that were used as catalysts for biodiesel production (Li & Yan, 2010; Robles-Medina et al., 2009; Yagiz et al., 2007). The main drawbacks of enzyme based-transesterification include high enzyme cost and restricted operational conditions due to denaturing of enzymes at elevated temperatures (Baskar and Aiswarya 2016).

2.6 Zeolitic-Catalyzed Transesterifications

The main advantages which zeolitic catalysts hold over other heterogeneous catalysts used in oil transesterification are their high surface area and controllable acidity, basicity and hydrophobicity.

2.6.1 Zeolitic alkali-heterogeneous transesterification

2.6.1.1 Synthetic alkali zeolite catalysts

Several basic zeolitic heterogeneous catalysts were tested for their activity in biodiesel production from oils. Originally, non-modified Na-form zeolites were tested and showed low catalytic activity and biodiesel yields. Marchetti et al. used Na-Y in its produced form in the transesterification of oleic acid and obtained an ester yield of 27% at 55 °C reaction temperature, 6.3:1 ethanol to oil molar ratio, and 2 h reaction time (Marchetti and Errazu 2008a).

Later studies evaluated the use of chemically modified zeolites for enhanced operational conditions and increased catalytic activity. Metal ions were used for catalyst preparation by impregnation method, the most common being potassium-based molecules (potassium hydroxide, potassium acetate) and sodium-based molecules (sodium hydroxide, sodium acetate). After loading the metals on the synthetic or natural zeolites, the produced catalysts are calcined at high temperatures (500-900 °C) in order to transform the K-based and Na-based molecules in both the zeolite matrix and surface into potassium and sodium oxides (K_2O, Na_2O), which represent the basic active sites of the zeolite catalysts (Al-Jammal et al., 2016; Intarapong et al., 2011; Leclercq et al., 2001; Otieno et al., 2018;

Ramos et al., 2008; Rezayan & Taghizadeh, 2018; Supamathanon et al., 2011; Suppes et al., 2004; Y. Y. Wang & Chen, 2016; Xue et al., 2009). Leclercq et al. studied the transesterification of rapeseed oil in the presence of cesium-exchanged NaX faujasite catalysts. High methanol to oil ratio of 275:1 and a long reaction time of 22 h were needed to obtain a conversion of 70% (Leclercq, Finiels, and Moreau 2001). Ramos et al. analyzed the catalytic performance of Na-based zeolites (mordenite, beta, and X) in the transesterification of sunflower oil. Achieved methyl ester yields were between 93.5 and 95.1 wt% at 60 °C. However, leaching studies showed that sodium was leaked in the reactants mixture, giving the reaction a homogeneous path (Ramos et al. 2008). Suppes et al. studied the transesterification of soybean oil at different reaction temperatures in the presence of NaX zeolites ETS-10, and their metal loaded versions. Due to the high basicity of ETS-10 zeolites and their larger pore structures, FAMEs yield exceeded 90% at temperatures of 150 °C and 120 °C after 24 h reaction time (Suppes et al. 2004). Intarapong et al. investigated FAMEs yield over different loadings of KOH on NaY zeolite catalysts for the transesterification of palm oil in a packed-bed reactor. 15 wt.% K loading on NaY zeolite was found to have the highest catalytic activity achieving an oil conversion of 92.18% at 60°C for 7 h. However, potassium molecules were found to leach after few recycling runs of the solid catalyst, decreasing thus its activity (Intarapong, Luengnaruemitchai, and Jai-In 2011). Biodiesel production from *Jatropha curcas* seed oil using different loadings of CH_3COOK over an artificial zeolite and different calcination times and temperatures was assessed by Xue et al. FAMEs yield exceeded 91% when the catalyst with 47 wt.% CH_3COOK loading was calcined at 550°C for 5 h, with optimal transesterification reaction conditions of 10:1 methanol to oil molar ratio, catalyst amount

of 2 wt.%, and a reaction time of 4h (Xue et al. 2009). Supamathanon et al. produced biodiesel from Jatropha Curcas using potassium impregnated zeolite NaY (K/NaY) at different metal loadings. The highest FAMEs yield (73.4%) was attained with 12 wt.% of potassium loading at 65 °C, a methanol to oil molar ratio of 16:1, and a reaction time of 3 h, (Supamathanon, Wittayakun, and Prayoonpokarach 2011). Al-Jammal et al., prepared several KOH/zeolite tuft catalysts by impregnation in KOH solutions for the production of biodiesel from waste sunflower vegetable oil. The impregnated 1-4M KOH/TZT catalyst produced by heating in a two-step impregnation method, provided the maximum biodiesel yield of 96.7% at 50 °C, methanol to oil molar ratio of 11.5:1, and 2 h reaction time. Higher KOH loadings on the zeolite resulted in a decreasing trend in the FAMEs yield due to the agglomeration of excess KOH covering the zeolite's active basic sites. Impregnation of KOH performed in one stage and without heating resulted in lower catalytic activity. The heating process during catalyst preparation was inevitable for the conversion of KOH into the more active K_2O (Al-Jammal, Al-Hamamre, and Alnaief 2016). To achieve better catalysis in the transesterification reaction of triolein, Wang et al. prepared beta zeolites treated with dilute NaOH solutions. The Na-loaded zeolites were used for biodiesel production by reflux heating and microwave irradiation. A conversion efficiency exceeding 90% was achieved within an hour of the reflux reaction with Na-treated zeolite catalysts which exhibited durable catalytic activity (nine consecutive cycles). The authors concluded that sodium cations present in the cages and the defect sites of the NaOH-treated beta zeolite can be brought to the external surface of the catalyst during the transesterification reaction, enhancing thus the catalysis (Wang & Chen, 2016). Otieno et al. used a cheap natural zeolite from Kenya (NZK) for the transesterification of *Jatropha curcas* oil to

biodiesel. The zeolites were loaded with Na, Cu and Pb ion metals by ion exchange to improve their catalytic activity. A better yield was achieved by Na-NZK in comparison to Cu-NZK and Pb–NZK zeolites (Otieno et al. 2018).

2.6.1.2 Natural alkali zeolite catalysts

The standard raw materials used for the synthesis of the previous discussed zeolites are silica and alumina. The preparation of zeolites from these chemical sources can be relatively expensive. Therefore, the possibility of using cheaper natural raw materials to produce zeolite catalysts and doping them with K-based and Na-based molecules was reported by different studies (Đặng et al., 2017; Kusuma et al., 2013; Volli & Purkait, 2015). Kusuma et al. studied the transesterification of palm oil using natural zeolites modified with KOH solution at different loadings. The catalyst prepared using a zeolite to KOH weight ratio of 1:4 produced the optimal FAMEs yield of 95.09% at 3 wt.% loading (Kusuma et al. 2013). Fereidooni et al. used a composite of chitosan and natural zeolite (clinoptilolite zeolite) treated with KOH for the transesterification of WFOs by electrolysis. KOH impregnation decreased the silica content of clinoptilolite by desilication and increased its active basic sites' content by the formation of hydroxylpotaslite. With acetone used as a co-solvent, a conversion yield of 93% was achieved with 1 wt.% catalyst concentration and alcohol to oil ratio of 1:7 at 40 V for 3 h (Fereidooni and Mehrpooya 2017). Dang et al. produced biodiesel from transesterification of triolein using NaOH-treated kaolin clay as an active catalyst possessing characteristics of zeolite LTA. An average conversion efficiency of 92.8% was reached with 36.6:1 mass ratio of methanol to

triolein, a catalyst loading at 72 wt.% , a reaction temperature of 62.9 °C, and a reaction time of 146 min (Đặng, Chen, and Lee 2017). Volli et al. discussed the application of coal fly ash for the synthesis of basic heterogeneous zeolite X and A catalysts for biodiesel production from mustard oil. The synthesized zeolites were ion-exchanged with potassium and used in the transesterification reaction. A conversion of 84.6% was reached using 12:1 methanol to oil molar ratio and a reaction time of 7 h at 65 °C (Volli and Purkait 2015).

2.6.1.3 Magnetic alkali zeolite catalysts

Despite adding value to waste (fly ash) and using natural zeolites to produce biodiesel, both synthetically and naturally produced zeolites have an issue related to their costly separation from the reaction products for the purpose of their reuse. Rezayan et al. resolved this problem through using magnetic catalysts which can be simply separated from the reaction solution by a magnetic field. Magnetic mesoporous basic nanocrystalline KOH/ZSM-5-Fe_3O_4 catalysts were employed in the transesterification of canola oil to biodiesel. Optimum biodiesel yield of 93.65% was achieved at 9.03% catalyst loading, 12.3:1 alcohol to oil molar ratio, 65 °C reaction temperature, and 3.26 h reaction time. The catalyst was easily separated from the reaction mix by an external magnetic field and reused for five successive cycles giving a biodiesel yield of 80% for three consecutive cycles (Rezayan and Taghizadeh 2018).

2.6.2 Zeolitic acid-heterogeneous transesterification

2.6.2.1 H-Type Acid Zeolite Catalysts

The stable crystalline aluminosilicate framework is formed by silica and alumina units' bounds. The charge imbalance between the bounds produces the zeolite's ability for ion exchange. This allows the conversion of the sodium form of zeolites to the hydrogen form mainly by ammonium ion exchange. H-type zeolites are the most common form of acid zeolite catalysts (Chung et al., 2008; Doyle et al., 2016; Doyle et al., 2017; Medina-Valtierra & Ramirez-Ortiz, 2013; Mowla et al., 2018).

Medina-Valtierra et al. produced biodiesel from WFOs in sub- and supercritical methanol on a zeolite H-Y solid acid catalyst. FAMEs yield exceeded 82 % after only 15 min of reaction time at 240 ºC, and a methanol to oil molar ratio of 5:1 (Medina-Valtierra and Ramirez-Ortiz 2013). Doyle et al. compared the catalytic activity of commercial H-Y zeolite and Zeolite H-Y prepared using kaolin in the esterification of oleic acid. At optimum conditions of 70 ºC, 5 wt.% catalyst loading, 1 h reaction time, and 6:1 ethanol to oleic acid molar ratio, the oleic acid conversion using Zeolite H-Y prepared from kaolin was 85%, while the resultant value for the synthetic H-Y zeolite was 76% (Doyle et al. 2016). In another study, the authors used acidic FAU-type zeolites prepared from shale rock and commercial H-Y zeolites in the esterification of oleic acid. The results demonstrated comparable structural characteristics and catalytic activity of both synthetic and natural zeolites, with oil conversion reaching 78% after 90 minutes in the latter case. (Doyle et al. 2017). Mowla et al. investigated a route for WFOs hydroesterification (hydrolysis and esterification of low quality fatty substrates) over acid heterogeneous

zeolites H-ZSM-5 and reported 40% conversion of WFOs into FFAs through hydrolysis, and 63% of FFAs esterification to biodiesel after 4h reaction (Mowla, Kennedy, and Stockenhuber 2018). Chung et al. compared different microporous acid zeolites (H-ZSM-5, H-FAU, H-BEA, H-MOR and silicalite zeolites) for the esterification of FFAs in WFOs. While the amount and strength of acid sites in the different zeolites played an important role in the extent of FFAs conversion, a major obstruction in the esterification of large FFA molecules was attributed to diffusion limitation of these molecules in the narrow intrinsic microporous zeolites such as in the case of H-ZSM-5 (5.1 × 5.4 Å - 5.4 × 5.6 Å) where most of the strong acid active sites are found. The authors demonstrated that in this case the esterification reaction occurred on the external acidic surface of the zeolite and that the increase in the external surface area and external acidity are at the basis of higher oil conversions (K. H. Chung, Chang, and Park 2008).

2.6.2.2 Modified Acid Zeolite Catalysts

It is established that the physical and chemical properties of zeolite catalysts directly affect the extent of oil conversion. Studies have been conducted to develop modified heterogeneous acid zeolite catalysts with stronger acidity, appropriate external surface properties, and increased pore volume and pore size, to improve their catalytic activity and selectivity in transesterification reactions. Many studies discussed post-synthesis modifications of zeolites using deposition and ion exchange techniques and dealumination to improve their catalytic performance (Alismaeel et al., 2018; Feyzi & Khajavi, 2014; Narkhede & Patel, 2014; Shu et al., 2007; Vieira et al., 2015, 2017), while few others

investigated the direct production of modified hierarchical zeolites, with improved mass transfer properties to carry out transesterification reactions (Carrero et al. 2011; Sun et al. 2015).

2.6.2.2.1 Post-synthesis modification of acid zeolite catalysts

Vieira et al. modified the external properties of H-ZSM-5 by dealumination with citric acid. Dealumination involves the removal of aluminum atoms from the zeolite framework through treatment with an acid, modifying thus the pore structure and acidity of the zeolites in addition to improving their reactivity in biodiesel production reactions. The modified material showed a slight increase in the external surface area and a reduction in Brønsted acid sites (Vieira et al. 2015). The authors later assessed the incorporation of sulfated lanthanum oxide (SO_4^{2-}/La_2O_3) on the external surface of the dealuminated solids to improve their catalytic activity in the transesterification of oleic acid. When compared to the parent HZSM-5 zeolites, the modified catalysts showed a higher catalytic activity achieving 100% oil conversion at 10 wt.% catalyst loading, 45:1 alcohol to oil molar ratio, 100 °C, and 4 h reaction time (Vieira et al. 2017). Shu et al. applied $La(NO_3)_3$ as the ion exchange precursor to incorporate La ion into zeolite beta and used it in the synthesis of biodiesel from soybean oil. La/zeolite beta showed higher stability and oil conversion than zeolite beta, which was associated with the greater concentration of external Brønsted acid sites available for the reactants. Triglycerides conversion of 48.9 wt% was obtained at 1.1 wt.% catalyst loading, using a methanol to oil molar ratio of 14.5:1, a reaction temperature of 60 ºC maintained over 4 h (Shu et al. 2007). Feyzi et al. investigated the catalytic activity

of strontium and barium supported on the ZSM-5 zeolite (Sr/ZSM-5 and yBa − xSr /ZSM-5) in the transesterification reaction of sunflower oil to biodiesel. The activity of yBa − xSr/ZSM-5 (where x = 6 wt% strontium based on the weight of ZSM-5 and y = 4 wt% Ba based on the weight of Sr) showed to be optimal for biodiesel production achieving a FAMEs yield of 87.7% at a methanol to oil ratio of 9/1, a reaction temperature of 60 °C, and a reaction time of 180 min. Catalyst characterization showed that the synthesis, impregnation, and calcination conditions had a noticeable outcome on the morphology and texture of the modified zeolite whereby fine particles and high specific surface area were registered for the yBa − xSr/ZSM-5 catalyst (Feyzi and Khajavi 2014). Narkhede and Patel studied the esterification of oleic acid and soybean oil over a monolacunary silicotungstate (SiW11) supported on zeolite H-beta solid acid catalyst. The catalyst was prepared with 30 wt.% SiW11 loaded on zeolite H-beta and showed high catalytic activity achieving 82% conversion of oleic acid (3.5 wt.% catalyst, 20:1 molar ratio of alcohol to oil, 60 °C, 10 h) and 96% of soybean oil (4 wt.% catalyst, 4:1molar ratio of alcohol to oil, 65 °C, 8 h). The catalyst showed consistency in its catalytic activity when it was reused up to four times (Narkhede and Patel 2014). Alismaeel et al. studied the esterification of oleic acid in a fixed-bed reactor over FAU-type zeolites synthesized using shale rock. Co, Ni and Pt were added to the zeolite to increase its catalytic activity. At a reaction temperature of 70 °C and reaction time of 1.5-2 h, oleic acid conversions reached respectively 93 and 89% under batch and continuous conditions using Co-Ni-Pt-FAU acid catalyst (Alismaeel et al. 2018).

2.6.2.2.2 Direct-synthesis modification of acid zeolite catalysts

Another interesting way of improving zeolites activity in the transesterification reaction, which was investigated by only few studies, is the production of hierarchical zeolites which combines the advantages of both microporous and mesoporous zeolites. The produced hierarchical zeolites overcome diffusion limitations by offering larger pores while maintaining the high reactivity of microporous acid zeolites. Carrero et al. carried out the transesterification of microalga lipids to biodiesel using hierarchical h-Beta zeolite as heterogeneous catalysts. The catalyst secondary mesoporosity improved the accessibility of microalga oil to the h-Beta acid sites by enhancing the mass transfer of large lipids into the zeolite framework. A conversion of 46% was reached at a reaction temperature of 115 °C after 4h (Carrero et al. 2011). Sun et al. tested microporous (Beta zeolite and ZSM-5 zeolite) and micro-mesoporous (MFI type ZRP-5 zeolite) acid zeolites in the esterification of oleic acid with ethanol to assess the effect of pore size on the oil mass transfer. ZRP-5 zeolite exhibited the lowest internal mass transfer limitations, but also the lowest catalytic activity associated to their hydrophilic surface favoring the adsorption of polar ethanol over the adsorption of oleic acid molecules. The highest conversion of oleic acid reached 73.6% and was achieved by the hydrophobic Beta zeolite used at a loading of 0.167 meq/g, with ethanol to oleic acid molar ratio of 20:1, a temperature of 78 °C, and a reaction time of 10 h (Sun et al. 2015). APPENDIX D: Table D summarizes the different studies on the use of zeolite catalysts in the production of biodiesel.

2.7 Factors Affecting Biodiesel Yield Using Zeolite Catalysts

The final FAMEs yield of the transesterification reaction over zeolite catalysts is influenced by several parameters, such as reaction temperature, reaction time, catalyst loading, and alcohol to oil ratio.

2.7.1 Reaction Temperature

The transesterification reaction temperature is one of the most important parameters affecting biodiesel yield. As the temperature increases, the reaction rate increases due to a higher transfer of heat energy. In addition, the viscosity of the oil decreases with increasing reaction temperature, which promotes high yield of biodiesel within a shorter time. The transesterification reaction is usually carried out at the boiling temperature of the alcohol. Methanol which is extensively used in this reaction has a boiling point between 60 and 70 °C under atmospheric pressure, depending on its purity. At this temperature range, different studies reported high biodiesel yields using zeolite catalysts. Feyzi et al. achieved a FAMEs yield of 87.7% at a reaction temperature of 60 °C and a reaction time of 3 h using Ba-Sr/ZSM-5 catalyst (Feyzi and Khajavi 2014). Doyle et al. reported that the conversion of oleic acid increased from approximately 40% at 40 °C to 85% at 70 °C using zeolite Y prepared from kaolin (Doyle et al. 2016). An optimum reaction temperature of 65 °C was reported for the transesterification of *Jatropha curcas* oil using Na-NZK at a reaction time of 5.5 h (Otieno et al. 2018).

Higher temperatures were used in pressurized systems, in other studies and achieved high yield at an increased reaction rate. Vieira et al. achieved a FAMEs yield of 80% after 1 h of reaction time at a temperature of 100 °C using SLO/HZSM5 as a catalyst (Vieira et al.

2013). Medira-Valtierra et al. reached a biodiesel yield of 82% from the transesterification of WFOs at a reaction temperature of 240 °C and a reaction time of only 20 min (Medina-Valtierra and Ramirez-Ortiz 2013).

2.7.2 Molar Ratio of Alcohol to Oil

Since the transesterification is a reversible reaction, the moles of alcohol must be in excess to force the reaction towards the formation of FAMEs and to achieve higher conversion rates (Qiu et al., 2011). Therefore, the alcohol to oil ratio is one of the most sensitive factors that affect the final biodiesel yield (Jacobson et al., 2008). The effect of the molar ratio of alcohol to oil on the conversion of oils was examined by different studies through varying the amount of methanol used in the process. Under similar reaction conditions, Sun et al. reported that the conversion rate of oleic acid increased from 62.5% to 73.6% as the molar ratio of ethanol to oleic acid shifted from 1:10 to 1:20 using hydrophobic Beta zeolites as catalysts (Sun et al. 2015). Shu et al. assessed different methanol to oil ratios in transesterification reactions using La beta catalyst, and found that FAMEs yield increased with increasing alcohol to oil ratio to 9:1 (Shu et al., 2007). Similarly, Feyzi et al reported increased FAMEs yield in transesterification reactions conducted over Ba–Sr/ZSM-5 catalyst at increased methanol to oil ratio of 14.5:1 (Feyzi & Khajavi, 2014). However, in the previous discussed studies, the authors reported a decreased FAMEs yield when the quantity of alcohol was further increased beyond optimal amounts. This phenomenon is due to the recombination of FAMEs and glycerol to form monoglycerides. Excess methanol is advantageous for the conversion of triglycerides into monoglycerides. However, monoglycerides affect the solubility of the nearly immiscible

glycerol and FAMEs encouraging thus the backward reaction to take place (Shu et al. 2007; Sun et al. 2015). Besides, glycerol separation gets more difficult as glycerol solubility in alcohol also increases (Fereidooni and Mehrpooya 2017).

2.7.3 Catalyst Type and Loading

The amount of zeolite catalyst used influences the conversions of triglycerides in a transesterification reaction. At higher catalyst loadings, a greater amount of active sites will be available for the oil to react and produce FAMEs (Liu et al., 2014). In fact, alcohol's solubility in oil is partial, the transesterification can thus only take place at the interface of these two phases. Increasing catalyst loading will increase the active sites' concentration in the interface which will enhance the formation of FAMEs and higher oil conversions (Shu et al. 2007). Doyle et al. registered an increase in the conversion of oleic acid from 70 to 85%, by increasing zeolite H-Y amount from 2 to 5 wt.% (Doyle et al. 2016). Volli et al. evaluated the effect of different catalyst concentrations (3, 5, 7 and 10 wt.%) on the conversion of mustard oil to biodiesel using zeolite X and A produced from fly ash and found that with an increase in catalyst concentration from 3 to 5 wt.%, biodiesel yield increased to 84.6% (Volli and Purkait 2015). In both studies, only a slight increase in the conversion of oils was observed at catalyst loadings higher than 5%. This was explained by the increased miscibility of the methanol and oil phases due to the formation of FAMEs which act as a mutual solvent driving the alcohol-oil mixture to become a single-phase. In this case, increasing the catalyst loading will no further enhance the reaction rate (Shu et al. 2007).

2.7.4 Reaction Time

In order to study the influence of reaction time on the conversion of oils, different studies fixed the zeolite loading, alcohol to oil ratio, and reaction temperature and varied the reaction time (Doyle et al. 2017; Medina-Valtierra and Ramirez-Ortiz 2013; Suppes et al. 2004; Volli and Purkait 2015). Biodiesel yield increases with reaction time but at long durations zeolite catalysts deactivation due to less reactant coverage might occur (Doyle et al. 2017). It is worth mentioning that optimum reaction time is dependent on the reaction parameters. Medina and Ramirez reported an optimum oil tansesterification time of 20 minutes (Medina-Valtierra & Ramirez-Ortiz, 2013) while Suppes et al. achieved maximum conversions at a reaction time of 24 h under different reaction conditions (Suppes et al., 2004).

2.8 Synthesis of Zeolite Catalysts

The production of zeolites follows either a hydrothermal synthesis in the presence or absence of a liquid phase (Arnold et al., 2003; Flanigen & Breck, 1960), or a non-aqueous synthesis referred to as “dry” production (Morris & Weigel, 1997). Hydrothermal zeolite synthesis is commonly used and typically follows the mechanistic pathways of induction period, evolution of order, nucleation and crystal growth.

During the induction period, amorphous individual reactants containing silica and alumina are mixed together with a cation source and a structuring agent, usually in a basic medium. The aqueous reaction mixture is heated, (at temperatures above 100 °C) in a sealed autoclave (Antonić-Jelić et al., 2003). The Si and Al elements are mineralized by the

alkali source to their oxide forms which will make up the microporous framework. These oxidic precursors are amorphous and contain Si-O and Al-O bonds (Cundy & Cox, 2003). Over a period of time and especially under the effect of heat, the solid phase is organized during the evolution of order step, and a new generated material having a similar chemical composition to that of the eventual zeolite product is formed. However, this semi-ordered gel lacks the periodical organization and is thus still amorphous (Lowe 1983; Zhdanov 1971). Zeolite nucleation is a phase transition event during which, a critical volume of the semi-ordered gel network is transformed into a structure which is sufficiently well-organized to form viable growth nuclei from which the crystal lattice can propagate. Growth centers can then increase in size (crystal growth phase) by either the addition of growth units or by aggregation (Cundy et al., 1995). And the emerging microcrystal grows to an ordered and crystalline material entity containing Si-O-Al linkages which form the tangible zeolite catalysts that are used in transesterification reactions among other applications (Cundy & Cox, 2005).

2.9 Characterization of Heterogeneous Zeolites

After zeolites' production and before their use in biodiesel production, the catalysts are carefully characterized as the nature and properties of zeolites affect the quality of the biodiesel produced. X-ray diffraction (XRD) is a technique used for the characterization of the composition and crystallinity of the produced zeolites. The specific surface area is calculated by the Barrett Joyner Hlenda (BJH) and Brunauer Emmett Teller (BET) methods. Pore volume and pore size distribution are also provided by the N_2 adsorption-desorption isotherms. Scanning electron microscope (SEM) is used to determine the

morphology of the prepared zeolites. Transmission electron microscopy (TEM) is a technique used to examine the particle's diameters and morphology. Fourier transform infra-red (FTIR) spectroscopy is sensitive to the assimilation of phases. For zeolite acidity studies, IR bands deriving from the stretching modes of the hydroxyl groups are studied to differentiate between Brønsted and Lewis acidity. The basic probe pyridine is commonly adsorbed on the acid zeolite and modifies the O-H bonds stretching frequency depending on the acid strength of the corresponding site. The characteristic IR bands of the pyridinium ion formed at the Brønsted acid sites and the coordination complexes at the Lewis sites are soundly distinguished at 1540 cm^{-1} and 1450 cm^{-1}, respectively (Derouane et al. 2013). Basicity can be assessed by FTIR as well. Dang et al. distinguished between LTA zeolites and their NaOH-treated form using FTIR. LTA activated with NaOH showed bands at 997.2 cm^{-1} associated with asymmetric Al–O vibrations in comparison with non-activated LTA zeolites (Đặng, Chen, and Lee 2017).

2.10 Economic and Environmental Considerations of Biodiesel Production by Zeolite Catalysts

The lower price of the catalyst would bring a direct reduction in the overall production cost. However, the main criteria in choosing an economically viable catalyst for the transesterification reactions is ruled by the feedstock character, such as FFAs and water content (Singh & Singh, 2010). For low quality feedstock with high FFAs and water content, transesterification performed by heterogeneous acid catalysts such as zeolites have the economic advantage of reducing unit cost of biodiesel production by being easily and cheaply recovered for reuse without the required process steps for product separation and

purification needed in homogeneous catalysis (Avhad & Marchetti, 2015; Lam et al., 2010; Zheng et al., 2006). Additional advantages of using heterogeneous zeolites in catalytic processes such as the transesterification of oils include the ease of separation from the liquid products, and the toxicity, corrosion and environmental pollution reduction (Lee and Saka 2010).

2.11 Summary of the Review

As the fruit of detailed research into biodiesel synthesis using numerous catalysts, some key conclusions can be drawn:

1. The present review helps identify benefits and challenges in various transesterification paths used for the production of biodiesel.
2. Information regarding chemical and physical characteristics of oil feedstock help determine the proper and most efficient catalytic method for biodiesel production.
3. An overview of various catalysts used in biodiesel production were investigated focusing on zeolitic catalysts which offer on one hand, high yield, better selectivity and regenerability in comparison with homogeneous catalysts, and on the other hand, higher surface area, and controllable acidity, basicity, and hydrophobicity, in comparison with other heterogeneous catalysts.
4. A better understanding of the transesterification reaction conditions using zeolitic catalysts such as, temperature, alcohol to oil ratio, catalyst loading, and reaction time allows optimizing the biodiesel yield.

CHAPTER 3

PRELIMINARY ECONOMIC ASSESSMENT OF THE USE OF WASTE FRYING OILS FOR BIODIESEL PRODUCTION IN BEIRUT, LEBANON

In this chapter, a method for assessing the costs of biodiesel production from waste frying oils in Beirut, Lebanon, is investigated with the aim of developing an economic evaluation of this alternative. A hundred restaurant and hotel enterprises in Beirut were surveyed and were promoted to participate in the biodiesel supply chain. The survey was a mean of data collection on waste frying oils generation, disposal methods and frequency, and acquisition cost. Also, waste frying oils were collected and converted into biodiesel using a one-step base catalyzed transesterification process. Physicochemical characteristics of the produced biodiesel were tested for conformity to international standards. Data produced from laboratory scale conversion of waste frying oils to biodiesel, as well as data collected from the only biodiesel plant in Lebanon are used to determine the production cost of biodiesel. A Geographic Information System is used to propose real-time vehicle routing model to establish the logistics costs associated with waste frying oils collection. Sensitivity and benefit analysis of biodiesel production from waste frying oils are also discussed.

3.1 Introduction

More and more countries around the world are turning to renewable energies to use as resources. Research has confirmed the wisdom of these efforts, as many studies have shown that an increased use of intermittent renewable energy sources can reduce carbon emissions (Lund 2007; Nelson et al. 2012; Solomon et al., 2014). Of these intermittent renewable

energy sources, biomass is the most frequent form (McKendry 2002; Uthman and Abdulkareem 2014) and can be converted to other utilizable forms of energy like biofuels. And, among these biofuels, biodiesel is one of the leading potential alternatives to petroleum (Tan et al., 2011; Veiga et al. 2014).

Literature on biodiesel has focused on the optimization of biodiesel production processes from waste frying oil which involve the transesterification of oils by a short chain alcohol in the presence of a suitable catalyst (Al-Hamamre and Yamin 2014; Alves et al. 2013; Fernando et al. 2007). Dias et al. compared the performance of different homogeneous alkali catalysts during the transesterification of waste and virgin oils (Dias et al., 2008). Sabudak and Yildz added to Dias's work by performing a two-step acid-base catalyzed transesterification and comparing biodiesel yields (Sabudak and Yildiz 2010). Uzun et al. determined the optimized reaction parameters by carrying out an alkali-catalyzed transesterification of WFOs under various conditions, permitting the investigation of the effects of catalyst type, catalyst concentration, reaction time, methanol/ethanol molar ratio, reaction temperature, and purification type on biodiesel yields (Uzun et al. 2012).

On another note, many studies have analyzed the economic feasibility of producing biodiesel from WFOs. In South Africa, large-scale biodiesel production was investigated based on a 2% blend with conventional diesel (Moodley, 2006). Small-scale, on-farm studies examined the potential of using biodiesel as an alternative local fuel (Pienaar and Brent 2012). Patle et al. analyzed trade-offs between profit and heat duty, and profit and organic waste generated in two biodiesel production processes. They deduced that the profit improves with the increase in heat duty, and that the profit increase is accompanied by larger amounts of organic waste, the main contributor to these increases being the waste cooking oil flow

rate (Patle et al. 2014). Araujo et al. proposed a method to evaluate the costs of biodiesel production from WFOs with the goal of assessing the economic feasibility of such an alternative. The method they used embraced a logistics perspective which proved to be relevant to the total biodiesel production cost (Araujo et al., 2010). Valizadeh et al. proposed a method for improving the economic performance of biofuel supply chain in Malaysia and recommended that by incorporating uncertainties including feedstock demand, the biodiesel supply chain would be optimized (Valizadeh et al., 2014). Mosarof et al., assessed the cost of biodiesel produced from palm oil by including the feedstock price, installation, operation, and maintenance costs of the biodiesel production plants, and by-products credit and concluded that economic prospects for the produced biodiesel are not yet promising due to factors such as production cost and fuel economy (Mosarof et al. 2015). Chanthawong and Dhakal contributed to the liquid biofuels' market analysis in illustrating import-export dynamics in Southeast Asian Countries in terms of policies and challenges (Chanthawong and Dhakal 2016).

This study aims at assessing the economic feasibility of biodiesel production from WFOs in the capital of Lebanon, Beirut, and uses data produced from laboratory scale conversion of WFOs to biodiesel, as well as data collected from the only biodiesel plant in Lebanon to determine the production cost of biodiesel. Data from 100 restaurants and hotels in Beirut aiming at evaluating WFOs generation and potential contribution of the food enterprises to the biodiesel supply chain were equally analyzed. This study presents an initial assessment of the economic feasibility of the implementation of biodiesel production at a large scale in Lebanon which was not addressed previously. Furthermore, the study proposes vehicle routing model scenarios to determine logistics network for the profitable reuse of

WFOs in Beirut. The assessment of the economic feasibility of biodiesel production from WFOs allows for a better understanding of cost interactions and acts as an initial ground for multiple actors such as government and WFOs and biodiesel producers, to jointly implement the recycling logistics system of WFOs in Beirut as well as in other cities.

3.2 Methodology

The study involved laboratory-scale biodiesel production, field research through visits, interviews, and the distribution of a structured questionnaire for data collection purposes from main WFOs producers including restaurants and hotels enterprises. The study also entailed the development of a vehicle routing model scenarios to determine logistics network for the profitable reuse of waste frying oil in Beirut.

3.2.1 Waste Frying Oils Collection

Fast food restaurants and hotels being the main sources of WFOs in Lebanon were chosen as the population. The sample included small, medium, large and chain restaurants and hotels in Lebanon's capital and most crowded city, Beirut. 36% of the enterprises had no more than 100 seats and 25% served more than 200 dinners per day. The types of food facilities ranged between ethnic, fast food, casual dining and fine dining. Structured questionnaires were carried out with the different restaurants and hotels to obtain information concerning how long is the oil used before it is disposed of, how much WFOs are generated, and for how much it is sold. In parallel, other interviews were performed with WFOs collection companies based in Lebanon and responsible for collecting and exporting the used oils for recycling outside Lebanon. All corresponding visits delivered entry data for the form

of collection of the oil, the capacity and cost of the collecting vehicles, and the time taken to achieve the rounds. The only company that produces biodiesel from WFOs, currently operating in Lebanon was also surveyed. This last step produced information about large-scale production costs, including general expenses, equipment, manufacturing costs and fixed capital. The different restaurants and hotels visited were mapped and georeferenced through a Geographical Information System (GIS). The location of the only biodiesel company in the country was also added to the map, thus helping develop a vehicle routing model that finds the best WFOs transportation sequence to the operating plant, minimizing the impedance and optimizing the logistics cost.

3.2.1.1 Data Collection

This paper opts for restaurant and hotel enterprises as the focuses for two reasons. First, the amount of WFOs produced by restaurants and hotels is much larger than that of families, giving a much more observable sample. Second, restaurants and hotels dispose of the WFOs in a more marketing approach. For these reasons, studying such subjects is more suitable to coordinate and manage a supply chain that helps in the establishment of the logistics cost and the WFOs acquisition cost. The capital of Lebanon, Beirut, was selected as the survey area since it holds a large number of restaurants and hotels. Over 70 restaurants and 30 hotels were surveyed. The return rate of the questionnaire was 87%. Descriptive statistics and graphics analysis were used to describe the basic features of the collected data including the quantity of vegetable oil consumed, WFOs disposal frequencies and methods, the willingness of the restaurants and hotels owners to cooperate in the WFOs supply chain,

and the acquisition cost of WFOs. They formed the basis of the subsequent quantitative analysis for the assessment of the economic profitability of biodiesel production from WFOs in the study city, Beirut.

3.2.1.2 Questionnaire Design

As a mechanism for obtaining information and opinion on WFOs commercialization and their potential use in biodiesel production, a structured questionnaire was designed to survey restaurants and hotels in the area of Beirut (APPENDIX E: Table E). The designed questionnaire adopted in this study included questions regarding the generation and disposal of WFOs, the recycling approach and motives and the willingness of the surveyed enterprises to participate in the WFOs supply chain for the production of biodiesel. The questionnaire covered basic information related to the number of seats, the type of food served, the number of meals per day, the types, amounts and costs of vegetable oil used, the period during which a batch of vegetable oil is used before disposal, the quantities and sale prices of WFOs produced, the methods of WFOs disposal, the awareness of WFOs recycling through biodiesel production, and the willingness to participate in the WFOs supply chain for biodiesel production. The questionnaire was also a mean to obtain WFOs samples in order to assess their biodiesel yield in the lab. The return rate of the sample collection was 22%. The physical appearance of the WFOs was examined at the time of the collection in order to confirm the information provided by the enterprises' owners towards the periods of use of the WFOs before they are discarded and differentiate between minimally used batches versus more exhausted ones.

3.2.2 Biodiesel Production

3.2.2.1 Reagents and Chemicals

The reagents used during the synthesis and purification procedures were: methanol 99% (Fischer Scientific), potassium hydroxide capsules 95% (KOH, Aldrich), sulfuric acid 99% (H_2SO_4, Aldrich), anhydrous magnesium sulphate 70% ($MgSO_4$, Aldrich) and anhydrous sodium sulphate 99% (Na_2SO_4, Aldrich).

3.2.2.2 WFOs Sampling and Preparation

WFOs' sampling was conducted during the summer season over a period of 2 months extending from mid-June until mid- August. Samples were collected in 0.5 L amber glass bottles and were subsequently randomly mixed to prepare the oil feedstocks for biodiesel production. All WFOs batches were produced from the mixture of at least three different supply sources including WFOs of different quality (WFOs discarded after a maximum of 4 days of use and those used for a longer period, ranging between 5 and 8 days). A total of 21 batches were reconstituted and used for the biodiesel production.

3.2.2.3 Pretreatment and Transesterification

The prepared WFOs mixtures were first filtered (Whatman GF/A 90mm Ø filter paper) to remove food residues. Most of the water was initially removed by gravity separation and the oil was then heated at 105–110 °C to remove any additional water until constant sample weight is reached. Next, the quality of WFOs mixture samples was examined

by testing the acid values. For mixtures of WFOs containing a level of free fatty acids (FFAs) lower than 5% (0.94% to 3.56%), biodiesel synthesis was carried out via a one-step base catalyzed transesterification, following a modified method used by Dias et al. (Dias et al., 2008). A defined amount of methanol (6:1 methanol/oil molar ratio) was pre-mixed with the KOH catalyst at a 0.75% of oil mass. The mixture of methanol and catalyst was then added to 200 g of WFOs preheated in a reactor at the reaction temperature (60 °C). The reactor consisted of a 1 L flat-bottom flask equipped with a magnetic stirrer. The reaction time was 1 h under stirring at 600 rpm. For FFAs content higher than 5% (6.73%) which consisted of only 5% of the mixed WFOs samples mixed, the synthesis method was different. On these samples which were of a visually poor quality and contained oil that had been used continually for a month, acid-catalyzed esterification was first carried out to ensure the conversion of FFAs to methyl esters. In this case a method by Inman et al. was adopted (Inman 1945). Briefly, methanol (77% of the weight of oil) and sulfuric acid (0.75% of the weight of oil) were added to the oil while stirring took place at 60 °C for 1 h. After neutralization, methanol (6:1 methanol/oil molar ratio) premixed with KOH (1.25% of the weight of oil) was added, and the mixture was stirred for an additional hour at 50 °C. The oil phase was analyzed and new FFAs average values of 2.7% were obtained. Since the fraction of oil mixtures with acid value higher than 5% was minimal (5% of the total oil mixtures prepared), it was disregarded from the study analysis and cost assessment of the biodiesel production was only based on the one step base catalyzed transesterification. This was deemed reasonable, as an initial step of acid esterification would erroneously increase the overall cost of the production and is unnecessary when considering the option of further decreasing the oil FFA content through mixing it with additional amount of oil of low acid

values. Samples of mixed WFOs were prepared in duplicates for the transesterification reactions. For each sample, the experimental errors were determined for the different reaction parameters including reaction temperature and weight of used chemicals. An experimental error of less than 0.5% was obtained.

3.2.2.4 Purification

At the end of the transesterification reaction, products were left to settle in a decantation funnel for 1 h to ensure the separation of the mixture into two layers. The upper layer contained methyl esters, and the lower one consisted of glycerin, remaining catalyst, excess methanol, soaps formed and some drawn methyl esters. Lower concentrations of glycerin, catalyst and methanol were in the upper methyl ester phase.

The upper phase was washed firstly with an acid solution (0.2% H_2SO_4) and then repeatedly with distilled water (ratio of 1:1), until the pH of the washing water was the same as the distilled water. To remove unreacted glycerides and water, 2 g of magnesium sulfate ($MgSO_4$) were added at 35 °C for 45 min (Felizardo et al. 2006). Biodiesel was later dried over anhydrous sodium sulphate (Na_2SO_4) for 1 h under room temperature, and then filtered under reduced vacuum in order to obtain the purified biodiesel.

3.2.2.5 Biodiesel Quality Characterization

The characteristics of the final biodiesel product were determined according to the ASTM D 6751 and EN 14214 standard test methods, which include the acid value (ASTM D664), kinematic viscosity (ASTM D445), density (ASTM D4052), flash point (ASTM

D93), and methyl ester content (EN 14103). Biodiesel samples were prepared in DCM. FAMEs concentration in biodiesel was determined according to the EN 14103:2011 method using an internal standard. The analysis was performed on a Trace Ultragas chromatogram equipped with a flame ionization detector and an HP-INNOWAX capillary column (30m×250μm×0.25 μm). The flow rate of helium carrier gas was 1 mL/min. The split flow rate was equal to 100 mL/min, the inlet temperature was held at 320 °C and the flame temperature was 250 °C. The sample injection volume was 1 μL. The oven temperature program was as follows: start at 60 °C (2 min), ramp at 10 °C/min to 200 °C, ramp at 5 °C/min to 240 °C (7 min).

3.2.3 Assessment of Economic Feasibility of Biodiesel Production

To assess the production feasibility of biodiesel from WFOs, several cost categories were investigated. These were: acquisition cost of the WFOs depending on source, logistics cost incurred in the WFOs collection, inputs cost counting the different reagents and chemicals used for the production of biodiesel as determined through the laboratory scale transesterification reactions, production costs considering general expenses, equipment and fixed capital at the scale of plant capacity as per the data provided by the only biodiesel plant in Lebanon, and finally labor and taxes costs.

3.3 Results and Discussion

3.3.1 Production

Product yield is defined as mass percentage of final product transesterified and purified relative to the initial mass of WFOs introduced into transesterification. For the

mixtures of WFOs containing a level of FFAs higher than 5%, the acid-base transesterification resulted in a final yield of biodiesel ranging between 19.1 and 35% (w/w). Much higher yields were obtained in the case of the one-step base catalyzed transesterification and ranged between 96.9 and 99.4% (w/w). Considering the very low yield and negligible fraction of the oil mixtures with FFA levels higher than 5%, this fraction was not included in any further analysis and only the one-step base catalyzed transesterification was considered in the assessment of biodiesel production cost.

3.3.2 Characterization of Biodiesel

The physico-chemical properties of the biodiesel samples produced through a one-step base catalyzed transesterification were determined and are presented in Table 1. Triplicate analysis was performed in each case and the average results were reported. All reported parameters are in accordance with ASTM D6751 and EN 14214 standards except for the acid value. The latter exceeds the limits. In fact, 85% of the biodiesel samples showed an acid value ranging between 0.1 to 0.4 mg KOH/g, and 95% of these samples exhibited acid values between 0.1 and 0.25 mg KOH/g. The remaining 15% recorded an acid value slightly higher than 0.5 mg KOH/g (0.55 to 0.65 mg KOH/g).

Table 1. Physical and chemical properties of the biodiesel produced from WFOs

Property	**Value**	**Limits (EN 14214)**	**Limits (ASTM D6751)**
Acid value (mg KOH/g)	0.1 - 0.65	0.5	0.5
Kinematic viscosity at 40°C (mm^2/s)	4.21 - 4.78	3.5 - 5.0	-
Density at 15°C (g/cm^3)	0.886 - 0.891	0.860 - 0.900	0.860 - 0.900
Flash point (°C)	165 – 178	-	130
Water content (% w/w)	0.02 - 0.04	0.05	-
Potassium content (mg/kg)	1.7 - 3.9	-	5

Sulphated ash (%)	0.006 - 0.017	0.02	0.02
Ester content of FAME (% w/w)	96.9 - 99.4	96.5	96.5

The produced biodiesel characteristics agree with the Standard Specifications for Biodiesel Fuel. High levels of free fatty acids will influence fuel aging (Felizardo et al. 2006; Predojević 2008) and affect biodiesel stability (Dias et al., 2008). 85% of the samples showed an acid value lower than the limit, with values ranging from 0.1 to 0.4 mg KOH/g. For all analyzed samples, flash point was much higher than the minimum standard limit. Values ranged from 165 to 178◦C. These high values indicate the recovery of excess methanol and safety in handling and storage (Encinar et al., 2007; Srivastava and Verma 2008). High yields of FAME (96.9% - 99.4%) obtained prevent carbon deposition that lead to negative impacts on fuel injector performance allowing fuel atomization and distribution in the engine (Meher et al., 2006). FAME yields are very much related to the viscosity and density which serve as indicators of the completeness of the transesterification reaction and which are in compliance with the ASTM and European Biodiesel Standard (Felizardo et al. 2006; De Filippis et al., 2005).

3.3.3 Analysis of the questionnaire

Data generated from the questionnaire was gathered for a typical working week. Amongst the surveyed facilities, the average weekly generation of WFOs was 70 kg/week/restaurant (variance =45.832). Figure 3a describes the quantity of edible oils consumed per week by the surveyed restaurants and hotels. It indicates that 43% of all enterprises use more than 90 kg/week/restaurant of edible oil of different types.

Figure 3b presents the disposal method of WFOs by the different surveyed restaurants and hotel enterprises. Among the facilities, 9% disposed of WFOs once per day. The largest amount (79%) of enterprises disposed of the WFOs by a frequency of 1-4 days, while 18% of the facilities changed their frying oil with a fresh one every 5-8 days. The survey showed that WFOs recycling was quite high, whereby 87% of the facilities sell the used oil for economic benefits with little or no knowledge of its fate. The main buyers were independent venders, companies that export WFOs for biodiesel production outside Lebanon, or the biodiesel production plant currently operating in Lebanon (Figure 3c).

After putting a slight effort into providing the restaurants and hotels facilities with an understanding about the significance and the motives behind recycling WFOs for biodiesel production, a total of 76% of restaurants and hotels enterprises expressed willingness to cooperate with biodiesel manufacturers (Figure 3d). The willingness rate was accompanied with two main cooperation demands, summarized in a door-to-door collection service and a sensible WFOs selling price.

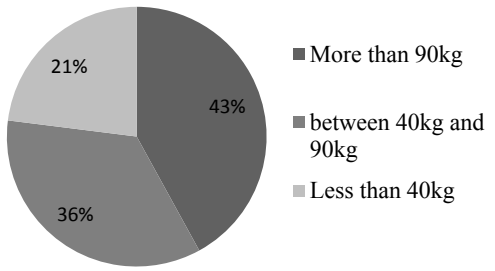

a: Quantity of vegetable oil consumed per week

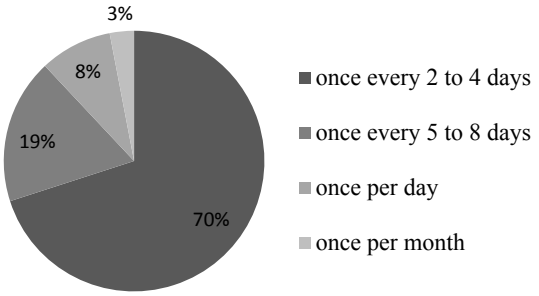

b: WFOs disposal frequency

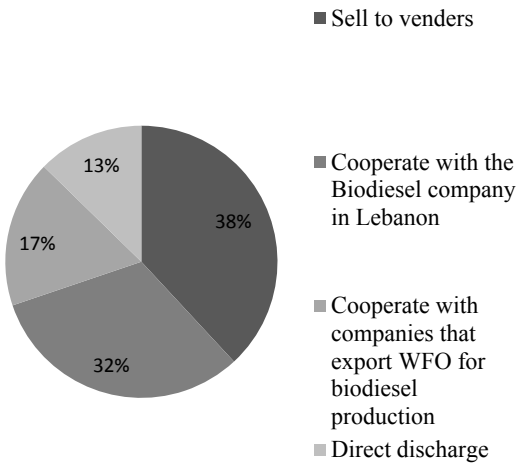

c: WFOs disposal method

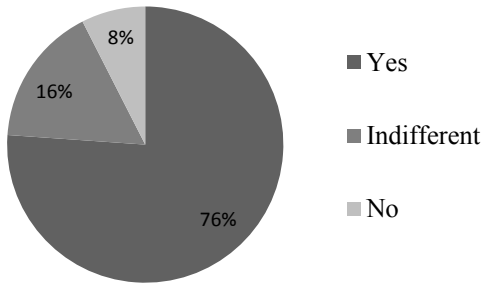

d: Willingness to cooperate with biodiesel producers

Figure 3. Questionnaire data per typical working week

3.3.4 Formation of the logistics costs

Logistics cost is of relevance to the total biodiesel production cost. WFOs need to be collected from the various supply sources that are geographically widespread, requiring planned collection. The cost of collection of WFOs from restaurants and hotels and its delivery to the biodiesel production plant should be embraced since the results obtained partially demonstrate the economic viability of biodiesel production from WFOs. To determine the logistics cost, different routing scenarios were developed, tested and compared based on the information acquired from the survey. The logistics cost per liter was calculated as the ratio of the total collection cost to the total volume of oil collected.

Upon conducting the survey in 100 restaurants and hotels in Beirut city, two major categories were strongly noted among the enterprises. 79% of the enterprises renew the frying oil they use every 4 days or less, while 19% of the enterprises replace the frying oil they use with fresh vegetable oil every 5 to 8 days. A very limited number of hotels change the frying oil used once every month. Since the amount of oil disposed of counted for only 0.03% of the total volume of oil, these corresponding hotels were no longer reckoned as collection points for the transportation design.

The assumptions for truck fuel was given a fixed cost of fuel of 0.2 $/km. The average driving speed for trucks in the city was set at 40 km/h and the fixed cost per vehicle adopted was $ 7.76 per hour, justifying the labor cost of the driver (owner of the truck) and his assistant. The regular working time for the driver and his assistant was calculated at 10 hours including the unloading time at the biodiesel production plant and the lunch-break. Justifiable over-times (traffic, unexpected events like accidents, and need for repair) were given an hourly rate of $ 8.7. Each enterprise was estimated to be visited once during a collection event and every visit calls for 10 minutes between the collections of WFOs and receipts.

To decide for the truck capacity, the total amount of WFOs from the hotels and restaurants were added accounting for a weight of 2 kg for each empty 20 L-container (Table 2).

A stationary collection system designed to gather WFOs stocks twice every 8 days. This system created separate collection times/routes/clusters for hotels and restaurants with similar WFOs disposal periods whereby the truck travels to and from the biodiesel production plant when fully loaded from the multiple collection points. The first collection was scheduled on

day 4 of the 8 day period and was geared to amass the WFOs from enterprises that changed the frying oil every 4 days or less; the second collection was planned for 4 days after the first collection to collect the WFOs generated from all restaurants and hotels including those that renew their oil every 4 days or less, having generated new stocks of WFOs.

Three scenarios were adopted, in which collection points were organized according to the categories discussed above and for which a routing system was created (available in supplementary information). Scenario 1 describes the collection of the WFOs twice every 8 days from the restaurants and hotels by the same truck of 6 t capacity (APPENDIX E: Figure E1). Scenario 2 defines the collection of WFOs by 1 vehicle of 5 t for the first collection and by two trucks of 5 t and 1 t capacity respectively during the second collection (APPENDIX E: Figure E2). Having observed that the different collection points could be easily separated into zones, Scenario 3 was chosen to proceed with the clustering technique which represents two different regions of Beirut: East zone and West zone. Each zone will be visited by a vehicle of 3 t each collection day (APPENDIX E: Figure E3).

Table 2. Determination of vehicle capacity based on the suggested collection scenarios

Parameters	**Scenario 1**		**Scenario 2**			**Scenario 3**			
WFOs collection	≤ 4 days	≤ 8 days	≤ 4 days	≤ 8 days		≤ 4 days		≤ 8 days	
Clusters	-	-	-	-		East	West	East	West
Amount of oil to collect (kg)	3851	4553	3851	3851	744	2423	1950	2632	2311
Weight of empty gallons (kg)	426	504	426	426	82	268	216	290	256
Total weight (kg)	4277	5057	4277	4277	826	2691	2166	2922	2567
Vehicle capacity (t)	6	6	5	5	1	3	3	3	3
Number of Vehicles	1		2			2			

Real distances were then generated on GIS which allowed the acquisition of the total travelling time, the cost per distance travelled, the driver's salary per operational day and the total cost per year for each scenario (Table 3).

Table 3. Total logistics cost per year for the different scenarios generated

	Scenario 1		**Scenario 2**			**Scenario 3**			
Parameters	**Generation of WFO ≤ 4 days**	**Generation of WFO ≤ 8 days**	**Generation of WFO ≤ 4 days**	**Generation of WFO ≤ 8 days**		**Generation of WFO ≤ 4 days**		**Generation of WFO ≤ 8 days**	
Cluster	-	-	-	-	-	**East zone**	**West zone**	**East zone**	**West zone**
Number of enterprises	64	79	64	64	15	31	33	38	41
Vehicle capacity (t)	6	6	5	5	1	3	3	3	3
Total distance traveled (km)	61.20	66.51	61.20	61.20	40.58	38.85	44.25	45.20	48.21
Total travelling time* (h)	15.41	18.09	15.41	15.41	6.56	8.24	8.72	9.59	10.18
Fixed fleet cost per distance ($/km)	12.24	13.30	12.24	12.24	8.12	7.77	8.85	9.04	9.64
Driver's salary per operational day ($/d)	113.77	137.08	113.77	113.77	66.70	66.70	66.70	66.70	68.27
Total cost per operational day ($/d)	126.01	150.38	126.01	126.01	74.82	74.47	75.55	75.74	77.91
Total cost including maintenance ($/yr)	35172.28		37795.60			36600.75			
Logistics cost ($/L)	0.08		0.09			0.08			

The development and testing of the different scenarios for vehicle routing permitted the comparison between these to determine the realistic WFOs collection routine with optimized logistics cost attached.

Logistics cost per liter is the ratio of the total collection cost to the total volume of oil collected twice every 8 days. The data corresponds to the collection for a typical year. The results show that the logistics cost for Scenarios 1 and 3 are similar. The increased distance in Scenario 3 is compensated by the total cost as the driver does not work for extra hours. Therefore, no extra fees beyond the 10 working hours are charged. Furthermore, the number of hours that the driver would need to satisfy in the event of driving a 6 t vehicle, is 5 to 8 hours beyond the 10 working hours. Such a scenario is not favored considering the appropriate and ethical working hours limit of any worker on one hand, and the means of being able to cover all the restaurants and hotels enterprises during opening hours on the other hand. In Scenario 2 the same vehicle of 5 t goes through the same routing system during the two collections. All the restaurants and hotels enterprises that change the frying oil every 5 to 8 days were grouped to be visited by a 1 t capacity vehicle. With this alternative, the logistics cost increased to 0.09 $/L of WFOs collected. Compared to the two other scenarios, scenario 3 presents results which show that the oil collected per vehicle is especially convenient to the maximum capacity of the vehicle (3 t), much as the number of hours consumed that is within the 10 hours working period, which demands no extra fee from the production plant. Therefore, clustering seems to optimize the commutation between cost and vehicle capacity. Taking scenario 3 into consideration, a possible variation in the agreement upon the amounts of WFOs supplied should be recognized. The offers are flexible enough to accommodate a variation of 25% accounting for tourism, seasonal flows, and

holidays. A logistics cost increase to 0.10 $/L of WFOs collected follows a decrease of 25% of the quantity of the WFOs offered (6,654 L every 8 days). That is mostly due to the shortage in the vehicles capacity filling. Whereas, in the case of an increase of 25% (13,820 L every 8 days), the logistics cost drops to 0.06 $/L of WFOs collected and the weight surcharge can be filled into the 3 t vehicles when well distributed.

3.3.5 Calculation of total cost

The final cost of large-scale biodiesel production from WFOs factors in the cost of acquiring the WFOs, the logistics cost incurred in WFOs collection, the cost of the different reagents and chemicals used for the production of biodiesel, production costs that include general expenses, equipment and fixed capital at the scale of a plant capacity, and finally labor and taxes costs. Logistics costs related to the distribution of the produced biodiesel to retail outlets were not included in the overall biodiesel costs as the studied biodiesel plant uses the ex-works method for the distribution of the end product.

3.3.5.1 Acquisition cost of WFOs

Large scale biodiesel production industries encounter some difficulties concerning raw material, among which is the unreliability of supplies (Y. Zhang et al. 2012). Findings in the field, state that the solution to this problem is to improve WFOs supply chain coordination and reduce the cost of WFOs supply (Peidong et al. 2009).

Figure 4 presents the acquisition cost of 20 L of WFOs (standard volume of the commonly used liquid storage container is 20 L). The average acquisition price of 1 L of WFO was found to be US$ 0.35 with a standard deviation of 0.05.

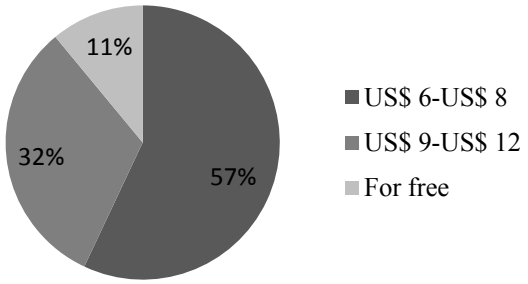

Figure 4. WFOs acquisition cost per 20 L WFOs

3.3.5.2 Capital, manufacturing and chemicals' cost

The present cost takes into account the capital cost, the equipment cost including material for WFOs transesterification and biodiesel purification, the maintenance cost, and the cost of production loss. It will be called production cost. Plant capacity is an important factor affecting production processes as well as the catalyst choice. Marchetti et al. studied a biodiesel plant of 36,036 t/yr capacity that uses an acid catalyst pretreatment process before the alkali base transesterification. The production cost of such a plant turned out to be 0.31 US$/L (Marchetti and Errazu 2008b). On the other hand, Bender studied a much larger biodiesel production plant (one that employs an alkali-catalyst), of 115,000 t/yr capacity. The production cost there turned out to be 0.10 US$/L (Bender 1999). In the present study, the production procedure for collected WFO did not need any acid catalyst pretreatment.

Therefore, additional equipment costs related to acid transesterification were omitted. The choice of alkali catalyst was validated by the Lebanese biodiesel production plant we interviewed. This biodiesel production plant is a medium scale plant of 4,000 t/yr capacity whose average production cost per liter of biodiesel is 0.20 US$/L (standard deviation = 0.05 US$/L).

For the tansesterification process to be established, the inputs adopted were the WFOs, alcohol and catalyst. For 100% biodiesel produced the technical coefficients of the different inputs to the production procedure were considered. Methanol was adopted at 20% consumption by volume and the catalyst, at 0.75% consumption by mass.

The methanol cost is based on the purchase price provided by the Lebanese biodiesel plant. The resulting average price was US$/L 0.60 with a standard deviation of 0.05. The catalyst cost adopted in the research was US$/L 0.11 with a standard deviation of 0.01. Therefore, involving the acquisition of methanol and catalyst, for each biodiesel liter produced, there is an average cost of US$ 0.12 (standard deviation = 0.01 US$/L) and US$ 0.00083.

3.3.5.3 Labor cost and Utility and taxes costs

For the 4,000 T/yr biodiesel plant operating in Lebanon, a total of 6 operators including 5 technical operators and 1 chemical operator, are employed. Since the production process is continuous and fully automated, it requires less supervision and therefore, the labor cost remains the same even when the plant capacity increases. The production plant consists of six total operators. Five technical operators are paid a total monthly salary of US$ 2500

and one chemical operator is satisfied a salary of US$/month 2000. Based on the operators' monthly salaries, the study found that for each biodiesel liter produced, there is a labor cost of US$/L 0.12.

Utility and taxes costs include value-added tax, city tax, security tax, electricity costs and insurance which add a total of US$/L 0.10 biodiesel produced. The source for this information was also the biodiesel plant.

3.3.5.4 Glycerin and FAEs credit

Glycerin is generated as a co-product of the transesterification reaction. It has many applications in the pharmaceutical, food and chemical industries (Dhar and Kirtania 2009). The process used to purify crude glycerin is composed of methanol removal, neutralization, distillation and bleaching (Xiao et al., 2013). The income from the sale of glycerin was considered in the calculation of the total cost and provided by the biodiesel production plant. A high total value of US$/L 0.10 of glycerin produced is what is currently marketed by the biodiesel plant to different companies. The glycerin acidification process separates the crude glycerin into three layers of FAEs on the top, glycerin rich layer in the middle and inorganic salts at the bottom. Fatty acids' esters (FAEs) is a high priced product that can be used as lubricant of tablets (Aoshima et al. 2005). According to the biodiesel plant, the net benefit from FAEs produced by the purification of glycerin is US$/L 0.30.

3.3.5.5 Biodiesel cost calculation and analysis

The main variables for the calculation of the cost of biodiesel from WFOs are the inputs used in the process of biodiesel production, taxes, and the logistics costs. The income from glycerin and FAEs is also considered in this calculation. As the values for most of the variables can vary, the calculation was done based on all possible combinations of the three different values for the logistics, WFOs acquisition, biodiesel production and methanol costs, yielding $3^4 = 81$ scenarios. The three values used for each variable represent a minimum, average and maximum cost based on the numbers obtained above. The optimum logistics values obtained for the clustered scenario were considered as the logistics costs. As the labor, taxes and the glycerin costs are assumed fixed and the catalyzer cost is not significant in the total cost composition, variations of these variables were not considered in the biodiesel total cost analysis. The minimum, average and maximum values of the variables used in the establishment of the cost of biodiesel are summarized in Table 4.

Table 4.Total fixed and varied costs for biodiesel production from WFOsTable 4: total fixed and varied costs for biodiesel production from WFOs

	Logistics	**Acquisition**	**Production**	**Methanol**	**Catalyst**	**Labor**	**Taxes**	**Glycerin +FA**
Minimum cost (US$/L)	0.06	0.30	0.15	0.11				
Medium cost (US$/L)	0.08	0.35	0.20	0.12	0.00083	0.12	0.10	- 0.40
Maximum cost (US$/L)	0.10	0.40	0.25	0.13				

Figure 5 presents the results for the total biodiesel cost obtained from the different 81 generated scenarios. The average biodiesel cost of the different scenarios is US$/L 0.57. The cost can drop to US$/L 0.42 in the best case scenario and rise to US$/L 0.71 in the worst case scenario. Hizari et al. (2014) reported a total cost of US$/L 1.2 for biodiesel produced from WFOs . The high share of costs was mainly due to the great expense of WFOs (US$/L 0.66) and the human labor payments (US$/L 0.33). Lee at al. conducted the economic analysis of three continuous biodiesel processes with production capacity of 40,000 t/yr and including a conventional alkali-catalyzed process using waste vegetable oil. Also, an alkali-catalyzed process of WFOs of a 40,000 t/yr of biodiesel produced a total biodiesel cost of US$/L 0.76 including glycerol credit and revenues from biodiesel sales. Glisic et al. performed a techno-economic analysis of biodiesel production from WFOs using, among other assessed production technologies, the homogeneous alkali catalyzed process. They reported a cost of 0.63 US$/L of produced biodiesel at process capacities of 100,000 t/yr (Glisic et al., 2016). Similarly, Patle et al., conducted a techno-economic analysis of an alkali catalyzed biodiesel production of waste palm oil and concluded that the process profitability increases with the increase in production capacity (Patle et al. 2014). The present study's lower average total biodiesel cost could be attributed to the low WFOs expenses and labor cost as well as the revenue from biodiesel production co-products.

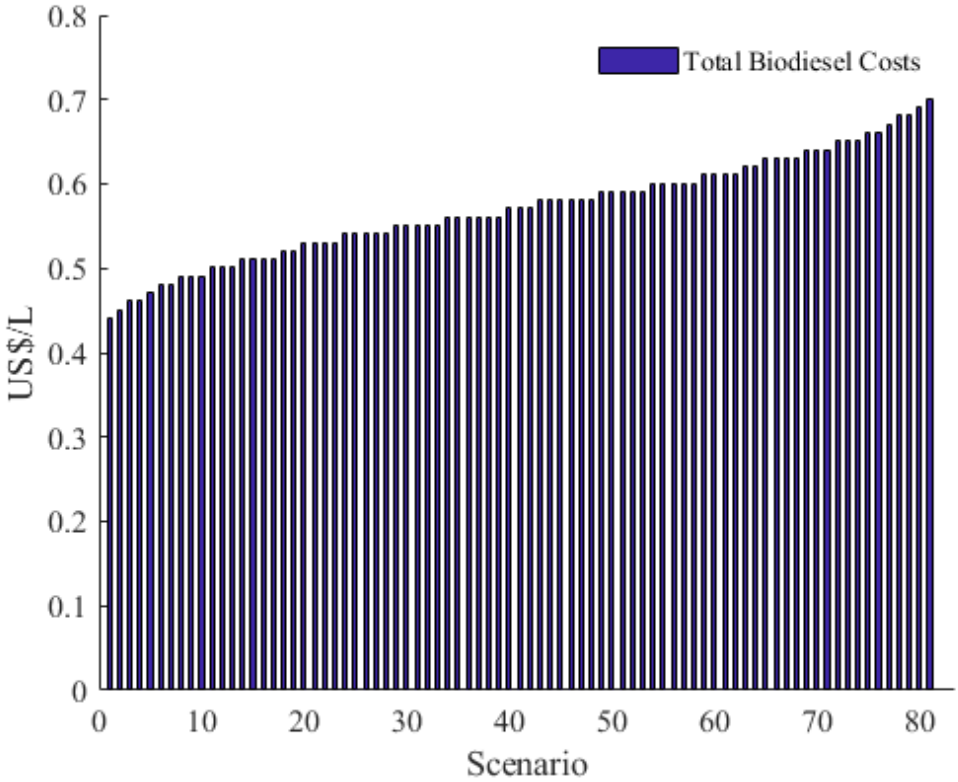

Figure 5. Total biodiesel cost

3.3.5.6 Sensitivity Analysis

A sensitivity analysis was performed in order to define the impact of key parameters on biodiesel cost variation. Important variables included logistics cost, WFOs acquisition cost, production cost and methanol cost.

Table 5. Influence of input parameter variation on Biodiesel cost

Varied input	Logistics (US$/L)	Acquisition (US$/L)	Production (US$/L)	Methanol (US$/L)	Input variation (%) [a]	Simulated biodiesel cost (US$/L)	Biodiesel cost variation (%) [b]	Relative sensitivity ζ [c]

Logistics	**0.08**	0.35	0.2	0.12		0.57		0.14
	0.06	0.35	0.2	0.12	-25	0.55	-3.5	
	0.1	0.35	0.2	0.12	25	0.59	3.5	
Acquisition	0.08	**0.35**	0.2	0.12		0.57		0.61
	0.08	**0.3**	0.2	0.12	-14.3	0.52	-8.8	
	0.08	**0.4**	0.2	0.12	14.3	0.62	8.8	
Production	0.08	0.35	**0.2**	0.12		0.57		0.35
	0.08	0.35	**0.15**	0.12	-25	0.52	-8.8	
	0.08	0.35	**0.25**	0.12	25	0.62	8.8	
Methanol	0.08	0.35	0.2	**0.12**		0.57		0.21
	0.08	0.35	0.2	**0.11**	-8.3	0.56	-1.8	
	0.08	0.35	0.2	**0.13**	8.3	0.58	1.8	

[a] Percent difference between the new input value and the value used for the base simulation, the latter being 0.08, 0.35, 0.2 and 0.12 for logistics, acquisition, production and methanol costs, respectively.
[b] Percent difference between the simulated biodiesel cost using the new input value and the biodiesel cost obtained in the base simulation (0.57083$/L)
[c] Relative Sensitivity = $\zeta=(\Delta Y/Y)/(\Delta X/X)$ where Y is the sensitivity index value (simulated biodiesel cost) and X is the input parameter value that is varied.

The absolute values of the relative sensitivity $|\zeta|$ were found to be 0.61, 0.35, 0.21 and 0.14 for the WFOs acquisition cost, production cost, methanol cost and logistics cost, respectively (Table 5). That is to say that the model is the most sensitive to the WFOs' acquisition cost followed by the production cost, almost equally least sensitive to the logistics cost and the methanol cost, nearly 2.5 times more sensitive to the production cost than to the logistics cost and nearly 2 times more sensitive to the WFOs acquisition cost than to the production cost.

3.3.5.7 Long-Term Economic Assessment of Biodiesel

The study's resulting production costs can be compared with the Lebanese market price of diesel fuel. Figure 6 presents break-even lines for biodiesel minimum, average, and

maximum costs, in relation to the minimum, average, and maximum prices of marketed diesel in Lebanon in years 2011 to 2017. For the years 2011, 2012, and 2013 biodiesel costs are lower than the minimum commercialized diesel for the respective years which demonstrates that transesterified WFOs could be an economically-sustainable fuel alternative to common diesels. Within the 81 scenarios, only 4 resulted in a cost higher than the minimum diesel fuel price for the year 2014. However, for the years 2015 through 2017, the average cost of biodiesel production is no longer competitive with the average petroleum diesel prices. In years 2015 and 2017, whereby diesel prices hovered at 0.48 US$/L, only the minimum biodiesel cost calculated in this study is in general competitive. This minimum cost is lower than the maximum tolerance for biodiesel viability in comparison with the minimum diesel cost in 2015 and minimum and average costs in 2016. This makes the viability of biodiesel as alternative fuel highly dependent on the actual cost of diesel commercialization.

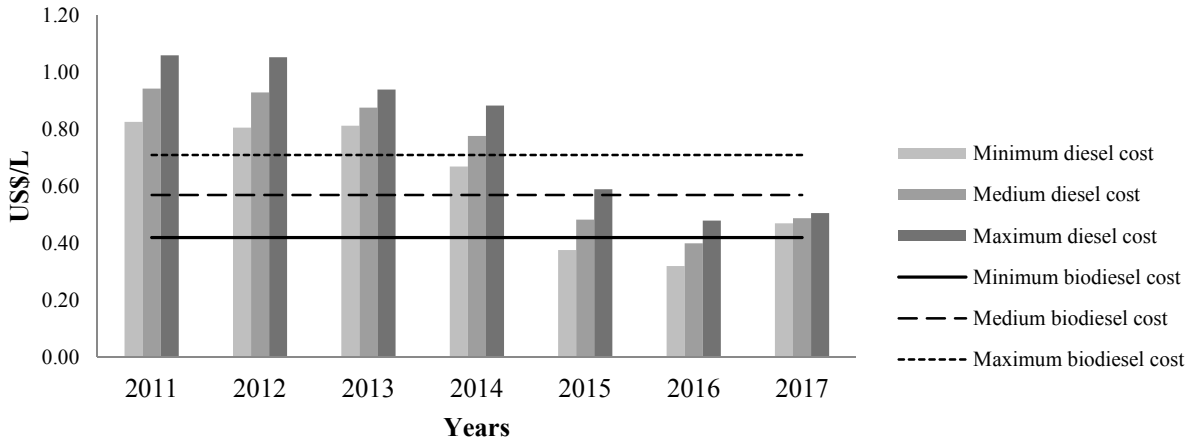

Figure 6. Variation of diesel oil cost in Lebanon

Therefore, government's intervention in the promotion of social and economic changes is vital to ensure the viability of biodiesel production from WFOs in Lebanon. Sufficient government enforcement and support leading to a significant reduction in overall WFOs acquisition cost to which the global biodiesel production is mostly sensitive can lead to the success and stability of the biodiesel production for the long term. This can be attained by adopting different measures that commit the government towards biodiesel industries. In this context, adequate government official policies will be critical in areas such as developing capital grants for biodiesel producers and increasing fuel levy rebates (Steenberghen and López 2008). Governmental measures would include encouraging restaurants and hotels to participate in the biodiesel supply chain, by implementing positive actions. Among these, the connection of relevant laws about WFOs with relevant laws related to renewable energy could be considered (Wiesenthal et al. 2009). Through firm directives, WFOs recycling could also be incorporated into the tax incentive system and into the health assessment, class assessment, and honor assessment of the restaurants and enterprises promoting competition (Schulte 2004; Wong et al., 1996).

3.3.6 Environmental and net energy benefit analysis

Aside from solving significant disposal problems, proper utilization and management of WFOs as raw material for biodiesel production reduce greenhouse gas emissions from engines. Substituting conventional petroleum diesel with biodiesel or its blends reduces particulate matter (PM) emissions by up to 75% (Von Wedel 1999). Total hydrocarbon emissions reductions of 70% were supported by EPA and a number of other studies (Alam et al. 2006; Nwafor, 2004). A carbon monoxide (CO) emission reduction of almost 50% with

biodiesel with respect to conventional diesel fuel is reported (Krahl et al. 2003; Peterson and Reece 1996). Also, biodiesel reduces net CO_2 emissions by 78.45% compared to petroleum diesel (Sheehan et al. 2000). To be a viable substitute for a fossil fuel, biodiesel should not only be economically competitive with petroleum diesel but also to have superior environmental benefits over it and provide a net energy gain over the energy sources used to produce it. Therefore, the energy requirements for the key steps in producing biodiesel and petroleum diesel were compared. Primary energy needed for the production of petroleum diesel by fractional distillation and for refining crude oil are 1.113 and 0.0650 MJ/MJ Diesel respectively (Sheehan et al. 2000), resulting in a total energy input of 1.178 MJ/MJ Diesel. For biodiesel production from WFOs in Lebanon, primary energy inputs are WFOs, methanol, KOH, human labor, electricity and machinery (including land). Total energy equivalent per liter biodiesel was obtained by multiplying energy equivalent of input by the quantity needed per unit volume of biodiesel (L) (Table 6). Total energy equivalent (MJ/L) was then converted to primary energy used to produce 1 MJ of biodiesel; using energy equivalent of Biodiesel produced which is 37.25 MJ/L (Kitani 1999). Total energy input for biodiesel production is 0.867 MJ/MJ Biodiesel. The slightly lower energy equivalent of biodiesel counter to that of petroleum diesel reflects a lower demand for process energy across the production of biodiesel from WFOs, making biodiesel more energy efficient than petroleum diesel. Also, a total energy input and energy output of biodiesel production are calculated as 32.274 and 44.614 MJ/L which show that biodiesel production results in a positive net energy balance. The energy output-input ratio is 1.38 whereby, for each MJ of energy consumed to produce biodiesel, 1.38 MJ of energy is obtained. The energy output-input ratio was obtained by the following equation

$$\frac{\text{Total output Energy equivalent per liter of biodiesel (MJ/L)}}{\text{Total input Energy equivalent per liter of biodiesel (MJ/L)}}.$$

Table 6. Total energy use for biodiesel production

	Energy production	Unit Energy	Quantity per unit volume of biodiesel (L)	Energy equivalent (MJ/unit)	Total Energy equivalent per liter of biodiesel (MJ/L)	Total Energy equivalent per energy equivalent of 1L of biodiesel (MJ/MJ biodiesel)
Inputs	Human labor	h	0.556	1.96[a]	1.090	0.029
	WFOs	L	1	23.16 [a]	23.160	0.622
	Methanol	L	0.271	26.60 [b]	7.209	0.194
	KOH	g	0.0075	19.87 [c]	0.149	0.004
	Electricity	kWh	0.013	11.93 [a]	0.155	0.004
	Machinery	h	0.009	57.78 [d]	0.520	0.014
Total					32.274	0.867
Outputs	Biodiesel	L	1	37.25 [e]	37.250	1
	Glycerin	L	0.12	25.30[f]	3.036	0.082
	Methanol	L	0.11	26.60 [b]	2.926	0.079
	Soap	L	0.019	42.105 [g]	0.80	0.021
	Glycerides	L	0.009	66.87 [g]	0.602	0.016
Total					44.614	1.198

[a] Source: Shirazi et al., 2014.
[b] Source: Singh and Mittal, 1992.
[c] Source:Al-Zuhair et al., 2012.
[d] Source: Huo et al., 2008.
[e] Source: Kitani and Jungbluth, 1999.
[f] Source: Sheehan et al., 2000; Krohn and Fripp, 2012.
[g] Source: Reusch, 1999.

Hence, biodiesel provides sufficient economic and environmental benefits to merit investment by NGOs and governmental agencies.

3.4 Conclusion

The study proposed vehicle routing model scenarios to determine logistics network for the profitable reuse of WFOs in Beirut and generated integrated total biodiesel cost. Despite being an economically-sustainable fuel alternative for the years 2011 through 2014,

the viability of biodiesel production from WFOs doesn't apply to the years 2015 to present. The economic sensitivity assessment of biodiesel production from WFOs allowed a better understanding of cost interactions and showed that biodiesel production cost is economically competitive with fossil diesel when a subsidy policy on WFOs acquisition cost is implemented by the government. Benefit analysis showed that biodiesel presents superior environmental benefits over petroleum diesel and its production provides a net energy gain. Accordingly, by interacting with local authorities and creating a more covered supply chain coordination system, it would be possible to successfully reuse WFOs for the production of biodiesel on a national scale for the long term, and reduce the environmental damages caused by their disposal.

CHAPTER 4

COMPARATIVE STUDY ON THE CATALYTIC PERFORMANCE OF HZSM-5 ZEOLITES FOR BIODIESEL PRODUCTION: STRATEGY TO INCREASE CATALYST EFFECTIVENESS.

In this chapter, strategies to improve molecular transport and accessibility of ZSM-5 zeolites were investigated for the esterification of linoleic acid with methanol as a model reaction for biodiesel production. Zeolite crystals with short diffusion paths and hierarchical porosity were compared with conventional coffin-shaped microcrystals for their catalytic activity in terms of acidic properties and pore structure. As-synthesized catalytic materials were characterized with instruments including XRD, SEM, TEM, BET/BJH porosimetry analysis, X-Ray fluorescence, and FTIR. The effect of pore size on the molecular diffusion limitation was investigated by Thiele modulus calculation.

4.1 Introduction

Biodiesel produced from waste renewable resources is a biodegradable, environmental friendly and non-toxic alternative fuel to the depleted petroleum diesel (Baskar and Aiswarya 2016; Amid. (2005) Demirbas 2005). Generally, biodiesel is produced by the transesterification reaction using a homogeneous base catalyst (Tubino et al., 2014). Despite being cheap, readily available and having high catalytic efficiency, this process is highly sensitive to water and free fatty acid (FFA) contents in the feedstock. At high contents, the reaction can change to saponification, which creates several problems in downstream purification and methyl ester recovery due to the difficult separation of

products and the increase in viscosity (Atapour & Kariminia, 2011; Tan et al., 2015). Freedman et al. reported that homogeneous acid catalysts are insensitive to FFA content and are better than the alkaline catalysts for the transesterification of oils with FFA greater than 1% (Freedman et al., 1984). However, this process also presents different drawbacks which can be overcome through the use of heterogeneous acid catalysts. These solid catalysts minimize the problems associated with homogeneous catalysis in terms of catalyst separation, recycling and regeneration (Chung et al., 2008; Fan et al., 2007). Further, transesterification of oils using solid acid catalysts is non-corrosive and eliminates extensive product purification step (Batonneau-gener et al., 2008; Saravanan et al, 2015). Nevertheless, one of the main problems associated with the use of heterogeneous catalysts in the transesterification reactions is the formation of three phases (alcohol, oil and solid catalyst) which lowers the rate of the reaction and the biodiesel yield, by limiting the diffusion of reagents and products (Helwani et al, 2009; Zabeti et al., 2009). Zeolites are crystalline solids with well-defined structures containing silicon, aluminum and oxygen in their framework (Auerbachet al., 2003). They have been finding applications in many areas of catalysis, especially in transesterification reactions for biodiesel production (Doyle et al., 2017; Mowla et al., 2018; Narkhede & Patel, 2014; Otieno et al., 2018; Thoai et al., 2017; Vieira et al., 2017). They exhibit high acid activity and total surface area with shape selective features not available in equivalent amorphous catalysts (Gardy et al., 2017; Park et al., 2010; Ramachandran et al., 2011; Thiruvengadaravi et al., 2012). However, they are usually synthesized with crystal sizes in the micrometer range and, therefore, with negligible external surface area. Both characteristics set severe limitations for their use in the conversion of bulky compounds. Alternative strategies enhancing mass transfer in

zeolite-catalyzed reactions by shortening the diffusion length and introducing a hierarchical porosity (micro- and mesoporosities) could make the active sites in the zeolites more accessible and thus the heterogeneous acid transesterification involving large molecules such as fatty acids more feasible. Only one study assessed the effect of pore size on the internal mass transfer limitation in the esterification of oleic acid with ethanol using microporous acid zeolites (Beta zeolite and ZSM-5 zeolite) and micro-mesoporous acid zeolites (MFI type ZRP-5 zeolite) (Sun et al. 2015). In the present study, the catalytic behavior of ZSM-5 zeolites exhibiting distinct crystal morphologies (conventional coffin-shaped microcrystals, nanocrystals, nanosheets, and nanosponges) was assessed in terms of acidic properties and pore structure in the esterification of linoleic acid, as a model reaction for biodiesel production. The influencing factors of esterification including reaction temperature, molar ratio of linoleic acid to methanol and reaction time were analyzed. Thiele modulus model was used to discuss the correlation between effective mass transfer within the pore size of the zeolites and their catalytic performance based on experimental results.

4.2 Experimental section

Tetrapropylammonium hydroxide is used as template for the conventional zeolites whereas bifunctional compounds which could generate micropores and mesopores simultaneously were specifically designed for the synthesis of hierarchical ZSM-5.

4.2.1 Structure directing agent synthesis

The di-quaternary ammonium-type surfactant $C_{22}H_{45}$-$N^+(CH_3)_2$-C_6H_{12}-$N^+(CH_3)_2$-$C_6H_{13}Br_2$ (abbreviated as C22-6-6), used for the ZSM-5 nanosheet synthesis were synthesized in two steps following the modified procedures reported by Na et al. (Na et al. 2010). First, 0.01 mol of 1-bromodocosane and 0.1 mol of N,N,N',N'–tetramethyl–1,6–diaminohexane were dissolved in 100 mL of acetonitrile/toluene mixture (1:1 v/v) and reacted under magnetic stirring at 60 °C for 10 h. After cooling to room temperature, the solvent was evaporated and the product [$C_{22}H_{45}$-$N^+(CH_3)_2$-C_6H_{12}-$N(CH_3)_2$]Br (denoted C22−6−0) was washed with diethyl ether and dried in a vacuum oven for 2 h at 50 °C. Second, 0.01 mol of C22-6-0 and 0.02 mol of 1-bromohexane were dissolved in 40 mL of acetonitrile and refluxed for 10 h under stirring.

For the synthesis of ZSM-5 nanosponges, the zeolite-SDA-functional surfactant $C_{18}H_{37}$–$N^+(CH_3)_2$–C_6H_{12}–$N^+(CH_3)_2$–C_6H_{12}– $N^+(CH_3)_2{}^-C_{18}H_{37}(Br^-)_3$ (abbreviated as 18–N_3–18) was prepared by separately synthesizing $C_{18}H_{37}$–$N^+(CH_3)_2$–C_6H_{12}–Br(Br^-) and $C_{18}H_{37}$–$N^+(CH_3)_2$–C_6H_{12}–$N(CH_3)_2$ through organic reactions as described by (Na et al. 2011). First, $C_{18}H_{37}$–$N^+(CH_3)_2$–C_6H_{12}–Br(Br^-) was prepared by dissolving 0.034 mol of N,N'–dimethyloctadecylamine and 0.34 mol of 1,6–dibromohexane in 1000 mL acetonitrile/toluene mixture (1:1 v/v). The mixture was heated under stirring at 60 °C for 12 h with reflux. Second, 0.030 mol of 1–bromooctadecane and 0.300 mol of N,N,N',N'–tetramethyl–1,6–diaminohexane were dissolved in 600 mL acetonitrile/toluene mixture (1:1 v/v) and heated at 60 °C for 12 h to obtain a solid product with the formula of $C_{18}H_{37}$–$N^+(CH_3)_2$–C_6H_{12}–$N(CH_3)_2$(Br^-). Finally, equimolar amounts of $C_{18}H_{37}$–$N^+(CH_3)_2$–C_6H_{12}–

Br(Br-) and $C_{18}H_{37}–N^{+}(CH_3)_2–C_6H_{12}–N(CH_3)_2(Br^-)$ were dissolved in acetonitrile (60 mL) and refluxed for 12 h under agitation to produce the 18–N_3–18 surfactant.

For all the reactions, solvent was evaporated after cooling to room temperature for product precipitation. The products were further filtered, washed with diethyl ether, and dried in a vacuum oven at 50 °C for 2 h.

The purity of the final solid organic products; C22-6-6 and 18–N_3–18 was analyzed by solution-state ^{1}H NMR, with $CDCl_3$ as the solvent.

4.2.2 Catalysts Synthesis

Typical ZSM-5 zeolite large crystals with coffin-shape morphology were synthesized by dissolving 0.26 g of sulfuric acid (Aldrich) and 3.19 g of tetraethoxysilane (TEOS, Aldrich, 98%) in 10.75 g of distilled water in a 45 ml teflon-lined stainless-steel autoclaves. 0.36 g of sodium hydroxide (Riedel de Haen, 99%) and 0.1 g of $Al_2(SO_4)_3.18H_2O$ (Rectapur, 99%) were added to the mixture. 3.03 g of tetrapropylammonium hydroxide (TPAOH) aqueous solution (25 wt%, Fluka) was finally added in order to set the molar composition of the gel to: $100SiO_2$: $1Al_2O_3$: $30Na_2O$: $18H_2SO_4$: 20TPAOH: $4000H_2O$ (Dhainaut et al. 2013). The gel was then stirred at 1000 rpm during 30 min, heated at 60 °C for 4 hours and finally placed in a tumbling oven at 150 °C for 4 days. The autoclaves were set at 30 rpm.

ZSM-5 zeolite nanocrystals were synthesized following the molar composition $50SiO_2$: $1C_9H_{21}O_3Al$: 6NaBr: 10TPAOH: $450H_2O$. 0.31 g of $C_9H_{21}O_3Al$ and 12.1 g of tertrapropylammonium hydroxide (25 wt% TPAOH aqueous solution, Fluka) were dissolved in 3 g of distilled water and stirred at room temperature for 20min. 0.93 g of

NaBr were added to the solution which was stirred for 20 additional minutes. 4.48 g of porous silica gel (100 mesh) was then added and well mixed with the solution. The gel was finally placed in an oven at 170 °C for 24 hours.

ZSM-5 nanosheets were synthesized in the same conditions described above for ZSM-5 zeolite large crystals with coffin-shape morphology. The only difference being the usage of 1.08 g of the diquaternary ammonium- type surfactant (C22-6-6) instead of tetrapropylammonium hydroxide aqueous solution (25 wt%). The composition of the gel therefore being, $100SiO_2 : 1Al_2O_3 : 30Na_2O : 18H_2SO_4 : 10C_{22}H_{45}–N^+(CH_3)_2–C_6H_{12}–N^+(CH_3)_2–C_6H_{13}Br_2 : 4000H_2O$.

To produce ZSM-5 nanosponges of molar composition $100SiO_2 : 2.5Al_2O_3 : 22Na_2O : 800EtOH : 5\ C_{18}H_{37}–N^+\ (CH_3)_2–C_6H_{12}–N^+\ (CH_3)_2–C_6H_{12}–\ N^+\ (CH_3)_2{}^-C_{18}H_{37}(Br^-)_3 : 7100H_2O$ as described by Na et al. (Na et al. 2011), 0.08 g of sodium aluminate ($NaAlO_2$ of 56.7 wt% Al_2O_3, 39.5 wt% Na_2O and 3.3 wt% H_2O), 0.26g of sodium hydroxide (Riedel de Haen, 99%), 3.54 g of tetraethoxysilane (TEOS, Aldrich, 98%), 3.07 g of EtOH (99%) and 1.28 g of $18–N_3–18$ were dissolved in distilled water under stirring, in a Teflon-lined stainless steel autoclave. The gel was stirred at 1000 rpm at room temperature during 30 min, then at 60 °C for 6 hours and finally placed in a tumbling oven at 150 °C for 5 days at 30 rpm.

After synthesis, the different ZSM-5 zeolites were filtered, washed with distilled water, dried overnight at 105 °C, and finally calcined at 550 °C for 8 h in air to remove the organic structuring agents.

The synthesized Na-type ZSM-5 zeolites were modified by an ion exchange process using NH_4Cl as a precursor. The dried zeolites were dispersed in 1 M solution of NH_4Cl

with a ratio of 1:20 and heated under stirring at 80 °C for 2 h in a round bottom flask fitted with a reflux condenser. The ion exchange process was repeated three times and the mixture was recurrently washed with distilled water, dried at 105 °C and then calcined in air at 550 °C for 10 h to obtain the H^+ exchanged zeolite ready for catalysis. The exchanged zeolites of HZSM-5 big crystals, nanocrystals, nanosheets and nanosponges were labeled MC-HZSM-5, NC-HZSM-5, NSh-HZSM-5, and NS-HZSM-5, respectively.

4.2.3 Catalysts Characterization

X-ray diffraction patterns and purity of the different zeolite materials were recorded using a PANalytical MPD X'Pert Pro diffractometer operating with Cu Kα radiation (λ = 0.15418 nm) equipped with an X'Celerator real-time multiple strip detector (active length = 2.122 ° 2θ). The powder pattern was collected at 22 °C in the low range $0.5 < 2\theta < 5°$ and wide range $3 < 2\theta < 50°$ with a 2θ angle step of 0.017° and a time step of 220 s.

The homogeneity and the morphology of the synthesized crystals were examined using a scanning electron microscopy (SEM) (Philips XL 30 FEG microscope) working at 7 kV accelerating voltage and a transmission electron microscope (TEM) (Philips model CM200), operating at 200 kV, with a point-to-point resolution of 0.3 nm.

The pore size, pore volume and surface area of the samples were measured by N_2 sorption (ASAP 2420 system, Micrometitics, USA) and calculated using BET and t-plot methods. Prior to each manometric measure, 50 mg of the zeolitic samples were outgassed to a residual pressure of less than 0.8 Pa at 300 °C for 15 h. Nitrogen sorption measurements were performed at −196 °C and mesoporous volume was calculated using the BJH method.

The Si/Al molar ratio of the synthesized samples and their successful exchange was evaluated by X-ray fluorescence (Philips, Magic X).

The amount of Brønsted and Lewis acid sites were measured by pyridine adsorption followed by infrared spectrometry in a Thermo Nicolet Magna 550-FT-IR spectrometer. Zeolite samples were pressed into a self-supported wafer of 20 mg. Each pellet was then introduced in the analysis cell and pretreated at 450 °C in air for 12 h. The temperature was then decreased at 200 °C under air and the cell was placed in vacuum during 1 h to remove physisorbed species. The temperature was then decreased to 150 °C, and the pyridine introduced in the cell for 5 min under vacuum for 1 h. The amounts of Brønsted [$PyrH^+$] and Lewis [PyrL] acid sites were determined from the integration of peaks' areas at 1545 cm^{-1} and 1454 cm^{-1} respectively, using extinction coefficients previously determined by Guisnet et al. (1997).

4.2.4 Esterification Reaction Procedure

For all types of HZSM-5 produced, the esterification reaction of linoleic acid (ACROS, 99 %) with methanol (Chromasolv, 99.9 %) was performed by reflux in a 50 ml round-bottomed flask, under stirring (550 rpm). The reactor was loaded with 0.6 ml (equivalent to 0.54 g and 1 mole) of linoleic acid and the desired amount of methanol (6:1, 12:1 or 25:1 methanol to linoleic acid by molar ratio) was then added. Esterification was carried out over a range of reaction temperatures (60, 140 and 180 ºC) at a catalyst loading of 10 wt% for 6 h. The desired amount of catalyst was dried before reaction at 105 ºC. Kinetics study was performed for the HZSM-5 type which showed the highest conversions at reaction times ranging between 0 and 24 h by sacrificing the solution in reaction flasks

consecutively with time. For the conditions used, the esterification reactions were performed in triplicates.

At the end of the esterification reactions, extraction of linoleic acid and produced methyl esters adsorbed to the solid zeolites was ensured. The content of the reaction flasks was extracted with 50 ml of methanol to dissolve the water produced during the esterification reaction, followed by two dichloromethane (DCM) (Fisher, 99.8 %) extractions of 50 mL each, to dissolve the residual linoleic acid and produced methyl esters. The liquid extracts were separated from the solid catalysts by gravity filtration through a bed of filtration beads and 0.2 um filter paper and analyzed for methyl esters and residual linoleic acid.

4.2.5 Fatty Acids and Methyl Esters analysis

Methyl linoelate content in the liquid extracts was determined by gas chromatography (GC) analysis (Trace Ultragas chromatogram). The GC was equipped with a HP-INNOWAX capillary column (30 m × 250 µm × 0.25 µm) and a flame ionization detector (FID). Helium was employed as carrier gas at 1 mL/min. The injector temperature was 250 °C at splitless conditions, the FID was set at 300 °C and the injection volume of the sample was 5µl. The initial oven temperature was set at 60 °C with an equilibration time of 2 min. After the isothermal period, oven temperature was increased to 200°C at a heating rate of 10°C/min and finally increased to 240°C at a ramp of 5°C/min and held for 7 min. Peaks of methyl esters (namely Methyl linoleate among other methyl esters) were identified

based on reference standards (Supelco 37 component FAME mix in DCM, TraceCert). The yield of the esterification reaction was determined by the following equation (4-1):

$$Yield\ (\%) = \frac{\sum C_{methyl\ esters} \times V_{extract}}{M_{0\ Linoleic\ acid}} \times 100 \qquad 4\text{-}1$$

Where, $C_{methyl\ esters}$ is the concentration in g/L quantified by GC/FID, $V_{extract}$ is the total volume (L) of the liquid extract, and $M_{0\ Linoleic\ acid}$, the initial mass of linoleic acid added to the reactor.

To close the linoleic acid conversion mass balance, residual FAs were determined using high-performance liquid chromatography (HPLC) according to the method described by Gratzfeld-HüSgen and Schuster (Gratzfeld-Husgen & Schuster, 2001) . whereby, prior to injection, FAs were derivatizated with bromophenacyl bromide (Fluka, Buchs SG, Switzerland), to obtain their corresponding esters. The analysis was performed on a 1100 series chromatographic system with a UV visible diode array detector (Agilent Technologies, CA, USA) using a C18 column (150 × 2.1 mm ZORBAX Eclipse XDB, 5 µm). The sample injection volume was 1 µL. A mix of water (A) and acetonirile + 1% tetrahydrofuran (B) was used as mobile phase with a solvent gradient of 30% B at 0 min; 70% B at 15 min; and 98% B at 25 min. The detection wavelength for the esters of FAs was 258 nm.

4.2.6 Determination of the kinetics of the esterification reaction

Equation (4-2) describes the stochiometric relationship of the reactants and products of the esterification reaction.

$$Linoleic\ acid + Methanol \xrightarrow{Catalyst} Methyl\ linoleate + H_2O \qquad 4\text{-}2$$

According to general eq (4-2), the reaction rate could be presented as follows (eq (4-3)):

$$-r_a = -\frac{dC_{LA}}{dt} = k' \,.\, C_{LA} \,.\, C_{Me} \qquad 4\text{-}3$$

where C_{LA} is the concentration of linoleic acid (mg.L^{-1}), C_{Me} that of methanol (mg.L^{-1}) and *k'* the reaction rate constant (h^{-1}).

Equation (4-3) follows a second order reaction rate law. However, the concentration of methanol throughout the reaction could be considered constant due to the excess amount of methanol used to shift the reaction to the products side. Consequently, the concentration of methanol does not change the reaction order which will behave as a first order reaction and obey pseudo-first order kinetics (eq. (4-4)) (Birla et al., 2012; Dang et al., 2013).

$$-r_a = -\frac{dC_{LA}}{dt} = k' . C_{LA} \,.\, C_{Me} = k \,.\, C_{LA} \qquad 4\text{-}4$$

where $k = k'.C_{Me} \approx cst$, when methanol is used in excess.

Assuming that the initial concentration of linoleic acid is $C_{0\ LA}$ at time $t = 0$ and becomes $C_{t\ LA}$ at time t. The integration of eq. (4-4) from $t = 0$ to $t = t$, and $C_{0\ LA}$ to $C_{t\ LA}$ gives eq. (4-5):

$$ln\, C_{0\ LA} - ln\, C_{t\ LA} = k\,.\,t \qquad 4\text{-}5$$

From the mass balance of the reaction,

$$X_{ML} = 1 - \frac{C_{t\ LA}}{C_{0\ LA}}$$

where X_{ML} is the methyl linoleate yield. Upon rearrangement of eq. (4-5), the kinetics of linoleic acid conversion could be expressed as follows (eq. (4-6)):

$$ln(1 - X_{ML}) = -k\,.\,t \qquad 4\text{-}6$$

4.3 Results and Discussion

4.3.1 Catalyst Characterization

As illustrated in Figure 7a and 7b, only crystalline MFI phase was obtained for all zeolites which confirms the high purity achieved for the different morphologies of ZSM-5. However, after exchange with NH_4^+, the hierarchical samples, denoted as NSh-HZSM-5 and NS-HZSM-5 presented less intense XRD peaks, suggesting the presence of smaller crystalline domains. In addition, XRD reflections of MC-HZSM-5 are sharper than those of NC-HZSM-5, NSh-HZSM-5 and NS-HZSM-5 which are relatively broader. This is explained by the bigger crystal size of HZSM-5 big crystals (MC-HZSM-5), in comparison

with HZSM-5 nanocrystals, nanosheets and nanosponges. It is important to note that NS-HZSM-5 reflection peaks are broader and less intense relatively to the other zeolites' diffractograms which may be explained by the smallest crystallite sizes they hold as shown through imaging. The use of C22-6-6 and C18-N_3-C18 as structure directing agents for NSh-ZSM-5 and NS-ZSM-5 respectively, produces nanosheets and nanosponges with meso-structuration recognized by the presence of broad peaks at low diffraction angles ($0.6^{o} < 2\Theta < 5^{o}$) as shown in Figure 7c. NSh-ZSM-5 broad peak at low diffraction angles decreases in intensity after calcination whereas it remains intact for NS-ZSM-5 (Figure 7d). This suggests that nanosponges samples have higher mesoporous volume which will be confirmed by N_2 sorption tests. At wide angles, only the diffraction peaks relative to the (*h0l*) crystallographic plane are strong enough to be properly indexed for NSh-HZSM-5. This indicates that the crystal growth along the *b*-crystal axis (perpendicular to the nanosheet layer) is prevented by the hydrophobic alkyl tail of C22-6-6 and that the zeolite layers are assembled in multilamellar arrays through hydrophobic interactions between the structure directing agent tails outside the zeolite layers, confirming thus the formation of nanosheets (Na et al. 2010). The wide angle XRD pattern of NS-HZSM-5 suggests a 2D hexagonal symmetry of micropores stacked in two different orientations (Na et al. 2011).

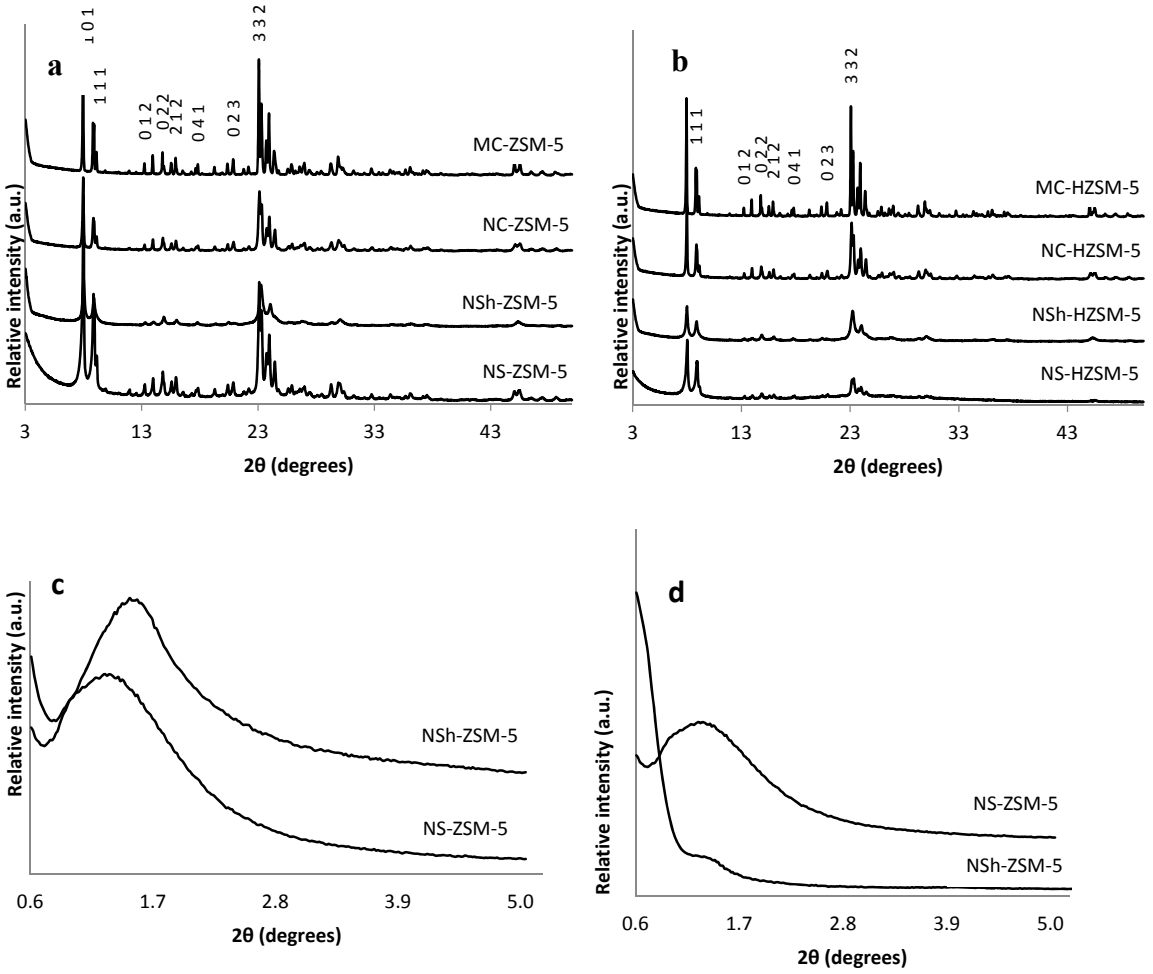

Figure 7. (a) Wide angle XRD patterns of calcined MC-ZSM-5, NC-ZSM-5, NSh-ZSM-5, and NS-ZSM-5, (b) Wide angle XRD patterns of exchanged and calcined MC-HZSM-5, NC-HZSM-5, NSh-HZSM-5, and NS-HZSM-5, (c) Low angle patterns of non-calcined NSh-ZSM-5, and NS-ZSM-5, (d) Low angle patterns of calcined NSh-ZSM-5, and NS-ZSM-5

The SEM images displayed in Figure 8 show the different morphologies observed for the HZSM-5 synthesized zeolites. Micrometric crystals with parallelepiped shape were obtained for the MC-HZSM-5, with crystal sizes ranging between 2.4 and 6 µm (Figure 8a). NC-HZSM-5 crystals have an average size of 85 to 210 nm (Figure 8b). The replacement of TPAOH by the bifunctional organic structure directing agent C_{22}-6-6 led to the production of lamellar materials for NSh-HZSM-5 (Figure 8c) of thickness ranging between 20 and 40

nm. It is clear from the figure that the zeolite nanosheets were well supported by silica pillars which retained the interlayer mesoporosity after removal of the surfactant by calcination. Upon the use of 18-N3-18 as structure directing agent, the increase in carbon chain length and in the number of quaternary ammonium generated the nanosponge morphology of NS-HZSM-5 (Figure 8d). The spiky-like nanomaterials are uniform in shape and size varying between 250 and 350 nm.

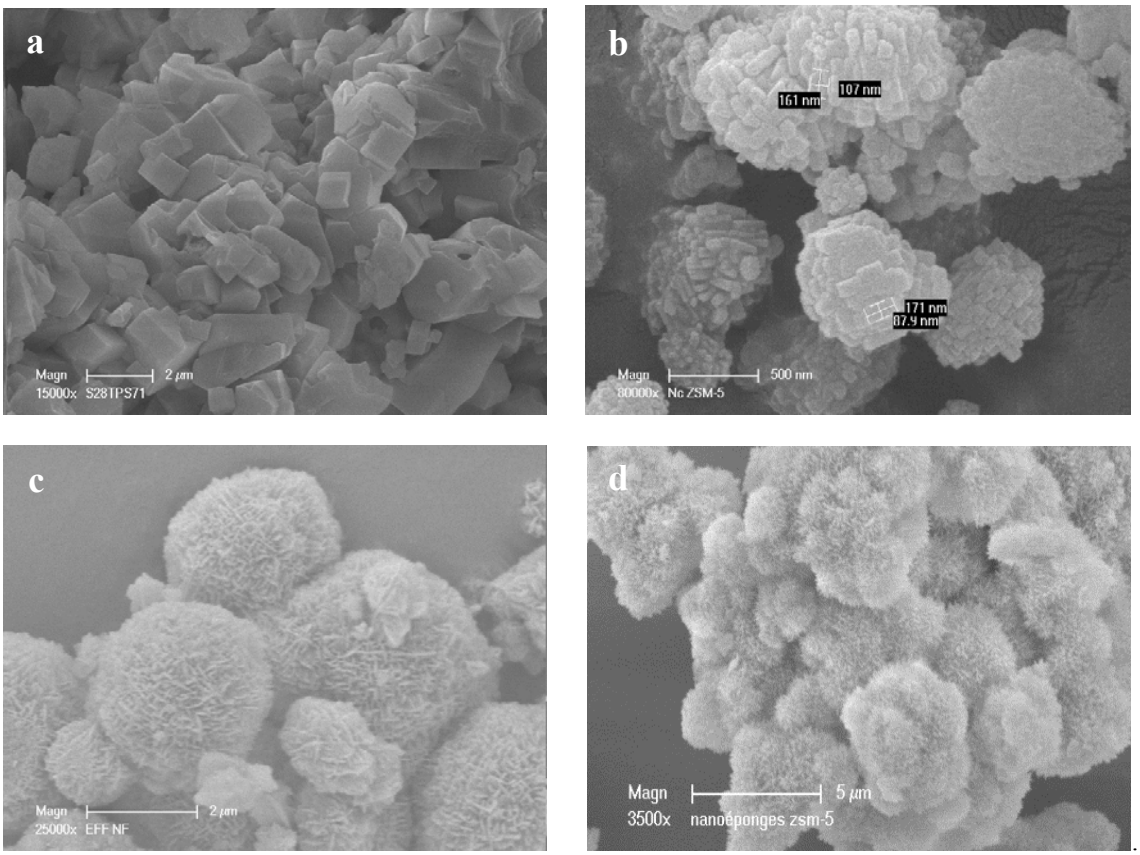

Figure 8. Scanning electronic microscopy (SEM) images of (a) MC-HZSM-5, (b) NC-HZSM-5, (c) NSh-HZSM-5, and (d) NS-HZSM-5.

From the TEM image (Figure 9a), it is well observable that several nanosheets of a single unit are parallel to each other, presenting an entirely ordered assembly of zeolite

nanosheets with a vertical diameter of 3.5 nm. TEM image of NS-HZSM-5 (Figure 9b) show hexagonal arrays of ordered and disordered mesopores and a microporous crystalline lattice within the mesopore walls.

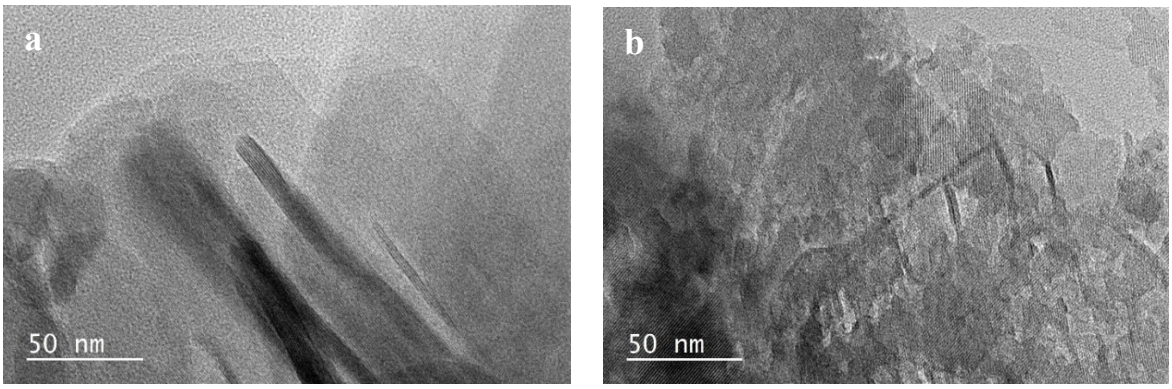

Figure 9. Transmittance electronic microscopy (TEM) images of (a) NSh-HZSM-5, and (b) NS-HZSM-5

The textural properties of the calcined HZSM-5 with different morphologies were investigated by adsorption-desorption of nitrogen (Figure 10). MC-HZSM-5 and NC-HZSM-5 displayed both an isotherm of type I as expected for microporous solids. A slight hysteresis was observed for NC-HZSM-5 due to the agglomeration of nanocrystals. Microporous volumes of MC-HZSM-5 and NC-HZSM-5 was 0.17 $cm^3.g^{-1}$ for both zeolites (Table 7). In the presence of the structure directing agent C22-6-6, NSh-HZSM-5 exhibited type I isotherms at $p/p_0 < 0.4$ (p is the vapor pressure and p_0 is the saturation vapor pressure of nitrogen) revealing the presence of micropores within the zeolite framework with a microporous volume of 0.19 $cm^3.g^{-1}$. At $0.4 < p/p_0 < 1$, the isotherms of NSh-HZSM-5 were of type IIb (Sing et al.1985) representative of mesoporous materials (mesoporous volume of 0.13 $cm^3.g^{-1}$). A hysteresis loop was also detected, characteristic of lamellar materials,

which in this case is due to the parallel stacking of nanosheets. The isotherms of NS-HZSM-5 are of type Ib at low p/p_0 with a microporous volume of 0.27 $cm^3.g^{-1}$ (Table 7). The highest microporous volume relatively to the other morphologies of HZSM-5 is explained by the presence of a secondary microporosity induced by the polar head of the 18-N_3-18 surfactant, in additional to the typical channels of the MFI-type lattice. The presence of mesopores on NS-HZSM-5 zeolite is indicated by the type IV and type II isotherms at $0.4 < p/p_0 < 0.6$ with an H4 hysteresis attributed to the capillary condensation of nitrogen gas in the mesopores, and $p/p_0 > 0.9$ respectively, holding a mesoporous volume of 0.35 $cm^3.g^{-1}$. The total pore volume presented in Table 1 increased from MC-HZSM-5 to NC-HZSM-5, from NC-HZSM-5 to NSh-HZSM-5 and from NSh-HZSM-5 to NS-HZSM-5, and the BET surface area was higher for the hierarchical materials relatively to the microporous zeolites. The BJH pore size distribution of Sh-HZSM-5 was monomodal with a mean mesoporous diameter of 35 Å. For NS-HZSM-5 zeolites, the BJH pore size distribution was more intense and quite broad, presenting an average mesopore diameter of 58 Å (Figure 11).

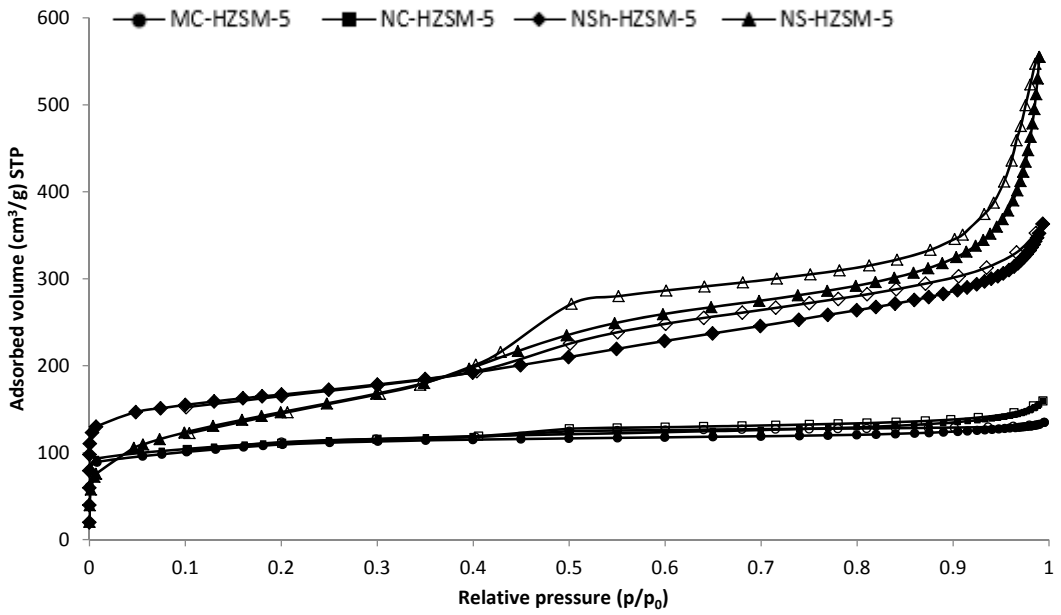

Figure 10. N2 adsorption/desorption isotherms at −196 °C of the calcined MC-HZSM-5, NC-HZSM-5, NSh-HZSM-5 and NS-HZSM-5 samples. Full bullets represent adsorption isotherms and empty bullets, the desorption ones.

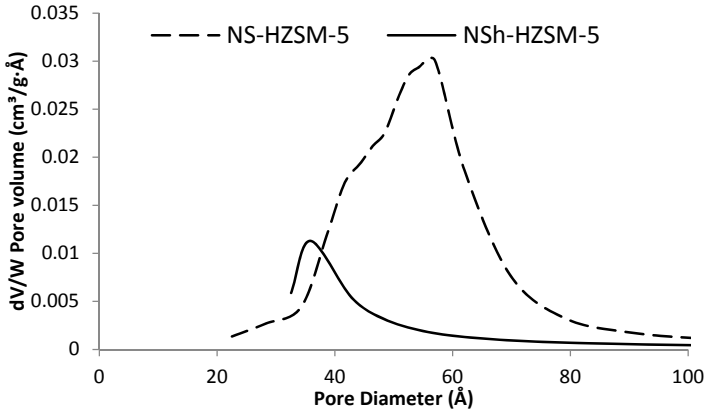

Figure 11 .Mesopore size distribution of the calcined exchanged hierarchical samples NSh-HZSM-5 and NS-HZSM-5

FTIR of adsorbed pyridine was used to quantify the acidity of the morphologically different HZSM-5 catalysts. Two reasons exist that make pyridine a well-adapted probe

molecule for the acidity quantification: 1) It can access the inner porosity of the zeolite since it presents a diameter of 2.8 Å, much lower than that of the HZSM-5 zeolite (5.5 Å) and, 2) It is a strong base with a nitrogen single electron pair that forms pyridium ion on protonic Brønsted sites ($PyrH^+$) and coordinated species on Lewis acidic sites (PyrL) (Derouane et al. 2013). The concentration of Lewis and Brønsted acidic sites were calculated from the bands at 1454 cm^{-1} and 1545 cm^{-1}, respectively. The results are reported in Table 7. Brønsted acidity decreases for hierarchical NSh-HZSM-5 and NS-HSZM-5 in respect to microporous MC-HZSM-5 and NC-HZSM-5 zeolites whereas Lewis acidity increases for the bi-porous zeolites relatively to the microporous zeolites.

Table 7. Textural properties by N2 sorption and acidity of the morphologically different HZSM-5 zeolites

HZSM-5 type	Si/Al ratio	S BET ($m^2.g^{-1}$)	Total porous volume ($cm^3.g^{-1}$)	Microporous volume ($cm^3.g^{-1}$)	Mesoporous volume ($cm^3.g^{-1}$)	$[PyrH^+]^a$ ($\mu mol.g^{-1}$)	$[PyrL]^b$ ($\mu mol.g^{-1}$)
MC-HZSM-5	45	395	0.17	0.17	-	351	44
NC-HZSM-5	25	411	0.17	0.17	-	301	76
NSh-HZSM-5	44	521	0.32	0.19	0.13	103	80
NS-HZSM-5	23	613	0.62	0.27	0.35	218	103

[a]Concentration of pyridine adsorbed on Brønsted acid sites after thermodesorption at 150 °C.
[b]Concentration of pyridine adsorbed on Lewis acid sites after thermodesorption at 150 °C.

4.3.2 Optimized Reaction Conditions of Esterification

4.3.2.1 Effect of Reaction Temperature on Esterification

To study the effect of reaction temperature on the conversion of linoleic acid, experiments using MC-HZSM-5, NC-HZSM-5, NSh-HZSM-5 and NS-HZSM-5 were

carried out at three different temperatures of 60, 140 and 180°C, under the same reaction conditions (methanol to linoleic acid molar ratio = 12:1, stirring rate = 550 rpm, catalyst loading = 10 wt%, and reaction time = 6 h). As shown in Figure 12, catalytic activity for all zeolites increased with increasing temperature except for MC-HZSM-5 and NC-HZSM-5 which showed no significant difference in linoleic acid conversion at 60 and 140 °C reaction temperatures with optimal methyl linoleate yield of 34.40 % (SD = 1.45) and 32.25 % (SD = 3.02), respectively, at 60 °C. For all zeolites, the order of conversion at the optimal reaction temperature of 180 °C was MC-HZSM-5 (45.76 %, SD = 4.85) < NC-HZSM-5 (51.31 %, SD = 5.33) < NS-HZSM-5 (68.60 %, SD = 3.47) < NSh-HZSM-5 (76.57 %, SD = 4.24). Higher temperatures achieved higher conversions which is explained by the decrease of fatty acid viscosity at high temperatures, promoting thus a better methanol/linoleic acid phase mixture and increasing methyl linoleate yield. However, results show that the increase of acid strength doesn't seem to be the only factor affecting the conversions obtained. The effect of pore size on the internal mass transfer limitation seems to play a major role in the esterification of linoleic acid.

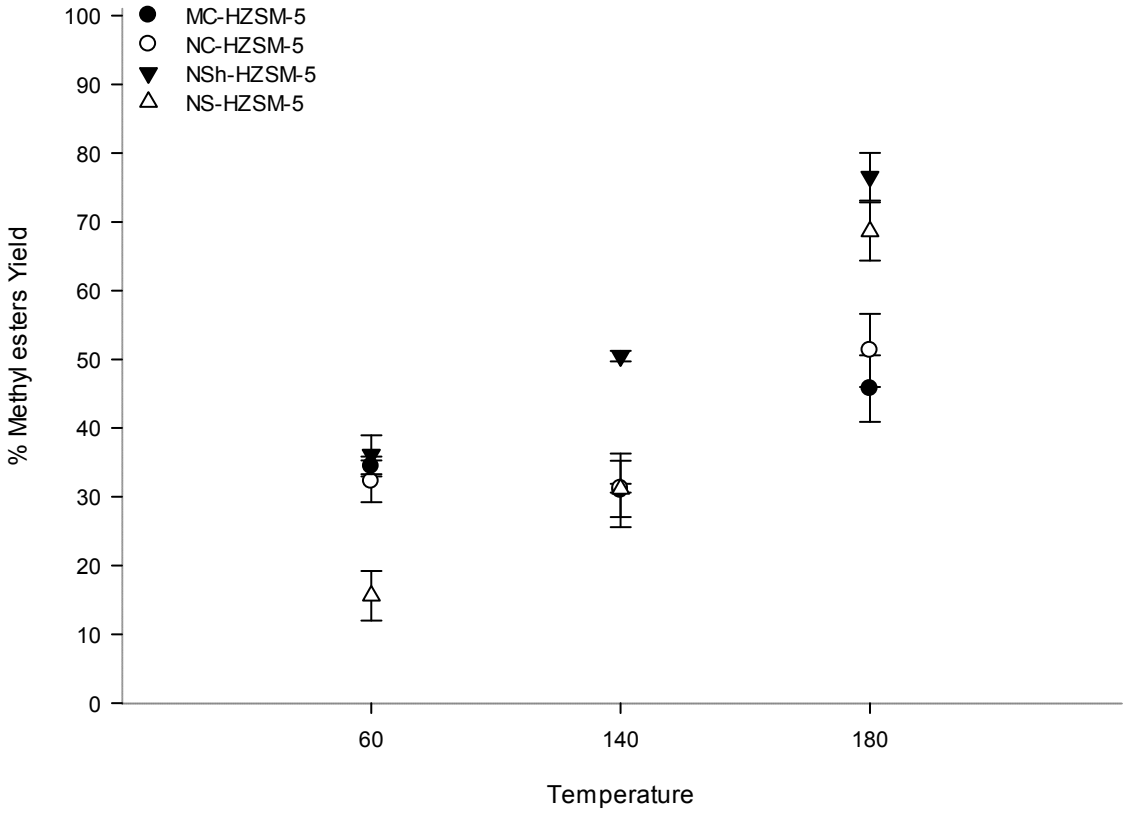

Figure 12. Effect of reaction temperature variation on the esterification of linoleic acid using MC-HZSM-5, NC-HZSM-5, NSh-HZSM-5, NS-HZSM-5 catalysts at methanol to linoleic acid molar ratio of 12:1, catalyst loading of 10 wt%, stirring rate of 550 rpm, and reaction time of 6 h

4.3.2.2 Effect of Methanol to Linoleic Acid Ratio on Esterification

Since the esterification is a reversible reaction, the moles of methanol must be in excess to force the reaction towards the formation of methyl linoleate (Qiu et al., 2011). The effect of methanol on the conversion of linoleic acid was examined through varying the amount of the alcohol to achieve a methanol/linoleic acid molar ratio of 6:1, 12:1, and 25:1 in the esterification reactions performed with the different catalysts (MC-HZSM-5, NC-

HZSM-5, NSh-HZSM-5, NS-HZSM-5). Similar reaction conditions were used and consisted of 10 wt% catalyst loading, 6 h reaction time, 550 rpm stirring rate, and fixed optimal temperature of 180°C. Figure 13 shows that the conversion rate of linoleic acid slightly increased from 46.68 % (SD = 6.58) to 51.31 %, (SD = 5.33) using NC-HZSM-5 as the molar ratio of methanol to linoleic acid increased from 6:1 to 12:1, and decreased to 34.50 (SD = 7.01) at the highest alcohol to linoleic acid molar ratio. For all other catalysts, the conversion rate of linoleic acid decreased as the molar ratio increased from 6:1 to 25:1. While it is a recognized principle that the equilibrium can be shifted towards the direction of methyl linoleate formation when an excess of methanol is used in the reaction (Xie and Zhao 2014), at higher methanol to linoleic acid molar ratios, the influence of reverse reaction is potentially greater than the forward reaction. This phenomenon is due to the slight recombination of methyl linoleate and water to form linoleic acid. Excess methanol could affect the solubility of the nearly immiscible water and methyl linoleate encouraging thus the backward reaction to take place (Shu et al., 2007). The methanol to linoleic molar ratio of 6:1was thus the optimal molar ratio with an order of conversion of NC-HZSM-5 (46.68 % SD = 6.58) < MC-HZSM-5 (76.62 %, SD =1.37) < NS-HZSM-5 (86.40 %, SD = 2.16) < NSh-HZSM-5 (90.76 %, SD = 1.17). It is noteworthy to mention that NC-HZSM-5 yielded lower methyl linoleate than MC-HZSM-5. Further investigations are needed to draw clear conclusions.

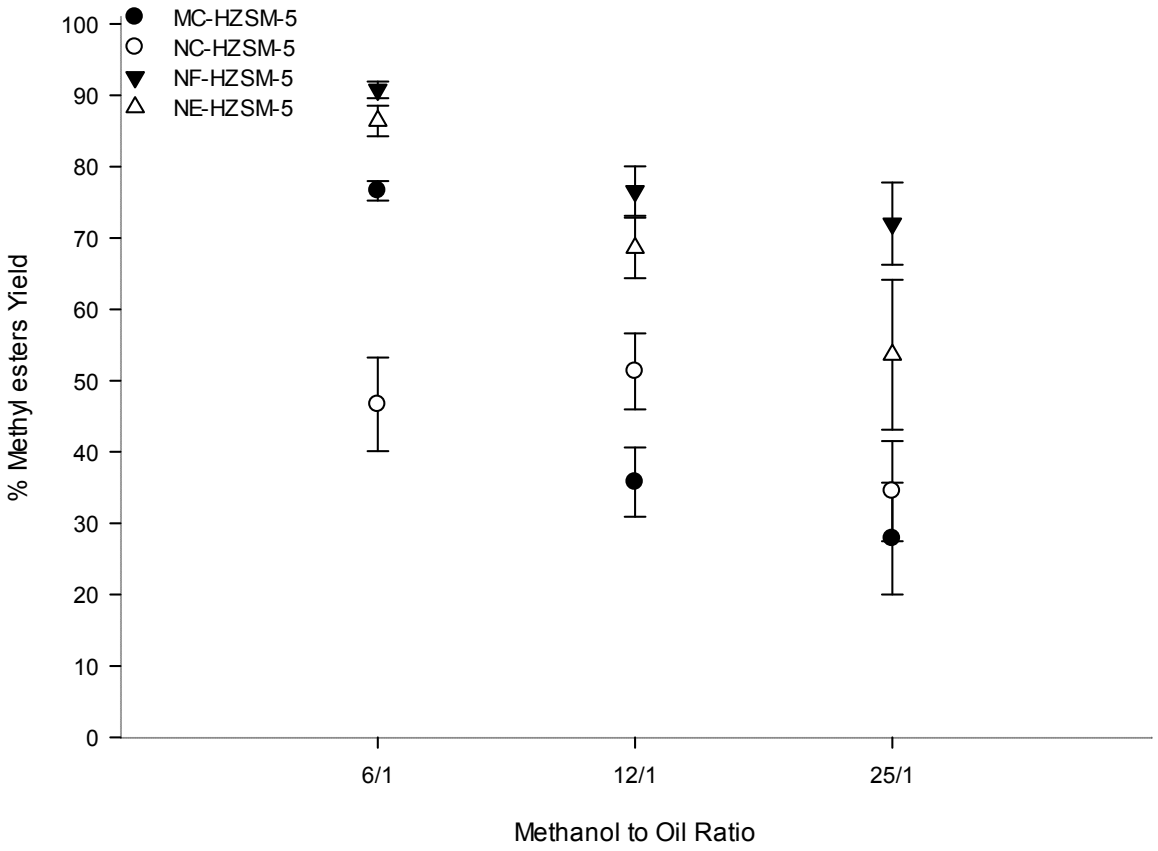

Figure 13.Effect of methanol to linoleic acid molar ration variation on the esterification of linoleic acid using MC-HZSM-5, NC-HZSM-5, NSh-HZSM-5, NS-HZSM-5 catalysts at catalyst loading of 10 wt%, reaction temperature of 180 °C, stirring rate of 550 rpm and reaction time of 6 h

4.3.2.3 Effect of Reaction Time on Esterification

In order to study the influence of reaction time on the conversion of linoleic acid, experiments were carried out using the catalyst which achieved the highest conversion of linoleic acid (hierarchical NSh-HZSM-5) at the optimal reaction conditions (methanol to linoleic acid molar ratio of 6:1, reaction temperature of 180 °C, catalyst loading of 10% and

stirring rate of 550 rpm) with the variation of reaction time in the range of 0 - 24 h. Figure 14 shows the effect of reaction time on methyl linoleate yield.

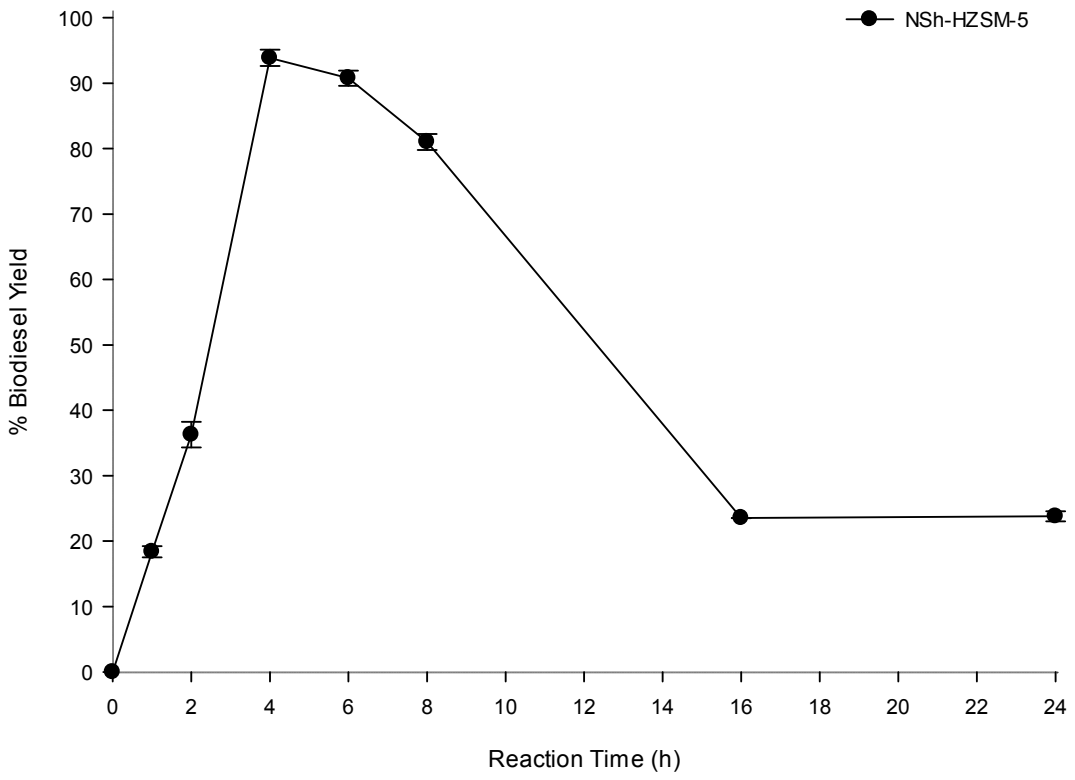

Figure 14. Effect of reaction time on the esterification of linoleic acid using NSh-HZSM-5 catalyst at catalyst loading of 10 wt%, methanol to linoleic molar ratio of 6:1, reaction temperature of 180 °C, and stirring rate of 550 rpm

According to the results, an increase in the reaction time from 1 to 2 h caused a marked increase in the conversion of linoleic acid from 18.38 % (SD = 0.85) to 36.26 % (SD = 1.95) and reached an optimal average yield of 93.87 % (SD = 1.25) with a maximum of 95.12 % after 4 h. No further enhancement in the conversion of linoleic acid was

observed after 4h of reaction time beyond which a decrease in the methyl ester yield was observed and was significant after 16 h of the reaction. At 16 and 24 h the aspect of the oil changed and seemed polymerized. Having the solution reacting for a long time at high temperatures might have resulted in overcooking the linoleic acid and changing its properties. Aside from yielding lower linoleic acid conversions, higher reactions times are not favorable for the esterification reactions due to the higher energy consumption they require. A reaction rate constant of 4.68×10^{-1} h^{-1} was calculated for NSh-HZSM-5 (Figure 15).

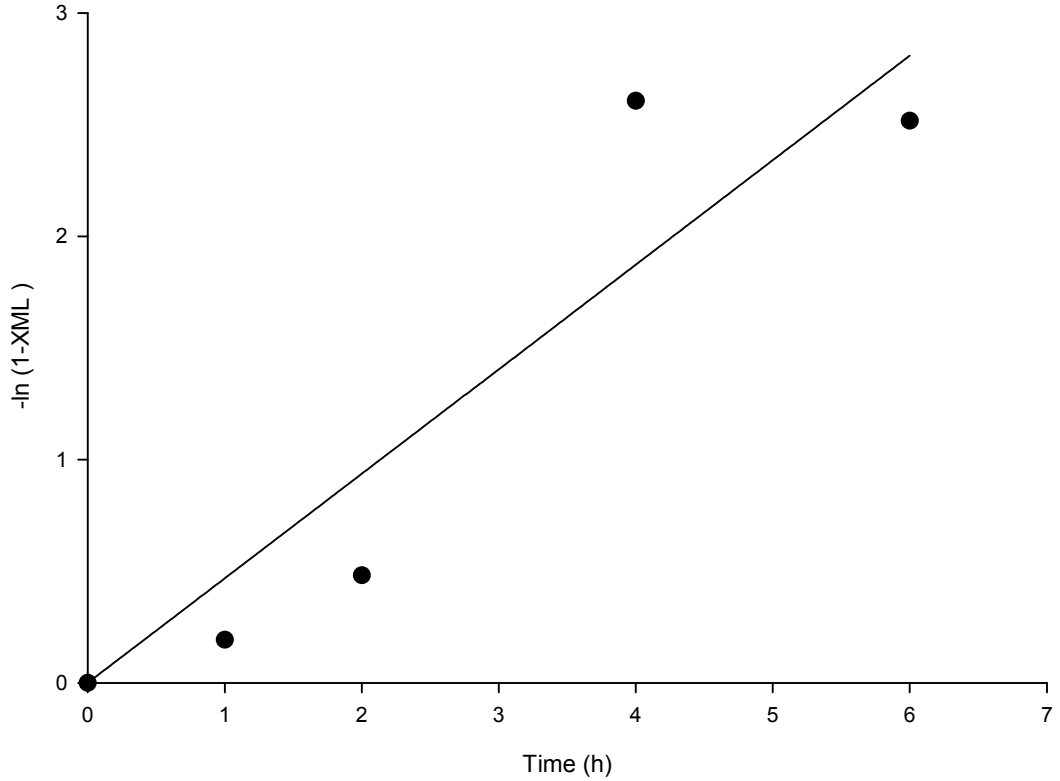

Figure 15. -ln(1-X_ML) versus reaction time plot at optimal reaction conditions using NSh-HZSM-5

For all the experiments carried out, residual linoleic acid was quantified using HPLC and mass balance closure was inspected. Table F in APPENDIX F presents numeric methyl esters yields and residual linoleic acid at the different reaction conditions.

4.3.3 Mass transfer evaluation of the synthesized catalysts on the esterification reaction

Although the presence of ordered micropores in zeolitic materials enhances their acidity, their sole presence seems to impose intercrystalline diffusion limitations, contributing to the low usage of the zeolite active volume in the catalyzed esterification reaction (Taguchi and Schüth 2005). In fact, microporous HZSM-5 zeolites have a small pore size (5.1 – 5.5 Å) and linoleic acid molecules possess a kinetic diameter of 8.08 Å estimated using eq. (4-7) (Wang & Frenklach, 1994).

$$\sigma = 1.234 \,.\, (M_W)^{1/3} \qquad \text{4-7}$$

where σ is the kinetic diameter estimated for hydrocarbons, and M_W is the molecular weight of linoleic acid in g. mol^{-1}.

This means that it is unlikely for such a molecule to penetrate the pores and reach the active intrinsic sites of the microporous zeolite such as MC-HZSM-5.

Alternative strategies leading to improved accessibility of the active sites confined in zeolites for linoleic acid esterification, were sought in this study by adopting two

different approaches: shortening the micropore diffusion path length (NC-HZSM-5) and introducing an additional (meso)porosity within the microporous zeolite crystal (NSh-HZSM-5 and NS-HZSM-5).

Reaction rate on the different morphologies of HZSM-5 were studied as a function of intrinsic diffusion rate by the estimation of Thiele modulus ($\emptyset$) to evaluate more precisely the extent of internal mass transfer limitations (eq. (4-8)) (Carberry 2001).

$$\emptyset = L \,.\, \sqrt{\frac{k}{D_{eff}}} \qquad \text{4-8}$$

where, L represents the characteristic diffusion length defined by the crystal size of the zeolites determined by SEM, k the reaction rate coefficient, and D_{eff} the effective diffusivity of linoleic acid and methanol molecules within the zeolite pores.

This method thus combines a theoretical calculation of the effective diffusion coefficient with the experimental value of the pseudo first-order rate constant k. A value of $\emptyset < 0.1$ indicates that the esterification reaction is free of any diffusion constraints and that observed reaction rate equals the intrinsic reaction rate. A reaction rate of 4.68×10^{-1} h^{-1} was calculated for the more active zeolite and used for all estimations.

The effective diffusion coefficient D_{eff} was calculated using eq. (4-9) (Poling et al., 2001):

$$D_{eff} = D_{AB} \,.\, \frac{\varepsilon}{\tau} \qquad \text{4-9}$$

Where, D_{AB} is the molecular diffusion coefficient of solute A (linoleic acid) at very low concentration in solvent B (methanol), ε is the particle porosity of the catalyst, and τ is the zeolite pore tortuosity.

In the present study, the molecular diffusion coefficient of linoleic acid in methanol was calculated based on the Wilke-Chang method, accounting for the reaction temperature of 180 °C (Wilke& Chang, 1955) and was 1.57×10^{-6} $m^2.s^{-1}$. ε for all zeolites were determined from the nitrogen adsorbed in pores fractions and τ was given a value of 4 as recommended for porous materials (Carberry 2001). Corresponding D_{eff} values for the zeolites used are listed in Table 8 along with Thiele modulus estimations.

Table 8. Thiele modulus variables data for linoleic acid esterification using MC-HZSM-5, NC-HZSM-5, NSh-HZSM-5 and NS-HZSM-5.

	MC-HZSM-5	**NC-HZSM-5**	**NSh-HZSM-5**	**NS-HZSM-5**
$\boldsymbol{\varepsilon}$	0.165	0.166	0.323	0.624
$\boldsymbol{D_{eff}}$ **($m^2.s^{-1}$)**	$6.50 .10^{-8}$	$6.52 .10^{-8}$	$1.27 .10^{-7}$	$2.45 .10^{-7}$
L **(nm)**	6000	210	20	250
∅	0.965	0.034	0.002	0.021

A Thiele modulus value of ~1 was obtained for micron-sized big crystals MC-HZSM-5, whereas ∅ = 0.034, 0.021 and 0.002 were estimated for NC-HZSM-5, NS-HZSM-5 and NSh-HZSM-5, respectively. Despite the high Brønsted acid concentration MC-HZSM-5 holds, the esterification reaction is hindered by mass transfer limitation whereby the zeolite active volume is not fully available to the linoleic acid molecules. MC-HZSM-5 diffusion properties can therefore rationalize the lower catalytic performance it held at different reaction temperatures, relatively to the other nanosized and hierarchical

zeolites respectively. NC-HZSM-5, NSh-HZSM-5 and NS-HZSM-5 had Thiele modulus values of $\emptyset < 0.1$, which prove that molecular transport effectiveness was enhanced by shortening diffusion length (NC-HZSM-5) and introducing a secondary mesoporosity (NSh-HZSM-5 and NS-HZSM-5). It is noteworthy that the catalytic performance over NC-HZSM-5 is lower than that of the hierarchical zeolites at the different reaction temperatures and methanol to linoleic acid ratios used. This shows that despite increasing the catalyst effectiveness, a shorter diffusion length in not sufficient to achieve high conversion yields. In addition to the short diffusion length, generating mesopores that are directly accessible to the linoleic acid molecules from the outer surface of the zeolite crystal, enhanced the molecular transport to and from the intrinsic active sites of the NSh-HZSM-5 and NS-HZSM-5 which showed the highest methyl linoleate yields at optimal esterification reaction conditions.

However, it is noticeable that between the two hierarchical HZSM-5 materials, NS-HZSM-5 zeolites which possess larger mesoporous diameter and volume (58 Å and 0.35 $cm^3.g^{-1}$, respectively, versus 35 Å and 0.13 $cm^3.g^{-1}$ for NSh-HZSM-5) along with a higher number of Brønsted acid sites (218 versus 103 $\mu mol.g^{-1}$ for NSh-HZSM-5), exhibit nearly similar catalytic activity as NS-HZSM-5 (86.40 % (SD = 2.16) versus 90.76 % (SD = 1.17) for NSh-HZSM-5).

Turnover frequencies (TOF) (methyl linoleate produced per Brønsted acid site per specific surface area in one hour) were therefore calculated for the hierarchical zeolites to provide insight into which fundamental factors affect catalytic activity within the hierarchical materials. TOF values were corrected by the BET surface areas found from the nitrogen adsorption/desorption isotherms of the hierarchical zeolites. TOF calculations yielded

values of 1.1×10^{-4} and 1.6×10^{-4} mol methyl linoleate .$\mu mol_{H^+}.m^{-2}.g.h^{-1}$ for NSh-HZSM-5 and NS-HZSM-5, respectively. The TOF values of the hierarchical zeolites are closely similar indicating that there is no significant influence of the specific nature of the acid sites of NSh-HZSM-5 and NS-HZSM-5 on their catalytic behavior. Introducing mesopores within microporous zeolite framework is effective for catalytic application if properly located in the crystal. The connectivity between the two types of pores is essential to optimize the efficiency of introducing different levels of porosity in catalyzed reaction and to satisfy the bulky molecules transfer from the outer mesoporous surface into the intrinsic active framework (Pérez-Ramírez et al., 2008). Despite the higher Brønsted acid sites concentrations in NS-HZSM-5, the disordered mesopores generated by surfactant aggregates could have been less effective than the orderly generated mesopores of NSh-HZSM-5 for the selective transport of linoleic acid to the totality of the intrinsic active acid sites, making NS-HZSM-5 zeolites not operating at their full potential. Consequently, engineered hierarchical zeolites for high catalytic selectivity, requires a careful design of mesopores harmoniously located with the micropores. However, it is difficult to assign such causation with certainty without further exploration and, therefore, this will not be considered further here.

Besides, the higher Si/Al ratio of NSh-HZSM-5 (Si/Al = 44) in comparison with that of NS-HZSM-5 (Si/Al = 23) may have led to a higher adsorption capacity of linoleic acid to the active surface of the zeolite. In fact, the more the zeolite is hydrophobic, the more it loses its acidic properties. However, it also avoids the adsorption of the water by-product that will lead to its deactivation by blocking access of the fatty acid (Kiss et al., 2006). It appears that water was more easily adsorbed to the surface of the more

hydrophilic NS-HZSM-5, hindering the linoleic acid molecules to react with the acid sites and thus, yielding lower conversions despite its higher acidity. In terms of diffusion limitation, reactant selectivity, and relative hydrophobicity, NSh-HZSM-5 offered the best catalytic performance in modelling biodiesel production.

4.4 Summary and Conclusion

Esterification of linoleic acid with methanol was successfully catalyzed using hierarchical HZSM-5 zeolite catalysts produced in nanosheet and nanosponge morphologies as compared to highly acidic conventional big and nano-crystals of HZSM-5 zeolites. Improved accessibility and molecular transport of linoleic acid from the outer mesoporous surface to the intrinsic active zeolitic framework resulted in achieving high conversions of 86.40 % (SD = 2.16) for NS-HZSM-5 and 90.76 % (SD = 1.17) for NSh-HZSM-5 at similar reaction conditions. A maximum methyl ester yield of 95.12 % was reached for the esterification of linoleic acid using NSh-HZSM-5 at 4 h reaction time, 10 wt% catalyst loading, 6:1 methanol to linoleic acid molar ratio and 180 °C. Although highly accessible and acidic, HZSM-5 nanosponges did not operate to their full potential as compared to HZSM-5 nanosheets given their higher hydrophilicity which favored water adsorption to their surface, and due to the connectivity between the different levels of porosity (micro and meso-porosity) that wasn't optimal for effective selective transport of linoleic acid and methyl linoleate molecules to and from the intrinsic active sites of the catalyst.

CHAPTER 5

HIERARCHICAL ZEOLITES AS CATALYSTS FOR BIODIESEL PRODUCTION FROM WASTE FRYING OILS TO OVERCOME MASS TRANSFER LIMITATIONS

ZSM-5 crystals with short diffusion path and hierarchical porosity were compared with conventional coffin-shaped microcrystals for their catalytic activity in terms of acidic properties and pore structure for the transesterification of waste frying oils with methanol for biodiesel production. Produced zeolitic catalytic materials were characterized with different instruments including XRD, SEM, TEM, BET/BJH porosimetry analysis, X-Ray fluorescence, and FTIR. The effect of pore size on the molecular diffusion limitation was investigated by Thiele modulus calculation and turnover frequencies (TOF) were used to discuss the correlation between acidic properties of the zeolites and their catalytic performance.

5.1 Introduction

In recent years, non-renewable resources have been over-exploited which led to the depletion of energy reserves, as well as an increase in the price of petroleum-based fuels (Živković et al. 2017). A suitable and sustainable alternative for conventional fuels is thus needed. Interest in biodiesel has been increasing in recent years due to its renewability, minor dependence on depleted resources and its lower pollution profile (OECD/FAO 2015). However, a major hurdle to its commercialization in comparison with petroleum-based fuels is its high cost due to the raw material used for its production (Harvey and

Pilgrim 2011). Besides the economic appeal it provides, waste frying oil (WFO) is one of the most promising biodiesel feedstocks by way of reducing the amounts of WFOs being dumped into sewers and landfills (Chakraborty and Das 2012). However, WFOs contain between 0.5 wt% and 15 wt% of free fatty acid (FFAs) compared to less than 0.5 wt% for refined vegetable oils (Kulkarni and Dalai 2006). Therefore, the use of basic homogeneous transesterification reactions is not recommended for the conversion of these inexpensive feedstocks. The base-catalyzed transesterification suffers from serious limitations such as the presence of high FFAs and water contents in the feedstock which promote the formation of soaps, increase of product viscosity and the difficult separation of glycerol from the produced methyl esters (Atadashi et al., 2013). Homogeneous acid catalysts are less sensitive to FFA content but require a long reaction time, a neutralization step and produce a large mass of salt residues, which is a cause of engine corrosion (Feyzi et al., 2017; Gardy et al., 2016). The high demand for cleaner methodologies made acid heterogeneous catalysts a better alternative, as they present advantages of environmental friendliness, easy removal, and non-corrosion (Lee & Saka, 2010; Saravanan et al., 2015). As one kind of heterogeneous solid acids, zeolites are crystalline and porous materials with high specific surface area, controllable acidity and hydrophobicity. Different studies followed an ion exchange procedure to form and compare between microporous H-type zeolites, which is the most common form of solid acid heterogeneous zeolite catalysts (Chung et al., 2008; Doyle et al., 2016; Doyle et al., 2017; Mowla et al., 2018). However, physical properties of microporous acid zeolites limit bulky molecules such as triglycerides from entering the narrow pores and reaching the internal active sites necessary for their conversion to fatty acid methyl esters (FAMEs). Further, molecules that were able to convert into more

valuable products have difficulty escaping the zeolite through the narrow micropores, yielding low feedstock conversion. An interesting way of improving zeolites activity for biodiesel production is the synthesis of zeolites with short diffusion paths and hierarchical porosity which overcome diffusional limitation by having secondary mesoporosity while maintaining the high reactivity of microporous acid zeolites. To our knowledge, no studies have yet assessed the transesterification of WFOs for the production of biodiesel using hierarchical zeolites. In the present study, the influence of acidic properties and pore structure of ZSM-5 zeolites exhibiting distinct crystal morphologies (conventional coffin-shaped microcrystals, nanocrystals, nanosheets, and nanosponges) has been assessed for the transesterification of WFOs to biodiesel. The catalytic behavior of the different ZSM-5 zeolites was optimized by varying the methanol to WFO molar ratio, the reaction temperature, the amount of catalyst and the reaction time. Thiele modulus model and turnover frequencies (TOF) were used to discuss the correlation between the pore size and acidic properties of the zeolites and their catalytic performance based on experimental results.

5.2 Experimental section

5.2.1 Structure directing agent synthesis

The di-quaternary ammonium-type surfactant $C_{22}H_{45}$-$N^+(CH_3)_2$-C_6H_{12}-$N^+(CH_3)_2$-$C_6H_{13}Br_2$ (abbreviated as C22-6-6), used for the ZSM-5 nanosheet synthesis were synthesized in two steps following a modified procedure reported by Na et al. (Na et al. 2010).

For the synthesis of ZSM-5 nanosponges, the zeolite-SDA-functional surfactant $C_{18}H_{37}–N^+ (CH_3)_2–C_6H_{12}–N^+ (CH_3)_2–C_6H_{12}– N^+ (CH_3)_2^-C_{18}H_{37}(Br^-)_3$ (abbreviated as 18–N_3–18) was prepared by separately synthesizing $C_{18}H_{37}–N_+(CH_3)_2–C_6H_{12}–Br(Br_-)$ and $C_{18}H_{37}– N_+(CH_3)_2–C_6H_{12}–N(CH_3)_2$ through organic reactions as described by Na et al. (Na et al. 2011).

The purity of the final solid organic products; C22-6-6 and 18–N_3–18 was analyzed by solution-state ^1H NMR, with $CDCl_3$ being used as solvent.

5.2.2 Catalysts Synthesis

To produce the ZSM-5 nanosheets, sulfuric acid (Aldrich) and tetraethoxysilane (TEOS, Aldrich, 98%) were dissolved in distilled water in a 45 ml Teflon-lined stainless-steel autoclave. Sodium hydroxide (Riedel de Haen, 99%) and $Al_2(SO_4)_3.18H_2O$ (Rectapur, 99%) were added to the mixture. The structuring agent C22-6-6 was finally added in order to set the molar composition of the gel to: $100SiO_2$: $1Al_2O_3$: $30Na_2O$: $18H_2SO_4$: $10C_{22}H_{45}–N^+(CH_3)_2–C_6H_{12}– N^+(CH_3)_2–C_6H_{13}Br_2$: $4000H_2O$. The gel was then stirred at 1000 rpm during 30 min, heated at 60 °C for 4 hours and finally placed in a tumbling oven at 150 °C for 4 days. The autoclaves were set at 30 rpm.

To produce ZSM-5 nanosponges of molar composition $100SiO_2$: $2.5Al_2O_3$: $22Na_2O$: 800EtOH : 5 $C_{18}H_{37}–N^+ (CH_3)_2–C_6H_{12}–N^+ (CH_3)_2–C_6H_{12}– N^+ (CH_3)_2^-C_{18}H_{37}(Br^-)_3$: $7100H_2O$ as described by Na et al. (Na et al. 2011), sodium aluminate ($NaAlO_2$ of 56.7 wt% Al_2O_3, 39.5 wt% Na_2O and 3.3 wt% H_2O) sodium hydroxide (Riedel de Haen, 99%), tetraethoxysilane (TEOS, Aldrich, 98%), EtOH (99%) and 18–N_3–18 were dissolved in distilled water under stirring, in a Teflon-lined stainless steel autoclave. The gel was stirred

at 1000 rpm at room temperature during 30 min, then at 60 °C for 6 hours and finally placed in a tumbling oven at 150 °C for 5 days at 30 rpm.

For comparison, ZSM-5 zeolite nanocrystals were synthesized following the molar composition $50SiO_2$: $1C_9H_{21}O_3Al$: 6NaBr: 10TPAOH: $450H_2O$. $C_9H_{21}O_3Al$ and tertrapropylammonium hydroxide (25 wt% TPAOH aqueous solution, Fluka) were dissolved in distilled water and stirred at room temperature for 20min. NaBr was added to the solution which was stirred for 20 additional minutes. Porous silica gel (100 mesh) was then added and well mixed with the solution. The gel was finally placed in an oven at 170 °C for 24 hours.

Typical ZSM-5 zeolite large crystals with coffin-shape morphology were synthesized under the same condition described above for ZSM-5 nanosheets. The only difference being the usage of a tetrapropylammonium hydroxide aqueous solution (25 wt%, Fluka) instead of the diquaternary ammonium- type surfactant, C22-6-6. The composition of the gel therefore being, $100SiO_2$: $1Al_2O_3$: $30Na_2O$: $18H_2SO_4$: 20TPAOH : $4000H_2O$ (Dhainaut et al. 2013).

After synthesis, the different ZSM-5 zeolites were filtered, washed with distilled water, dried overnight at 105 °C, and finally calcined at 550◦C for 8 h in air to remove the organic structuring agents.

All the ZSM-5 samples were NH_4^+-ion-exchanged with a 1 M NH_4Cl aqueous solution at 80 °C during 2 h. The solution was stirred in a round bottom flask fitted with a reflux condenser. The ion exchange process was repeated three times at a zeolite mass (g) to solution volume (ml) ratio of 1:20. NH_4^+-ion-exchanged zeolites were repetitively washed with distilled water. After filtration and drying at 105 °C for 12 h, NH_4^+-ion-

exchanged samples were calcined in air at 550◦C for 10 h to obtain the zeolite H^+ form. The different prepared and exchanged HZSM-5 big crystals, nanocrystals, nanosheet and nanosponges were labeled MC-HZSM-5, NC-HZSM-5, NSh-HZSM-5, and NS-HZSM-5 respectively.

5.2.3 Catalysts Characterization

The purity and the crystallinity of the different calcined zeolites were checked by XRD analysis. X-ray diffraction patterns of the different samples were recorded using a PANalytical MPD X'Pert Pro diffractometer operating with Cu Kα radiation (λ = 0.15418 nm) equipped with an X'Celerator real-time multiple strip detector (active length = 2.122 ° 2θ).

The size and the morphology of the calcined zeolites were determined by scanning electron microscopy (SEM) using a Philips XL 30 FEG microscope. A transmission electron microscope (TEM) (Philips model CM200) was used to investigate the homogeneity of the synthesized zeolites.

Nitrogen adsorption/desorption isotherms were measured using a Micromeritics ASAP 2420 apparatus. Prior to the adsorption measurements, the calcined samples were outgassed at 300°C for 15 h under vacuum. The specific surface area (S_{BET}) and microporous volume (V_{micro}) were calculated using the BET (p/p^0 range of 0.05-0.25) and *t*-plot methods, respectively (Brunauer et al., 1938; Lippens, 1965). Mesoporous volume was calculated using the BJH method.

The Si/Al molar ratio and the outcome of ion exchange of the different zeolites were estimated using the X-Ray fluorescence (Philips, Magic X).

Infrared spectra (FTIR) of pyridine , adsorbed at 150 °C, were recorded on a Nicolet Magna 550-FTIR spectrometer with a 2 cm^{-1} optical resolution for the different HZSM-5 samples. After establishing a pressure of 1 Torr at equilibrium, the pressed pellets of zeolite samples were evacuated at 200 °C under vaccum to remove all physisorbed species. The temperature was then lowered to 150 °C and the pyridine introduced in the cell. The amount of pyridine adsorbed on the Brønsted [$PyrH^+$] and Lewis [PyrL] sites were determined from the integration of the band at 1545 and 1454 cm^{-1}, using extinction coefficients previously determined by Guisnet et al., 1997.

5.2.4 Esterification Reaction Procedure

For all types of HZSM-5 produced, the transesterification reaction of WFOs with methanol (Chromasolv, 99.9 %) was performed in triplicates in a 50 ml round-bottomed flask, which was equipped with a mechanical stirrer and a reflux condenser. The reactor was loaded with 0.6 ml of WFO, equivalent to 1 mol or 0.54 g of WFO (MW = 876.5 g/mol). Methanol was added in the desired amount to achieve alcohol/oil molar ratios of 6:1, 12:1 or 25:1. The catalyst loading was also varied at 5, 7.5, or 10 wt% with respect to the WFO mass. The desired amount of catalyst was dried before reaction at 105 ºC. The reactor contents were heated at 140 ºC for 6 h. Reaction temperature and time were optimized for the HZSM-5 type which showed the highest conversions. Reaction temperatures were 60, 140 and 180 ºC and the kinetics study was performed at reaction times ranging between 0 and 24 h by sacrificing the solution in the reaction flasks consecutively with time.

When the reactions were completed, the produced fatty acid methyl esters (FAMEs) and remaining FFAs and triglycerides (TGCs) were extracted for analysis. The reactors were first extracted with 50 mL methanol followed by two DCM (Fisher, 99.8 %) extractions of 50 mL each. The liquid extracts were separated from the catalysts by gravity filtration through a bed of filtration beads and a 0.2 µm filter paper.

5.2.5 Chemical Analysis

The extracts were analyzed for FAMEs content on a Trace Ultragas chromatograph equipped with a flame ionization detector. An HP-INNOWAX capillary column (30 m × 250 µm × 0.25 µm) was used for the separation of FAMEs. Helium was used as a carrier gas at a flow rate of 1mL/min. 5 µL of sample were injected at 250 °C under splitless mode and the FID temperature was set at 300 °C. The oven temperature program was as follows: start at 60 °C (2 min), ramp at 10 °C/min to 200 °C (0 min), ramp at 5 °C/min to 240 °C (7 min). Reference standards (Supelco 37 component FAME mix in DCM, TraceCert) were used for the identification and quantification of the produced FAMEs. The biodiesel yield was determined by the following equation (5-1):

$$Yield\ (\%) = \frac{\sum C_{FAMEs} \times V_{extract}}{M_{0\ WFO}} \times 100 \qquad 5\text{-}1$$

where, C_{FAMEs} is the concentration of FAMES in g/L quantified by GC/FID, $V_{extract}$ is the volume (L) of the liquid extract, and $M_{0\ WFO}$, the initial mass of WFO added to the reactor (g).

Residual FFAs and triglycerides were determined by reversed-phase HPLC on an 1100 Series Chromatographic System with a diode array detector (Agilent Technologies, CA, USA).Two different methods, developed by Gratzfeld-HüSgen and Schuster (Gratzfeld-Husgen & Schuster, 2001), were used. For both protocols, a C_8 column (150 × 2.1 mm ZORBAX Eclipse XDB, 5 μm) was required. For the determination of FFAs residual content, a detection wavelength of 258 nm was used. FFAs were derivatizated with bromophenacyl bromide (Fluka, Buchs SG, Switzerland) prior to sample injection to obtain their corresponding esters and a mix of water (A) and acetonirile + 1% tetrahydrofuran (B) was used as mobile phase. The solvent gradient used for this method was as follow: at 0 min 30% B; at 15 min 70% B; at 25 min 98% B. For triglycerides determination, the composition of the mobile phase was water (A) and acetonitrile/methyl-*t*-butyl-ether (9:1) (B). The solvent gradient used covered 87% B at 0 min; and 100% B at 25 min. The analytes were detected at 215 nm.

5.2.6 Determination of the kinetics of the esterification reaction

Transesterification reaction is divided into three steps whereby, triglycerides are converted to diglycerides, diglycerides are converted to monoglycerides, and finally monoglycerides to glycerol. Each step produces one ester molecule by consuming one mole of methanol and, consequently, the reaction generates three ester molecules from one triglyceride molecule (Sharma and Singh 2008). The reaction will be assumed to be a single step transesterification following the stochiometric relationship between the initial reactants and final products (eq. (5-2)):

$$Triglyceride + 3Methanol \xrightarrow{Catalyst} 3Fatty\ acid\ methyl\ esters\ +\ Glycerol \qquad 5\text{-}2$$

According to the general eq (5-2), the reaction rate could be expressed as follows (eq (5-3)):

$$-r_a = -\frac{dC_{TGCs}}{dt} = k'\,.\,C_{TGCs}\,.\,C_{Me}^3 \qquad 5\text{-}3$$

where C_{TGCs} is the concentration of triglycerides (mg.L^{-1}), C_{Me} the concentration of methanol (mg.L^{-1}), and *k'* the reaction rate constant (h^{-1}).

Eq. (5-3) follows a second order reaction rate. However, the transesterification reaction is a reversible reaction and excess methanol is needed to shift the equilibrium to the product side, (Chisti 2007). Therefore, the change in methanol concentration could be considered as constant during the transesterification reaction which will thus obey pseudo-first order kinetics (Birla et al., 2012; Dang et al., 2013). The reaction rate can then be expressed as described in eq. (5-4):

$$-r_a = -\frac{dC_{TGCs}}{dt} = k'.\,C_{TGCs}\,.\,C_{Me}^3 = k\,.\,C_{TGCs} \qquad 5\text{-}4$$

where $k = k'.\,C_{ME}^3 \approx cst$, when methanol is used in excess.

Assuming that the initial concentration of triglycerides is $C_{0\,TGCs}$ at time $t = 0$ and becomes $C_{t\,TGCs}$ at time t, the integration of eq. (5-4) from $t = 0$ to $t = t$, and $C_{0\,TGCs}$ to $C_{t\,TGC}$ gives eq. (5-5):

$$ln\, C_{0\,TGCs} - ln\, C_{t\,TGCs} = k\,.\,t \qquad 5\text{-}5$$

From the mass balance of the reaction,

$$X_{FAMEs} = 1 - \frac{C_{TGCs}}{C_{0\,TGCs}}$$

where X_{FAMEs} is the fatty acid methyl ester yield. Upon rearrangement of eq. (5-5), the kinetics of triglycerides conversion could be expressed as follows (eq. (5-6)):

$$ln(1 - X_{FAMEs}) = -k\,.\,t \qquad 5\text{-}6$$

5.3 Results and Discussion

5.3.1 Catalyst Characterization

The crystallinity and purity of the different morphologies of ZSM-5 and H-ZSM-5 zeolites were examined by XRD (Fig.1). As illustrated in Figure 16a, 16b, 16c and 16d the different synthesized zeolites are pure as the sole crystalline MFI phase was obtained. In Figure 16a and 16b, MC-HZSM-5 and NC-HZSM-5 samples are well crystallized. However, XRD reflections of NC-HZSM-5 show broader peaks than those of MC-HZSM-5 indicating the presence of smaller crystal sizes. After exchange with $NH4^{+}$, the hierarchical

samples, denoted as NSh-HZSM-5 and NS-HZSM-5 presented the least intense XRD peaks, suggesting the presence of even smaller crystalline domains which will be shown below through imaging (Figure 16b and 16d). At wide angles, the main portion of diffraction peaks that can be accurately indexed, belongs to the h0l crystallographic plane for NSh-HZSM-5. This indicates that the crystal growth along the b-crystal axis (perpendicular to the nanosheet layer) is inhibited by the hydrophobic alkyl tail of C22-6-6, confirming thus the formation of nanosheets (Na et al. 2010). A 2D hexagonal symmetry of micropores stacked in two different orientations is suggested for the wide angle XRD pattern of NS-HZSM-5 (Na et al. 2011).The use of C22-6-6 and 18-N_3-18 as structure directing agents for NSh-ZSM-5 and NS-ZSM-5 respectively, produces nanosheets and nanosponges with meso-structuration further recognized by the presence of broad peaks at low diffraction angles ($0.6^{o} < 2\Theta < 4.7^{o}$) as shown in Figure 16c and 16d. NSh-ZSM-5 broad peak at low diffraction angles decreases in intensity after calcination whereas it remains intact for NS-ZSM-5. This indicates that nanosponges samples have higher mesoporous volume which will be confirmed below by N_2 sorption tests.

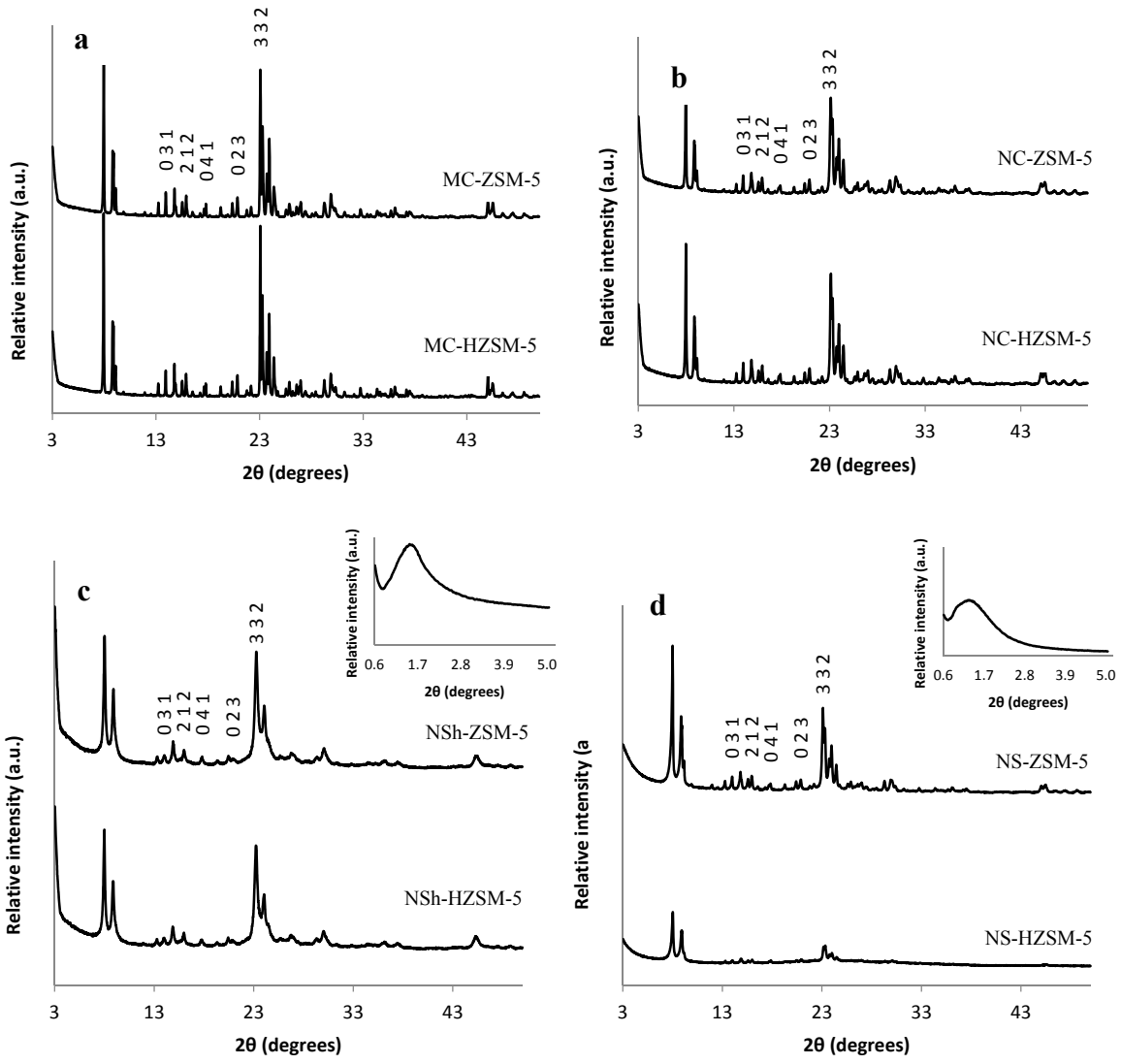

Figure 16. XRD diffractograms of (a) calcined MC-ZSM-5 and MC-HZSM-5 at wide angle patterns, (b) calcined NC-ZSM-5 and NC-HZSM-5 at wide angle patterns, (c) calcined NSh-ZSM-5 and NSh-HZSM-5 at low and wide-angle patterns, (c) calcined NS-ZSM-5 and NS-HZSM-5 at low and wide-angle patterns

The SEM images in the Figure 17 show the different morphologies observed for the HZSM-5 synthesized zeolites. Micrometric crystals were obtained for the MC-HZSM-5, with crystal sizes ranging between 2.4 and 6 µm (Figure 17a). NC-HZSM-5 crystals have

an average size of 85 to 210 nm (Figure 17b). The usage of bifunctional organic structure directing agent C_{22}-6-6 for the production of NSh-HZSM-5 led to the production of lamellar materials of thickness ranging between 20 and 40 nm (Figure 17c). The SEM figure of NSh-HZSM-5 demonstrates the existence of interlayer mesoporosity after the removal of the surfactant by calcination.

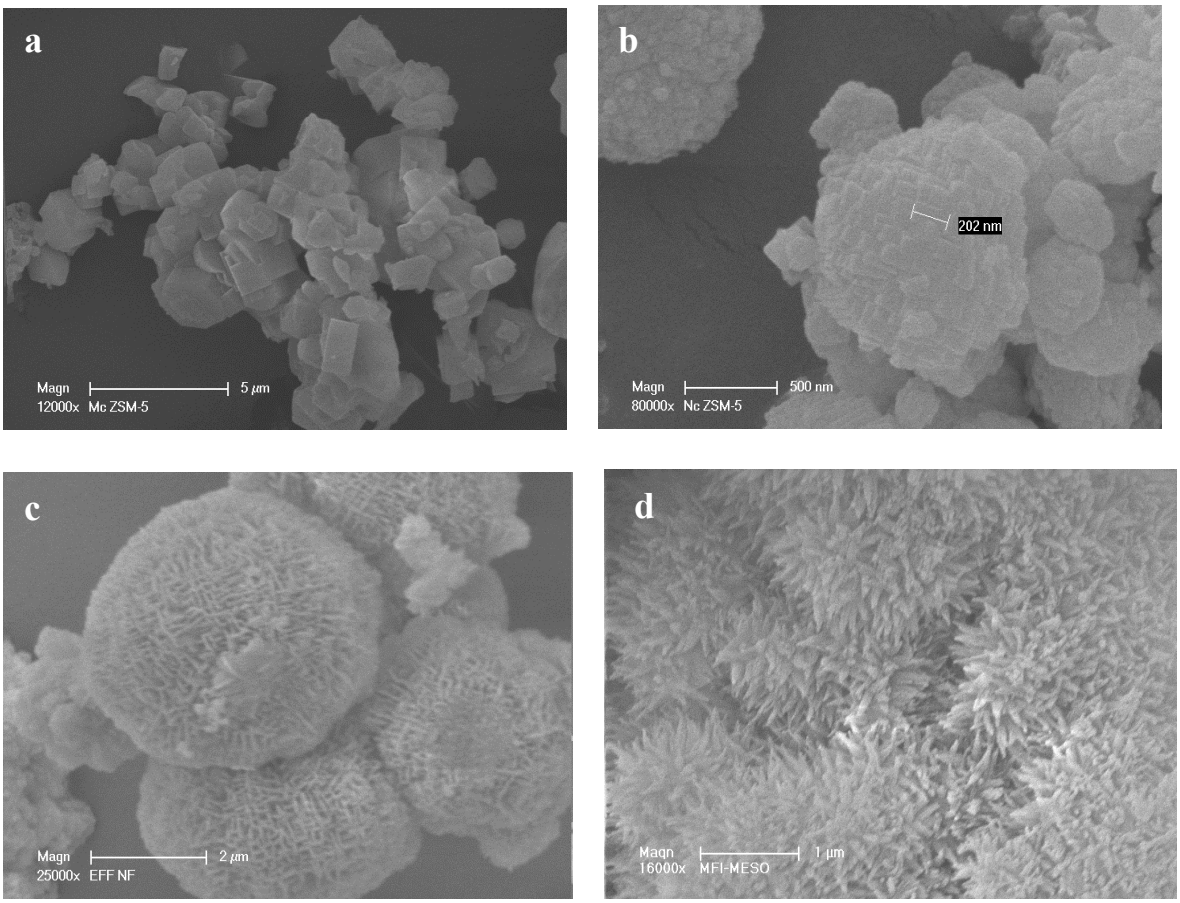

Figure 17. Scanning electronic microscopy (SEM) images of (a) MC-HZSM-5, (b) NC-HZSM-5, (c) NSh-HZSM-5, and (d) NS-HZSM-5. NS look beautiful in this picture

.

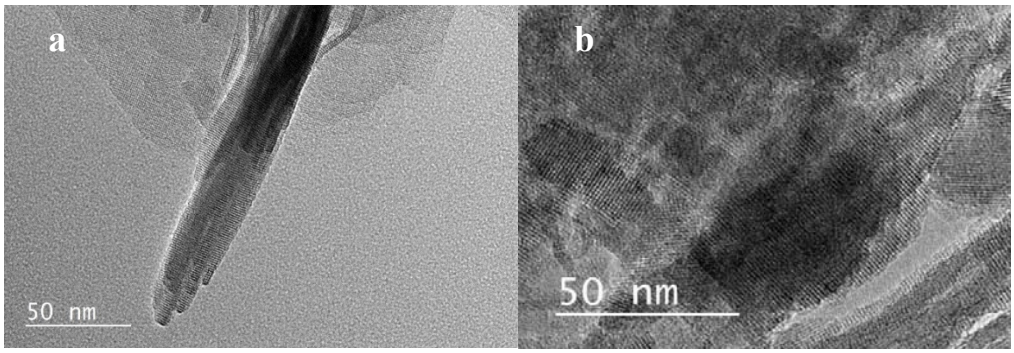

Figure 18. Transmission electronic microscopy (TEM) images of (a) NSh-HZSM-5, and (b) NS-HZSM-5.

TEM images (Figure 18a), show that several nanosheets are parallel to each other, whereby the thickness of each nanosheet is around 3.5 nm. When 18-N_3-18 is used as structure directing agent, the increase in carbon chain length and in the number of quaternary ammonium generate the nanosponge morphology of NS-HZSM-5 (Figure 17d). The spiky-like nanomaterials are uniform in shape and size ranging between 250 and 350 nm. TEM image of NS-HZSM-5 (Figure 18b) taken perpendicularly to the mesopore walls show crystal lattice borders with uniform spacing, representative of mesopore walls which have a zeolitic microporous crystalline framework.

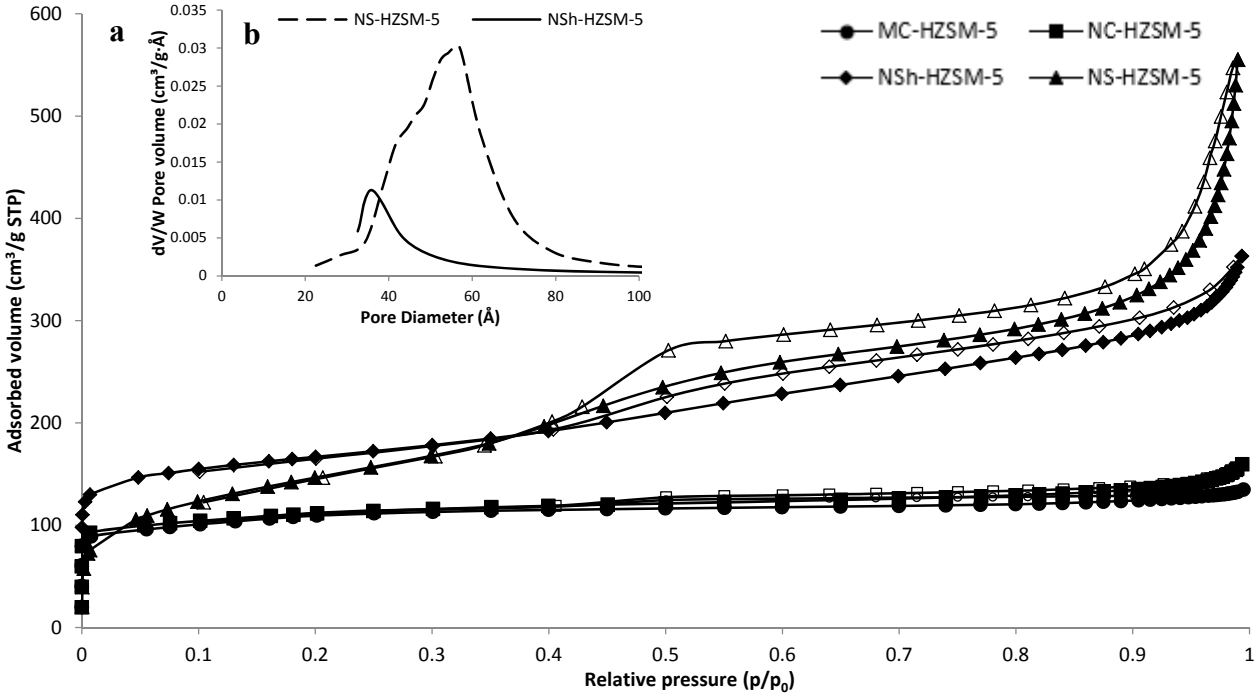

Figure 19. (a)Adsorption/desorption isotherms of nitrogen on the calcined MC-HZSM-5, NC-HZSM-5, NSh-HZSM-5 and NS-HZSM-5 samples, at −196 °C, (b) Mesopore size distribution of the calcined exchanged hierarchical samples.

The adsorption-desorption isotherms of nitrogen in the calcined HZSM-5 with different morphologies are shown in Figure 19a. As expected for microporous solids, MC-HZSM-5 and NC-HZSM-5 displayed both isotherms of type I. Microporous volumes of MC-HZSM-5 and NC-HZSM-5 were 0.17 $cm^3.g^{-1}$ for both zeolites (Table 9). However, a slight hysteresis was observed for NC-HZSM-5 due to the agglomeration of nanocrystals. The isotherms of NSh-HZSM-5 are of type I at low p/p_0 (p is the vapor pressure and p_0 is the saturation vapor pressure of nitrogen), which is characteristic of the presence of micropores with a microporous volume of 0.19 $cm^3.g^{-1}$ (Table 9). NSh-HZSM-5 isotherm is of type IIb at $0.4 < p/p_0 < 1$ revealing the presence mesopores having a volume of 0.13

$cm^3.g^{-1}$. A hysteresis loop is also noticed and is representative of lamellar materials, which in this case is due to the stacking of nanosheets. NS-HZSM-5 zeolites have type Ib isotherms at $p/p_0 < 0.4$ with a microporous volume of 0.27 $cm^3.g^{-1}$ (Table 9). In addition to the typical microporous channels of the MFI-type lattice, the presence of by the polar head of the 18-N_3-18 surfactant induced a secondary microporosity which contributed to the highest microporous volume observed among the different morphologies of HZSM-5. At $0.4 < p/p_0 < 1$, the isotherms of NS-HZSM-5 are of type IV ($0.4 < p/p_0 < 0.6$) and II ($p/p_0 > 0.9$) with a hysteresis, indicating the presence of mesopores due to capillary condensation and inter-particular adsorption of nitrogen respectively. Accordingly, NS-HZSM-5 exhibit mesopores with a mesoporous volume of 0.35 $cm^3.g^{-1}$. The BJH pore size distribution of NS-HZSM-5 is intense and broad with a mean mesoporous diameter of 58 Å (Figure 19b). For NSh-HZSM-5 zeolites, the BJH pore size distribution is less intense and quite narrow, presenting an average mesopore diameter of 35 Å. The BET surface area and total pore volume presented in Table 1 are higher for the hierarchical materials relatively to the microporous zeolites.

Table 9. Textural properties by N2 sorption of the morphologically different HZSM-5 zeolites

HZSM-5 type	Si/Al ratio	S BET (m^2/g)	Total porous volume (cm^3/g)	Microporous volume (cm^3/g)	Mesoporous volume (cm^3/g)
MC-HZSM-5	45	395	0.17	0.17	-
NC-HZSM-5	25	411	0.17	0.17	-
NSh-HZSM-5	44	521	0.32	0.19	0.13
NS-HZSM-5	23	613	0.62	0.27	0.35

For zeolite acidity characterization, FTIR was used. The bands originated by the adsorption of basic probe molecules of pyridine were measured. Pyridine allows the identification and quantification of the acidity of the active sites and distinguishes between the acidic OH groups, which are the Brønsted acid centers by forming pyridium ions on protonic sites ($PyrH^+$), and the weaker Lewis acid groups to which pyridine is physically bonded (PyrL). Also, the probe molecule has a diameter of 2.8 Å which makes possible its accessibility to the inner porosity of the HZSM-5 zeolite of 5.5 Å pore diameter. The concentrations of Brønsted and Lewis sites able to retain pyridine at 150 ◦C were determined using the absorbance areas of the bands at 1545 and 1454 cm^{-1}, respectively, using the extinction coefficients previously determined (1.13 and 1.28 $cm.mol^{-1}$ for pyridine interacting with Brønsted and Lewis centers, respectively (Guisnet, M., Ayrault, P., & Datka 1997)). The results are reported in Table 10. Brønsted acidity decreases for the hierarchical zeolites in respect to the microporous ones, and Lewis acidity increases for the NSh-HZSM-5 and NS-HSZM-5 zeolites relatively to the microporous MC-HZSM-5 and NC-HZSM-5.

Table 10. Brønsted and Lewis acidity of the morphologically different HZSM-5 catalysts

HZSM-5 type	**$[PyrH^+]^a$ ($\mu mol.g^{-1}$)**	**$[PyrL]^b$ ($\mu mol.g^{-1}$)**
MC-HZSM-5	351	44
NC-HZSM-5	301	76
NSh-HZSM-5	103	80
NS-HZSM-5	218	103

[a]Concentration of pyridine adsorbed on Brønsted acid sites after thermodesorption at 150 °C.
[b]Concentration of pyridine adsorbed on Lewis acid sites after thermodesorption at 150 °C.

5.3.2 Optimized Reaction Conditions of Transesterification

5.3.2.1 Effect of Catalyst Loading

The influence of catalyst loading on the conversion of triglycerides was investigated for MC-HZSM-5, NC-HZSM-5, NSh-HZSM-5 and NS-HZSM-5. Experiments were performed with loadings of 5, 7.5, and 10 wt% with respect to the used mass of WFO, at similar reaction conditions of 140 °C reaction temperature, 12:1 methanol to WFOs molar ratio, 550 rpm stirring rate, and 6 h reaction time. For all zeolite catalysts, FAMEs yield increased with increasing catalyst loading with an order of conversion of MC-HZSM-5 (15.60 %, SD = 0.57) <NC-HZSM-5 (17.29%, SD = 0.14) < NS-HZSM-5 (19.43 %, SD = 0.18) < NSh-HZSM-5 (26.83%, SD = 1.59) (Figure 20). Relatively to each catalyst type, at higher catalyst loadings, a greater amount of acid active sites will be available for the oil to react and produce FAMEs (Liu et al., 2014). In fact, oil's solubility in methanol is limited which leads to the formation of three phases in the heterogeneous transesterification (methanol, WFO, and solid zeolite). The transesterification can thus only take place at the interface of the methanol and WFO phases. Increasing catalyst loading will increase the concentration of the active sites at the interface between the oil and methanol which will enhance the formation of FAMEs and hence, higher conversions of oil will be achieved (Shu et al., 2007).

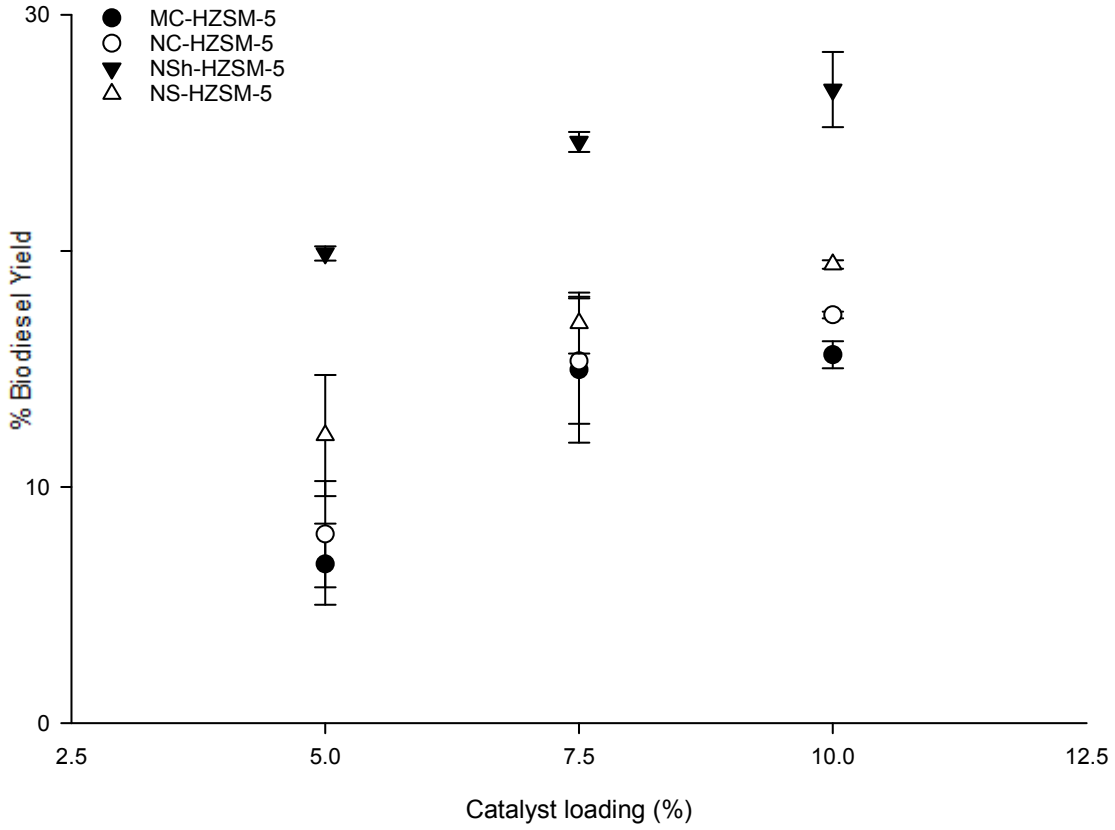

Figure 20. Effect of MC-HZSM-5, NC-HZSM-5, NSh-HZSM-5, and NS-HZSM-5 catalysts loading on the transesterification of WFO at the molar ratio of methanol to WFO of 12:1, reaction temperature of 140°C, stirring rate of 550 rpm, and reaction time of 6 h

5.3.2.2 Effect of Methanol to WFO ratio on Transesterification

The transesterification is a reversible reaction. Therefore, the moles of methanol must be in excess to force the reaction towards the formation of FAMEs (Qiu et al., 2011). The effect of the molar ratio of methanol to WFO on the conversion of triglycerides was examined through varying the amount of methanol used for the different MC-HZSM-5, NC-HZSM-5, NSh-HZSM-5, NS-HZSM-5 catalysts (6:1, 12:1, 25:1). Similar reaction conditions were used for the esterification reactions and consisted of fixed optimal 10 wt%

catalyst loading, 6 h reaction time, 550 rpm stirring rate, and 140°C reaction temperature. Figure 21 shows that the conversion rate of WFO increased for all the catalysts morphologies as the molar ratio of methanol to WFO increased from 6:1 to 12:1. The excess of methanol was proved favorable to the conversion of triglycerides into FAMEs. However, for all the catalyst types used, when the methanol to WFO molar ratio was further increased to 25:1, FAMEs yield decreased. This phenomenon is due to the slight recombination of FAMEs and glycerol to form monoglycerides. Excess methanol is advantageous for the conversion of triglycerides into monoglycerides. However, monoglycerides affect the solubility of the nearly immiscible glycerol and FAMEs encouraging thus the backward reaction to take place (Shu et al. 2007; Sun et al. 2015). 12:1 methanol to WFOs molar ratio was consequently the optimal molar ratio used for the rest of the optimization tests, with an order of conversion that was kept at MC-HZSM-5 (15.60 %, SD = 0.57) < NC-HZSM-5 (17.29%, SD = 0.14) < NS-HZSM-5 (19.43 %, SD = 0.18) < NSh-HZSM-5 (26.83%, SD = 1.59).

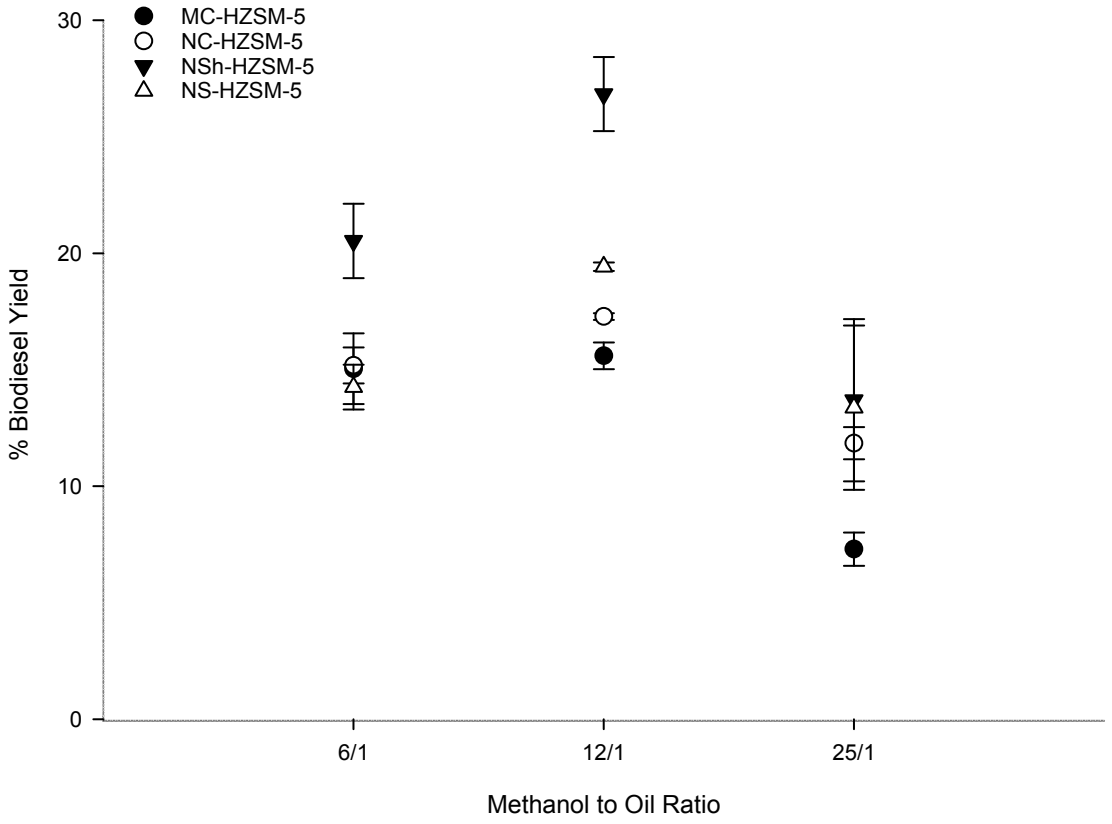

Figure 21. Effect of methanol to WFO molar ration variation on the transesterification of WFO using MC-HZSM-5, NC-HZSM-5, NSh-HZSM-5, and NS-HZSM-5 catalysts, at catalyst loading of 10 wt%, reaction temperature of 140 °C, stirring rate of 550 rpm and reaction time of 6 h

5.3.2.3 Effect of Reaction Temperature on Transesterification

To study the effect of reaction temperature on the conversion of WFOs, experiments using optimal hierarchical NSh-HZSM-5 catalyst, which achieved the highest conversion rates of WFO in the previous experiments, were carried out at three different temperatures of 60, 140 and 180 °C, under the same reaction conditions (optimal methanol to WFOs molar ratio = 12/1, optimal catalyst loading = 10%, stirring rate = 550 rpm, and reaction

time = 6 h). As shown in Figure 22, catalytic activity of NSh-HZSM-5 increased with increasing temperature with the highest FAMEs yield of 43.57 % (SD = 4.44) registered for reaction temperature of 180 °C. Higher temperatures achieved higher conversions which is explained by the decrease of WFO viscosity at high temperatures, promoting thus a better methanol/WFOs phase mixture, and increasing FAMEs yield (Borges et al. 2013).

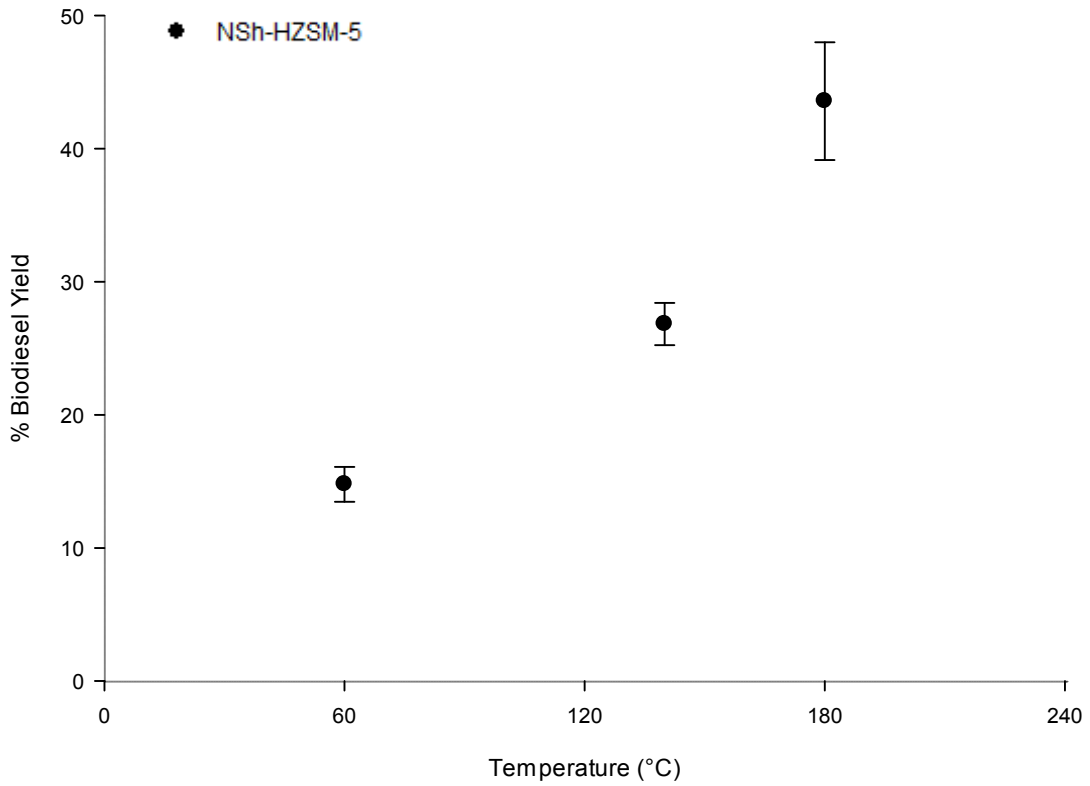

Figure 22. Effect of reaction temperature variation on the transesterification of WFO using NSh-HZSM-5 catalyst at catalyst loading of 10 wt%, methanol to WFO molar ratio of 12:1, stirring rate of 550 rpm and reaction time of 6 h.

5.3.2.4 Effect of Reaction Time on Transesterification

In order to study the influence of reaction time on FAMEs production from the transesterification of WFO, experiments were carried out using optimal catalyst (hierarchical NSh-HZSM-5) at the optimal reaction conditions of 12:1 methanol to WFO molar ratio, 180 °C reaction temperature, catalyst loading of 10% and stirring rate of 550 rpm, with the variation of reaction time in the range of 0 - 24 h. Figure 23 shows the effect of reaction time on FAMEs yield.

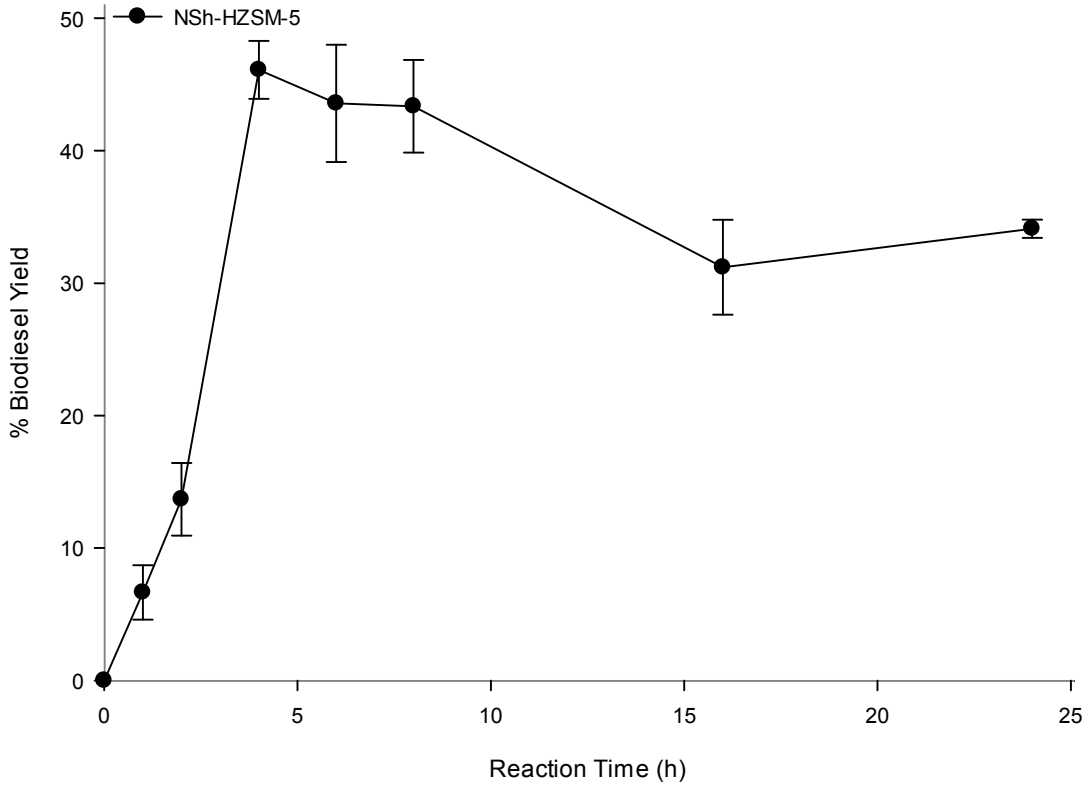

Figure 23. Effect of reaction time on the transesterification of WFO using NSh-HZSM-5 catalyst at catalyst loading of 10 wt%, methanol to WFOs molar ratio of 12:1, reaction temperature of 180 °C, and stirring rate of 550 rpm

According to the results, an increase in the reaction time from 1 to 2 h almost doubled the biodiesel yield which increased from 6.65 % (SD = 2.05) to 13.68 % (SD = 2.74). Further increase in the reaction time resulted in a significant improvement in FAMEs yield reaching a maximum of 48.29 % after 4 h. No significant enhancement was observed in WFO conversions beyond 4 h and up to 8 h of reaction time, after which a decrease in FAMEs yield was observed at 16 and 24 h reaction time. The latter decrease in the oil conversion is most probably due to the oil polymerization at prolonged heating time. Indeed, a solid mass was observed at the bottom of the reactors after 16 h and remained insoluble in DCM used for the oil extraction. Apart from yielding lower triglycerides conversions, higher reactions times are not favorable for the transesterification reactions due to the higher energy consumption they require. A reaction rate constant of 8.82×10^{-2} h^{-1} was calculated for NSh-HZSM-5 (Figure 24).

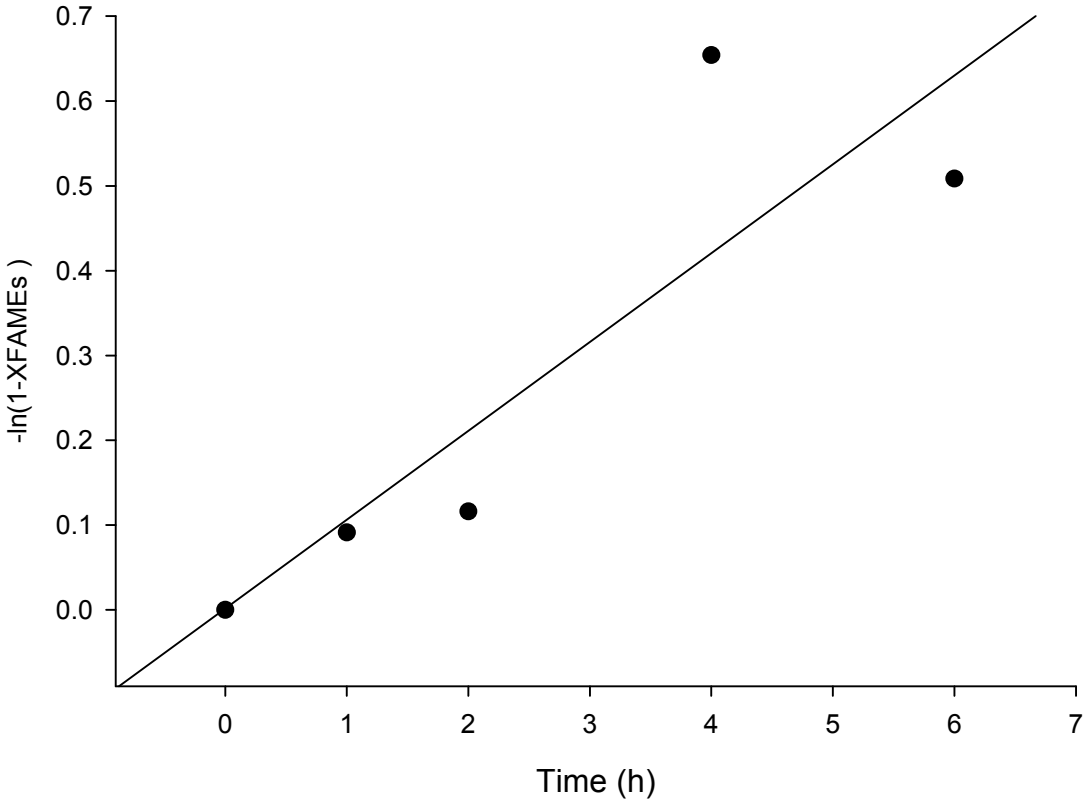

Figure 24.-ln(1-X_FAMEs) versus reaction time plot at optimal reaction conditions using NSh-HZSM-5

For all the experiments carried out, residual triglycerides and FFAs were quantified using HPLC and mass balance closure was inspected. Table G in APPENDIX G presents numeric FAMEs yields and residual triglycerides and FFAs contents at the different reaction conditions.

5.3.3 Mass transfer evaluation of the synthesized catalysts on the esterification reaction

Results from the experiments showed that the increase of acid strength doesn't seem to be the only factor affecting the conversions obtained. Therefore, the effect of pore size on the internal mass transfer limitation was investigated below.

The presence of ordered micropores in zeolitic materials enhances their acidity. However, the presence of this one type of porosity seems to contribute to the low usage of the zeolite active volume by imposing limitations on the accessibility and the molecular transport of bulky molecules such as triglycerides into the intercrystalline active acid sites (Taguchi and Schüth 2005). In fact, microporous HZSM-5 zeolites have a small pore size (5.1 – 5.5 Å) and triglycerides molecules possess a kinetic diameter of around 11.81 Å estimated using eq. (5-7) (Wang & Frenklach, 1994).

$$\sigma = 1.234 \,.\, (M_W)^{1/3} \qquad 5\text{-}7$$

where σ is the kinetic diameter estimated for hydrocarbons molecule, and M_W is the molecular weight of WFOs (876.5 g mol^{-1}).

This implies that the transport of triglycerides in pores of microporous zeolites such as HZSM-5 is hindered.

Strategies to enhance molecular mobility and accessibility to the active sites confined in zeolites for WFO transesterification were evaluated in this study by adopting

two different approaches: shortening the micropore diffusion path length (NC-HZSM-5) and introducing an secondary (meso)porosity within the microporous zeolite crystal (NSh-HZSM-5 and NS-HZSM-5).

In order to assess more precisely the extent of internal mass transfer limitations of the different zeolites on triglycerides conversions, reaction rates on the different morphologies of HZSM-5 were studied as a function of intrinsic diffusion rate by the estimation of Thiele modulus (∅)(eq. (5-8)) (Carberry 2001).

$$\emptyset = L \, . \sqrt{\frac{k}{D_{eff}}} \qquad 5\text{-}8$$

where, L represents the characteristic diffusion length defined by the crystal size of the zeolite determined by SEM, k is the reaction rate coefficient, and D_{eff} the effective diffusivity of triglyceride and methanol molecules within the zeolitic pores.

This method thus combines a theoretical calculation of the effective diffusion coefficient with the experimental value of the pseudo first-order rate constant k. A ∅ value < 0.1 indicates that the transesterification reaction is not limited in terms of mass transfer and that observed reaction rate equals the intrinsic reaction rate. A reaction rate constant of 8.82×10^{-2} h^{-1} was calculated for the more active zeolite and used for all estimations.

The effective diffusion coefficient D_{eff} was calculated using eq. (5-9) (Poling et al., 2001):

$$D_{eff} = D_{AB} \cdot \frac{\varepsilon}{\tau} \qquad 5\text{-}9$$

where, D_{AB} is the molecular diffusion coefficient of solute A (WFO) at very low concentration in solvent B (methanol), ε is the particle porosity of the catalyst, and τ is the zeolite pore tortuosity.

In the present study, the molecular diffusion coefficient of triglycerides in methanol was calculated based on the Wilke-Chang method (Wilke & Chang, 1955) and was 1.57×10^{-6} $m^2.s^{-1}$ at the reaction temperature of 180 °C. ε for all zeolites were determined from the nitrogen adsorbed in pore fractions and τ was given a value of 4 as recommended for porous materials (Carberry 2001). Corresponding D_{eff} values for the zeolites used are listed in Table 11 along with Thiele modulus estimations.

Table 11. Thiele modulus variables data for triglycerides transesterification using MC-HZSM-5, NC-HZSM-5, NSh-HZSM-5 and NS-HZSM-5

	MC-HZSM-5	**NC-HZSM-5**	**NSh-HZSM-5**	**NS-HZSM-5**
$\boldsymbol{\varepsilon}$	0.165	0.166	0.323	0.624
$\boldsymbol{D_{eff}}$ **($m^2.s^{-1}$)**	$1.28 .10^{-7}$	$1.29 .10^{-7}$	$2.51 .10^{-7}$	$4.85 .10^{-7}$
***L* (nm)**	6000	210	20	250
∅	0.298	0.010	0.0007	0.006

A Thiele modulus value of ~0.3 was obtained for micron-sized big crystals MC-HZSM-5, whereas ∅ = 0.010, 0.006 and 0.0007 were estimated for NC-HZSM-5, NS-HZSM-5 and NSh-HZSM-5 respectively. Despite the high Brønsted acid concentration MC-HZSM-5 holds, the transesterification reaction was hindered by mass transfer

limitation whereby the zeolite active volume was not fully available to the triglycerides molecules. MC-HZSM-5 diffusion properties can therefore justify the lower catalytic performance it detained at different catalysts loading and methanol to WFO molar ratios, relatively to the other nanosized and hierarchical zeolites respectively. NC-HZSM-5, NSh-HZSM-5 and NS-HZSM-5 had Thiele modulus values of $\emptyset < 0.1$, which prove that molecular transport effectiveness was enhanced by shortening diffusion length (NC-HZSM-5) and introducing an additional (meso)porosity (NSh-HZSM-5 and NS-HZSM-5). It is noteworthy that the catalytic performance over NC-HZSM-5 is lower than that of the hierarchical zeolites at the different catalysts loading and methanol to WFO molar ratios. This shows that despite increasing the catalyst effectiveness by shortening its diffusion length, it is not enough condition to reach high conversion yields. In addition to the short diffusion length, generating mesopores that are directly accessible to the triglycerides and FFA molecules from the outer surface of the zeolite crystal, enhanced the molecular transport to and from the active sites of the NSh-HZSM-5 and NS-HZSM-5 which showed the highest FAMEs yields at optimal transesterification reaction conditions.

However, it is noticeable that between the two hierarchical HZSM-5 materials, NS-HZSM-5 zeolites which possess larger mesoporous diameter and volume (58 Å and 0.35 $cm^3.g^{-1}$ respectively versus 35 Å and 0.13 $cm^3.g^{-1}$ for NSh-HZSM-5) along with a higher number of Brønsted acid sites (218 versus 103 $\mu mol.g^{-1}$ for NSh-HZSM-5), exhibit lower catalytic activity than NSh-HZSM-5 (19.43 % (SD = 0.18) for NS-HZSM-5 versus 26.83 % (SD = 1.59) for NSh-HZSM-5) at the following reaction conditions: (10 wt% catalyst loading, 6 h reaction time, 550 rpm stirring rate, and 140 °C reaction temperature).

Turnover frequencies (FAMEs produced per strong acid site per specific surface area in one hour) were therefore calculated for the hierarchical zeolites to provide insight into which fundamental factors affect catalytic activity. TOF calculation yielded values of 1.12×10^{-5} and 1.21×10^{-5} $mol_{produced\ methyl\ linoleate}.\mu mol_{H^+}.m^{-2}.g.h^{-1}$ for NSh-HZSM-5 and NS-HZSM-5 respectively. The TOF values of the hierarchical zeolites are closely similar whereas their reactivity was significantly different. This indicates that there is no significant influence of the specific nature of the acid sites of NSh-HZSM-5 and NS-HZSM-5 on their catalytic behavior.

Generally, in addition to the number of porosity levels, hierarchical zeolites are characterized by their individual geometry. NS-HZSM-5 nanosponges have a disordered geometry in comparison with the very ordered NSh-HZSM-5 nanosheets geometry (Na et al. 2010, 2011). The primary purpose of using hierarchical zeolites as catalysts is to couple the catalytic character of micropores and the improved molecular transport by introducing additional mesopores, in a single material. However, the connectivity between the two types of pores is essential to optimize the effectiveness of bi-porosity in catalyzed reaction (Pérez-Ramírez et al., 2008) and consequently, to facilitate the transport of bulky materials from the outer mesoporous surface of the hierarchical zeolite into the active intercristalline space. Despite the higher Brønsted acid sites concentration in NS-HZSM-5, the disordered mesopores generated by surfactant aggregates could have been less effective than the orderly generated mesopores of NSh-HZSM-5 for the selective transport of triglycerides and FFAs to the totality of the intrinsic active acid sites. Consequently, engineered hierarchical zeolites for high catalytic selectivity, requires a careful design of mesopores harmoniously located with the micropores. However, it is difficult to assign such causation

with certainty without further exploration and, therefore, this will not be considered further here.

Alternatively, a competing adsorption phenomenon might have existed between all reaction components on the surface of NS-HZSM-5 catalyst. The relatively more hydrophilic NS-HZSM-5 (Si/Al = 23, versus Si/Al = 44 for NSh-HZSM-5) adsorbed glycerol by-product more strongly than less polar reactants and consequently blocked the access of methanol, triglycerides and FFAs to the active sites of the zeolite (Khalid et al., 2004). However, when the Si/Al ratio was high, as it is the case for NSh-HZSM-5, glycerol produced in the transesterification reaction desorbed rapidly from the more hydrophobic surface of zeolites, increasing thus the outer mesoporous surface coverage of methanol, triglycerides and FFAs and their diffusion into the internal active sites. In terms of diffusion limitation, relative hydrophobicity and reactant selectivity, NSh-HZSM-5 offered the best catalytic performance in transesterification reactions for biodiesel production.

5.4 Conclusion

Despite their higher acidic strength, conventional big and nano-crystals of HZSM-5 zeolites achieved lower yields than hierarchical HZSM-5 zeolite catalysts produced in nanosheet and nanosponge morphologies, for the transesterification of WFO with methanol. Enhanced accessibility and molecular transfer of triglycerides and FFAs from the outer mesoporous surface to the intra-crystalline active zeolite resulted in achieving high conversions of 19.43 % (SD = 0.18) for NS-HZSM-5 and 26.83 % (SD = 1.59) for NSh-HZSM-5 at similar reaction conditions. A maximum FAMEs yield of 48.29 % was reached for the esterification of WFO using NSh-HZSM-5 at 4 h reaction time, 10 wt% catalyst

loading, 12:1 methanol to linoleic acid molar ratio and 180 °C. Although highly accessible and acidic, HZSM-5 nanosponges did not operate to their full potential as compared to with HZSM-5 nanosheets as their relatively lower Si/Al ratio made the zeolite's surface more prone to adsorb glycerol by-product than the less polar reactants, and because the connectivity between the two levels of porosity wasn't optimal for effective selective transport of reactant and product molecules to and from the active sites of the catalyst.

CHAPTER 6

CATALYTIC STUDY ON THE ESTERIFICATION OF LINOLEIC ACID USING HZSM-5 ZEOLITES WITH DIFFERENT SI/AL RATIOS

In this chapter, microporous HZSM-5 zeolite crystals with different Si/Al ratios (45, 25 and 11.5) were compared for the esterification of linoleic acid with methanol as a model reaction for biodiesel production. As-synthesized catalytic materials were characterized with instruments including XRD, SEM, TEM, BET/BJH porosimetry analysis, X-Ray fluorescence, and FTIR. The catalytic behavior of HZSM-5 zeolites with different Si/Al ratios was assessed by varying reaction temperature and time, methanol to linoleic acid molar ratio, and catalyst loading. The external mass transfer limitation of HZSM-5 zeolites was investigated and the correlation between the surface hydrophobicity and acidity of the zeolites with different Si/Al ratios and their catalytic performance was assessed based on experimental results.

6.1 Introduction

On account of the high demand for diesel fuel and the adverse environmental and health impacts of its direct combustion, biodiesel production and application have been globally increasing as a promising substitute for petroleum-based diesel (Baskar and Aiswarya 2016; Živković et al. 2017). Biodiesel is commonly produced by the esterification of free fatty acids (FFAs) or the transesterification of triglycerides from different renewable feedstocks, with an excess of short-chain alcohol such as methanol, in the presence of a homogeneous acid or base catalyst (Yaakob et al., 2014). However, a

large amount of wastewater is generated for the purification of biodiesel produced using homogeneous catalysts, increasing thus the costs (Granados et al. 2007). Other problems associated with homogeneous catalysts include difficulty in the separation of the catalysts from the reaction mixture (Tan et al., 2015; Veljković et al., 2015). The use of heterogeneous insoluble acid catalysts minimizes the problems associated with homogeneous catalysis. They can be easily separated from the products by filtration and used several times after recycling (Chung et al., 2008). They are also non-corrosive, don't promote soap formation and eliminate product purification steps offering thus, a more environmental and economic pathway for biodiesel production (Saravanan et al., 2015). Park et al. compared acid solid sulfated zirconia, amberlyst 15, and tungsten oxide zirconia catalysts for biodiesel production from WFOs, and recorded highest yield for tungsten oxide zirconia (WO_3/ZrO_2) (Park et al., 2010). Feng et al. used the cation-exchange resins NKC-9, 001x7 and D61 as heterogeneous acid catalysts in biodiesel production from WFOs. NKC-9 had the best catalytic activity yielding 90% conversion (Feng et al. 2010). Gardy et al. grused mesoporous $TiO_2/PrSO_3H$ solid acid catalyst (4.5 wt%) for the transesterification of WFOs which resulted in 98.3% yield at 60 °C (Gardy et al., 2017).

ZSM-5 zeolite, which is most commonly synthesized using the hydrothermal route (Shirazi et al., 2008), is a medium pore (5.1-5.6 Å) zeolite with three-dimentional channels defined by 10-membered rings (Sang et al. 2004). Due to its unique shape selectivity, solid acidity, ion exchangeability, thermal stability and structural network, ZSM-5 has been widely used as catalyst in petroleum and petrochemical industry (Falamaki et al., 1997). The catalytic properties of the zeolite are often influenced by their physical and chemical properties. Some studies observed that the conversion of oil molecules decreases with

increasing Si/Al ratio of the acid zeolite (Chung & Park, 2009;Chung et al., 2008). The amount of acid sites decreases as the Si increases over Al in the framework of the zeolite reducing thus its catalytic activity. However, other studies found that zeolites with high Si/Al ratios have better catalytic performance in transesterification reactions (Doyle et al., 2016; Sun et al., 2015) as the strength of the acid sites increases despite their lower number in comparison with zeolites of low Si/Al ratios. In the present study, the effect of acidic properties and Si/Al ratio of HZSM-5 zeolite catalysts on the esterification of linoleic acid as a model reaction for biodiesel production was discussed. The catalytic behavior of HZSM-5 zeolites of Si/Al ratios of 11.5, 25, and 45 was assessed by varying reaction temperature and time, methanol to linoleic acid molar ratio, and catalyst loading. The external mass transfer limitation of HZSM-5 zeolites was investigated and the correlation between the surface hydrophobicity and acidity of the zeolites with different Si/Al ratios and their catalytic performance was assessed based on experimental results.

6.2 Experimental section

6.2.1 Catalysts Synthesis

ZSM-5 zeolite (Si/Al = 45) were synthesized by dissolving 0.26 g of sulfuric acid (Aldrich) and 3.19 g of tetraethoxysilane (TEOS, Aldrich, 98%) in 10.75 g of distilled water in a 45 ml teflon-lined stainless-steel autoclaves. 0.36 g of sodium hydroxide (Riedel de Haen, 99%) and 0.1 g of $Al_2(SO_4)_3.18H_2O$ (Rectapur, 99%) were added to the mixture. An amount of 3.03 g of tetrapropylammonium hydroxide (TPAOH) aqueous solution (25 wt%, Fluka) was finally added in order to set the molar composition of the gel to: $100SiO_2$:

$1Al_2O_3$: $30Na_2O$: $18H_2SO_4$: 20TPAOH: $4000H_2O$ (Dhainaut et al. 2013). The gel was then stirred at 1000 rpm during 30 min, heated at 60 °C for 4 hours and finally placed in a tumbling oven at 150 °C for 4 days. The autoclaves were set at 30 rpm.

ZSM-5 zeolite (Si/Al = 25) were synthesized following a modified method developed by Kim and Kim (Kim and Kim, 2008).To achieve a molar composition of $100SiO_2$: $2Al_2O_3$: $10Na_2O$: $2250H_2O$, 9.39 g of colloidal silica (Sigma-Aldrich, LUDOX HS 40 wt.% SiO_2 in water) and 3.27g of NaOH (10 wt% in water) were added to 5.12 g of distilled water in a 45 ml teflon-lined stainless steel autoclaves. The mixture was stirred at 200 rpm for 3h, at room temperature. In a separate beaker, 0.28 g of NaOH (10 wt% in water) and 0.24 g of sodium aluminate ($NaAlO_2$ of 53 wt% AL_2O_3, 42 wt% Na_2O, and 5 wt% H_2O) were dissolved in 9.87 g of distilled water and stirred at 200 rpm for 3 h. An amount of 4.67 g of distilled water were then added to the beaker mixture. At the end of the 3 hours, the beaker content was added to the solution present in the teflon-lined stainless-steel autoclaves, and the mixture was stirred for 1 hour at room temperature. The reaction temperature was then increased to 190 °C for 2 hours under stirring and finally placed in an oven at 150 °C for 35 h.

For comparison, commercial ZSM-5 zeolite (Si/Al = 11.5) was purchased.
To convert the prepared ZSM-5 zeolites from Na^+ to NH_4^+ form, 1 g of prepared Na-ZSM-5 zeolites was mixed with 20 ml of 1 M solution of NH_4Cl at 80°C for 2 h and stirred in a round bottom flask fitted with a reflux condenser. The ion exchange process was repeated three times. NH_4^+-type zeolites were recovered by filtration, washed with deionized water and dried at 105°C for 6 h. the samples were finally calcined in air at 550 °C for 10 h to give zeolites in H^+ form. The prepared zeolites (H-ZSM5) were denoted by their Si/Al ratio

in the parenthesis after each zeolite name as follows: HZSM-5 (45), HZSM-5 (25) and HZSM-5 (11.5).

6.2.2 Catalysts Characterization

Powder X-ray diffraction (XRD) was performed in the reflection geometry using a Philips X'Pert Pro diffractometer with Cu Kα radiation (wavelength 1.5418 Å) equipped with an X'Celerator real-time multiple strip detector (active length = 2.122 ° 2θ). The powder pattern was collected at 22°C in the range $3 < 2\theta < 50°$.

The morphology and particle size of the synthesized samples were determined using a scanning electron microscope (SEM) (Philips XL30 FEG) working at 7 kV accelerating voltage.

The Si/Al molar ratio of the synthesized samples was estimated by X-ray fluorescence (Philips, Magic X).

A Micromeritics 2420 ASAP was used for nitrogen sorption measurements. Prior to each experiment, 50 mg of the calcined zeolitic samples were outgassed to a residual pressure of less than 0.8 Pa at 300 °C for 15 h. Nitrogen sorption measurements were performed at −196 °C. Specific surface areas were determined according to the Brunauer–Emmett–Teller (BET) method, in the p/p^0 range of 0.05-0.25. Total pore volume was determined from the nitrogen adsorbed volume at $p/p^0 = 0.90$ and the *t*-plot method was used to distinguish micropores from mesopores (p is the vapor pressure and p_0 is the saturation vapor pressure of nitrogen). The mesopore size distribution was calculated using the BJH method.

To determine the number of Brønsted acid sites present in the different solid acids, infrared spectra (FTIR) of pyridine adsorbed at 150 °C were recorded on a Nicolet Magna 550-FT-IR spectrometer with a 2 cm^{-1} optical resolution. After establishing a pressure of 1 Torr at

equilibrium, the self-supported pellets of HZSM-5 were each evacuated at 200 °C under vaccum (10^{-6} bar) for 1 h, to remove all physisorbed species. The concentrations of pyridine adsorbed on the Brønsted [$PyrH^+$] and Lewis [PyrL] sites were determined from the integration of the bands at 1545 and 1454 cm^{-1} respectively, using the extinction coefficients previously determined by Guisnet et al., 1997.

6.2.3 Esterification Reaction Procedure

Linoleic acid (ACROS, 99 %) conversion into methyl linoleate in the presence of methanol was used as a model reaction for biodiesel production. The experiments were performed in triplicates by reflux in a 50 ml batch reactor placed in thermostatic oil bath under stirring. Increased quantities of methanol (Riedel De Haen, 99.9 %) were added to 0.6 mL of linoleic acid (equivalent to 1 mol, 0.54 g), in order to achieve methanol to oil molar ratios of 6:1, 12:1 and 25:1. Optimization of reaction temperature was done by performing reactions at 60, 140 and 180 °C, respectively. The stirring speed was fixed at 550 rpm. The effect of the chemically modified zeolites of different Si/Al ratios on FAMEs production was investigated by using catalysts in loadings of 10 wt% relatively to the quantity of linoleic acid. The desired amount of catalyst was dried before the reaction at 105 ºC. The esterification reaction kinetics were also studied under the same conditions using the optimal determined reaction temperature and methanol to oil molar ratio.

At the end of the reactions, the reactors were extracted with 50 ml methanol followed by two dichloromethane (DCM) (Fisher, 99.8 %) extractions of 50 mL each. The liquid extracts were filtered under gravity through a bed of filtration beads and 0.2 µm filter paper and analyzed for residual fatty acid and produced FAMES, namely methyl linoleate.

6.2.4 Method of Analysis

The analysis of FAMEs content was performed on a Trace Ultragas chromatogram equipped with a flame ionization detector and an HP-INNOWAX capillary column (30 m × 250 µm × 0.25 µm). The flow rate of helium carrier gas was 1 mL/min. The split flow rate was equal to 100 mL/min, the inlet temperature was held at 300 °C and the flame temperature was 250 °C. The sample injection volume was 5 µL. The oven temperature program was as follows: start at 60 °C (2 min), ramp at 10 °C/min to 200 °C (0 min), ramp at 5 °C/min to 240 °C (7 min). Peaks of methyl esters (namely methyl linoleate among other methyl esters) were identified and quantified using reference standards (Supelco 37 component FAME mix in DCM, TraceCert). The yield of methyl esters was determined by the following equation (6-1):

$$Yield\ (\%) = \frac{\sum C_{ME} \times V_{extract}}{M_{0\ Linoleic\ acid}} \times 100 \qquad 6\text{-}1$$

where, C_{ME} is the concentration of methyl esters in g/L quantified by GC/FID, $V_{extract}$ is the extract volume (L) , and $M_{0\ Linoleic\ acid}$, the initial mass of linoleic acid added to the reactor (0.54 g).

Analysis was also performed by high-performance liquid chromatography (HPLC) on an 1100 Series Chromatographic System with a diode array detector (Agilent Technologies, CA, USA) to determine residual linoleic acid concentration. The method developed by Gratzfeld-HüSgen and Schuster (Gratzfeld-Husgen & Schuster, 2001) was followed and a C8 column (150 × 2.1 mm ZORBAX Eclipse XDB, 5 µm) was used. Prior

to injection, FFAs were derivatizated with bromophenacyl bromide (Fluka, Buchs SG, Switzerland), to obtain their corresponding esters. The composition of the mobile phase used was: water (A) and acetonirile + 1% tetrahydrofuran (B), at a solvent gradient of 30% B at 0 min; 70% B at 15 min; and 98% B at 25 min. The detection wavelength for the esters of fatty acids was 258 nm.

6.2.5 Determination of the kinetics of the esterification reaction

To determine the kinetics of the reaction, the effect of time on linoleic acid conversion was measured. A general equation of reaction rate based on the stochiometric relationship of the reactants and products could be presented as follows (eq. (6-2)):

$$-r_a = -\frac{dC_{LA}}{dt} = k' \,.\, C_{LA} \,.\, C_{Me}^3 \qquad \text{6-2}$$

where C_{LA} is the concentration of linoleic acid (mg.L^{-1}), C_{Me} the concentration of methanol (mg.L^{-1}), and *k'* the reaction rate constant (h^{-1}).

Eq. (6-2) follows a second order reaction rate law. However, excess methanol is used in the reversible esterification reaction to shift the equilibrium towards the formation of methyl linoleate. Correspondingly, a pseudo-first order reaction could well describe the esterification mechanism (eq. (6-3)) (Birla et al., 2012; Dang et al., 2013):

$$-r_a = -\frac{dC_{LA}}{dt} = k' . C_{LA} \,.\, C_{Me}^3 = k \,.\, C_{LA} \qquad \text{6-3}$$

where $k = k' . C_{ME}^3 \approx cst$, when methanol is used in excess.

The initial concentration of linoleic acid is set as $C_{0\,LA}$ at time $t = 0$ and as $C_{t\,LA}$ at time t. The integration of eq. (6-3) from $t = 0$ to $t = t$, and $C_{0\,LA}$ to $C_{t\,LA}$ gives eq. (6-4):

$$ln\, C_{0\,LA} - \ln C_{t\,LA} = k\,.\,t \qquad \text{6-4}$$

From the mass balance of the reaction,

$$X_{ML} = 1 - \frac{C_{LA}}{C_{0\,LA}}$$

where X_{ML} is the methyl linoleate yield. Upon rearrangement of eq. (6-4), the kinetics of linoleic acid conversion could be expressed as follows (eq. (6-5)):

$$\ln(1 - X_{ML}) = -k\,.\,t \qquad \text{6-5}$$

6.3 Results and Discussion

6.3.1 Catalyst Characterization

As illustrated in Figure 25, the sole crystalline MFI phase was obtained for all zeolites which confirms the high purity and crystallinity achieved during synthesis. XRD reflections of HZSM-5 (25) are broader than those of HZSM-5 (45) and HZSM-5 (11.5). This is explained by the smaller crystal size that HZSM-5 (25) holds as compared to HZSM-5 (45) and HZSM-5 (11.5) as confirmed by SEM imaging.

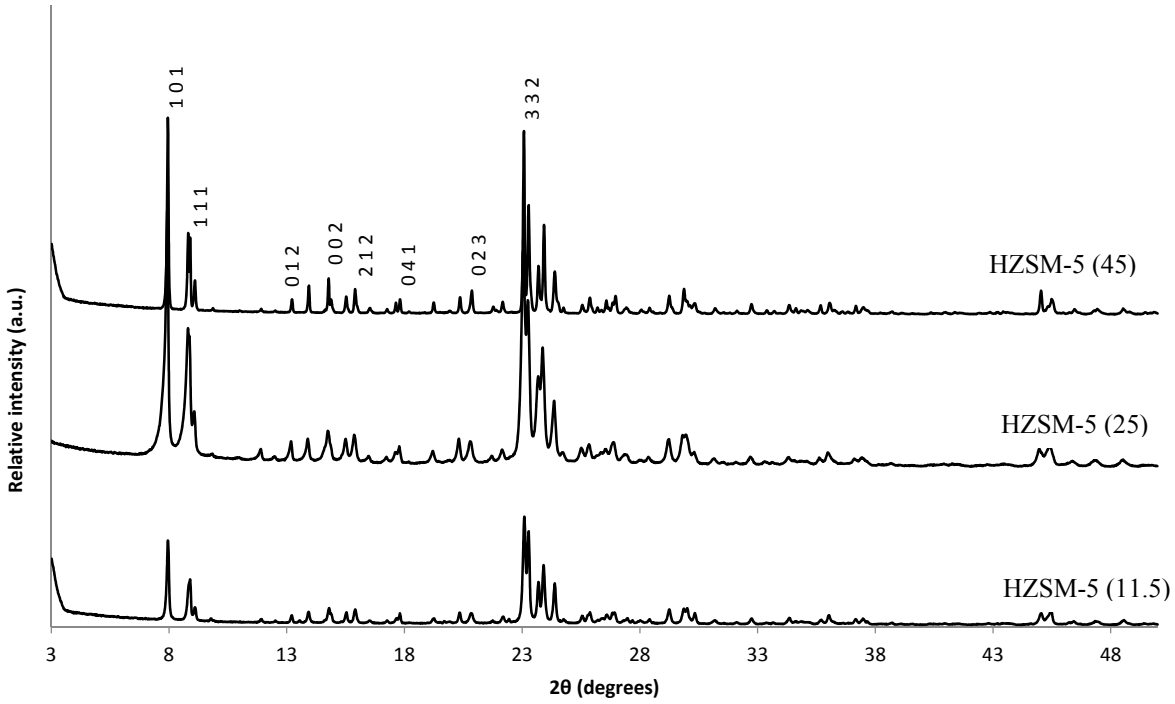

Figure 25. Wide angle XRD patterns of exchanged and calcined HZSM-5 (45), HZSM-5 (25), and HZSM-5 (11.5)

The SEM micrographs shown in Figure 26 reveal the shape of the HZSM-5 zeolites of different Si/Al ratios. HZSM- 5 (45) crystals have crystal sizes ranging between 2.4 and 6 µm (Figure 26a). HZSM-5 (25) crystals show lower average sizes of 1.5 to 5.5 µm (Figure 26b) and HZSM-5 (11.5) zeolites have crystal sizes of 2 to 6 µm (Figure 26c).

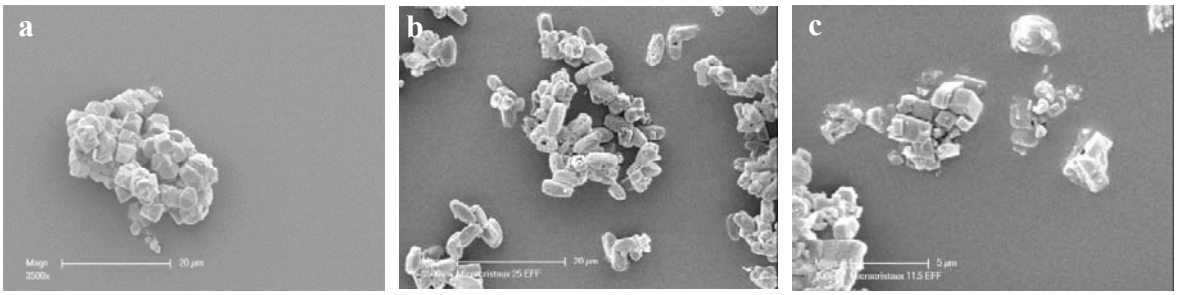

Figure 26. Scanning electronic microscopy (SEM) images of (a) HZSM-5 (45), (b) HZSM-5 (25), and (c) HZSM-5 (11.5)

The textural data of the synthesized samples HZSM-5 (45), H-ZSM-5 (25) and HZSM-5 (11.5) are summarized in Table 12. Type I adsorption isotherms are obtained for conventional MFI-type zeolites (Figure 27), which is typical for completely microporous materials. A slight hysteresis was observed for the three zeolite samples, due to the agglomeration of microcrystals and the formation of inter-particular voids in which nitrogen was adsorbed. BET surface areas of the three samples were also similar and measured 380 $m^2.g^{-1}$. The microporous volume of HZSM-5 (45) with the highest Si/Al ratio was, 0.17 $cm^3.g^{-1}$, while a lower value of 0.15 $cm^3.g^{-1}$ was measured for HZSM-5 (25) and HZSM-5 (11.5).

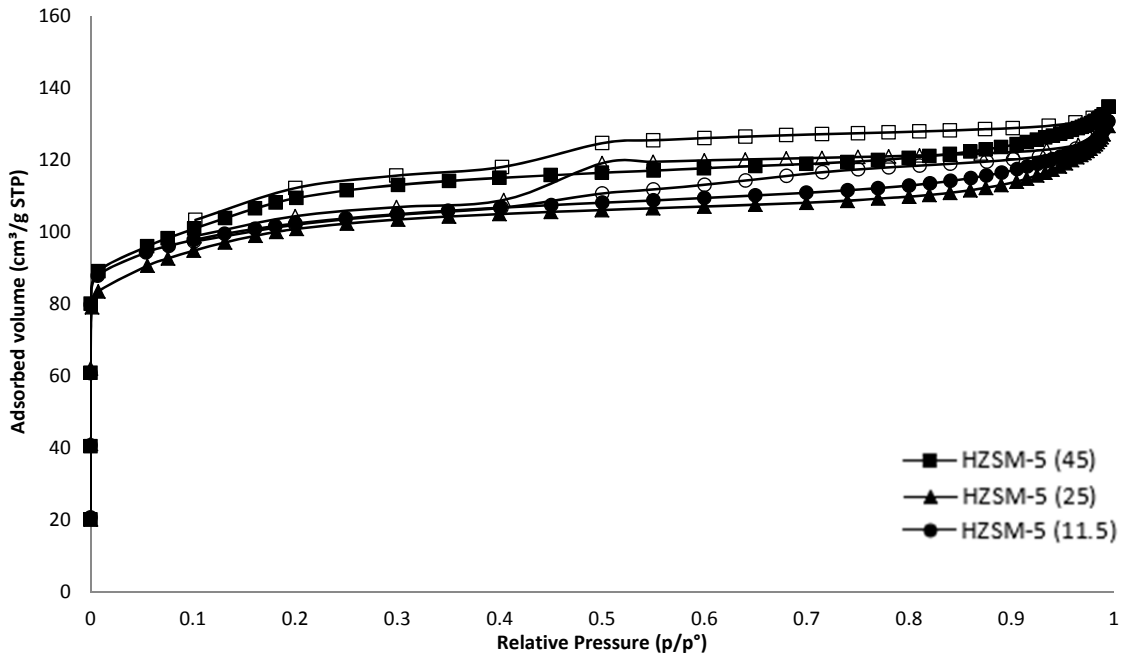

Figure 27. N_2 adsorption/desorption isotherms at −196 °C of the calcined HZSM-5 (45), HZSM-5 (25), and HZSM-5 (11.5) samples. Full bullets represent adsorption isotherms and empty bullets, the desorption ones.

The quantification of the acidity of HZSM-5 with different Si/Al ratios was done by FTIR of adsorbed strong base pyridine molecule. In addition to its ability to access the inner pores of the zeolites, it distinguishes between protonic Brønsted acid sites ($PyrH^+$) and coordinated Lewis acidic sites (PyrL) (Derouane et al. 2013). The concentrations of Lewis and Brønsted acidic sites were calculated from the bands at 1454 cm^{-1} and 1545 cm^{-1}, respectively and the results are reported in Table 12. It is interesting to observe the effect of Si/Al ratio on the acidity of the zeolites. As Si/Al ratio increases for the HZSM-5 zeolites, the total concentration of acid sites ($PyrH^+$ and PyrL) decreases, making the number of total acid sites a function of the Si/Al ratio. This is not surprising because as Al content decreases in the zeolite, charge imbalance associated to the Al content also

decreases, yielding a lower H^+ exchange capacity. However, the strong Brønsted acidic sites concentrations don't undertake the same trend for the different zeolites. Although the amount of total acid sites and acid strength was the highest for HZSM-5 (11.5), [$PyrH^+$] of HZSM-5 (25) was lower than that of HZSM-5 (45), whereby a higher relative density of the total acid sites of HZSM-5 (25) existed as Lewis sites in comparison with HZSM-5 (45).

Table 12. BET surface area, porous volume and acidity of the H-ZSM5 catalysts with different Si/Al ratios

HZSM-5 types	S BET (m^2/g)	Total porous volume (cm^3/g)	Microporous volume (cm^3/g)	[$PyrH^+$][a] ($\mu mol.g^{-1}$)	[PyrL][b] ($\mu mol.g^{-1}$)
HZSM-5 (45)	395	0.17	0.17	351	44
HZSM-5 (25)	373	0.15	0.15	347	126
HZSM-5 (11.5)	387	0.15	0.15	749	173

[a]Concentration of pyridine adsorbed on Brønsted acid sites after thermodesorption at 150 °C.
[b]Concentration of pyridine adsorbed on Lewis acid sites after thermodesorption at 150 °C.

6.3.2 Optimized Reaction Conditions of Esterification

6.3.2.1 Effect of Reaction Temperature on Esterification

To study the effect of reaction temperature on the conversion of linoleic acid, experiments using HZSM-5 (45), HZSM-5 (25) and HZSM-5 (11.5) were carried out at three different temperatures of 60, 140 and 180°C, under the same reaction conditions (methanol to linoleic acid molar ration = 12/1, stirring rate = 550 rpm, catalyst loading = 10 wt%, and reaction time = 6 h). As shown in Figure 28, catalytic activity increased with increasing temperature except for HZSM-5 (45) and HZSM-5 (25) which showed no significant difference in linoleic conversion at 60 and 140 °C. For all zeolites, the highest

linoleic acid conversions were reached at the optimal reaction temperature of 180°C, with the order of conversion being HZSM-5 (45) (45.76 %, SD = 4.85) > HZSM-5 (25) (43.73 %, SD = 4.43) > HZSM-5 (11.5) (27.96 %, SD = 2.23). Higher temperatures achieved higher conversions which is explained by the decrease of the FA viscosity at high temperatures, promoting thus a better methanol/linoleic acid phase mixture, increasing thus methyl linoleate yield. It is noteworthy to mention that at the different reaction temperatures used, linoleic acid conversions using HZSM-5 (45) were the highest, followed by HZSM-5 (25) and HZSM-5 (11.5), respectively. While HZSM-5 (11.5) has the highest strong acid sites concentration, it exhibits the lower catalytic performance. The increase of acid strength doesn't seem to be the only factor affecting the conversions obtained, as will be later discussed.

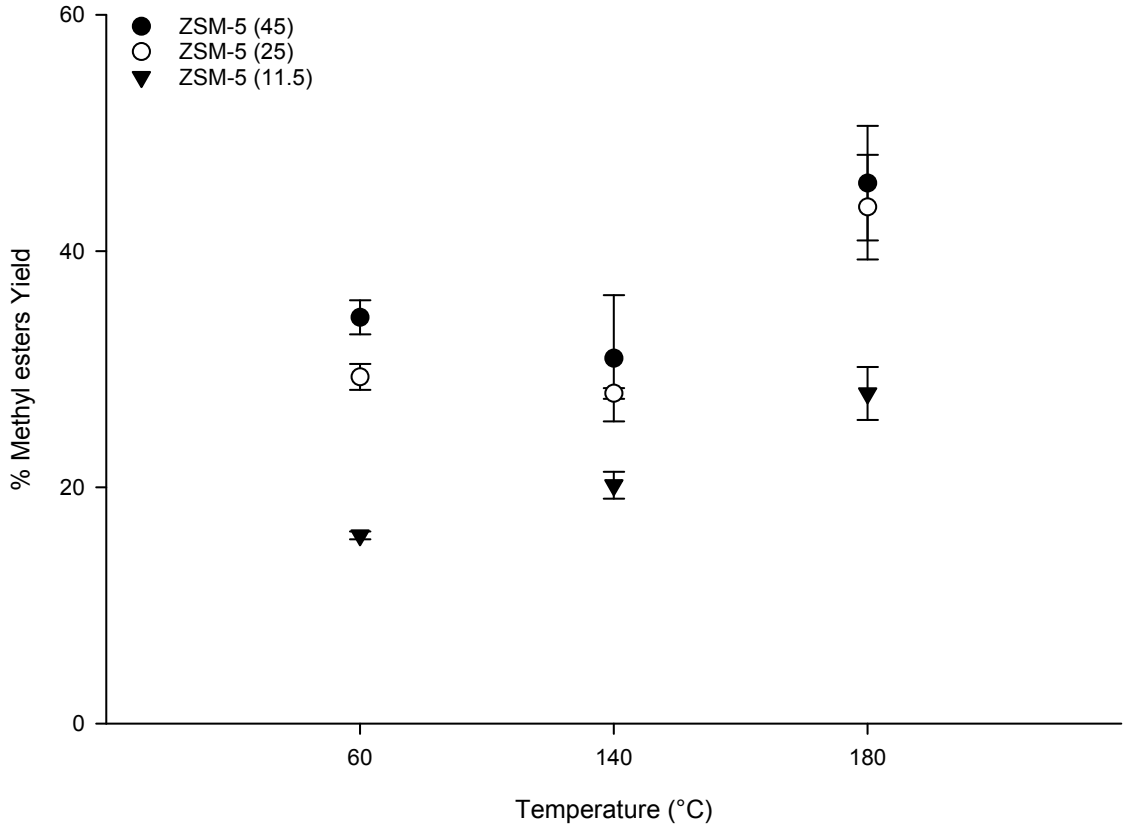

Figure 28. Effect of reaction temperature variation on the esterification of linoleic acid using HZSM-5 (45), HZSM-5 (25), and HZSM-5 (11.5) catalysts at the molar ratio of methanol to linoleic acid molar ratio of 12:1, catalyst loading of 10 wt%, stirring rate of 550 rpm, and reaction time of 6 h

6.3.2.2 Effect of Methanol to Linoleic Acid Ratio on Esterification

The effect of the molar ratio of methanol to linoleic acid on the conversion of the latter was examined through varying the amount of methanol used for the different HZSM-5 (45), HZSM-5 (25), HZSM-5 (11.5) catalysts. Methanol to linoleic acid molar ratios of 6:1, 12:1, and 25:1 were used to provide excess methanol to force the reversible esterification reaction towards the formation of methyl linoleate (Qiu et al. 2011). Similar

reaction conditions were used for the esterification reactions and consisted of 10 wt% catalyst loading, 6 h reaction time, 550 rpm stirring rate, and fixed optimal temperature of 180°C. Figure 29 shows that the conversion rate of linoleic acid decreased for all zeolite catalysts as the molar ratio of methanol to linoleic acid increased from 6:1 to 12:1 and from 12:1 to 25:1. At higher methanol to linoleic acid molar ratios, the influence of reverse reaction is potentially greater than the forward esterification reaction. This phenomenon is due to the slight recombination of methyl linoleate and water to form linoleic acid. Excess methanol could affect the solubility of the nearly immiscible water and methyl linoleate encouraging thus the backward reaction to take place (Shu et al., 2007). Also, the conversion may have decreased due to the adsorption of more water produced when the quantity of methanol was further increased to react with linoleic acid. Methanol to linoleic molar ratio of 6;1 was thus the optimal molar ratio with an order of conversion of HZSM-5 (45) (78.62 %, SD = 0.63) > HZSM-5 (25) (61.56 %, SD = 2.30) > HZSM-5 (11.5) (27.96 %, SD = 1.99).

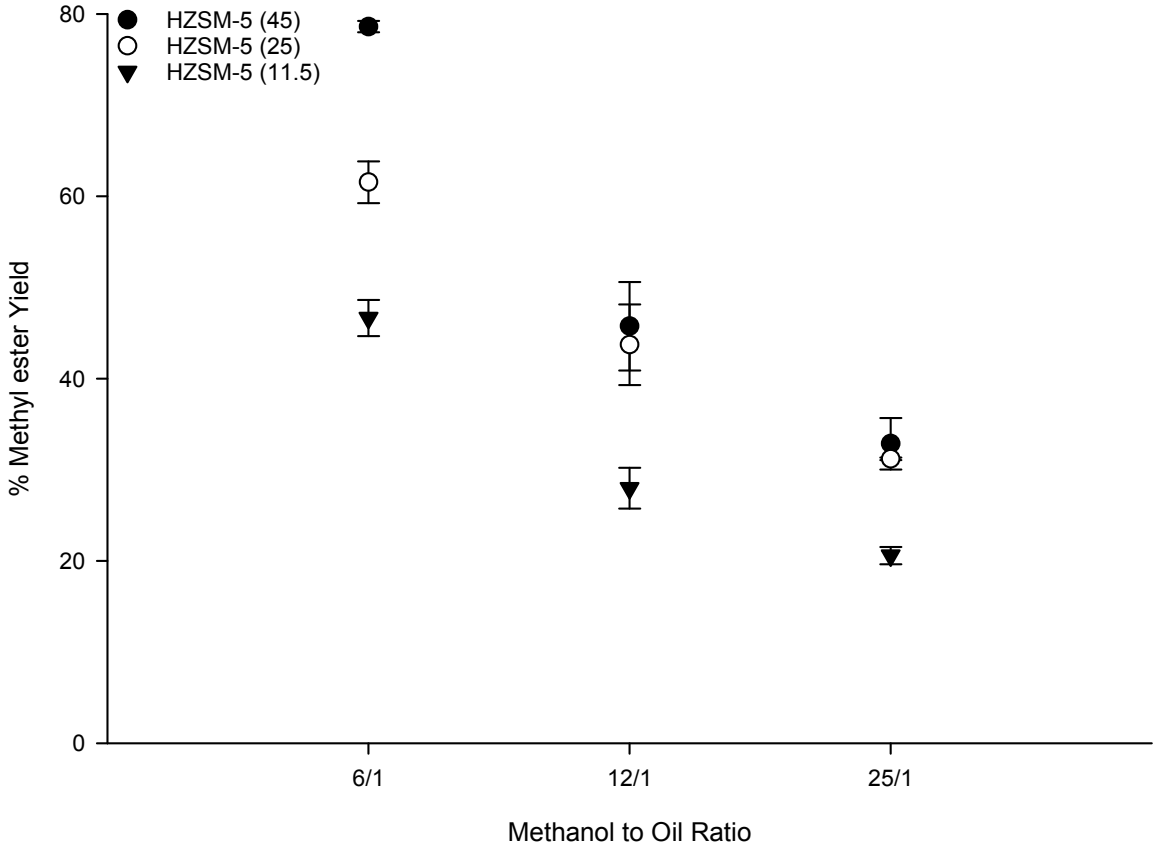

Figure 29. Effect of methanol to linoleic acid molar ration variation on the esterification of linoleic acid using HZSM-5 (45), HZSM-5 (25), and HZSM-5 (11.5) catalysts at catalyst loading of 10 wt%, reaction temperature of 180 °C, stirring rate of 550 rpm and reaction time of 6 h

For all the experiments carried out, residual linoleic acid was quantified using HPLC and mass balance closure was inspected. Table H in APPENDIX H presents numeric methyl esters yields and residual linoleic acid content at the different reaction conditions.

6.3.2.3 Effect of External Mass Transfer Limitation

Microporous HZSM-5 zeolites have a small pore size (5.1 – 5.5 Å) and linoleic acid molecules possess a kinetic diameter of 8.08 Å estimated using eq. (6-6) (Wang & Frenklach, 1994).

$$\sigma = 1.234 \,.\, (M_W)^{1/3} \qquad 6\text{-}6$$

where σ is the kinetic diameter estimated for hydrocarbonmolecules, and M_W is the molecular weight of linoleic acid in g mol^{-1}.

Meaning that it is unlikely for such a molecule to penetrate the pores and reach the active intrinsic sites of the microporous zeolite such as microporous HZSM-5.

Therefore, the esterification reaction is more likely to happen on the external surface of microporous HZSM-5 (Vieira et al. 2015, 2017). However, the mass transfer between the bulk fluid and the external catalytic surface should be examined. In a homogeneous catalytic reaction, the effect of mass transfer is negligible, as all substances (reactants, catalysts and products) are in the same phase. In a heterogeneous catalytic reaction as is the case in this study, the catalyst is in a different phase than the reactants and diffusion of the reactants from the bulk phase to the external surface of the catalyst particle can be hindered if proper stirring is not provided.

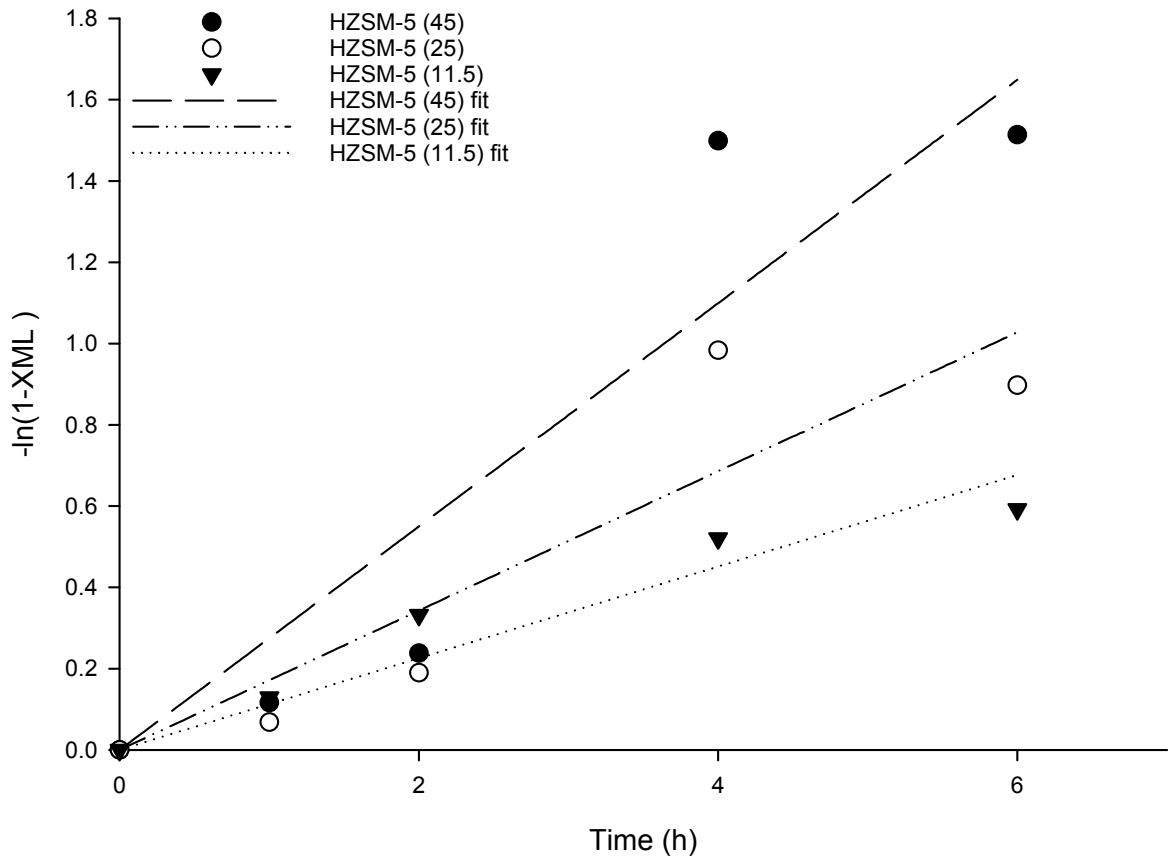

Figure 30. $-ln(1-X_{ML})$ versus reaction time plot at optimal reaction conditions using HZSM-5 with different Si/Al ratios

At 550 rpm stirring rate, the effect of external mass transfer limitations could be examined using the dimensionless Mears criterion (C_M) (Ju et al. 2011):

$$C_M = \frac{r_0 \ \rho \ d \ n}{2 \ k_c \ C_0} \qquad 6\text{-}7$$

where, r_0 is the initial reaction rate which is equal to the reaction rate of linoleic acid esterification at 60 min (= $\frac{moles\ of\ methyl\ esters\ produced\ in\ the\ reaction\ time\ (mol)}{catalyst\ loading\ (g) \times reaction\ time\ (min)}$ (Sert et al., 2013), ρ is the framework density of HZSM-5, d is the mean diameter of the catalyst particles, C_0 is the initial concentration of linoleic acid, n is the reaction order (the esterification reaction obeyed the pseudo first-order reaction kinetics as shown in Figure 30 with reaction rates of 2.75×10^{-1}, 1.71×10^{-1}, and 1.13×10^{-1} for HZSM-5 (45), HZSM-5 (25) and HZSM-5 (11.5), respectively), and k_c is the mass transfer coefficient, estimated by the Dwivedi-Upadhyay equation (Dwivedi& Upadhyay, 1977):

$$k_c = \frac{2D_{AB}}{d_z} + 0.31\, N_S^{\frac{2}{3}} \left(\frac{\Delta\rho\ \mu_c\ g}{\rho_c^2}\right)^{1/3} \qquad 6\text{-}8$$

where D_{AB} is the molecular diffusion coefficient of solute A (linoleic acid) at very low concentration in solvent B (methanol), calculated based on the Wilke-Chang method, accounting for the reaction temperature of 180 °C (Wilke & Chang, 1955), d_z is the diameter of the catalyst particle, μ_c is the viscosity of the solvent, g is the gravitational acceleration, N_S is the Schmidt number, and $\Delta\rho$ is the difference between density of the solution and the catalyst and ρ_c the density of the solvent.

If the value of the Mears parameter is lower than 0.15, the external mass transfer diffusion resistance is negligible in the kinetic study. C_M were 2.71×10^{-7}, 1.35×10^{-7}, and 2.84×10^{-7} for HZSM-5 (45), HZSM-5 (25) and HZSM-5 (11.5) respectively. This indicates that the external mass transfer limitations in the solid-liquid interface were

overcome when the stirring speed was 550 rpm and that the esterification reaction mainly took place on the totality of the external surface of the zeolite.

6.3.2.4 Effect of Reaction Time on Esterification

In order to study the influence of reaction time on the conversion of linoleic acid, experiments were carried out using HZSM-5 (45), HZSM-5 (25), HZSM-5 (11.5) catalysts at the optimal reaction conditions (methanol to linoleic acid molar ratio of 6:1, reaction temperature of 180 °C, catalyst loading of 10% and stirring rate of 550 rpm) with the variation of reaction time in the range of 0 - 24 h. Figure 31 shows the effect of reaction time on methyl linoleate yield for the different Si/Al ratio catalysts. According to the results, an increase in the reaction time from 1 to 4 h causes a marked increase of conversion of linoleic acid reached a maximum yield of 79.78 % and 62.60 % registered for HZSM-5 (45) and HZSM-5 (25) at 4 h. For these two zeolites, no further significantly different conversion was observed in the reaction time from 4 to 8 h, making thus the 4 h the optimal reaction time for the model reaction of biodiesel. A maximum yield of 48.66% was however achieved at 6 h reaction time for HZSM-5 (11.5). The general increase in catalytic activity for the HZSM-5 zeolites of higher Si/Al ratios will be explained in detail below. Aside from yielding lower linoleic acid conversions, higher reaction times are not favorable for the esterification reactions due to the higher energy consumption they require.

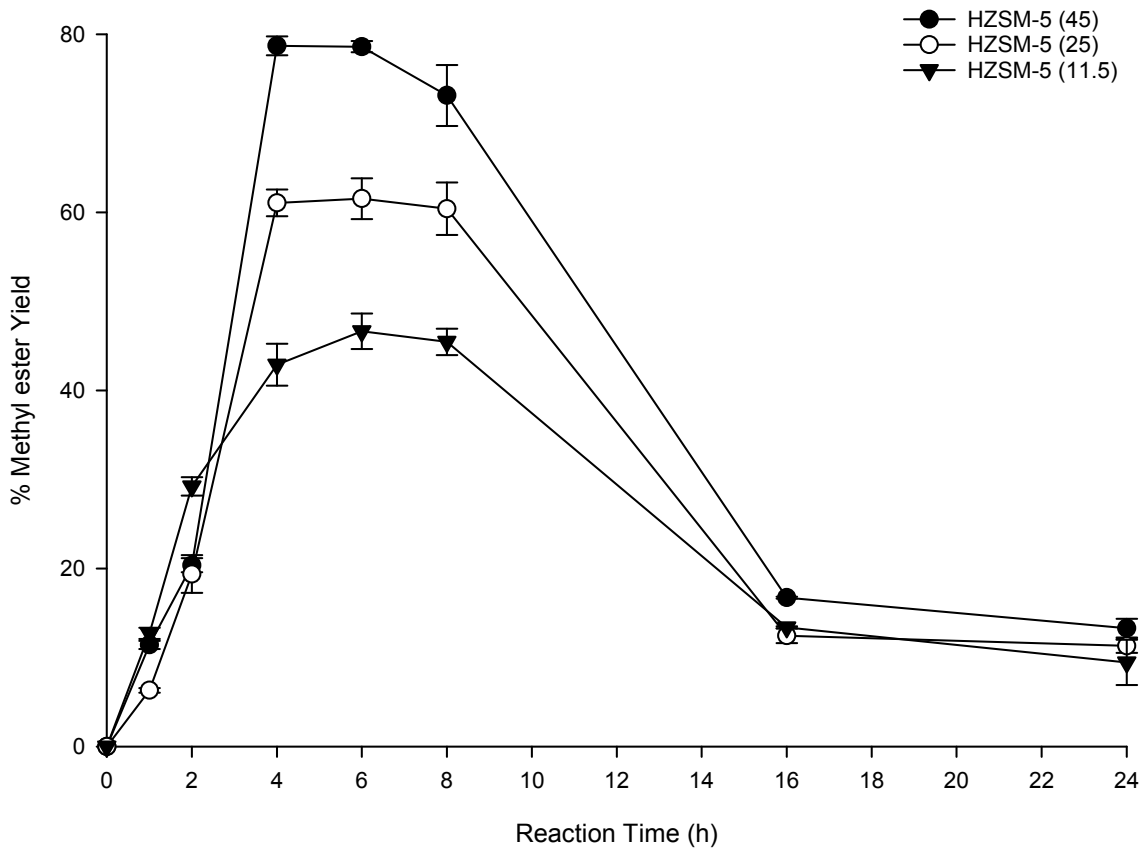

Figure 31. Effect of reaction time on the esterification of linoleic acid using HZSM-5 (45), HZSM-5 (25), and HZSM-5 (11.5) catalysts at catalyst loading of 10 wt%, methanol to linoleic molar ratio of 6:1, reaction temperature of 180 °C, and stirring rate of 550 rpm

6.3.3 Effect of Si/Al Ratio on Esterification

The difference in activity between HZSM-5 zeolites with different Si/Al ratios is interesting (Fig.7). At early stages of the esterification reactions (up to 2 h), a higher catalytic activity was observed for the HZSM-5 zeolite with the lower Si/Al, agreeing with the fact that the activity improves as the number of strong acid sites increases (at lower Si/Al ratios). After 4 h of reaction time, the activity of linoleic acid on zeolites increased with increasing Si/Al ratio. Doyle et al. reported a similar increase in activity for the HY

zeolites with lower Si/Al ratio, during the initial stages of the reaction (Doyle et al. 2016). However, for a lower Si/Al ratio, the zeolite presents a more hydrophilic character which makes it more prone to adsorbing on its surface the water produced from the esterification reactions, blocking thus the access of the fatty acids to the external active sites. As water is produced, it competes with less polar methanol and linoleic acid for the adsorption sites of the zeolites surface. This explains the lower linoleic acid conversions registered for the more hydrophilic HZSM-5 (11.5) zeolites starting 4 h reaction time. On another hand, although zeolites with high Si/Al ratio may lose their acidic properties, their higher hydrophobic character allow them to rapidly desorb the produced water during the esterification reaction which could lead to the catalysts deactivation. This results in an increase in the surface coverage of linoleic acid. Therefore, Si/Al ratio of HZSM-5 determines the acidity and relative hydrophobic character of the zeolite, both influencing the kinetics and ultimate yield from the esterification reactions. At early stages of the esterification reaction the acidity of the zeolites took over the hydrophilic character of HZSM-5 (11.5) as water molecules were not yet produced in quantities high enough to compete with linoleic acid adsorption to acid sites. HZSM-5 (11.5) registered a maximum conversion of 30.28 % at 2 h reaction time in comparison with 21.49 % and 21.15 % for HZSM-5 (25) and HZSM-5 (45), respectively. However, at later stages of the reactions (beyond 4 h), the relative hydrophobic character of HZSM-5 zeolites allowed rapid desorption of produced water molecules and more coverage of linoleic acid which resulted in higher methyl esters production) yields despite the lower acidity. Linoleic acid conversion reached a maximum of 79.78 % and 62.60 % for HZSM-5 (45) and HZSM-5 (25) at 4 h reaction time, respectively, whereas it only reached a maximum of 45.27% at a

similar reaction time for HZSM-5 (11.5). Thus, HZSM-5 (11.5) zeolite exhibited the highest Bronsted acidity but the lower catalyst performance, and the zeolites with high Si/Al ratios had better catalyst performance.

6.4 Conclusion

Esterification of linoleic acid with methanol was carried out over HZSM-5 zeolites with different Si/Al ratios. A maximum methyl ester yield of 79.78 % was reached for the esterification of linoleic acid using HZSM-5 (45) at 4 h reaction time, 10 wt% catalyst loading, 6:1 methanol to linoleic acid molar ratio and 180 °C. It was shown that Si/Al ratio of HZSM-5 zeolites determines their acidity and hydrophobic character with a combined effect on the esterification reactions. As the reaction time progresses, water molecules are produced and are rapidly adsorbed to more hydrophilic surfaces (zeolites with low Si/Al), decreasing the surface coverage of linoleic acid and yielding lower conversions despite the zeolites' higher acidity. The conversion rate of linoleic acid with methanol could thus be enhanced by designing zeolites with adequate relative hydrophobicity and acidity.

CHAPTER 7
CONCLUSION

For the application of HZSM-5 zeolite catalyst in esterification and transesterification reactions, the catalytic performance of zeolites depends on their acidic properties, hydrophobic character and on their pore size.

7.1 Important conclusions

7.1.1 With respect to the economic viability of homogeneous transesterification from WFOs in Lebanon

Despite being an economically-sustainable fuel alternative for the years 2011 through 2014, the viability of biodiesel production from WFOs doesn't apply to the years 2015 to present in Lebanon. The economic sensitivity assessment of biodiesel production from WFOs allowed a better understanding of cost interactions and showed that biodiesel production cost is economically competitive with fossil diesel when a subsidy policy on WFOs acquisition cost is implemented by the government. Benefit analysis showed that biodiesel presents superior environmental benefits over petroleum diesel and its production provides a net energy gain. Accordingly, by interacting with local authorities and creating a more covered supply chain coordination system, it would be possible to successfully reuse WFOs for the production of biodiesel on a national scale for the long term, and reduce the environmental damages caused by their disposal.

7.1.2 With respect to the application of hierarchical heterogeneous zeolites for biodiesel production

Esterification of linoleic acid and WFOs with methanol was successfully catalyzed using hierarchical HZSM-5 zeolite catalysts produced in nanosheet and nanosponge morphologies as compared to highly acidic conventional big and nano-crystals of HZSM-5 zeolites. Improved accessibility and molecular transport of linoleic acid from the outer mesoporous surface to the intrinsic active zeolitic framework resulted in achieving high conversions for HZSM-5 nanosheets and HZSM-5 nanosponges at similar reaction conditions. Maximum methyl ester yields of 95.12 % and 48.29 % were reached for the esterification of linoleic acid and WFOs respectively, using NSh-HZSM-5 at 4 h reaction time, 10 wt% catalyst loading, respective 6:1 and 12:1 methanol to oil molar ratio and 180 °C. Although highly accessible and acidic, HZSM-5 nanosponges did not operate to their full potential as compared to HZSM-5 nanosheets given their higher hydrophilicity which hindered fatty acid and triglycerides adsorption to their surface and subsequently their transfer from the outer surfaces of the mesopores to the intrinsic active sites. Also, the connectivity between the two levels of porosity could have not been optimal for effective selective transport of reactant and product molecules to and from the active sites of the nanosponge catalysts.

7.1.3 With respect to the effect of acidic and hydrophobic characters on the catalytic performance of zeolites with different Si/Al ratios

It was shown that Si/Al ratio presents a trade-off between the acidity and the hydrophobic character of the zeolite. As the esterification reaction time progresses, polar by-product molecules are produced and are rapidly adsorbed to more hydrophilic surfaces (low Si/Al), decreasing the surface coverage of less polar fatty acids and methanol and yielding lower conversions despite the zeolites' higher acidity. FAMEs yield could thus be enhanced by designing zeolites with higher hydrophobicity.

7.2 Future Work

Recommended future work includes:

7.2.1 Shape selective effect of channels and cages of different hierarchical zeolites for biodiesel production

Hierarchical porous solids can be characterized by the number of porosity levels in the material and their individual geometry. As exemplified by the mesoporous ZSM-5 in this study, the prime aim of hierarchical zeolites is coupling in a single material the catalytic features of micropores and the improved access and transport consequence of additional pores of larger size. However, the connectivity between the various levels of pores is essential to take full advantage of the benefits of hierarchy in catalyzed reactions. Thus, introducing mesopores in zeolites could be unsuccessful for selective catalytic application of bulky molecules if not properly located in the crystal as might have been the case with HZSM-5 nanosponges. A closer look at produced hierarchical zeolites should be taken into consideration aiming not only at extensively generating large pores, but

principally at locating them in harmony with the micropores. This is captured well by the quote by the French architect Robert Le Ricolais, which can be adapted to this topic as “the art of making hierarchical materials is where to put the pore”.

7.2.2 Factors affecting biodiesel yield variation between linoleic acid esterification and WFOs transesterification

For both linoleic acid esterification and waste frying oil transesterification, HZSM-5 nanosheets showed the best catalytic performance in comparison to the other tested zeolites. However, the maximum yields found for both reactions were very different. A maximum methyl ester yield of 95.12 % was reached for the esterification of linoleic acid using HZSM-5 nanosheets at 4 h reaction time, 10 wt% catalyst loading, 6:1 methanol to linoleic acid molar ratio and 180 °C, whereas, at the same reaction conditions except for the methanol to WFO ratio of 12:1, a maximal yield of FAMEs of 48.29% was achieved. In addition to FFAs and triglycerides, WFOs contain impurities and are subject to autoxidation giving rise to supplementary compounds like peroxides. Selectivity of the acid catalyst towards all molecules present in the waste oil should be investigated. Peroxides and other compounds present in oil could compete with triglycerides and FFAs molecules for directly accessing the mesopores of the hierarchical zeolite from the outer surface of the zeolite crystal and be transported to the intrinsic active sites, hindering and possibly obstructing thus the conversion of the desired reactants to FAMEs.

7.2.3 Quantification of enhanced acid site accessibility in hierarchical zeolites

Brønsted and Lewis acid sites can coexist on the surface of the zeolite, in the openings of the mesopores and inside the microporous lattice (Derouane et al., 2013). It is relevant to identify the location of the acid sites and distinguish between Brønsted and Lewis sites in the different pore levels of the hierarchical zeolite. Although generally difficult, it is often possible to distinguish between acid sites that are located inside the zeolite pores micropores and acid sites that reside at the mesopores openings and on the outer surface, by using suitably large probe base molecules. In this study, pyridine molecules were used for the qualitative and quantitative analysis of the acid sites by FTIR spectroscopy. Pyridine can access the zeolites' micropores, mesopores and external surface and react with the corresponding acid sites either ionically (on Brønsted sites) or covalently (on Lewis sites) which is lacking in more valuable information. A probe molecule like collidine, which is too bulky to diffuse into the HZSM-5 micropores, can be used to exclusively study the mesopore formation and accessibility to active sites. The approach of using molecular probes of different sizes can thus provide valuable information regarding the location and the strength of active sites in hierarchical zeolite.

BIBLIOGRAPHY

Aarthy, M. et al. 2014. "Enzymatic Transesterification for Production of Biodiesel Using Yeast Lipases: An Overview." *Chemical Engineering Research and Design* 92(8): 1591–1601. http://linkinghub.elsevier.com/retrieve/pii/S0263876214001841.

Adewale, Peter, Marie-Josée Dumont, and Michael Ngadi. 2015. "Recent Trends of Biodiesel Production from Animal Fat Wastes and Associated Production Techniques." *Renewable and Sustainable Energy Reviews* 45: 574–88. http://linkinghub.elsevier.com/retrieve/pii/S1364032115001276.

Agarwal, Avinash Kumar. 2007. "Biofuels (Alcohols and Biodiesel) Applications as Fuels for Internal Combustion Engines." *Progress in Energy and Combustion Science* 33(3): 233–71. http://linkinghub.elsevier.com/retrieve/pii/S0360128506000384.

Aghbashlo, Mortaza, and Ayhan Demirbas. 2016. "Biodiesel: Hopes and Dreads." *Biofuel Research Journal* 3(2): 379–379. http://www.biofueljournal.com/article_15282.html.

Akbar, E., Binitha, N., Yaakob, Z., Kamarudin, S. K., & Salimon, J. 2009. "Preparation of Na Doped SiO 2 Solid Catalysts by the Sol-Gel Method for the Production of Biodiesel from Jatropha Oil." *Green Chemistry* 11(11): 1862–66.

Akia, Mandana et al. 2014. "A Review on Conversion of Biomass to Biofuel by Nanocatalysts." *Biofuel Research Journal* 01(01): 16–25. http://www.biofueljournal.com/pdf_4747_5a92b5c3cb64907a765d44d1e7a57be5.htm.

Al-Hamamre, Zayed, and Jehad Yamin. 2014. "Parametric Study of the Alkali Catalyzed Transesterification of Waste Frying Oil for Biodiesel Production." *Energy Conversion and Management* 79: 246–54. http://linkinghub.elsevier.com/retrieve/pii/S0196890413008030.

Al-Jammal, Noor, Zayed Al-Hamamre, and Mohammad Alnaief. 2016. "Manufacturing of Zeolite Based Catalyst from Zeolite Tuft for Biodiesel Production from Waste Sunflower Oil." *Renewable Energy* 93: 449–59. http://dx.doi.org/10.1016/j.renene.2016.03.018.

Al-Widyan, Mohamad I., and Ali O. Al-Shyoukh. 2002. "Experimental Evaluation of the Transesterification of Waste Palm Oil into Biodiesel." *Bioresource Technology* 85(3): 253–56. http://linkinghub.elsevier.com/retrieve/pii/S0960852402001359.

Alam, M, J Song, V Zello, and A Boehman. 2006. "Spray and Combustion Visualization of a Direct-Injection Diesel Engine Operated with Oxygenated Fuel Blends." *International Journal of Engine Research* 7(6): 503–21.

http://journals.sagepub.com/doi/10.1243/14680874JER01506.

Alismaeel, Ziad T., Ammar S. Abbas, Talib M. Albayati, and Aidan M. Doyle. 2018. "Biodiesel from Batch and Continuous Oleic Acid Esterification Using Zeolite Catalysts." *Fuel* 234(February): 170–76. https://linkinghub.elsevier.com/retrieve/pii/S0016236118312250.

Alves, C.T. et al. 2013. "Transesterification of Waste Frying Oil Using a Zinc Aluminate Catalyst." *Fuel Processing Technology* 106: 102–7. http://linkinghub.elsevier.com/retrieve/pii/S0378382012002688.

Antonić-Jelić, Tatjana et al. 2003. "Experimental Evidence of the 'Memory' Effect of Amorphous Aluminosilicate Gel Precursors." *Microporous and Mesoporous Materials* 64(1–3): 21–32. http://linkinghub.elsevier.com/retrieve/pii/S1387181103004980.

Aoshima, Hiroyuki et al. 2005. "Glycerin Fatty Acid Esters as a New Lubricant of Tablets." *International Journal of Pharmaceutics* 293(1–2): 25–34. http://linkinghub.elsevier.com/retrieve/pii/S0378517305000050.

Araujo, Victor Kraemer Wermelinger Sancho, Silvio Hamacher, and Luiz Felipe Scavarda. 2010. "Economic Assessment of Biodiesel Production from Waste Frying Oils." *Bioresource Technology* 101(12): 4415–22. http://linkinghub.elsevier.com/retrieve/pii/S0960852410001872.

Arnold, Andreas, Stefan Steuernagel, Michael Hunger, and Jens Weitkamp. 2003. "Insight into the Dry-Gel Synthesis of Gallium-Rich Zeolite [Ga]Beta." *Microporous and Mesoporous Materials* 62(1–2): 97–106. http://linkinghub.elsevier.com/retrieve/pii/S1387181103003974.

Arumugam, A., and V. Ponnusami. 2014. "Enzymatic Transesterification of Calophyllum Inophyllum Oil by Lipase Immobilized on Functionalized SBA-15 Synthesized from Low-Cost Precursor." *Biomass Conversion and Biorefinery* 4(1): 35–41. http://link.springer.com/10.1007/s13399-013-0087-1.

Atadashi, I.M., M.K. Aroua, A.R. Abdul Aziz, and N.M.N. Sulaiman. 2012. "The Effects of Water on Biodiesel Production and Refining Technologies: A Review." *Renewable and Sustainable Energy Reviews* 16(5): 3456–70. http://linkinghub.elsevier.com/retrieve/pii/S1364032112001840.

Atadashi, I. M., Aroua, M. K., Aziz, A. A., & Sulaiman, N. M. N. 2013. "The Effects of Catalysts in Biodiesel Production: A Review." *Journal of Industrial and Engineering Chemistry* 19(1): 14–26. http://linkinghub.elsevier.com/retrieve/pii/S1226086X1200233X.

Atapour, Mehdi, and Hamid-Reza Kariminia. 2011. "Characterization and

Transesterification of Iranian Bitter Almond Oil for Biodiesel Production." *Applied Energy* 88(7): 2377–81. http://linkinghub.elsevier.com/retrieve/pii/S0306261911000171.

Auerbach, S. M., Carrado, K. A., & Dutta, P. K. 2003. *Handbook of Zeolite Science and Technology.*

Avhad, M.R., and J.M. Marchetti. 2015. "A Review on Recent Advancement in Catalytic Materials for Biodiesel Production." *Renewable and Sustainable Energy Reviews* 50: 696–718. http://linkinghub.elsevier.com/retrieve/pii/S1364032115004979.

Ayodele, Olubunmi O., and Folasegun A. Dawodu. 2014. "Production of Biodiesel from Calophyllum Inophyllum Oil Using a Cellulose-Derived Catalyst." *Biomass and Bioenergy* 70: 239–48. http://linkinghub.elsevier.com/retrieve/pii/S0961953414004085.

Azcan, Nezihe, and Ozlem Yilmaz. 2013. "Microwave Assisted Transesterification of Waste Frying Oil and Concentrate Methyl Ester Content of Biodiesel by Molecular Distillation." *Fuel* 104: 614–19. http://linkinghub.elsevier.com/retrieve/pii/S0016236112005133.

Babajide, Omotola, Nicholas Musyoka, Leslie Petrik, and Farouk Ameer. 2012. "Novel Zeolite Na-X Synthesized from Fly Ash as a Heterogeneous Catalyst in Biodiesel Production." *Catalysis Today* 190(1): 54–60. http://dx.doi.org/10.1016/j.cattod.2012.04.044.

Balat, M. 2008. "Biodiesel Fuel Production from Vegetable Oils via Supercritical Ethanol Transesterification." *Energy Sources, Part A: Recovery, Utilization, and Environmental Effects* 30(5): 429–40. http://www.tandfonline.com/doi/abs/10.1080/15567030600826531.

Barnwal, B.K., and M.P. Sharma. 2005. "Prospects of Biodiesel Production from Vegetable Oils in India." *Renewable and Sustainable Energy Reviews* 9(4): 363–78. http://linkinghub.elsevier.com/retrieve/pii/S136403210400067X.

Baskar, G., and R. Aiswarya. 2016. "Trends in Catalytic Production of Biodiesel from Various Feedstocks." *Renewable and Sustainable Energy Reviews* 57: 496–504. http://linkinghub.elsevier.com/retrieve/pii/S1364032115014847.

Basu, H. N., & Norris, M. E. 1996. "Process for Production of Esters for Use as a Diesel Fuel Substitute Using a Non-Alkaline Catalyst." : 525,126.

Batonneau-gener, Isabelle et al. 2008. "Influence of Steaming and Acid-Leaching Treatments on the Hydrophobicity of HBEA Zeolite Determined under Static Conditions." *Microporous and Mesoporous Materials* 110(2–3): 480–87.

http://linkinghub.elsevier.com/retrieve/pii/S1387181107003976.

Beetul, Keshini et al. 2014. "An Investigation of Biodiesel Production from Microalgae Found in Mauritian Waters." *Biofuel Research Journal*: 58–64. http://www.biofueljournal.com/pdf_5547_50e0bbfdff41df3912228dc354083b27.html.

Bender, Martin. 1999. "Economic Feasibility Review for Community-Scale Farmer Cooperatives for Biodiesel." *Bioresource Technology* 70(1): 81–87. http://linkinghub.elsevier.com/retrieve/pii/S0960852499000097.

Benesi, H. A. 1956. "Acidity of Catalyst Surfaces. I. Acid Strength from Colors of Adsorbed Indicators." *JAOCS, Journal of the American Oil Chemists' Society* 78(21): 5490–94.

Birla, Ashish, Bhaskar Singh, S.N. Upadhyay, and Y.C. Sharma. 2012. "Kinetics Studies of Synthesis of Biodiesel from Waste Frying Oil Using a Heterogeneous Catalyst Derived from Snail Shell." *Bioresource Technology* 106: 95–100. http://linkinghub.elsevier.com/retrieve/pii/S0960852411016762.

BOLTON, A. 1970. "A Mechanism for the Isomerization of the Hexanes Using Zeolite Catalysts." *Journal of Catalysis* 18(1): 1–11. http://linkinghub.elsevier.com/retrieve/pii/0021951770903040.

Borges, Luciana D. et al. 2013. "Investigation of Biodiesel Production by HUSY and Ce/HUSY Zeolites: Influence of Structural and Acidity Parameters." *Applied Catalysis A: General* 450: 114–19. http://linkinghub.elsevier.com/retrieve/pii/S0926860X12006576.

El Boulifi, N., A. Bouaid, M. Martinez, and J. Aracil. 2010. "Process Optimization for Biodiesel Production from Corn Oil and Its Oxidative Stability." *International Journal of Chemical Engineering* 2010: 1–9. http://www.hindawi.com/journals/ijce/2010/518070/.

Brito, A., M. E. Borges, and N. Otero. 2007. "Zeolite Y as a Heterogeneous Catalyst in Biodiesel Fuel Production from Used Vegetable Oil." *Energy & Fuels* 21(6): 3280–83. http://pubs.acs.org/doi/abs/10.1021/ef700455r.

Brunauer, Stephen, P. H. Emmett, and Edward Teller. 1938. "Adsorption of Gases in Multimolecular Layers." *Journal of the American Chemical Society* 60(2): 309–19. http://pubs.acs.org/doi/abs/10.1021/ja01269a023.

Cao, Fenghua et al. 2008. "Biodiesel Production from High Acid Value Waste Frying Oil Catalyzed by Superacid Heteropolyacid." *Biotechnology and Bioengineering* 101(1): 93–100. http://doi.wiley.com/10.1002/bit.21879.

Carberry, J. J. 2001. “Chemical and Catalytic Reaction Engineering.” *Courier Corporation.*

Carrero, A. et al. 2011. “Hierarchical Zeolites as Catalysts for Biodiesel Production from Nannochloropsis Microalga Oil.” *Catalysis Today* 167(1): 148–53. http://dx.doi.org/10.1016/j.cattod.2010.11.058.

Cerveró, José María, José Coca, and Susana Luque. 2008. “Production of Biodiesel from Vegetable Oils.” *Grasas y Aceites* 59(1). http://grasasyaceites.revistas.csic.es/index.php/grasasyaceites/article/view/494/496.

Chakraborty, Rajat, and Sujit K. Das. 2012. “Optimization of Biodiesel Synthesis from Waste Frying Soybean Oil Using Fish Scale-Supported Ni Catalyst.” *Industrial & Engineering Chemistry Research* 51(25): 8404–14. http://pubs.acs.org/doi/10.1021/ie2030745.

Chanthawong, Anuman, and Shobhakar Dhakal. 2016. “Liquid Biofuels Development in Southeast Asian Countries: An Analysis of Market, Policies and Challenges.” *Waste and Biomass Valorization* 7(1): 157–73. http://link.springer.com/10.1007/s12649-015-9433-9.

Chavarria-Hernandez, Juan et al. 2017. “Perspectives on the Utilization of Waste Fat from Beef Cattle and Fowl for Biodiesel Production in Mexico.” *Journal of Chemical Technology & Biotechnology* 92(5): 899–905. http://doi.wiley.com/10.1002/jctb.5057.

Chen, Guo, and Baishan Fang. 2011. “Preparation of Solid Acid Catalyst from Glucose–starch Mixture for Biodiesel Production.” *Bioresource Technology* 102(3): 2635–40. http://linkinghub.elsevier.com/retrieve/pii/S0960852410017554.

Chisti, Yusuf. 2007. “Biodiesel from Microalgae.” *Biotechnology Advances* 25(3): 294–306. http://linkinghub.elsevier.com/retrieve/pii/S0734975007000262.

Chisti, Y. 2013. “Constraints to Commercialization of Algal Fuels.” *Journal of Biotechnology* 167(3): 201–14. http://linkinghub.elsevier.com/retrieve/pii/S0168165613003167.

Chung, Kyong-Hwan, and Byung-Geon Park. 2009. “Esterification of Oleic Acid in Soybean Oil on Zeolite Catalysts with Different Acidity.” *Journal of Industrial and Engineering Chemistry* 15(3): 388–92. http://linkinghub.elsevier.com/retrieve/pii/S1226086X09001117.

Chung, Kyong Hwan, Duck Rye Chang, and Byung Geon Park. 2008. “Removal of Free Fatty Acid in Waste Frying Oil by Esterification with Methanol on Zeolite Catalysts.” *Bioresource Technology* 99(16): 7438–43.

Cundy, C.S., M.S. Henty, and R.J. Plaisted. 1995. “Investigation of Na, TPA-ZSM-5

Zeolite Synthesis by Chemical Methods." *Zeolites* 15(4): 342–52. http://linkinghub.elsevier.com/retrieve/pii/014424499400042Q.

Cundy, Colin S., and Paul A. Cox. 2003. "The Hydrothermal Synthesis of Zeolites: History and Development from the Earliest Days to the Present Time." *Chemical Reviews* 103(3): 663–702. http://pubs.acs.org/doi/abs/10.1021/cr020060i.

Cundy, C. S., & Cox, P. A. 2005. "The Hydrothermal Synthesis of Zeolites: Precursors, Intermediates and Reaction Mechanism." *Microporous and Mesoporous Materials* 82(1–2): 1–78. http://linkinghub.elsevier.com/retrieve/pii/S1387181105000934.

Cvengroš, Ján, and Zuzana Cvengrošová. 2004. "Used Frying Oils and Fats and Their Utilization in the Production of Methyl Esters of Higher Fatty Acids." *Biomass and Bioenergy* 27(2): 173–81. http://linkinghub.elsevier.com/retrieve/pii/S096195340300206X.

Dang, Tan Hiep, Bing Hung Chen, and Duu Jong Lee. 2013. "Application of Kaolin-Based Catalysts in Biodiesel Production via Transesterification of Vegetable Oils in Excess Methanol." *Bioresource Technology* 145: 175–81. http://dx.doi.org/10.1016/j.biortech.2012.12.024.

Đặng, Tấn Hiệp, Bing Hung Chen, and Duu Jong Lee. 2017. "Optimization of Biodiesel Production from Transesterification of Triolein Using Zeolite LTA Catalysts Synthesized from Kaolin Clay." *Journal of the Taiwan Institute of Chemical Engineers* 79: 14–22.

Datta, Ambarish, and Bijan Kumar Mandal. 2016. "A Comprehensive Review of Biodiesel as an Alternative Fuel for Compression Ignition Engine." *Renewable and Sustainable Energy Reviews* 57: 799–821. http://linkinghub.elsevier.com/retrieve/pii/S1364032115015531.

Dawodu, Folasegun A., Olubunmi Ayodele, Jiayu Xin, Suojiang Zhang, et al. 2014. "Effective Conversion of Non-Edible Oil with High Free Fatty Acid into Biodiesel by Sulphonated Carbon Catalyst." *Applied Energy* 114: 819–26. http://linkinghub.elsevier.com/retrieve/pii/S0306261913008246.

Dawodu, Folasegun A., Olubunmi O. Ayodele, Jiayu Xin, and Suojiang Zhang. 2014. "Application of Solid Acid Catalyst Derived from Low Value Biomass for a Cheaper Biodiesel Production." *Journal of Chemical Technology & Biotechnology* 89(12): 1898–1909. http://doi.wiley.com/10.1002/jctb.4274.

Demirbas, A. (2005). 2005. "Biodiesel Production from Vegetable Oils by Supercritical Methanol."

Demirbas, Ayhan. 2006. "Biodiesel Production via Non-Catalytic SCF Method and

Biodiesel Fuel Characteristics." *Energy Conversion and Management* 47(15–16): 2271–82. http://linkinghub.elsevier.com/retrieve/pii/S0196890405003237.

Demirbas, A. 2009. "Progress and Recent Trends in Biodiesel Fuels." *Energy Conversion and Management* 50(1): 14–34. http://linkinghub.elsevier.com/retrieve/pii/S0196890408003294.

Derouane, E.G. et al. 2013. "The Acidity of Zeolites: Concepts, Measurements and Relation to Catalysis: A Review on Experimental and Theoretical Methods for the Study of Zeolite Acidity." *Catalysis Reviews* 55(4): 454–515. http://www.tandfonline.com/doi/abs/10.1080/01614940.2013.822266.

Dhainaut, Jérémy et al. 2013. "One-Pot Structural Conversion of Magadiite into MFI Zeolite Nanosheets Using Mononitrogen Surfactants as Structure and Shape-Directing Agents." *CrystEngComm* 15(15): 3009. http://xlink.rsc.org/?DOI=c3ce40118a.

Dhar, Bipro Ranjan, and Kawnish Kirtania. 2009. "Excess Methanol Recovery in Biodiesel Production Process Using a Distillation Column: A Simulation Study." *Chemical Engineering Research Bulletin* 13(2). http://banglajol.info/index.php/CERB/article/view/3538.

Dias, Joana M., Maria C.M. Alvim-Ferraz, and Manuel F. Almeida. 2008. "Comparison of the Performance of Different Homogeneous Alkali Catalysts during Transesterification of Waste and Virgin Oils and Evaluation of Biodiesel Quality." *Fuel* 87(17–18): 3572–78. http://linkinghub.elsevier.com/retrieve/pii/S0016236108002561.

Dimian, Alexandre C., C.S. Bildea, F. Omota, and A.A. Kiss. 2009. "Innovative Process for Fatty Acid Esters by Dual Reactive Distillation." *Computers & Chemical Engineering* 33(3): 743–50. http://linkinghub.elsevier.com/retrieve/pii/S0098135408001919.

Doyle, Aidan M., Talib M. Albayati, Ammar S. Abbas, and Ziad T. Alismaeel. 2016. "Biodiesel Production by Esterification of Oleic Acid over Zeolite Y Prepared from Kaolin." *Renewable Energy* 97: 19–23. http://dx.doi.org/10.1016/j.renene.2016.05.067.

Doyle, Aidan M., Ziad T. Alismaeel, Talib M. Albayati, and Ammar S. Abbas. 2017. "High Purity FAU-Type Zeolite Catalysts from Shale Rock for Biodiesel Production." *Fuel* 199: 394–402. http://dx.doi.org/10.1016/j.fuel.2017.02.098.

Dwivedi, P. N., & Upadhyay, S. N. 1977. "Particle-Fluid Mass Transfer in Fixed and Fluidized Beds." *Industrial & Engineering Chemistry Process Design and Development* 16(2): 157–65.

El-Gendy, N. Sh., S. F. Deriase, and A. Hamdy. 2014. "The Optimization of Biodiesel

Production from Waste Frying Corn Oil Using Snails Shells as a Catalyst." *Energy Sources, Part A: Recovery, Utilization, and Environmental Effects* 36(6): 623–37. http://www.tandfonline.com/doi/abs/10.1080/15567036.2013.822440.

Elkady, M. F., Ahmed Zaatout, and Ola Balbaa. 2015. "Production of Biodiesel from Waste Vegetable Oil via KM Micromixer." *Journal of Chemistry* 2015: 1–9. http://www.hindawi.com/journals/jchem/2015/630168/.

Encinar, J.M., J.F. González, and A. Rodríguez-Reinares. 2007. "Ethanolysis of Used Frying Oil. Biodiesel Preparation and Characterization." *Fuel Processing Technology* 88(5): 513–22. http://linkinghub.elsevier.com/retrieve/pii/S0378382007000045.

Falamaki, Cavus, Mohammad Edrissi, and Morteza Sohrabi. 1997. "Studies on the Crystallization Kinetics of Zeolite ZSM-5 With 1,6-Hexanediol as a Structure-Directing Agent." *Zeolites* 19(1): 2–5. http://linkinghub.elsevier.com/retrieve/pii/S0144244997000250.

Fan, Yu et al. 2007. "Realumination of Dealuminated HZSM-5 Zeolite by Citric Acid Treatment and Its Application in Preparing FCC Gasoline Hydro-Upgrading Catalyst." *Microporous and Mesoporous Materials* 98(1–3): 174–81. http://linkinghub.elsevier.com/retrieve/pii/S1387181106003295.

Felizardo, Pedro et al. 2006. "Production of Biodiesel from Waste Frying Oils." *Waste Management* 26(5): 487–94. http://linkinghub.elsevier.com/retrieve/pii/S0956053X05001236.

Feng, Yaohui et al. 2010. "Biodiesel Production Using Cation-Exchange Resin as Heterogeneous Catalyst." *Bioresource Technology* 101(5): 1518–21. http://linkinghub.elsevier.com/retrieve/pii/S0960852409010190.

Fereidooni, Leila, and Mehdi Mehrpooya. 2017. "Experimental Assessment of Electrolysis Method in Production of Biodiesel from Waste Cooking Oil Using Zeolite/Chitosan Catalyst with a Focus on Waste Biorefinery." *Energy Conversion and Management* 147: 145–54. http://dx.doi.org/10.1016/j.enconman.2017.05.051.

FERNANDO, S, P KARRA, R HERNANDEZ, and S JHA. 2007. "Effect of Incompletely Converted Soybean Oil on Biodiesel Quality." *Energy* 32(5): 844–51. http://linkinghub.elsevier.com/retrieve/pii/S0360544206001496.

Feyzi, Mostafa, Nahid Hosseini, Nakisa Yaghobi, and Rohollah Ezzati. 2017. "Preparation, Characterization, Kinetic and Thermodynamic Studies of MgO-La 2 O 3 Nanocatalysts for Biodiesel Production from Sunflower Oil." *Chemical Physics Letters* 677: 19–29. https://linkinghub.elsevier.com/retrieve/pii/S0009261417302270.

Feyzi, Mostafa, and Gelareh Khajavi. 2014. "Investigation of Biodiesel Production Using

Modified Strontium Nanocatalysts Supported on the ZSM-5 Zeolite." *Industrial Crops and Products* 58: 298–304. http://dx.doi.org/10.1016/j.indcrop.2014.04.014.

Feyzi, Mostafa, Leila Nourozi, and Mohammad Zakarianezhad. 2014. "Preparation and Characterization of Magnetic CsH 2 PW 12 O 40 /Fe–SiO 2 Nanocatalysts for Biodiesel Production." *Materials Research Bulletin* 60: 412–20. http://linkinghub.elsevier.com/retrieve/pii/S0025540814005078.

De Filippis, Paolo, Carlo Borgianni, and Martino Paolucci. 2005. "Rapeseed Oil Transesterification Catalyzed by Sodium Phosphates." *Energy & Fuels* 19(6): 2225–28. http://pubs.acs.org/doi/abs/10.1021/ef0500686.

Flanigen, E. M., & Breck, D. W. 1960. "137th Meet, ACS, Div. Inorg. Chem."

Freedman, B. E. H. P., Pryde, E. H., & Mounts, T. L. 1984. "Variables Affecting the Yields of Fatty Esters from Transesterified Vegetable Oils." *Journal of the American Oil Chemists Society* 60(10): 1638–43.

Fukuda, Hideki, Akihiko Kondo, and Hideo Noda. 2001. "Biodiesel Fuel Production by Transesterification of Oils." *Journal of Bioscience and Bioengineering* 92(5): 405–16. http://linkinghub.elsevier.com/retrieve/pii/S1389172301802887.

G. Knothe. 2001. "ANALYTICAL METHODS USED IN THE PRODUCTION AND FUEL QUALITY ASSESSMENT OF BIODIESEL." *Transactions of the ASAE* 44(2). http://elibrary.asabe.org/abstract.asp??JID=3&AID=4740&CID=t2001&v=44&i=2&T=1.

Gardy, Jabbar et al. 2017. "Biodiesel Production from Used Cooking Oil Using a Novel Surface Functionalised TiO 2 Nano-Catalyst." *Applied Catalysis B: Environmental* 207: 297–310. http://linkinghub.elsevier.com/retrieve/pii/S0926337317300978.

Gardy, Jabbar, Ali Hassanpour, Xiaojun Lai, and Mukhtar H. Ahmed. 2016. "Synthesis of Ti(SO 4)O Solid Acid Nano-Catalyst and Its Application for Biodiesel Production from Used Cooking Oil." *Applied Catalysis A: General* 527: 81–95. http://linkinghub.elsevier.com/retrieve/pii/S0926860X16304495.

Gaurav, Aashish, Flora T.T. Ng, and Garry L. Rempel. 2016. "A New Green Process for Biodiesel Production from Waste Oils via Catalytic Distillation Using a Solid Acid Catalyst – Modeling, Economic and Environmental Analysis." *Green Energy & Environment* 1(1): 62–74. http://linkinghub.elsevier.com/retrieve/pii/S2468025716300164.

Van Gerpen, J., & Knothe, G. 2005. *The Biodiesel Handbook*.

Glisic, Sandra B., Jelena M. Pajnik, and Aleksandar M. Orlović. 2016. "Process and

Techno-Economic Analysis of Green Diesel Production from Waste Vegetable Oil and the Comparison with Ester Type Biodiesel Production." *Applied Energy* 170: 176–85. http://linkinghub.elsevier.com/retrieve/pii/S0306261916302586.

Goering, C. E., Schwab, A. W., Daugherty, M. J., Pryde, E. H., & Heakin, A. J. 1982. "Fuel Properties of Eleven Vegetable Oils." *Transactions of the ASAE* 25(6): 1472–77.

Granados, M. López et al. 2007. "Biodiesel from Sunflower Oil by Using Activated Calcium Oxide." *Applied Catalysis B: Environmental* 73(3–4): 317–26. http://linkinghub.elsevier.com/retrieve/pii/S0926337307000045.

Gratzfeld-Husgen, A., & Schuster, R. 2001. "HPLC for Food Analysis." *Agilent Technologies* 136.

Gude, Veera, Georgene Grant, Prafulla Patil, and Shuguang Deng. 2013. "Biodiesel Production from Low Cost and Renewable Feedstock." *Open Engineering* 3(4). http://www.degruyter.com/view/j/eng.2013.3.issue-4/s13531-013-0102-0/s13531-013-0102-0.xml.

Guisnet, M., Ayrault, P., & Datka, J. 1997. "Acid Properties of Dealuminated Mordenites Studied by IR Spectroscopy. 2. Concentration, Acid Strength and Heterogeneity of OH Groups." *Polish journal of chemistry* 71(10): 1455–61.

Hajjari, Masoumeh, Meisam Tabatabaei, Mortaza Aghbashlo, and Hossein Ghanavati. 2017. "A Review on the Prospects of Sustainable Biodiesel Production: A Global Scenario with an Emphasis on Waste-Oil Biodiesel Utilization." *Renewable and Sustainable Energy Reviews* 72: 445–64. http://linkinghub.elsevier.com/retrieve/pii/S1364032117300291.

Halim, Siti Fatimah Abdul, Azlina Harun Kamaruddin, and W.J.N. Fernando. 2009. "Continuous Biosynthesis of Biodiesel from Waste Cooking Palm Oil in a Packed Bed Reactor: Optimization Using Response Surface Methodology (RSM) and Mass Transfer Studies." *Bioresource Technology* 100(2): 710–16. http://linkinghub.elsevier.com/retrieve/pii/S0960852408006500.

Hammett, Louis P., and Alden J. Deyrup. 1932. "A Series of Simple Basic Indicators. I. The Acidity Functions of Mixtures of Sulfuric and Perchloric Acids with Water1." *Journal of the American Chemical Society* 54(7): 2721–39.

Harvey, Mark, and Sarah Pilgrim. 2011. "The New Competition for Land: Food, Energy, and Climate Change." *Food Policy* 36: S40–51. http://linkinghub.elsevier.com/retrieve/pii/S0306919210001235.

Hashmi, S., Gohar, S., Mahmood, T., Nawaz, U., & Farooqi, H. 2016. "Biodiesel Production by Using CaO-Al2O3 Nano Catalyst." *International Journal of*

Engineering Research & Science 2(3): 2395–6992.

Hatefi, H, M Mohsennia, and H Niknafs. 2014. "Transesterification of Corn Oil Using MgO and ZnO as Catalysts." In *International Conference on Chemistry, Biomedical and Environment Engineering*, , 37–41.

Helwani, Z. et al. 2009. "Solid Heterogeneous Catalysts for Transesterification of Triglycerides with Methanol: A Review." *Applied Catalysis A: General* 363(1–2): 1–10. http://linkinghub.elsevier.com/retrieve/pii/S0926860X09003652.

Hosseini, Seyed Ehsan, Amin Mahmoudzadeh Andwari, Mazlan Abdul Wahid, and Ghobad Bagheri. 2013. "A Review on Green Energy Potentials in Iran." *Renewable and Sustainable Energy Reviews* 27: 533–45. http://linkinghub.elsevier.com/retrieve/pii/S1364032113004607.

Hosseinpour, Soleiman, Mortaza Aghbashlo, Meisam Tabatabaei, and Esmail Khalife. 2016. "Exact Estimation of Biodiesel Cetane Number (CN) from Its Fatty Acid Methyl Esters (FAMEs) Profile Using Partial Least Square (PLS) Adapted by Artificial Neural Network (ANN)." *Energy Conversion and Management* 124: 389–98. http://linkinghub.elsevier.com/retrieve/pii/S0196890416306057.

Intarapong, P., A. Luengnaruemitchai, and S. Jai-In. 2011. "Transesterification of Palm Oil over KOH/NaY Zeolite in a Packed-Bed Reactor." *International Journal of Renewable Energy Research* 1(4): 271–80.

Issariyakul, Titipong, Mangesh G. Kulkarni, Ajay K. Dalai, and Narendra N. Bakhshi. 2007. "Production of Biodiesel from Waste Fryer Grease Using Mixed Methanol/Ethanol System." *Fuel Processing Technology* 88(5): 429–36. http://linkinghub.elsevier.com/retrieve/pii/S0378382007000069.

JACOBSON, K, R GOPINATH, L MEHER, and A DALAI. 2008. "Solid Acid Catalyzed Biodiesel Production from Waste Cooking Oil." *Applied Catalysis B: Environmental* 85(1–2): 86–91. http://linkinghub.elsevier.com/retrieve/pii/S0926337308002488.

Jahirul, Mohammad et al. 2014. "Biodiesel Production from Non-Edible Beauty Leaf (Calophyllum Inophyllum) Oil: Process Optimization Using Response Surface Methodology (RSM)." *Energies* 7(8): 5317–31. http://www.mdpi.com/1996-1073/7/8/5317.

Ju, In Bum et al. 2011. "Kinetic Study of Catalytic Esterification of Butyric Acid and N-Butanol over Dowex 50Wx8-400." *Chemical Engineering Journal* 168(1): 293–302. http://linkinghub.elsevier.com/retrieve/pii/S1385894711000234.

K.G. Inman. 1945. "U.S. Patent No. 2,383,601No Title." : U.S. Patent and Trademark Office, Washington, DC.

van Kasteren, J.M.N., and A.P. Nisworo. 2007. “A Process Model to Estimate the Cost of Industrial Scale Biodiesel Production from Waste Cooking Oil by Supercritical Transesterification.” *Resources, Conservation and Recycling* 50(4): 442–58. http://linkinghub.elsevier.com/retrieve/pii/S0921344906001558.

Kaur, Navjot, and Amjad Ali. 2015. “Preparation and Application" *Renewable Energy* 81: 421–31. http://linkinghub.elsevier.com/retrieve/pii/S0960148115002335.

Keera, S.T., S.M. El Sabagh, and A.R. Taman. 2018. “Castor Oil Biodiesel Production and Optimization.” *Egyptian Journal of Petroleum*. http://linkinghub.elsevier.com/retrieve/pii/S1110062117304105.

Khalid, Mohamed, Guy Joly, Arlette Renaud, and Patrick Magnoux. 2004. “Removal of Phenol from Water by Adsorption Using Zeolites.” *Industrial & Engineering Chemistry Research* 43(17): 5275–80. http://pubs.acs.org/doi/abs/10.1021/ie0400447.

Khan, N. A., & Dessouky, H. 2009. “Biodiesel Production from Corn Oil by Transesterification Process.” *Nucleus* 46(3): 241–52.

Kiss, Anton A., Alexandre C. Dimian, and Gadi Rothenberg. 2006. “Solid Acid Catalysts for Biodiesel Production –-Towards Sustainable Energy.” *Advanced Synthesis & Catalysis* 348(1–2): 75–81. http://doi.wiley.com/10.1002/adsc.200505160.

Kiss, Anton Alexandru, and Costin Sorin Bildea. 2011. “Integrated Reactive Absorption Process for Synthesis of Fatty Esters.” *Bioresource Technology* 102(2): 490–98. http://linkinghub.elsevier.com/retrieve/pii/S0960852410014471.

Kitani, O. 1999. “CIGR Handbook of Agricultural Engineering.” *Energy and biomass engineering* 5: 330.

Kligerman, Debora Cynamon, and Edward J. Bouwer. 2015. “Prospects for Biodiesel Production from Algae-Based Wastewater Treatment in Brazil: A Review.” *Renewable and Sustainable Energy Reviews* 52: 1834–46. http://linkinghub.elsevier.com/retrieve/pii/S136403211500876X.

Knothe, Gerhard, Christopher A. Sharp, and Thomas W. Ryan. 2006. “Exhaust Emissions of Biodiesel, Petrodiesel, Neat Methyl Esters, and Alkanes in a New Technology Engine †.” *Energy & Fuels* 20(1): 403–8. http://pubs.acs.org/doi/abs/10.1021/ef0502711.

Knothe, Gerhard, and Kevin R. Steidley. 2009. “A Comparison of Used Cooking Oils: A Very Heterogeneous Feedstock for Biodiesel.” *Bioresource Technology* 100(23): 5796–5801. http://linkinghub.elsevier.com/retrieve/pii/S0960852409006981.

Krahl, Jürgen et al. 2003. “Influence of Biodiesel and Different Designed Diesel Fuels on the Exhaust Gas Emissions and Health Effects.” http://papers.sae.org/2003-01-3199/.

Kulkarni, Mangesh G., and Ajay K. Dalai. 2006. “Waste Cooking OilAn Economical Source for Biodiesel: A Review.” *Industrial & Engineering Chemistry Research* 45(9): 2901–13. http://pubs.acs.org/doi/abs/10.1021/ie0510526.

Kusdiana, Dadan, and Shiro Saka. 2004. “Effects of Water on Biodiesel Fuel Production by Supercritical Methanol Treatment.” *Bioresource Technology* 91(3): 289–95. http://linkinghub.elsevier.com/retrieve/pii/S0960852403002013.

Kusuma, Ricky Indra et al. 2013. “Natural Zeolite from Pacitan Indonesia, as Catalyst Support for Transesterification of Palm Oil.” *Applied Clay Science* 74: 121–26. http://dx.doi.org/10.1016/j.clay.2012.04.021.

Lam, Man Kee, Keat Teong Lee, and Abdul Rahman Mohamed. 2010. “Homogeneous, Heterogeneous and Enzymatic Catalysis for Transesterification of High Free Fatty Acid Oil (Waste Cooking Oil) to Biodiesel: A Review.” *Biotechnology Advances* 28(4): 500–518. http://linkinghub.elsevier.com/retrieve/pii/S0734975010000388.

Lapuerta, Magín et al. 2008. “Effect of the Alcohol Type Used in the Production of Waste Cooking Oil Biodiesel on Diesel Performance and Emissions.” *Fuel* 87(15–16): 3161–69. http://linkinghub.elsevier.com/retrieve/pii/S0016236108002159.

Leclercq, Elisabeth, Annie Finiels, and Claude Moreau. 2001. “Transesterification of Rapeseed Oil in the Presence of Basic Zeolites and Related Solid Catalysts.” *JAOCS, Journal of the American Oil Chemists’ Society* 78(11): 1161–65.

Lee, Jin-Suk, and Shiro Saka. 2010. “Biodiesel Production by Heterogeneous Catalysts and Supercritical Technologies.” *Bioresource Technology* 101(19): 7191–7200. http://linkinghub.elsevier.com/retrieve/pii/S0960852410007571.

Lertsathapornsuk, V., R. Pairintra, K. Aryusuk, and K. Krisnangkura. 2008. “Microwave Assisted in Continuous Biodiesel Production from Waste Frying Palm Oil and Its Performance in a 100 KW Diesel Generator.” *Fuel Processing Technology* 89(12): 1330–36. http://linkinghub.elsevier.com/retrieve/pii/S0378382008001586.

Leung, Dennis Y.C., Xuan Wu, and M.K.H. Leung. 2010. “A Review on Biodiesel Production Using Catalyzed Transesterification.” *Applied Energy* 87(4): 1083–95. http://linkinghub.elsevier.com/retrieve/pii/S0306261909004346.

Li, Qin, and Yunjun Yan. 2010. “Production of Biodiesel Catalyzed by Immobilized Pseudomonas Cepacia Lipase from Sapium Sebiferum Oil in Micro-Aqueous Phase.” *Applied Energy* 87(10): 3148–54. http://linkinghub.elsevier.com/retrieve/pii/S0306261910000632.

de Lima da Silva, Nívea et al. 2010. “Biodiesel Production from Integration Between Reaction and Separation System: Reactive Distillation Process.” *Applied Biochemistry and Biotechnology* 161(1–8): 245–54. http://link.springer.com/10.1007/s12010-009-8882-7.

LIPPENS, B. 1965. “Studies on Pore Systems in Catalysts V. The t Method.” *Journal of Catalysis* 4(3): 319–23. http://linkinghub.elsevier.com/retrieve/pii/0021951765903076.

Liu, Wei et al. 2014. “Biodiesel Production from Esterification of Free Fatty Acid over PA/NaY Solid Catalyst.” *Energy Conversion and Management* 82: 83–91. http://linkinghub.elsevier.com/retrieve/pii/S0196890414001812.

Lou, Wen-Yong, Min-Hua Zong, and Zhang-Qun Duan. 2008. “Efficient Production of Biodiesel from High Free Fatty Acid-Containing Waste Oils Using Various Carbohydrate-Derived Solid Acid Catalysts.” *Bioresource Technology* 99(18): 8752–58. http://linkinghub.elsevier.com/retrieve/pii/S0960852408003581.

Lourinho, Gonçalo, and Paulo Brito. 2015. “Advanced Biodiesel Production Technologies: Novel Developments.” *Reviews in Environmental Science and Bio/Technology* 14(2): 287–316. http://link.springer.com/10.1007/s11157-014-9359-x.

Lowe, Barrie M. 1983. “An Equilibrium Model for the Crystallization of High Silica Zeolites.” *Zeolites* 3(4): 300–305. http://linkinghub.elsevier.com/retrieve/pii/0144244983901732.

Lund, Henrik. 2007. “Renewable Energy Strategies for Sustainable Development.” *Energy* 32(6): 912–19. http://linkinghub.elsevier.com/retrieve/pii/S036054420600301X.

Lv, Dan, Wei Du, Guoling Zhang, and Dehua Liu. 2010. “Mechanism Study on NS81006-Mediated Methanolysis of Triglyceride in Oil/Water Biphasic System for Biodiesel Production.” *Process Biochemistry* 45(4): 446–50. http://linkinghub.elsevier.com/retrieve/pii/S1359511309003407.

Ma, Fangrui, and Milford A Hanna. 1999. “Biodiesel Production: A Review1Journal Series #12109, Agricultural Research Division, Institute of Agriculture and Natural Resources, University of Nebraska–Lincoln.1.” *Bioresource Technology* 70(1): 1–15. http://linkinghub.elsevier.com/retrieve/pii/S0960852499000255.

Macario, Anastasia et al. 2010. “Biodiesel Production Process by Homogeneous/Heterogeneous Catalytic System Using an Acid–base Catalyst.” *Applied Catalysis A: General* 378(2): 160–68. http://linkinghub.elsevier.com/retrieve/pii/S0926860X10001146.

Madhuvilakku, Rajesh, and Shakkthivel Piraman. 2013. “Biodiesel Synthesis by TiO2–

ZnO Mixed Oxide Nanocatalyst Catalyzed Palm Oil Transesterification Process." *Bioresource Technology* 150: 55–59. http://linkinghub.elsevier.com/retrieve/pii/S0960852413015198.

Mahdavi, Mohmmad, Ebrahim Abedini, and Amir hosein Darabi. 2015. "Biodiesel Synthesis from Oleic Acid by Nano-Catalyst (ZrO 2 /Al 2 O 3) under High Voltage Conditions." *RSC Advances* 5(68): 55027–32. http://xlink.rsc.org/?DOI=C5RA07081C.

Van Manh, Do et al. 2011. "Biodiesel Production from Tung Oil and Blended Oil via Ultrasonic Transesterification Process." *Journal of the Taiwan Institute of Chemical Engineers* 42(4): 640–44. http://linkinghub.elsevier.com/retrieve/pii/S1876107010002257.

Marchetti, J. M., and A. F. Errazu. 2008a. "Comparison of Different Heterogeneous Catalysts and Different Alcohols for the Esterification Reaction of Oleic Acid." *Fuel* 87(15–16): 3477–80.

Marchetti, J.M., and A.F. Errazu. 2008b. "Technoeconomic Study of Supercritical Biodiesel Production Plant." *Energy Conversion and Management* 49(8): 2160–64. http://linkinghub.elsevier.com/retrieve/pii/S019689040800071X.

McKendry, Peter. 2002. "Energy Production from Biomass (Part 1): Overview of Biomass." *Bioresource Technology* 83(1): 37–46. http://linkinghub.elsevier.com/retrieve/pii/S0960852401001183.

Medina-Valtierra, Jorge, and Jorge Ramirez-Ortiz. 2013. "Biodiesel Production from Waste Frying Oil in Sub- and Supercritical Methanol on a Zeolite Y Solid Acid Catalyst." *Frontiers of Chemical Science and Engineering* 7(4): 401–7.

MEHER, L, D VIDYASAGAR, and S NAIK. 2006. "Technical Aspects of Biodiesel Production by Transesterification—a Review." *Renewable and Sustainable Energy Reviews* 10(3): 248–68. http://linkinghub.elsevier.com/retrieve/pii/S1364032104001236.

Meher, Lekha Charan, Mangesh G. Kulkarni, Ajay K. Dalai, and Satya Narayan Naik. 2006. "Transesterification of Karanja(Pongamia Pinnata) Oil by Solid Basic Catalysts." *European Journal of Lipid Science and Technology* 108(5): 389–97. http://doi.wiley.com/10.1002/ejlt.200500307.

Moodley, N. 2006. "Biofuels Strategy Approved for Consultation." *Engineering News*.

Moradi, Gholamreza, Majid Mohadesi, and Zahra Hojabri. 2014. "Biodiesel Production by CaO/SiO2 Catalyst Synthesized by the Sol–gel Process." *Reaction Kinetics, Mechanisms and Catalysis* 113(1): 169–86. http://link.springer.com/10.1007/s11144-014-0728-9.

Morris, R. E., & Weigel, S. J. 1997. "The Synthesis of Molecular Sieves from Non-Aqueous Solvents." *Chemical Society Reviews* 26(4): 309–17.

Mosarof, M.H. et al. 2015. "Implementation of Palm Biodiesel Based on Economic Aspects, Performance, Emission, and Wear Characteristics." *Energy Conversion and Management* 105: 617–29. http://linkinghub.elsevier.com/retrieve/pii/S0196890415007669.

Motasemi, F., and F.N. Ani. 2012. "A Review on Microwave-Assisted Production of Biodiesel." *Renewable and Sustainable Energy Reviews* 16(7): 4719–33. http://linkinghub.elsevier.com/retrieve/pii/S1364032112002535.

Mowla, Omid, Eric Kennedy, and Michael Stockenhuber. 2018. "In-Situ FTIR Study on the Mechanism of Both Steps of Zeolite-Catalysed Hydroesterification Reaction in the Context of Biodiesel Manufacturing." *Fuel* 232(May): 12–26. https://doi.org/10.1016/j.fuel.2018.05.096.

Murugesan, A., C. Umarani, R. Subramanian, and N. Nedunchezhian. 2009. "Bio-Diesel as an Alternative Fuel for Diesel Engines—A Review." *Renewable and Sustainable Energy Reviews* 13(3): 653–62. http://linkinghub.elsevier.com/retrieve/pii/S1364032107001438.

Na, Kyungsu et al. 2010. "Pillared MFI Zeolite Nanosheets of a Single-Unit-Cell Thickness." *Journal of the American Chemical Society* 132(12): 4169–77. http://pubs.acs.org/doi/abs/10.1021/ja908382n.

Na, K., Jo, C., Kim, J., Cho, K., Jung, J., Seo, Y., ... & Ryoo, R. 2011. "Directing Zeolite Structures into Hierarchically Nanoporous Architectures." *Science* 333(6040): 328–32. http://www.sciencemag.org/lookup/doi/10.1126/science.1204452.

Narkhede, Nilesh, and Anjali Patel. 2014. "Efficient Synthesis of Biodiesel over a Recyclable Catalyst Comprising a Monolacunary Silicotungstate and Zeolite Hβ." *RSC Advances* 4(110): 64379–87.

Nelson, James et al. 2012. "High-Resolution Modeling of the Western North American Power System Demonstrates Low-Cost and Low-Carbon Futures." *Energy Policy* 43: 436–47. http://linkinghub.elsevier.com/retrieve/pii/S0301421512000365.

Nomanbhay, S., & Ong, M. Y. 2017. "A Review of Microwave-Assisted Reactions for Biodiesel Production." *Bioengineering* 4(4): 57. http://www.mdpi.com/2306-5354/4/2/57.

Nomanbhay, S., Ong, M.Y. 2017. "A Review of Microwave-Assisted Reactions for Biodiesel Production." *Bioengineering* 4(4): 57. http://www.mdpi.com/2306-

5354/4/2/57.

Nwafor, O.M.I. 2004. “Emission Characteristics of Diesel Engine Operating on Rapeseed Methyl Ester.” *Renewable Energy* 29(1): 119–29. http://linkinghub.elsevier.com/retrieve/pii/S0960148103001332.

OECD/FAO. 2015. “Biofuels.” In *OECD-FAO Agricultural Outlook 2015*, , 126–142. http://www.oecd-ilibrary.org/agriculture-and-food/oecd-fao-agricultural-outlook-2015/biofuels_agr_outlook-2015-13-en.

Okuhara, Toshio. 2002. “Water-Tolerant Solid Acid Catalysts.” *Chemical Reviews* 102(10): 3641–66. http://pubs.acs.org/doi/abs/10.1021/cr0103569.

Ong, H.C., T.M.I. Mahlia, H.H. Masjuki, and R.S. Norhasyima. 2011. “Comparison of Palm Oil, Jatropha Curcas and Calophyllum Inophyllum for Biodiesel: A Review.” *Renewable and Sustainable Energy Reviews* 15(8): 3501–15. http://linkinghub.elsevier.com/retrieve/pii/S1364032111002085.

Ong, Hwai Chyuan et al. 2014. “Optimization of Biodiesel Production and Engine Performance from High Free Fatty Acid Calophyllum Inophyllum Oil in CI Diesel Engine.” *Energy Conversion and Management* 81: 30–40. http://linkinghub.elsevier.com/retrieve/pii/S0196890414001204.

Orsavova, Jana et al. 2015. “Fatty Acids Composition of Vegetable Oils and Its Contribution to Dietary Energy Intake and Dependence of Cardiovascular Mortality on Dietary Intake of Fatty Acids.” *International Journal of Molecular Sciences* 16(12): 12871–90. http://www.mdpi.com/1422-0067/16/6/12871.

Otieno, Stephen O et al. 2018. “ScienceDirect Optimizing Production of Biodiesel Catalysed by Chemically Tuned Natural Zeolites.” *Materials Today: Proceedings* 5(4): 10561–69. https://doi.org/10.1016/j.matpr.2017.12.388.

Panichelli, Luis, Arnaud Dauriat, and Edgard Gnansounou. 2009. “Life Cycle Assessment of Soybean-Based Biodiesel in Argentina for Export.” *The International Journal of Life Cycle Assessment* 14(2): 144–59. http://link.springer.com/10.1007/s11367-008-0050-8.

Park, Ji-Yeon, Zhong-Ming Wang, Deog-Keun Kim, and Jin-Suk Lee. 2010. “Effects of Water on the Esterification of Free Fatty Acids by Acid Catalysts.” *Renewable Energy* 35(3): 614–18. http://linkinghub.elsevier.com/retrieve/pii/S0960148109003528.

Park, Young-Moo et al. 2010. “Tungsten Oxide Zirconia as Solid Superacid Catalyst for Esterification of Waste Acid Oil (Dark Oil).” *Bioresource Technology* 101(17): 6589–93. http://linkinghub.elsevier.com/retrieve/pii/S0960852410005869.

Patle, Dipesh S., Shivom Sharma, Z. Ahmad, and G.P. Rangaiah. 2014. "Multi-Objective Optimization of Two Alkali Catalyzed Processes for Biodiesel from Waste Cooking Oil." *Energy Conversion and Management* 85: 361–72. http://linkinghub.elsevier.com/retrieve/pii/S0196890414004452.

Peidong, Zhang et al. 2009. "Bioenergy Industries Development in China: Dilemma and Solution." *Renewable and Sustainable Energy Reviews* 13(9): 2571–79. http://linkinghub.elsevier.com/retrieve/pii/S1364032109001154.

Pérez-Ramírez, Javier et al. 2008. "Hierarchical Zeolites: Enhanced Utilisation of Microporous Crystals in Catalysis by Advances in Materials Design." *Chemical Society Reviews* 37(11): 2530. http://xlink.rsc.org/?DOI=b809030k.

Peterson, Charles L., and Daryl L. Reece. 1996. "Emissions Testing with Blends of Esters of Rapeseed Oil Fuel With and Without a Catalytic Converter." http://papers.sae.org/961114/.

Phan, Anh N., and Tan M. Phan. 2008. "Biodiesel Production from Waste Cooking Oils." *Fuel* 87(17–18): 3490–96. http://linkinghub.elsevier.com/retrieve/pii/S0016236108002743.

Pienaar, Johan, and Alan C. Brent. 2012. "A Model for Evaluating the Economic Feasibility of Small-Scale Biodiesel Production Systems for on-Farm Fuel Usage." *Renewable Energy* 39(1): 483–89. http://linkinghub.elsevier.com/retrieve/pii/S0960148111005076.

Poling, B. E., Prausnitz, J. M., & O'connell, J. P. 2001. "The Properties of Gases and Liquids." *New York: Mcgraw-hill* 5.

Predojević, Zlatica J. 2008. "The Production of Biodiesel from Waste Frying Oils: A Comparison of Different Purification Steps." *Fuel* 87(17–18): 3522–28. http://linkinghub.elsevier.com/retrieve/pii/S0016236108002706.

Qiu, Fengxian et al. 2011. "Heterogeneous Solid Base Nanocatalyst: Preparation, Characterization and Application in Biodiesel Production." *Bioresource Technology* 102(5): 4150–56. http://linkinghub.elsevier.com/retrieve/pii/S0960852410020341.

Ramachandran, Kasirajan, Pandian Sivakumar, Tamilarasan Suganya, and Sahadevan Renganathan. 2011. "Production of Biodiesel from Mixed Waste Vegetable Oil Using an Aluminium Hydrogen Sulphate as a Heterogeneous Acid Catalyst." *Bioresource Technology* 102(15): 7289–93. http://linkinghub.elsevier.com/retrieve/pii/S0960852411006390.

Ramos, María Jesús et al. 2008. "Transesterification of Sunflower Oil over Zeolites Using Different Metal Loading: A Case of Leaching and Agglomeration Studies." *Applied*

Catalysis A: General 346(1–2): 79–85.

Rezayan, Armin, and Majid Taghizadeh. 2018. "Synthesis of Magnetic Mesoporous Nanocrystalline KOH/ZSM-5-Fe3O4for Biodiesel Production: Process Optimization and Kinetics Study." *Process Safety and Environmental Protection* 117: 711–21. https://doi.org/10.1016/j.psep.2018.06.020.

Robles-Medina, A., P.A. González-Moreno, L. Esteban-Cerdán, and E. Molina-Grima. 2009. "Biocatalysis: Towards Ever Greener Biodiesel Production." *Biotechnology Advances* 27(4): 398–408. http://linkinghub.elsevier.com/retrieve/pii/S0734975009000445.

Rosillo-Calle, F., Pelkmans, L., & Walter, A. 2009. A global overview of vegetable oils, with reference to biodiesel.

Ruhul, A. M. et al. 2015. "State of the Art of Biodiesel Production Processes: A Review of the Heterogeneous Catalyst." *RSC Advances* 5(122): 101023–44. http://xlink.rsc.org/?DOI=C5RA09862A.

Sabudak, T., and M. Yildiz. 2010. "Biodiesel Production from Waste Frying Oils and Its Quality Control." *Waste Management* 30(5): 799–803. http://linkinghub.elsevier.com/retrieve/pii/S0956053X10000164.

Salamatinia, B., Hashemizadeh, I., & Ahmad Zuhairi, A. 2013. "Alkaline Earth Metal Oxide Catalysts for Biodiesel Production from Palm Oil: Elucidation of Process Behaviors and Modeling Using Response Surface Methodology." *Iranian Journal of Chemistry and Chemical Engineering (IJCCE)* 32(1): 113–26.

Sang, Shiyun et al. 2004. "Difference of ZSM-5 Zeolites Synthesized with Various Templates." *Catalysis Today* 93–95: 729–34. http://linkinghub.elsevier.com/retrieve/pii/S0920586104003281.

Saravanan, K., Beena Tyagi, Ram S. Shukla, and H.C. Bajaj. 2015. "Esterification of Palmitic Acid with Methanol over Template-Assisted Mesoporous Sulfated Zirconia Solid Acid Catalyst." *Applied Catalysis B: Environmental* 172–173: 108–15. http://linkinghub.elsevier.com/retrieve/pii/S092633731500065X.

Schuchardt, Ulf, Ricardo Sercheli, and Rogério Matheus Vargas. 1998. "Transesterification of Vegetable Oils: A Review." *Journal of the Brazilian Chemical Society* 9(3). http://www.scielo.br/scielo.php?script=sci_arttext&pid=S0103-50531998000300002&lng=en&nrm=iso&tlng=en.

Schulte, I. 2004. "Issues Affecting the Acceptance of Hydrogen Fuel." *International Journal of Hydrogen Energy* 29(7): 677–85. http://linkinghub.elsevier.com/retrieve/pii/S0360319903002428.

Sdrula, Nicolae. 2010. “A Study Using Classical or Membrane Separation in the Biodiesel Process.” *Desalination* 250(3): 1070–72. http://linkinghub.elsevier.com/retrieve/pii/S0011916409011424.

Sert, Emine, Aslı Deniz Buluklu, Simge Karakuş, and Ferhan Sami Atalay. 2013. “Kinetic Study of Catalytic Esterification of Acrylic Acid with Butanol Catalyzed by Different Ion Exchange Resins.” *Chemical Engineering and Processing: Process Intensification* 73: 23–28. http://linkinghub.elsevier.com/retrieve/pii/S0255270113001517.

Shamshirband, Shahaboddin et al. 2016. “Support Vector Machine-Based Exergetic Modelling of a DI Diesel Engine Running on Biodiesel–diesel Blends Containing Expanded Polystyrene.” *Applied Thermal Engineering* 94: 727–47. http://linkinghub.elsevier.com/retrieve/pii/S1359431115011990.

Sharma, Y.C., and B. Singh. 2008. “Development of Biodiesel from Karanja, a Tree Found in Rural India.” *Fuel* 87(8–9): 1740–42. http://linkinghub.elsevier.com/retrieve/pii/S0016236107003663.

Sheehan, J et al. 2000. *An Overview of Biodiesel and Petroleum Diesel Life Cycles*. Golden, CO (United States). http://www.osti.gov/servlets/purl/771560/.

Shirazi, L., E. Jamshidi, and M. R. Ghasemi. 2008. “The Effect of Si/Al Ratio of ZSM-5 Zeolite on Its Morphology, Acidity and Crystal Size.” *Crystal Research and Technology* 43(12): 1300–1306. http://doi.wiley.com/10.1002/crat.200800149.

Shu, Qing et al. 2007. “Synthesis of Biodiesel from Soybean Oil and Methanol Catalyzed by Zeolite Beta Modified with La3+.” *Catalysis Communications* 8(12): 2159–65.

Silitonga, A.S. et al. 2011. “A Review on Prospect of Jatropha Curcas for Biodiesel in Indonesia.” *Renewable and Sustainable Energy Reviews* 15(8): 3733–56. http://linkinghub.elsevier.com/retrieve/pii/S1364032111002462.

Sing, K. S. W., Everett, D. H., Haul, R. A. W., Moscou, L., Pierotti, L. A., Rouquerol, J., & Siemieniewska, T. 1985. “International Union of Pure and Applied Chemistry Physical Chemistry Division Reporting Physisorption Data for Gas/Soils Systems with Special Reference to the Determination of Surface Area and Porosity.” *Pure Appl Chem* 57: 603–19.

Singh, S.P., and Dipti Singh. 2010. “Biodiesel Production through the Use of Different Sources and Characterization of Oils and Their Esters as the Substitute of Diesel: A Review.” *Renewable and Sustainable Energy Reviews* 14(1): 200–216. http://linkinghub.elsevier.com/retrieve/pii/S1364032109001695.

Singh, Veena, Faizal Bux, and Yogesh Chandra Sharma. 2016. “A Low Cost One Pot

Synthesis of Biodiesel from Waste Frying Oil (WFO) Using a Novel Material, β-Potassium Dizirconate (β-K 2 Zr 2 O 5).” *Applied Energy* 172: 23–33. http://linkinghub.elsevier.com/retrieve/pii/S0306261916302914.

Solomon, A.A., Daniel M. Kammen, and D. Callaway. 2014. “The Role of Large-Scale Energy Storage Design and Dispatch in the Power Grid: A Study of Very High Grid Penetration of Variable Renewable Resources.” *Applied Energy* 134: 75–89. http://linkinghub.elsevier.com/retrieve/pii/S0306261914007867.

Srivastava, P.K., and Madhumita Verma. 2008. “Methyl Ester of Karanja Oil as an Alternative Renewable Source Energy.” *Fuel* 87(8–9): 1673–77. http://linkinghub.elsevier.com/retrieve/pii/S0016236107003754.

Steenberghen, Thérèse, and Elena López. 2008. “Overcoming Barriers to the Implementation of Alternative Fuels for Road Transport in Europe.” *Journal of Cleaner Production* 16(5): 577–90. http://linkinghub.elsevier.com/retrieve/pii/S0959652606004215.

Sun, Kaian et al. 2015. “A Comparative Study on the Catalytic Performance of Different Types of Zeolites for Biodiesel Production.” *Fuel* 158: 848–54. http://dx.doi.org/10.1016/j.fuel.2015.06.048.

Sun Shuzhen, Zhang Liping, Meng Xin, Ma Cong, and Xin Zhong. 2014. “Biodiesel Production By Transesterification Of Corn Oil With Dimethyl Carbonate Under Heterogeneous Base Catalysis Conditions Using Potassium Hydroxide.” *Chemistry and Technology of Fuels and Oils* Vol. 50(No. 2): 99–107.

Supamathanon, Nuttinee, Jatuporn Wittayakun, and Sanchai Prayoonpokarach. 2011. “Properties of Jatropha Seed Oil from Northeastern Thailand and Its Transesterification Catalyzed by Potassium Supported on NaY Zeolite.” *Journal of Industrial and Engineering Chemistry* 17(2): 182–85. http://dx.doi.org/10.1016/j.jiec.2011.02.004.

Suppes, Galen J. et al. 2004. “Transesterification of Soybean Oil with Zeolite and Metal Catalysts.” *Applied Catalysis A: General* 257(2): 213–23.

Szczęsna Antczak, Mirosława, Aneta Kubiak, Tadeusz Antczak, and Stanisław Bielecki. 2009. “Enzymatic Biodiesel Synthesis – Key Factors Affecting Efficiency of the Process.” *Renewable Energy* 34(5): 1185–94. http://linkinghub.elsevier.com/retrieve/pii/S096014810800431X.

Taguchi, Akira, and Ferdi Schüth. 2005. “Ordered Mesoporous Materials in Catalysis.” *Microporous and Mesoporous Materials* 77(1): 1–45. http://linkinghub.elsevier.com/retrieve/pii/S1387181104003038.

Takase, Mohammed, Alexander Nii Moi Pappoe, Ernest Amankwa Afrifa, and Michael Miyittah. 2018. "High Performance Heterogeneous Catalyst for Biodiesel Production from Non-Edible Oil." *Renewable Energy Focus* 25(June): 24–30. https://doi.org/10.1016/j.ref.2018.03.002.

Talebi, Ahmad Farhad et al. 2015. "Biochemical Modulation of Lipid Pathway in Microalgae Dunaliella Sp. for Biodiesel Production." *BioMed Research International* 2015: 1–12. http://www.hindawi.com/journals/bmri/2015/597198/.

Tan, K.T., K.T. Lee, and A.R. Mohamed. 2011. "Potential of Waste Palm Cooking Oil for Catalyst-Free Biodiesel Production." *Energy* 36(4): 2085–88. http://linkinghub.elsevier.com/retrieve/pii/S0360544210002665.

Tan, Yie Hua, Mohammad Omar Abdullah, and Cirilo Nolasco-Hipolito. 2015. "The Potential of Waste Cooking Oil-Based Biodiesel Using Heterogeneous Catalyst Derived from Various Calcined Eggshells Coupled with an Emulsification Technique: A Review on the Emission Reduction and Engine Performance." *Renewable and Sustainable Energy Reviews* 47: 589–603. http://linkinghub.elsevier.com/retrieve/pii/S1364032115002014.

Tang, Ying, Mei Meng, Jie Zhang, and Yong Lu. 2011. "RETRACTED: Efficient Preparation of Biodiesel from Rapeseed Oil over Modified CaO." *Applied Energy* 88(8): 2735–39. http://linkinghub.elsevier.com/retrieve/pii/S0306261911001322.

Tao, Haixiang et al. 2013. "Space-Confined Synthesis of Nanorod Oriented-Assembled Hierarchical MFI Zeolite Microspheres." *Journal of Materials Chemistry A* 1(44): 13821. http://xlink.rsc.org/?DOI=c3ta12989f (May 21, 2018).

Thanh, Le Tu et al. 2010. "A Two-Step Continuous Ultrasound Assisted Production of Biodiesel Fuel from Waste Cooking Oils: A Practical and Economical Approach to Produce High Quality Biodiesel Fuel." *Bioresource Technology* 101(14): 5394–5401. http://linkinghub.elsevier.com/retrieve/pii/S0960852410003718.

Thanh, Le Tu, Kenji Okitsu, Luu Van Boi, and Yasuaki Maeda. 2012. "Catalytic Technologies for Biodiesel Fuel Production and Utilization of Glycerol: A Review." *Catalysts* 2(1): 191–222. http://www.mdpi.com/2073-4344/2/1/191.

Thiruvengadaravi, K.V. et al. 2012. "Acid-Catalyzed Esterification of Karanja (Pongamia Pinnata) Oil with High Free Fatty Acids for Biodiesel Production." *Fuel* 98: 1–4. http://linkinghub.elsevier.com/retrieve/pii/S0016236112001706.

Thoai, Dang Nguyen et al. 2017. "A Novel Chemical Method for Determining Ester Content in Biodiesel." *Energy Procedia* 138: 536–43. http://linkinghub.elsevier.com/retrieve/pii/S1876610217350993.

Tubino, Matthieu, José Geraldo Rocha Junior, and Glauco Favilla Bauerfeldt. 2014. "Biodiesel Synthesis with Alkaline Catalysts: A New Refractometric Monitoring and Kinetic Study." *Fuel* 125: 164–72. http://linkinghub.elsevier.com/retrieve/pii/S001623611400115X.

Uthman, H., and A. S. Abdulkareem. 2014. "The Production and Characterization of Ethyl Ester (Biodiesel) from Waste Vegetable Oil as Alternative to Petro Diesel." *Energy Sources, Part A: Recovery, Utilization, and Environmental Effects* 36(19): 2135–41. http://www.tandfonline.com/doi/abs/10.1080/15567036.2011.563274.

Uzun, Başak Burcu et al. 2012. "Biodiesel Production from Waste Frying Oils: Optimization of Reaction Parameters and Determination of Fuel Properties." *Energy* 44(1): 347–51. http://linkinghub.elsevier.com/retrieve/pii/S0360544212004756.

Valizadeh, Maryam, S. Syafiie, and I. S. Ahamad. 2014. "Optimal Planning of Biodiesel Supply Chain Using a Linear Programming Model." In *2014 IEEE International Conference on Industrial Engineering and Engineering Management*, IEEE, 1280–84. http://ieeexplore.ieee.org/document/7058844/.

Veiga, Paula Moraes et al. 2014. "Zn,Al-Catalysts for Heterogeneous Biodiesel Production: Basicity and Process Optimization." *Energy* 75: 453–62. http://linkinghub.elsevier.com/retrieve/pii/S0360544214009372.

Velázquez, Janice M. 2007. "Conversion of Corn Oil to Alkyl Esters."

Veljković, Vlada B., Ivana B. Banković-Ilić, and Olivera S. Stamenković. 2015. "Purification of Crude Biodiesel Obtained by Heterogeneously-Catalyzed Transesterification." *Renewable and Sustainable Energy Reviews* 49: 500–516. http://linkinghub.elsevier.com/retrieve/pii/S1364032115003676.

Venkatesh Kamath, H., I. Regupathi, and M.B. Saidutta. 2011. "Optimization of Two Step Karanja Biodiesel Synthesis under Microwave Irradiation." *Fuel Processing Technology* 92(1): 100–105. http://linkinghub.elsevier.com/retrieve/pii/S0378382010002912.

Verma, Puneet, and M.P. Sharma. 2016. "Review of Process Parameters for Biodiesel Production from Different Feedstocks." *Renewable and Sustainable Energy Reviews* 62: 1063–71. http://linkinghub.elsevier.com/retrieve/pii/S1364032116300879.

Vicente, Gemma, Mercedes Martínez, and José Aracil. 2004. "Integrated Biodiesel Production: A Comparison of Different Homogeneous Catalysts Systems." *Bioresource Technology* 92(3): 297–305. http://linkinghub.elsevier.com/retrieve/pii/S096085240300230X.

Vieira, Sara S. et al. 2013. "Biodiesel Production by Free Fatty Acid Esterification Using

Lanthanum (La3+) and HZSM-5 Based Catalysts." *Bioresource Technology* 133: 248–55. http://dx.doi.org/10.1016/j.biortech.2013.01.107.

Vieira, S. S., Magriotis, Z. M., Ribeiro, M. F., Graça, I., Fernandes, A., Lopes, J. M. F., ... & Saczk, A. A. 2015. "Use of HZSM-5 Modified with Citric Acid as Acid Heterogeneous Catalyst for Biodiesel Production via Esterification of Oleic Acid." *Microporous and Mesoporous Materials* 201(C): 160–68. http://dx.doi.org/10.1016/j.micromeso.2014.09.015.

Vieira, S. S., Magriotis, Z. M., Graça, I., Fernandes, A., Ribeiro, M. F., Lopes, J. M. F., ... & Saczk, A. A. 2017. "Production of Biodiesel Using HZSM-5 Zeolites Modified with Citric Acid and SO42−/La2O3." *Catalysis Today* 279: 267–73.

Vipin, V.C., Jilse Sebastian, C. Muraleedharan, and A. Santhiagu. 2016. "Enzymatic Transesterification of Rubber Seed Oil Using Rhizopus Oryzae Lipase." *Procedia Technology* 25: 1014–21. http://linkinghub.elsevier.com/retrieve/pii/S2212017316305497.

Volli, Vikranth, and M. K. Purkait. 2015. "Selective Preparation of Zeolite X and A from Flyash and Its Use as Catalyst for Biodiesel Production." *Journal of Hazardous Materials* 297: 101–11. http://dx.doi.org/10.1016/j.jhazmat.2015.04.066.

W.J. Kim and S.D. Kim. 2008. "U.S. Pat. 7,361." : 328.

Wang, Deju et al. 2010. "Hierarchical Structured ZSM-5 Zeolite of Oriented Nanorods and Its Performance in the Alkylation of Phenol with Isopropanol." *Journal of Colloid and Interface Science* 350(1): 290–94. https://www.sciencedirect.com/science/article/pii/S0021979710006090 (May 21, 2018).

WANG, H, and M FRENKLACH. 1994. "Transport Properties of Polycyclic Aromatic Hydrocarbons for Flame Modeling☆." *Combustion and Flame* 96(1–2): 163–70. http://linkinghub.elsevier.com/retrieve/pii/0010218094901678.

Wang, Yong, Shiyi Ou Pengzhan Liu, and Zhisen Zhang. 2007. "Preparation of Biodiesel from Waste Cooking Oil via Two-Step Catalyzed Process." *Energy Conversion and Management* 48(1): 184–88. http://linkinghub.elsevier.com/retrieve/pii/S0196890406001543.

Wang, Yu Yuan, and Bing Hung Chen. 2016. "High-Silica Zeolite Beta as a Heterogeneous Catalyst in Transesterification of Triolein for Biodiesel Production." *Catalysis Today* 278: 335–43. http://dx.doi.org/10.1016/j.cattod.2016.03.012.

Wang, Yun et al. 2009. "Preparation of Mesoporous Nanosized KF/CaO–MgO Catalyst and

Its Application for Biodiesel Production by Transesterification." *Catalysis Letters* 131(3–4): 574–78. http://link.springer.com/10.1007/s10562-009-9972-4.

Warabi, Yuichiro, Dadan Kusdiana, and Shiro Saka. 2004. "Reactivity of Triglycerides and Fatty Acids of Rapeseed Oil in Supercritical Alcohols." *Bioresource Technology* 91(3): 283–87. http://linkinghub.elsevier.com/retrieve/pii/S0960852403002025.

Von Wedel, R. 1999. *Technical Handbook for Marine Biodiesel in Recreational Boats*.

Wen, Libai et al. 2010. "Preparation of KF/CaO Nanocatalyst and Its Application in Biodiesel Production from Chinese Tallow Seed Oil." *Fuel* 89(9): 2267–71. http://linkinghub.elsevier.com/retrieve/pii/S0016236110000360.

Wiesenthal, Tobias et al. 2009. "Biofuel Support Policies in Europe: Lessons Learnt for the Long Way Ahead." *Renewable and Sustainable Energy Reviews* 13(4): 789–800. http://linkinghub.elsevier.com/retrieve/pii/S1364032108000166.

Wilke, C. R., & Chang, P. 1955. "AI Ch. EJ, 1, 264."

Wong, Veronica, William Turner, and Paul Stoneman. 1996. "Marketing Strategies and Market Prospects for Environmentally-Friendly Consumer Products1." *British Journal of Management* 7(3): 263–81. http://doi.wiley.com/10.1111/j.1467-8551.1996.tb00119.x.

Xiao, Yang, Guomin Xiao, and Arvind Varma. 2013. "A Universal Procedure for Crude Glycerol Purification from Different Feedstocks in Biodiesel Production: Experimental and Simulation Study." *Industrial & Engineering Chemistry Research* 52(39): 14291–96. http://pubs.acs.org/doi/10.1021/ie402003u.

Xie, Wenlei, and Liangliang Zhao. 2014. "Heterogeneous CaO–MoO3–SBA-15 Catalysts for Biodiesel Production from Soybean Oil." *Energy Conversion and Management* 79: 34–42. http://linkinghub.elsevier.com/retrieve/pii/S0196890413007620.

Xue, Wei et al. 2009. "Synthesis of Biodiesel from Jatropha Curcas L. Seed Oil Using Artificial Zeolites Loaded with CH3COOK as a Heterogeneous Catalyst." *Natural Science* 01(01): 55–62. http://www.scirp.org/journal/PaperDownload.aspx?DOI=10.4236/ns.2009.11010.

Yaakob, Zahira et al. 2014. "A Review on the Oxidation Stability of Biodiesel." *Renewable and Sustainable Energy Reviews* 35: 136–53. http://linkinghub.elsevier.com/retrieve/pii/S1364032114002275.

Yagiz, Funda, Dilek Kazan, and A. Nilgun Akin. 2007. "Biodiesel Production from Waste Oils by Using Lipase Immobilized on Hydrotalcite and Zeolites." *Chemical Engineering Journal* 134(1–3): 262–67.

http://linkinghub.elsevier.com/retrieve/pii/S138589470700191X.

Yusuf, N.N.A.N., S.K. Kamarudin, and Z. Yaakub. 2011. "Overview on the Current Trends in Biodiesel Production." *Energy Conversion and Management* 52(7): 2741–51. http://linkinghub.elsevier.com/retrieve/pii/S0196890410005352.

Yusuf, Nik N.A.N., Siti K. Kamarudin, and Zahira Yaakob. 2012. "Overview on the Production of Biodiesel from Jatropha Curcas L. by Using Heterogenous Catalysts." *Biofuels, Bioproducts and Biorefining* 6(3): 319–34. http://doi.wiley.com/10.1002/bbb.345.

Zabeti, Masoud, Wan Mohd Ashri Wan Daud, and Mohamed Kheireddine Aroua. 2009. "Activity of Solid Catalysts for Biodiesel Production: A Review." *Fuel Processing Technology* 90(6): 770–77. http://linkinghub.elsevier.com/retrieve/pii/S0378382009000629.

Zhang, Dongdong et al. 2015. "High Performance Catalytic Distillation Using CNTs-Based Holistic Catalyst for Production of High Quality Biodiesel." *Scientific Reports* 4(1): 4021. http://www.nature.com/articles/srep04021.

Zhang, Yong et al. 2012. "Analysing the Status, Obstacles and Recommendations for WCOs of Restaurants as Biodiesel Feedstocks in China from Supply Chain' Perspectives." *Resources, Conservation and Recycling* 60: 20–37. http://linkinghub.elsevier.com/retrieve/pii/S0921344911002497.

Zhdanov, S. P. 1971. "Some Problems of Zeolite Crystallization." *Advances in chemistry series* 101(20).

Zheng, S., M. Kates, M.A. Dubé, and D.D. McLean. 2006. "Acid-Catalyzed Production of Biodiesel from Waste Frying Oil." *Biomass and Bioenergy* 30(3): 267–72. http://linkinghub.elsevier.com/retrieve/pii/S0961953405001790.

Zhu, Mulan et al. 2010. "Preparation and Characterization of PSSA/PVA Catalytic Membrane for Biodiesel Production." *Fuel* 89(9): 2299–2304. http://linkinghub.elsevier.com/retrieve/pii/S0016236110000499.

Živković, Snežana B. et al. 2017. "Technological, Technical, Economic, Environmental, Social, Human Health Risk, Toxicological and Policy Considerations of Biodiesel Production and Use." *Renewable and Sustainable Energy Reviews* 79: 222–47. http://linkinghub.elsevier.com/retrieve/pii/S1364032117306846.

APPENDIX

APPENDIX A

Table A. Physical and chemical properties of feedstock oils

Type of Oil	Species	Acid Value (mg KOH/g)	Viscosity (at 40°C)	Fatty Acid Composition
Edible Oil	Soybean	0.2	32.9	C16:0, C18:1, C18:2
	Rapeseed	2.92	35.1	C16:0, C18:0, C18:1, C18:2
	Sunflower		32.6	C16:0, C18:0, C18:1, C18:2
	Palm	0.1	39.6	C16:0, C18:0, C18:1, C18:2
	Peanut	3	22.7	C16:0, C18:0, C18:1, C18:2, C20:0, C22:0
	Canola	0.4	38.2	C16:0, C18:0, C18:1, C18:2, C18:3
Non-Edible Oil	Jatropha Curcas	28	29.4	C16:0, C16:1, C18:0, C18:1, C18:2
	Pongamina pinnata	5.06	27.8	C16:0, C18:0, C18:1, C18:2, C18:3
	Nile Tilapia	2.81	32.1	C16:0, C18:1, C20:5, C22:6, Other acids
Others	WFOs*	2.5	44.7	Depends on fresh cooking oil

*WFOs: waste frying oils.
Adapted from (Barnwal and Sharma 2005; Thanh et al. 2012; Venkatesh Kamath, Regupathi, and Saidutta 2011)

APPENDIX B

Table B. Properties of biodiesel produced from oil feedstock and petroleum diesel fuel

Diesel type	**Biodiesel**				**Petroleum diesel**
Property	**ASTM D6751-12**		**EN 14214:2012**		
	Test	**Standard value**	**Test**	**Standard value**	**Standard value**
Flash point, min (ºC)	D93	>130	EN ISO 2719	>101	67-85
Water, max (mg/kg)	D2709	<300	EN ISO 12937	<500	200-500
Kinematic viscosity (mm^2/s)	D445	1.9-6.0	EN ISO 3104	3.5-5.0	1.9-4.1
Density (kg/m^3)		860-900	EN ISO 3675	860-900	750-840
Ester content (%)	D6751	97.5	EN 14103	96.50%	-
Sulfated Ash, max (Mass)	D5453	0.02%	ISO 3987	0.02%	
Sulfur, max (%)	D130	0.05	EN ISO 20846	0.05	0.35-0.55
Copper strip corrosion, max	D613	No 3	EN ISO 2160	class 1	
Cetane number, min		>47	EN ISO 5165	>51	40-46

Adapted from (Azcan and Yilmaz 2013; V. Singh, Bux, and Sharma 2016; Thoai et al. 2017)

APPENDIX C

Table C. Advantages and disadvantages associated with the catalyst transesterification process

		Advantages	Disadvantages	References
Single -Step Transesterification	**Homogeneous Base Catalyst**	• Fast reaction rate • High FAMEs yield • Low reaction temperature and pressure required	• Sensitive to FFAs (> 2%) and water content • Soap Formation • High purification cost • Large energy consumption for biodiesel refining	Ayhan Demirbas, 2009; Dias, Alvim-Ferraz, & Almeida, 2008; Leung, Wu, & Leung, 2010
	Homogeneous Acid Catalyst	• No soap formation • Insensitive nature to FFAs content	• High Alcohol to oil molar ratio •Slow reaction rate • Corrosive action to engines • High Purification cost	Atadashi, Aroua, Abdul Aziz, & Sulaiman, 2013; J.-Y. Park, Wang, Kim, & Lee, 2010; Vieira et al., 2017
	Heterogeneous Catalyst	• High reaction rate and conversion yield • Catalyst can be easily separated from the product and regenerated •Operational stability of the catalyst up to 4-5 cycles •Potentially cheaper •Environmentally friendly	• High Cost associated with Solid Catalyst production • High temperature and pressure conditions required during process	Kaur & Ali, 2015; Nomanbhay, S., & Ong, 2017; Ruhul et al., 2015; Verma & Sharma, 2016
	Enzymatic catalyst	• High operational stability • Higher yield of byproduct with high FFA level • Reduces complication of downstream process •Possibility of reuse	• High cost • Slow reaction rate • Enzyme culture handling • Chances of cross contamination •Denaturation of enzymes at high temperatures	Arumugam & Ponnusami, 2014; Cerveró, Coca, & Luque, 2008; Fukuda, Kondo, & Noda, 2001
Two-Step Transesterification		• High FAME yield • Commercially Applicable	• Cost intensive process	Atadashi et al., 2013; Nomanbhay, S., & Ong, 2017

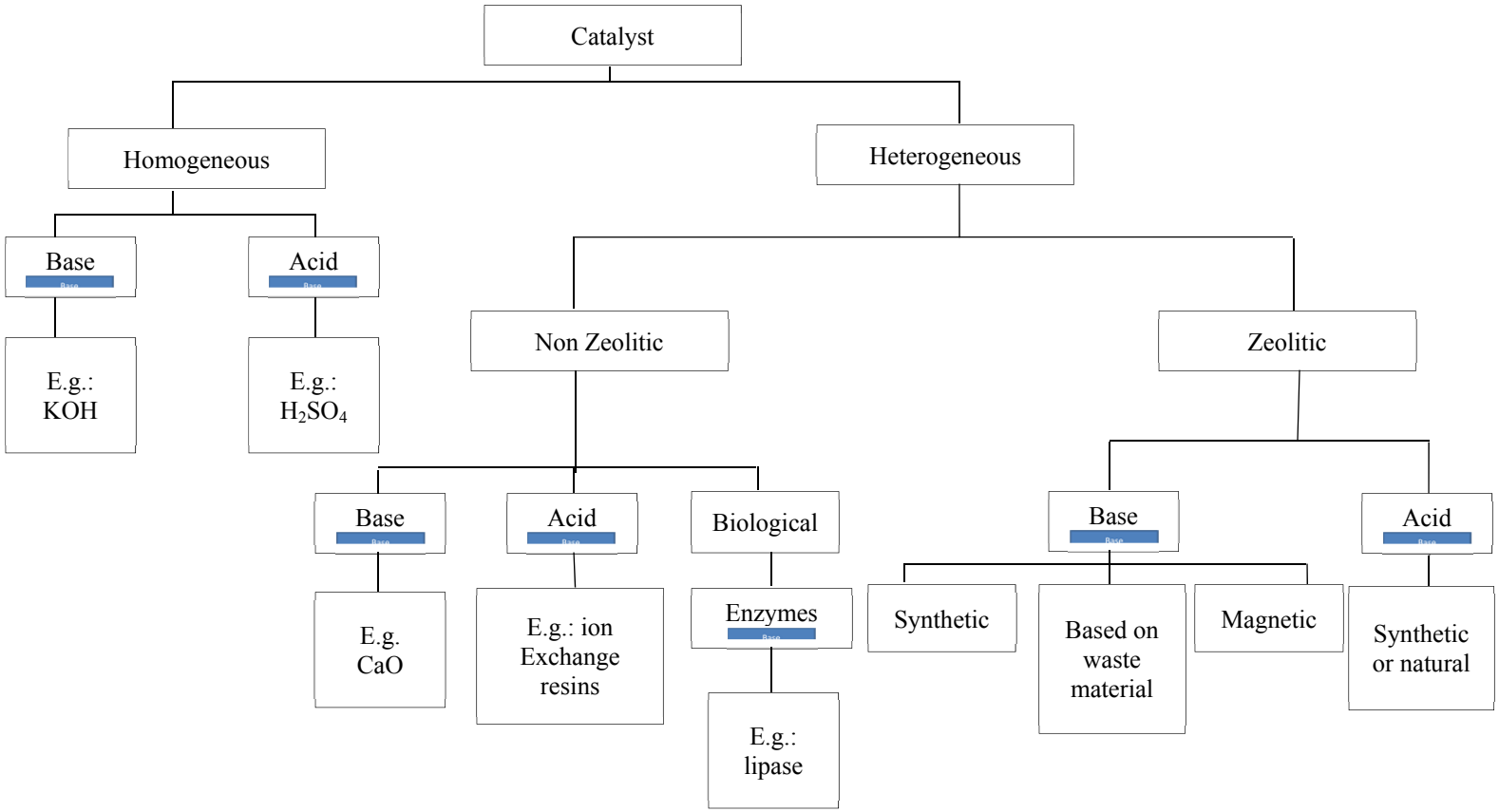

Figure C. General scheme of different types of catalysts used in biodiesel production

APPENDIX D

Table D. Summary of studies that used zeolitic catalysts for biodiesel production

		Catalyst Type	Oil Type	Catalyst Loading	Temperature	Alcohol:Oil Ratio	Reaction Time	Method	Yield	Reference Article
Alkaline	Synthetic	Alkali Natural Zeolite Na-NZK>Cu-NZK>Pb-NZK	Jatropha Curcas Oil	10g 1/1, 2/1, 1/2	65 °C	11ml	5.5h	Reflux at 600 rpm	57%	Otieno et al., 2018
		Magnetic zeolites KOH/ZSM-5: Fe_3O_4	Carola Oil	9.03 wt.%	65 °C	12.3:1	3.26h	100 ml 2-neck flask reflux	93.65%	Rezayan and Taghizadeh, 2018
		Cesium-exchanged NaX Faugasite	Rapeseed Oil	0.5g		275.0:1	22h	Reflux at 700 rpm	70%	Leclercq et al., 2001
		Artificial Zeolite loaded with potassium acetate	Jatropha Curcas Oil	2 wt.%	Reflux T °C	10.0:1	4h	250 ml reflux	91.00%	Xue et al., 2009
		KOH impregnated on Zeolite	Palm Oil	3 wt.%	60 °C	7.0:1	2h	500 ml reflux at 500rpm	95.09%	Vieira et al., 2013
		Nax Faugasite ETS-10 Metal Catlysts NaO_X/Na_X, NaO_X/Na_X^*	Soybean Oil	10 wt.%	120 °C	6.0:1	24h	0.8 ml glass capillary tubes or 1ml sealed glass vials	90%	Suppes et al., 2004

		BEA impregnated with NaOH	Triolein Oil	1/1	65 °C	15.0:1	1h	250 ml reflux at 700 rpm	90%	Wang and Chen, 2016
		Zeolite tylt impregnated with KOH	Synflower Oil	6.40 wt.%	50 °C	11.5:1	2h	250 ml reflux at 800 rpm	96.70%	Al-Jammal et al., 2016
		NaY and K/NaY (12%)	Jatropha Seed oil	0.2g	65 °C	16.0:1	3h	50ml reflux	73.40%	Supamathanon et al., 2011
		NaY/KOH (15%)	Palm Oil	12 wt.%	60 °C	15.0:1	7h	Reflux at 300 rpm	92.18%	Intarapong et al., 2011
		Modernite, Beta and X + Metal Loading	Sunflower Oil	10 wt.%	60 °C	6.0/1	7h	500 ml reflux at 600 rpm	93.5% to 95.1%	Ramos et al., 2008
	Natural	LTA from Kaolin impregnated NaOH	Triolein Oil	72 wt.%	62.9 °C	36.6 (mass ratio)	146 min	Reflux at 600 rpm	92.80%	Thoai et al., 2017
		Faujasite from shale rock impregnated with Co-Ni-Pt	Oleic Acid		70 °C	6.0:1	1.5h	500 ml batch reactor with stirring Continuous stirring	Batch: 89% Continuous: 93%	Alismaeel et al., 2018
		Fly ash used for Production of X and A exchanged with potassium	Mustard Oil	5 wt.%	65 °C	12.0/1	7h	-	84.60%	Volli and Purkait, 2015
		Zeolite HY from Kaolin with Commercial HY	Oleic Acid	5 wt.%	70 °C	6.0/1	1h	500 ml Rbf stirring reflux	Commercial HY: 76% Kaolin HY: 85%	Doyle et al., 2016

		Zeolite chitosan impregnated with KOH	WFO	1 wt.%	40V	7.0/1	3h	Electrolysis with acetone (co-solvent)	93%	Fereidooni and Mehrpooya, 2017
		NA-X from Fly ash	Vegetable Oil	3 wt.%	65 °C	6.0/1	8h	100 ml Rbf Reflux at 600rpm	83.53%	Babajide et al., 2012
		LTA from Kaolin	Soybean Oil Palm Oil	Soybean oil: 50-55 wt.% Palm oil: 10 wt.%	60 °C	Soybean oil: 20.0/1 Palm oil: 10.0/1	2h	Vial Sealed by Teflon Cap 600 rpm	Soybean: 97% Palm: 95.4%	Dang et al., 2013
Acid		H-ZSM-5 dealuminated with citric acid and modified with sulfated lanthanum oxide	Oleic Acid	5 wt.%	100 °C	20.0/1	4h	Glass Batch Reactor	H-ZSM-5: 35% at 1:20 SLO/HZ: 100% at 1:45	Vieira et al., 2017
		HZSM-5	WFO	5 wt.%	Hydrolysis: 100 °C Esterification: 77 °C	3.0/1	4h	Hydroesterification	Hydrolysis from WFO to FA: 40% Esterification to biodiesel: 63%	Mowla et al., 2018
		Zeolite HY	WFO	-	476 °C	6.0:1	21.99min	continuous tubular steel reactor	26.60%	Brito et al., 2007
		H-ZSM-5 and SLO/ H-ZSM-5	Oleic Acid	10 wt.%	100 °C	H-ZSM-5: 20.0:1 SLO: 10.0:1	1h to 7h	In batch	H-ZSM-5: 80% SLO: 100%	Vieira et al., 2013
		Hierarchical Beta	Algae Oil	2 wt.%	115 °C	100.0:1	4h	0.1 L Sirred Batch autoclave	25%	Carrero et al., 2011
		Beta La/Zeolite	Soybean Oil	1.1 wt.%	60 °C	14.5:1	4h	250 ml Rbf + Reflux Condenser	48.9% 500 rpm	Shu et al., 2007

	Beta								
	H-MFI, H-MOR, H-BEA, H-FAU, H-SILICALITE	FFA of WFO	1g	60 °C	1.0:30	3h	Rbf at 600rpm	80%	Chung et al., 2008
	Zeolite HY	WFO	0.2g	240 °C	5.0:1	20 min	Reactor	82% Wt FAME	Medina-Valtierra and Ramirez-Ortiz, 2013
	Sr_ZSM5 Ba_ZSM5 yBa-xSr (y:6% of ZSM5 and x:4% of Ba)	Sunflower Oil	3 wt.%	60 °C	9.0:1	180 min	250 ml Rbf +cond 500 rpm	87.70%	Feyzi and Khajavi, 2014
	Microporous: BEA - HZSM-5 Meso Microporous: HZRP-5	Oleic Acid	0.167 meq/g	78 °C	20.0:1	10h	250 ml Rbf + cond 600 rpm	73.60%	Sun et al., 2015
	FAU using Shale Rock	Oleic Acid		70 °C	6.0:1	90 min	500 ml Rbf Reflux	78%	Doyle et al., 2017
	H-Beta	Oleic Acid and Soybean Oil	Oleic Acid: 3.5 wt.% Soybean Oil: 4 wt.%	Oleic Acid: 60 °C Soybean Oil: 65 °C	Oleic Acid: 20.0:1 Soybean Oil: 4.0:1	Oleic Acid: 10h Soybean Oil: 8h	50 ml batch reactor + stiring	Oleic Acid: 82% Soybean Oil: 96%	Narkhede and Patel, 2014
	HZSM-5 modified with citric acid	Oleic Acid	10 wt.%	100 °C	45.0:1	4h	100 ml Batch Reactor	83%	Vieira et al., 2015

APPENDIX E

Table E: WFOs questionnaire for restaurants and hotels

1. Name of restaurant/hotel	
2. Location of restaurant/hotel	
3. Area of restaurant/hotel	
4. Number of seats	
5. Number of servings per day	
6. Type of food served	
7. Type of oil used (sunflower, canola, Corn, peanut…)	
8. Quantity of vegetable oil used per week	
9. Cost of vegetable oil used per week	
10. How long do you use the oil before disposing of it?	
11. In what form do you dispose of the used oil?	
12. What is the quantity of waste oil generated before disposal?	
13. What companies is the oil used sold to?	
14. If it is sold, for how much are 20L (a typical container) sold?	
15. Are you familiar with used oil recycling techniques?	
16. Do you know what biodiesel is?	
17. Would you be interested in being part of a biodiesel supply chain?	
18. Could you supply us a simple quantity of used oil?	

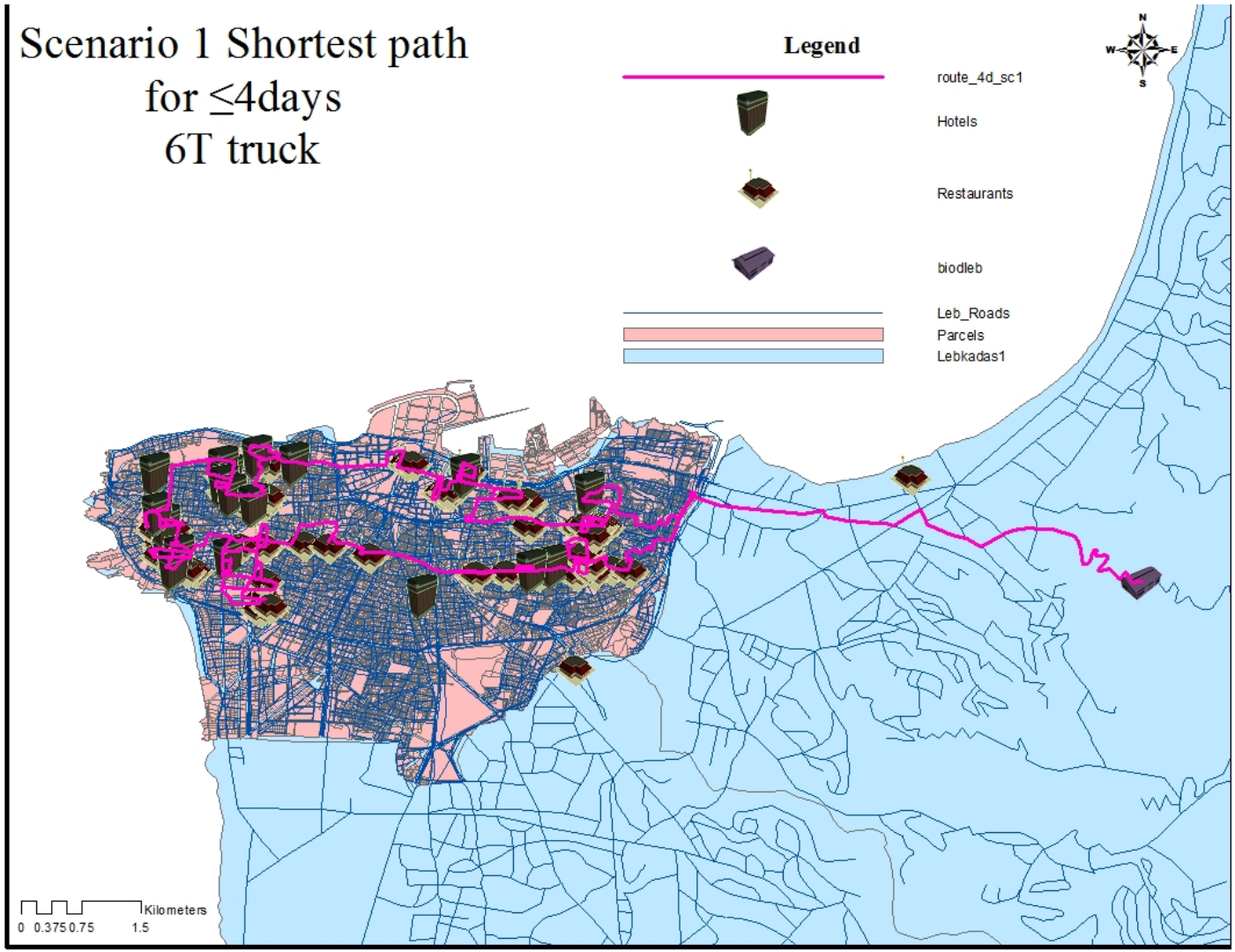
Scenario 1 Shortest path
for ≤4days
6T truck
Legend
route_4d_sc1
Hotels
Restaurants
biodleb
Leb_Roads
Parcels
Lebkadas1
N
W
E
S
Kilometers
0 0.375 0.75 1.5

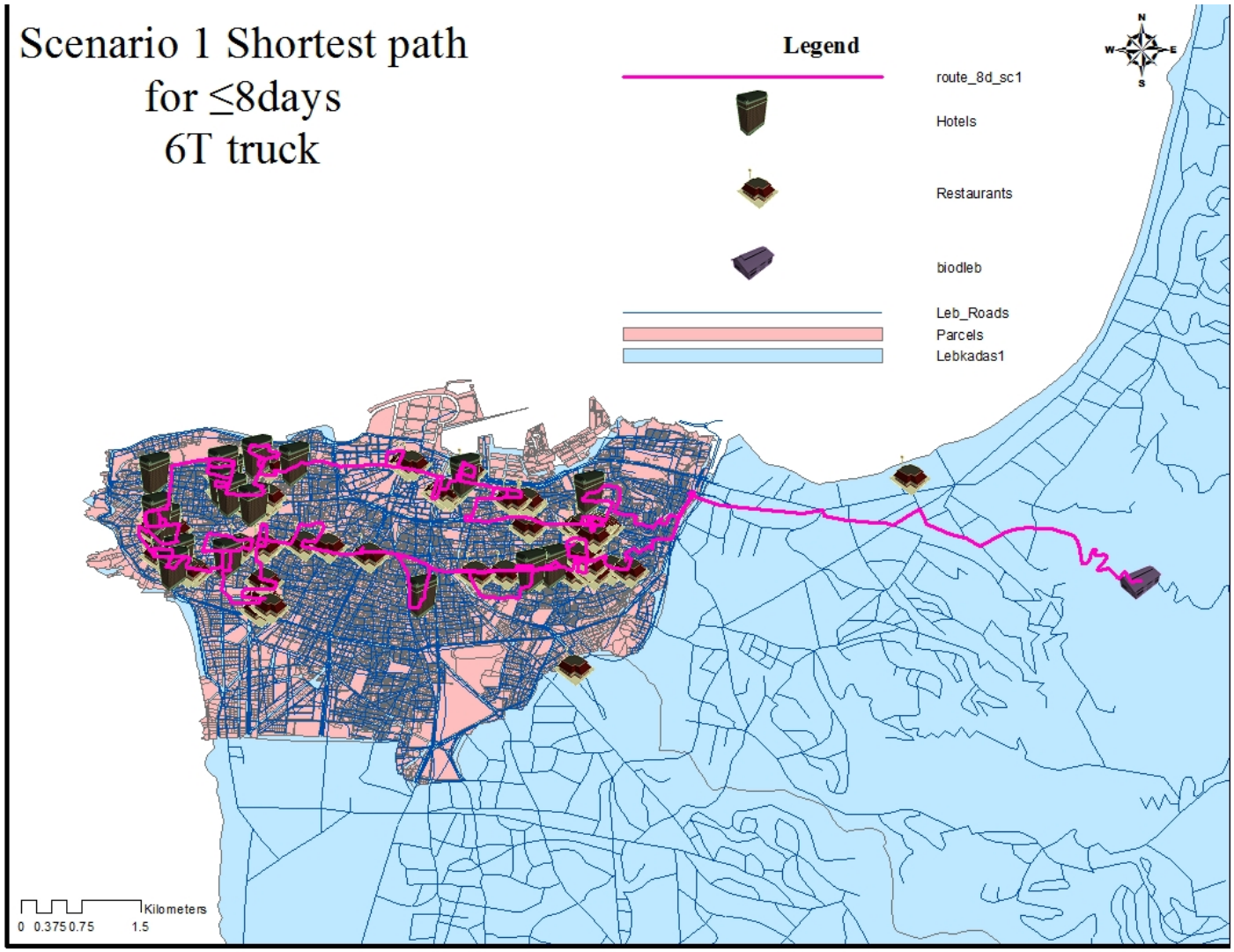

E1: Scenario 1

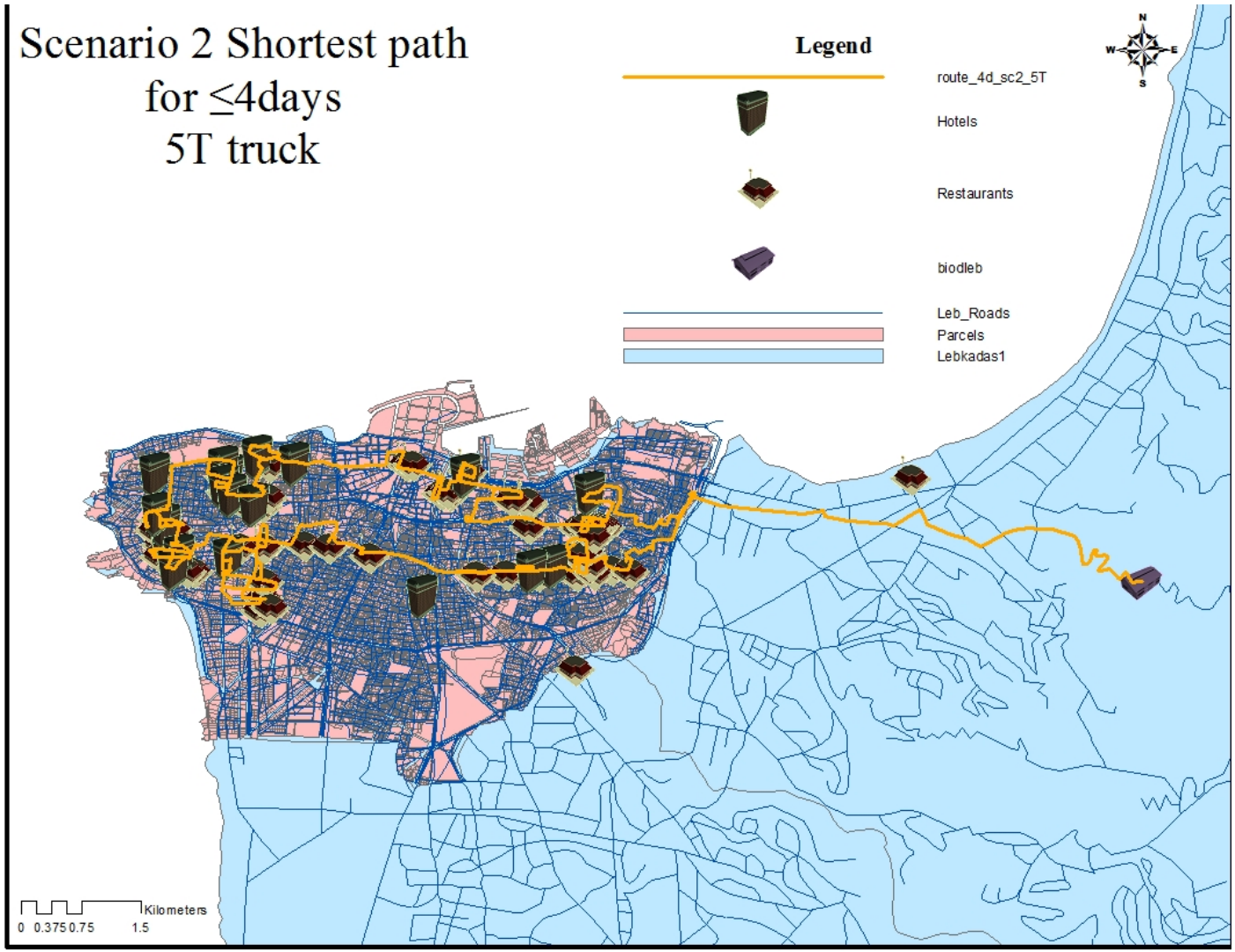
Scenario 2 Shortest path
for ≤4days
5T truck
Legend
route_4d_sc2_5T
Hotels
Restaurants
biodleb
Leb_Roads
Parcels
Lebkadas1
N
W
E
S
Kilometers
0 0.375 0.75 1.5

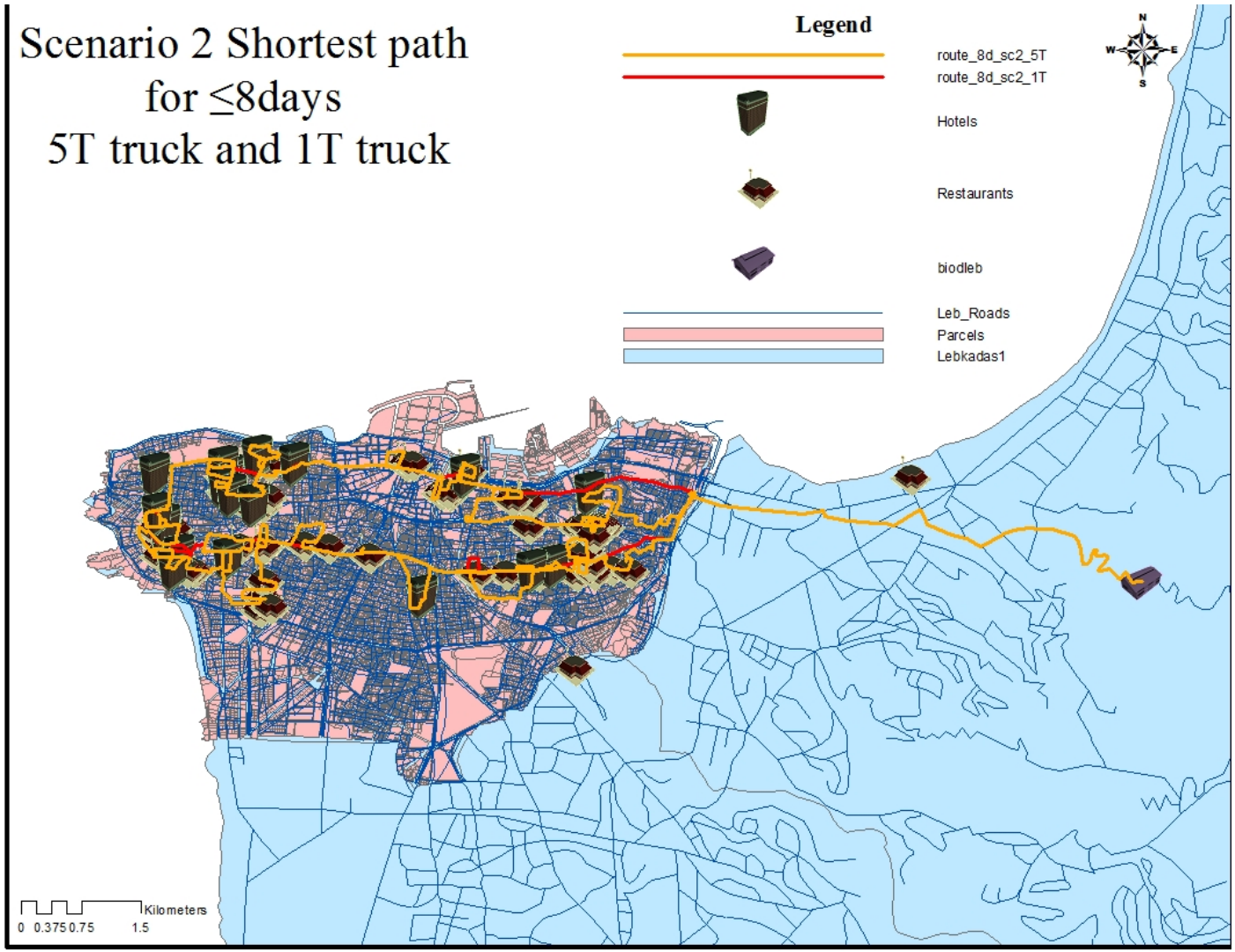

E2: Scenario 2

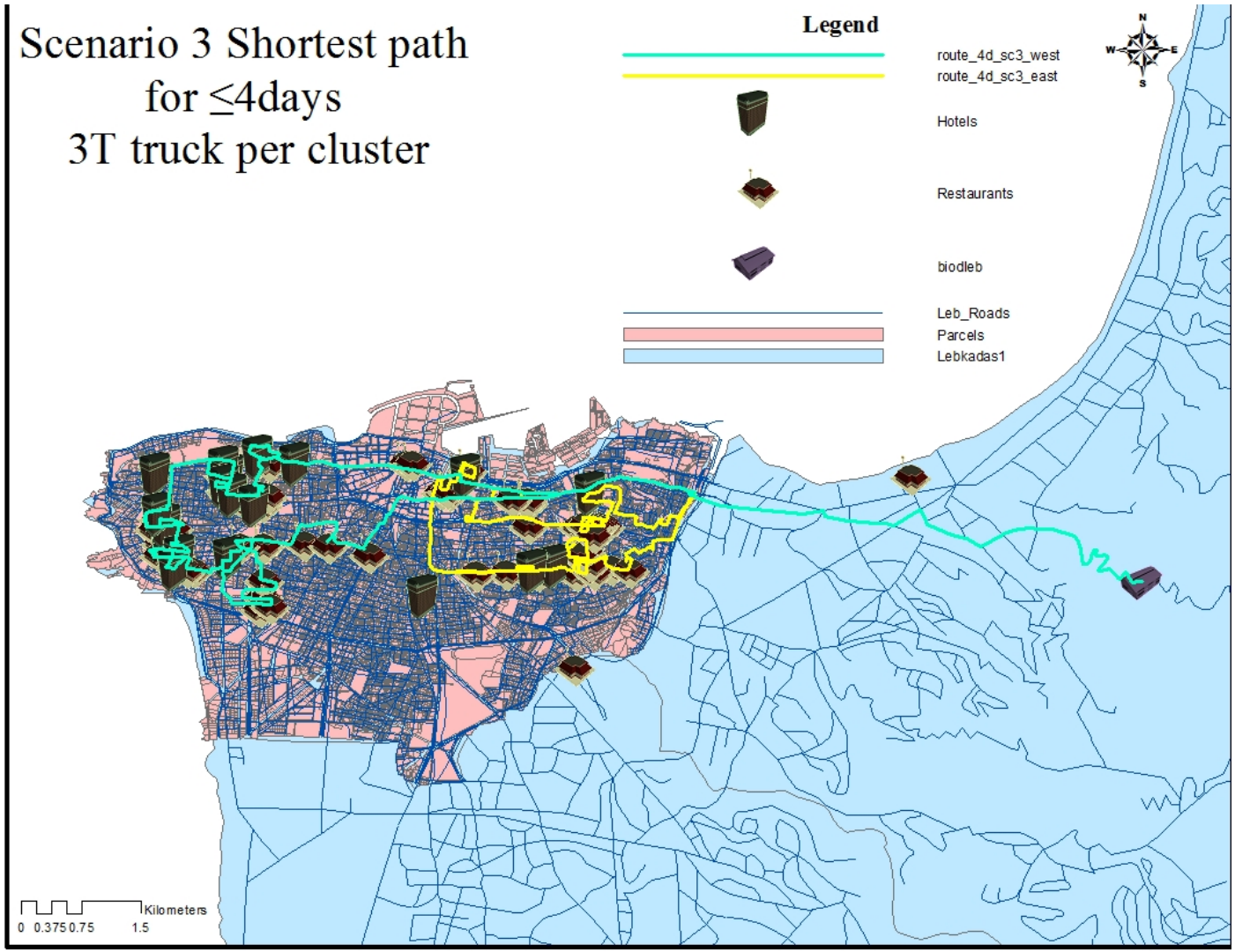
Scenario 3 Shortest path
for ≤4days
3T truck per cluster
Legend
route_4d_sc3_west
route_4d_sc3_east
Hotels
Restaurants
biodleb
Leb_Roads
Parcels
Lebkadas1
N
W
E
S
Kilometers
0 0.375 0.75 1.5

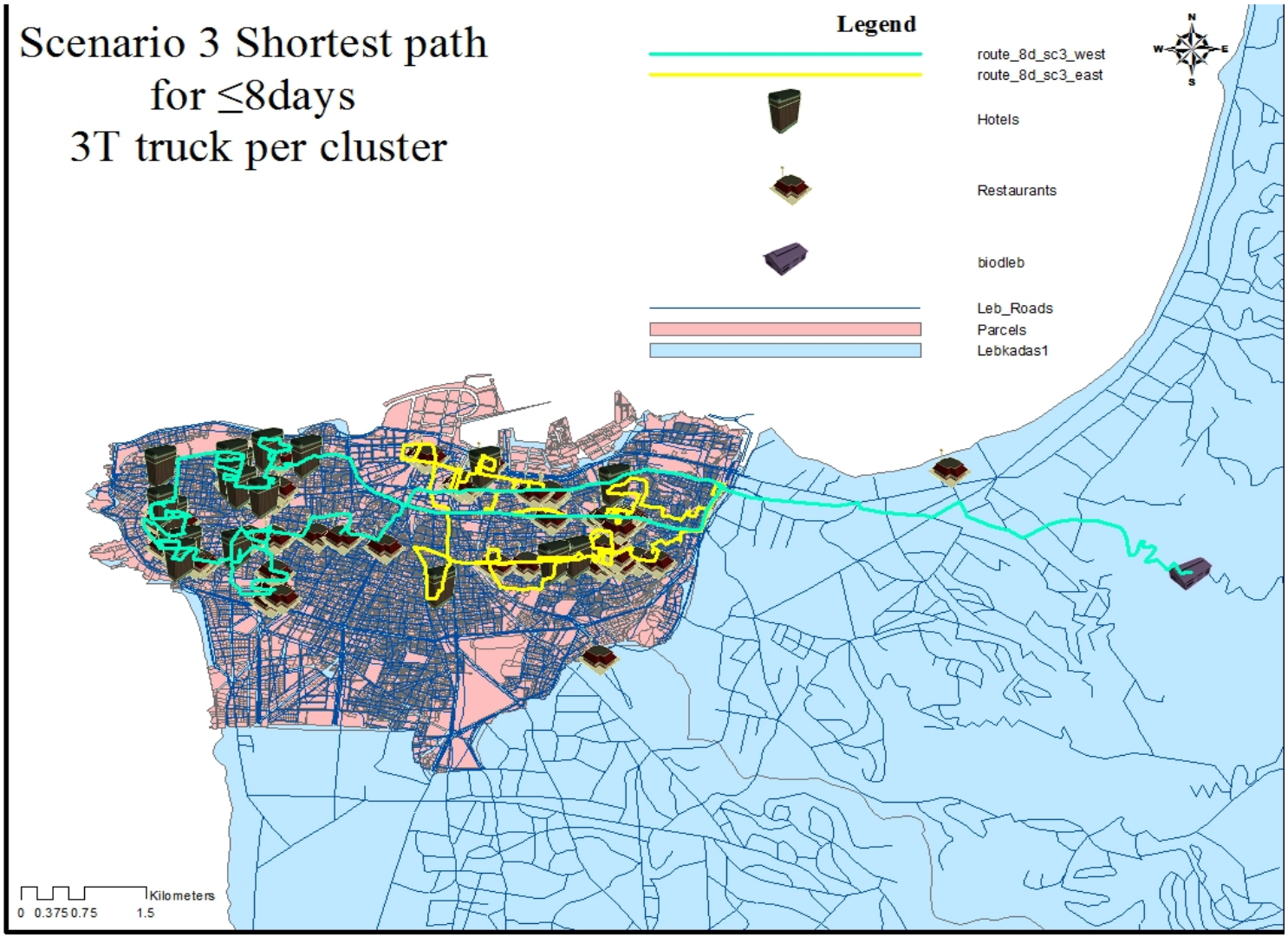

E3: Scenario 3

Figure E: Routing systems for the different scenarios

APPENDIX F

Table F: Yields of produced methyl esters and residual linoleic acid using MC-HZSM-5, NC-HZSM-5, NSh-HZSM-5 and NS-HZSM-5 zeolite catalysts

		MC-HZSM-5		NC-HZSM-5		NSh-HZSM-5		NS-HZSM-5	
Temperature (□C)		Average (%)	SD	Average (%)	SD	Average (%)	SD	Average (%)	SD
60	Methyl esters	34.40	1.45	32.25	3.02	36.12	2.83	15.60	3.60
	Linoleic acid	64.48	1.83	61.56	4.62	63.51	9.46	68.38	5.83
140	Methyl esters	30.93	5.34	31.25	0.66	50.48	0.78	31.16	4.10
	Linoleic acid	60.33	4.58	61.97	2.55	55.97	13.69	41.72	1.52
180	Methyl esters	45.76	4.85	51.31	5.33	76.58	3.47	68.60	4.24
	Linoleic acid	47.74	4.55	57.50	10.87	52.23	23.75	23.67	1.42
Methanol to LA ratio									
6 to 1	Methyl esters	76.62	1.37	46.68	6.58	90.76	1.17	86.40	2.16
	Linoleic acid	14.98	8.17	46.22	8.88	10.44	0.23	5.00	4.16
12 to 1	Methyl esters	45.76	4.85	51.31	5.33	76.58	3.47	68.60	4.24
	Linoleic acid	47.74	4.55	62.39	6.83	23.67	1.42	12.95	5.61
25 to 1	Methyl esters	27.85	7.83	34.50	7.01	72.01	5.77	53.62	10.51
	Linoleic acid	68.70	10.98	59.95	4.66	19.16	7.17	56.18	6.71
Reaction time (h)									
1	Methyl esters					18.38	0.85		
	Linoleic acid					74.02	3.75		
2	Methyl esters					36.26	1.95		
	Linoleic acid					52.84	4.55		
4	Methyl esters					93.87	1.25		
	Linoleic acid					6.83	2.85		
6	Methyl esters					90.76	1.17		
	Linoleic acid					5.34	1.77		

8	Methyl esters	81.01	1.21
	Linoleic acid	18.54	3.26
16	Methyl esters	23.53	0.02
	Linoleic acid	73.62	3.73
24	Methyl esters	23.78	0.78
	Linoleic acid	67.02	1.32

APPENDIX G

Table G: Yields of produced FAMEs and residual triglycerides and FFAs using MC-HZSM-5, NC-HZSM-5, NSh-HZSM-5 and NS-HZSM-5 zeolite catalysts

		MC-HZSM-5		NC-HZSM-5		NSh-HZSM-5		NS-HZSM-5	
Catalyst loading (wt%)		Avergae (%)	SD	Avergae (%)	SD	Avergae (%)	SD	Avergae (%)	SD
	FAMEs	6.73	1.72	8.00	2.25	19.90	0.31	12.18	2.57
5	Triglycerides	55.17	5.02	53.80	11.47	38.10	5.41	38.87	1.32
	FFAs	1.83	0.02	2.91	0.45	2.66	0.31	1.23	0.75
	FAMEs	14.97	3.10	15.34	2.66	24.62	0.42	16.94	1.29
7.5	Triglycerides	56.78	3.35	50.26	2.36	37.63	3.23	50.06	4.49
	FFAs	1.18	1.05	1.04	0.22	1.81	0.65	2.97	0.64
	FAMEs	15.60	0.57	17.29	0.14	26.84	1.59	19.43	0.18
10	Triglycerides	52.55	1.78	51.11	3.06	46.76	3.29	41.12	2.17
	FFAs	2.12	1.05	4.86	0.79	1.54	0.29	1.26	0.08
Methanol to LA ratio									
	FAMEs	15.04	1.52	15.19	0.77	20.53	1.59	14.26	0.96
6 to 1	Triglycerides	34.06	17.72	44.36	6.42	50.37	0.89	47.49	1.19
	FFAs	1.71	0.63	1.07	0.83	4.17	2.79	2.31	0.36
	FAMEs	15.60	0.57	17.29	0.14	26.84	1.59	19.43	0.18
12 to 1	Triglycerides	52.55	1.78	51.11	3.06	46.76	3.29	41.12	2.17
	FFAs	2.12	1.05	4.86	0.79	1.54	0.29	1.26	0.08
	FAMEs	7.29	0.72	11.84	0.69	13.70	3.49	13.38	3.53
25 to 1	Triglycerides	64.96	0.23	52.41	1.74	55.45	2.44	61.87	2.58
	FFAs	1.91	0.28	2.11	0.34	1.50	0.81	1.37	0.08
Temperature (^{0}C)									
	FAMEs					14.77	1.31		
60	Triglycerides					58.68	3.16		
	FFAs					1.63	0.49		

	FAMEs	26.84	1.59
140	Triglycerides	45.26	2.39
	FFAs	1.71	0.24
	FAMEs	43.58	4.43
180	Triglycerides	38.99	5.64
	FFAs	1.02	0.26
Reaction time (h)			
	FAMEs	6.65	2.05
1	Triglycerides	61.65	0.95
	FFAs	1.25	0.25
	FAMEs	13.68	2.74
2	Triglycerides	55.57	2.69
	FFAs	2.22	0.44
	FAMEs	46.11	2.19
4	Triglycerides	31.64	0.36
	FFAs	2.84	0.84
	FAMEs	43.58	4.43
6	Triglycerides	26.02	2.73
	FFAs	3.32	0.57
	FAMEs	43.36	3.50
8	Triglycerides	32.54	1.10
	FFAs	1.64	0.40
	FAMEs	31.21	3.58
16	Triglycerides	37.64	5.77
	FFAs	1.39	1.08
	FAMEs	34.11	0.69
24	Triglycerides	30.54	6.14
	FFAs	1.49	0.19

APPENDIX H

Table H: Yields of produced methyl esters and residual linoleic acid using HZSM-5 (45), HZSM-5 (25) and HZSM-5 (11.5) zeolite catalysts

		HZSM-5 (45)		HZSM-5 (25)		HZSM-5 (11.5)	
Temperature (^{0}C)		Average (%)	SD	Average (%)	SD	Average (%)	SD
60	Methyl esters	34.40	1.45	29.36	1.09	15.93	0.33
	Linoleic acid	64.48	1.83	66.79	2.64	74.07	0.03
140	Methyl esters	30.93	5.34	27.96	0.46	20.18	1.14
	Linoleic acid	60.33	4.58	68.14	1.96	73.12	4.84
180	Methyl esters	45.76	4.85	43.73	4.43	27.96	2.23
	Linoleic acid	47.74	4.55	59.57	4.33	73.59	2.52
Methanol to LA ratio							
6 to 1	Methyl esters	78.62	0.63	61.56	2.30	46.66	1.99
	Linoleic acid	14.98	8.17	29.19	0.75	54.44	3.89
12 to 1	Methyl esters	45.76	4.85	43.73	4.43	27.96	2.23
	Linoleic acid	47.74	4.55	59.57	4.33	73.59	2.52
25 to 1	Methyl esters	27.85	7.83	31.18	0.14	20.58	0.95
	Linoleic acid	68.70	10.98	65.17	9.11	80.72	5.45
Reaction time (h)							
1	Methyl esters	11.42	0.45	6.31	0.26	12.71	0.63
	Linoleic acid	74.02	3.75	85.89	3.26	81.24	1.02
2	Methyl esters	20.36	0.79	19.38	2.11	29.23	1.03
	Linoleic acid	52.84	4.55	72.47	0.24	67.57	0.43
4	Methyl esters	78.72	1.06	61.08	1.52	42.92	2.35
	Linoleic acid	6.83	2.85	39.12	2.52	46.28	2.65
6	Methyl esters	78.62	0.63	61.56	2.30	46.66	1.99
	Linoleic acid	5.34	1.77	29.04	5.30	43.14	2.59
8	Methyl esters	73.15	3.42	60.42	2.95	45.48	1.49
	Linoleic acid	18.54	3.26	30.03	1.00	41.57	3.14
16	Methyl esters	16.72	0.12	12.44	0.82	13.39	0.11
	Linoleic acid	73.62	3.73	77.86	7.08	92.86	4.64
24	Methyl esters	13.29	1.05	11.30	0.78	9.45	2.54
	Linoleic acid	67.02	1.32	81.40	3.78	85.45	5.46